



UNEXMIN DELIVERABLE D2.1

PARAMETER FRAMEWORK REPORT UNEXMIN: AN AUTONOMOUS UNDERWATER EXPLORER FOR FLOODED MINES

Summary:



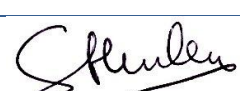
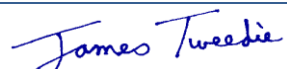

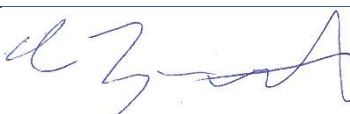
This is a summary documentation about the possible instrumentation that could provide meaningful geo-scientific data during underwater mine exploration missions.

Author:

Csaba Vörös, Endre Turai PhD, Réka Kavanda, Krisztián Baracza PhD, József Subert Viktor Füvesi PhD, József Lénárt, László Rónai, Ildikó Bölkeny, Ferenc Kristály PhD, Norbert Zajzon PhD, Ferenc Móricz



Lead beneficiary: UNIM			
Other beneficiaries:			
Due date: M8			
Nature: Public			
Diffusion			
Revision history	Author	Delivery date	Summary of changes
Version 1.0	Csaba Vörös		
Version 2.0	Norbert Zajzon		
Version 3.0	Stephen Henley		
Version 4.0	Gorazd Žibret		
Version 4.1			

Approval status			
Function	Name	Date	Signature
Deliverable responsible	Csaba Vörös	30.09.2016	
Reviewer 1	Gorazd Žibret	23.09.2016	
Reviewer 2	Jasminka Alijagić	23.09.2016	
Reviewer 3	Stephen Henley	29.09.2016	
Reviewer 4	James Tweedie	29.09.2016	
WP leader	Csaba Vörös	30.09.2016	
Project leader	Norbert Zajzon	30.09.2016	

Disclaimer: This report reflects only the author's view. The European Commission is not responsible for any use that may be made of the information it contains.

Table of Contents

1	Introduction - Goals of this deliverable	12
2	Temperature measurement	13
2.1	Theoretical Background	13
2.2	Measured parameter	13
2.3	Target parameter	13
2.4	Measuring methods	13
2.4.1	Thermometers: Glass Tube Thermometers	13
2.4.2	Probes	14
2.4.3	Notes	17
2.5	Conclusion	17
2.6	References	18
3	Hydrostatic level measurement	19
3.1	Theoretical Background	19
3.2	Measured parameter	19
3.3	Measuring method	19
3.3.1	Level measurement in open vessels	19
3.3.2	Level measurement in covered vessels	20
3.4	Target parameter	21
3.5	Applicability	21
3.6	Accuracy	21
3.7	Increasing the accuracy	21
3.8	Compensation	21
3.9	Response to disturbances	22
3.10	Advantages of the method	22
3.11	Disadvantages and limitations of the method	22
3.12	Industrial solutions – Purchasable instruments	23
3.12.1	Types of hydrostatic level sensors	23
3.12.2	Process connection, membranes, cleaning	24
3.12.3	Differential pressure transmitters	24
3.13	Purchasable instrument: Hydrostatic level meter WIKA S-11 pressure transmitter	25
3.13.1	Specifications	25
3.13.2	Dimensions	25
3.14	Conclusion	25
3.15	References	26
4	pH measurement	27
4.1	Theoretical Background	27
4.2	Measured parameter	28
4.3	Measuring method	28
4.4	Aimed parameter	28
4.5	Applicability	28
4.5.1	Advantages of the method	28
4.5.2	Disadvantages of the method	29

4.6	Handling electrodes	29
4.7	Effects on the accuracy	29
4.7.1	Real pH electrodes are not ideal	29
4.7.2	Effects of Temperature on pH measurements	30
4.7.3	Effects of concentration change on pH measurements	30
4.7.4	Effects of Liquid Temperature Coefficient Variation on the calibration buffer and the sample	30
4.8	Industrial solutions – Purchasable instruments	31
4.8.1	Cylindrical, high pressure glass membrane pH electrode - IDRONAUT, Italy	31
4.8.2	Ocean Seven 305 Plus CTD - IDRONAUT, Italy	32
4.8.3	Glass pH sensor - Corr Instruments, USA	33
4.8.4	Reference electrode - Corr Instruments, USA	34
4.8.5	Analog pH Meter Kit - DFRobot	35
4.9	Case Study	35
4.10	Conclusion	36
4.11	References	37
5	Conductivity measurement	38
5.1	Definition of Conductivity	38
5.2	Measured parameter	38
5.3	Target parameter	38
5.4	Theoretical Background	38
5.5	Measuring method	38
5.5.1	Inductive loops	39
5.5.2	Measurement by AC excited electrodes	39
5.6	Electronic interface	40
5.7	Applicability	41
5.8	Advantages of the method	41
5.9	Disadvantages of the method	41
5.10	Industrial solutions – Purchasable instruments	42
5.10.1	EC sensor - Corrinstruments, USA	42
5.10.2	Analog Electrical Conductivity Meter with Temperature Compensation – DFR0300 - DFRobot	42
5.11	Case Study	43
5.12	Conclusion	43
5.13	References	44
6	ISE measurement	45
6.1	Basic theory of ISE measurements	45
6.2	Differences Between pH and Other Ion-Selective Electrodes	46
6.3	Types of Ion-Selective Electrodes	46
a)	Impregnated-PVC-Membrane Electrodes	47
b)	Crystal-Membrane Electrodes	47
6.4	Handling Ion Selective Electrodes	47
6.5	Reference electrodes	47
6.6	Combination Electrodes	47
6.7	Advantages	48

6.8	Disadvantages.....	48
6.9	Industrial solutions – Purchasable instruments	48
6.10	Case Study	48
6.11	Conclusion	48
6.12	References	49
7	Spontaneous Potential, Self Potential	50
7.1	Theoretical Background	50
7.2	Measured parameter	50
7.3	Target parameters.....	50
7.4	Limitations	50
7.5	Components and types of Self Potential	51
7.6	Applicability in water or any aqueous solutions of ion compounds.....	52
7.7	Case Study	53
7.8	Advantages of the method	53
7.9	Disadvantages of the method.....	53
7.10	Conclusion	54
7.11	References	55
8	Natural gamma ray measurements.....	56
8.1	Theoretical Background	56
8.2	Measured parameter	56
8.3	Measuring method.....	56
8.3.1	Measurement in field	59
8.3.2	Aerial measurement.....	60
8.3.3	Measurement in marine environment.....	61
8.3.4	Measurement in borehole	62
8.4	Target parameter	63
8.5	Applicability	63
8.6	Advantages of the method	63
8.7	Disadvantages of the method.....	63
8.8	Industrial solutions – Purchasable instruments	64
8.8.1	NP4-2 Gamma-ray Energy Spectrometer.....	64
8.8.2	FD-908 Portable γ Spectrometer	65
8.8.3	FD-3022 microcomputer four channel γ Spectrometer	66
8.8.4	Geometrics GR-101 Scintillometer	67
8.8.5	NaI(Tl) Gamma spectrometer for iPhone\iPad\Android AtomSpectra 3.....	68
8.8.6	IH-99DNC dose rate meter for high dose rate measurement.....	69
8.9	Case Study	69
8.10	Conclusion	72
8.11	References	73
9	Hyper/multispectral Imaging.....	74
9.1	Theoretical background	74
9.2	Measured parameter	75
9.3	Aim	75
9.4	Hyper/Multispectral camera type	76

9.5	Spectral range considerations.....	77
9.6	Problem with underwater infrared imaging	77
9.7	Advantages of the method	78
9.8	Disadvantages of the method.....	78
9.9	Industrial solutions – Purchasable instruments	78
9.10	Conclusion	79
9.11	References	80
10	Induced Polarization (IP).....	81
10.1	Theoretical Background	81
10.2	Measured parametres	81
10.3	In Frequency Domain.....	82
10.3.1	Static parametres	82
10.3.2	Dynamic parametre.....	82
10.4	In Time Domain	83
10.4.1	Static parametres	83
10.4.2	Dynamic parametres.....	83
10.5	Measuring method.....	85
10.6	Aimed parametre	85
10.7	Applicability	85
10.8	Advantages of the method	85
10.9	Disadvantages of the method.....	85
10.10	Industrial solutions – Purchasable instruments	86
10.10.1	SYSCAL Junior (2 channels - 100 W resistivity meter) [19].....	86
10.10.2	SYSCAL R1 Plus (2 channels - 200 W resistivity metre) [20].....	88
10.10.3	SYSCAL R2 (Resistivity and IP system for sounding and profiling) [21].....	90
10.10.4	SYSCAL Pro (10 channels - 250W resistivity metre) [22].....	92
10.10.5	SYSCAL Pro Deep Marine (10/20 channels - 2500W resistivity metre) [23]	93
10.10.6	SYSCAL Junior Switch 72 (2 channels - 100 W resistivity metre 72 electrodes string) [24]	94
10.10.7	SYSCAL Pro Switch (10 channels - 250W resistivity metre 48 to 96 electrodes string) [22]	95
10.10.8	SYSCAL Pro for continuous land survey [22].....	95
10.10.9	SYSCAL Pro for river and sea survey [22].....	97
10.11	Case Study Examples.....	97
10.11.1	Geotechnical Study.....	97
10.11.2	Mineral Exploration Study.....	98
10.11.3	Gold Exploration Study.....	99
10.11.4	Refuse Dump Study.....	99
10.11.5	Waste Site Study.....	100
10.11.6	Oil Contaminated Site Study	101
10.11.7	Red Sludge Tailings Study.....	102
10.12	Conclusion	103
10.13	References	104
11	Water sampler and storage	105
11.1	Theoretical Background	105
11.2	Theoretical summary of possible design	105

11.3	Processes with the stored samples	106
11.3.1	Hydrogeochemistry Package ME-MS14HR	106
11.3.2	Hydrogeochemistry Package ME-MS14L	107
11.4	Industrial solutions – Purchasable instruments	107
11.4.1	Aqua Monitor	108
11.4.2	AquaLab	108
11.4.3	BallTrap	109
11.4.4	BoWa_Snapper - Multihorizon-Bottom Water Sampler K/MT 421	110
11.4.5	Bottom Water Sampler K/MT 420	111
11.4.6	NWS-11C5	111
11.4.7	Niskin Bottles	112
11.4.8	SBE 32 Carousel Water Sampler	113
11.4.9	SBE 55 ECO Water Sampler	113
11.4.10	Water Sampler with CTD	114
11.4.11	KIPS – Deep Sea Water Sampling	115
11.5	Comparison of some available water samplers	116
11.6	Development of water sampler	119
11.7	Conclusion	119
11.8	Referencies	120
12	Side-Scan Sonar	122
12.1	Theoretical Background	122
12.2	Measured parameter	123
12.3	Measuring method	124
12.3.1	Survey Speed	124
12.3.2	The Multi-beam Solution	124
12.4	Range and resolution	125
12.5	Target parameters	126
12.6	Applicability	127
12.7	Advantages of the method	127
12.8	Industrial solutions – Purchasable instruments	127
12.8.1	EdgeTech 2200 and 2205 [12]	127
12.8.2	Marine Sonic Technologie's Sea Scan® PC AUV/ROV	129
12.8.3	Other manufacturers:	131
12.9	Case Study	131
12.10	Conclusion	131
12.11	References	132
13	Magnetic Method	133
13.1	Theoretical Background	133
13.2	Measured parameter	133
13.3	Measuring method	133
13.4	Target parameter	134
13.5	Applicability	135
13.6	Advantages of the method	136
13.7	Disadvantages of the method	136
13.8	Industrial solutions – Purchasable instruments	136

13.9	Conclusion	139
13.10	References	140
14	Microgravimetry surveying.....	141
14.1	Theoretical Background	141
14.2	Measured parameter	142
14.3	Measuring method.....	142
14.4	Target parameter	146
14.5	Applicability	146
14.5.1	Advantages of the method	147
14.5.2	Disadvantages of the method.....	147
14.6	Industrial solutions – Purchasable instruments	147
14.6.1	Worden gravimeters	147
14.6.2	INO sea-floor gravimeter.....	150
14.7	Conclusion	151
14.8	References	152
15	Reflection Seismic Tomography	153
15.1	Theoretical Background	153
15.2	Measured parameter	154
15.3	Measuring method.....	154
15.4	Applicability	157
15.4.1	Advantages of the method	157
15.4.2	Disadvantages of the method.....	157
15.5	Industrial solutions – Purchasable instruments	157
15.6	Conclusion	161
15.7	References	162
16	Raman spectroscopy.....	163
16.1	Theoretical Background	163
16.2	Measured parameter	164
16.3	Measuring method.....	166
16.4	Target parameters.....	167
16.5	Applicability	167
16.5.1	Pore water analysis.....	168
16.6	Advantages of the method	169
16.7	Disadvantages of the method.....	169
16.8	Industrial solutions – Purchasable instruments	171
16.8.1	Lasers	172
16.8.2	Optical fibre, fibre probes	172
16.8.3	Filters.....	172
16.8.4	Benchtop instruments [17]	172
16.8.5	Handheld spectrometers and probes [19].....	173
16.9	Conclusion	174
16.10	References	175
17	Laser-induced breakdown spectroscopy - LIBS.....	176
17.1	Theoretical Background	176

17.2	Measured parameter	176
17.3	Measuring method.....	176
17.3.1	Single-Pulse LIBS.....	178
17.3.2	Dual-Pulse LIBS	178
17.4	Target parameter	181
17.5	Applicability	181
17.6	Advantages of the method	182
17.7	Disadvantages of the method.....	182
17.8	Industrial solutions – Purchasable instruments	183
17.8.1	SciAps Z – High Performance, Handheld LIBS Analyzer [9].....	183
17.8.2	Handheld LIBS Analyzer for Metal Alloys – mPulse [10]	183
17.8.3	PMI-analytical EOS Handheld LIBS [11]	184
17.9	Conclusion	184
17.10	References.....	185
18	X-ray diffraction (XRD) and X-ray fluorescence (XRF) spectrometry	186
18.1	Theoretical Background	186
18.2	Measured parameters	186
18.3	Measuring method.....	187
18.4	Target parameter	187
18.5	Advantages of the methods.....	187
18.6	Disadvantages of the methods	187
18.7	Conclusion	188
18.8	References	189
19	Summary.....	190
19.1	Geophysical methods.....	191
19.2	Water Testing Methods	191
19.3	Optical methods	192

1 INTRODUCTION- GOALS OF THIS DELIVERABLE

The main goal of WP2 of the UNEXMIN project is to prepare the scientific instrumentation which will be mounted on the UX1 robot. Besides the instrumentation providing attitude control the robot needs other instruments which provide relevant geological information. During the realisation of the proposal we aim to choose the optimal solution taking into account both the given budget and the procurable information. According to the main goal of Task 2.1 of the UNEXMIN project is to identify those methods that give maximum information and which are realizable in an autonomous underwater robot.

The best way to generate meaningful geoscientific data in the underground flooded mine is to analyse mineral samples from the mining wall. A rock sample can be investigated after grinding. These investigations could be based on optical spectrometry, gamma emissions or direct chemical analytical methods. Most of these methods can be adapted for high pressure and/or wet environment, so the identification of different minerals is a solvable task.

There are many deep-sea solutions available for mineral investigation. Within the framework of the UNEXMIN project an almost constantly moving robot must be equipped with appropriate scientific instruments to obtain useful information. Direct rock sampling methods cannot be used because it is impossible to predefine the sampling locations of for a robot whose main goal is mapping, and for which a project requirement is avoidance of direct contact with the wall. These obstacles are manageable, but solving them is not the goal of the UNEXMIN project.

Because direct investigation methods cannot be used, procedures which can replace these methods need to be applied. The available methods can be divided into three classes:

1. Observation based optical methods: The methods in this class can be used to investigate the surface of the mine wall from distances up to 2 m.
2. Geophysical methods: We can infer the type of minerals indirectly with the help of classical geophysical methods in this class.
3. Water sampling methods: The simplest task is to investigate the parameters of the ambient water. The physical-chemical properties of the water provide indirect information about the surrounded mine site.

All information about the applicability of each of the methods is summarized and the advantages, disadvantages and possible restrictive factors are described.

We have investigated whether commercially available equipment can be used and also investigated the possibilities of its installation into the UX1 robot. Energy consumption, overall dimensions, suitability of the environmental parameters (pressure and temperature limitations) as well the connectivity and communication solutions were the selection criteria. The summary contains our opinions about specific equipment, and our preference whether its use is suggested or not to be installed into UX1.

All chapters contain a specific paragraph called "Industrial solutions – Purchasable instruments". These sections demonstrate the available devices, their features and properties. The collected and presented materials include technical descriptions and specifications from public materials such as brochures and websites of given manufacturers. The inserted texts of these paragraphs are almost without changes and mared with different font. The relevant sources are listed in References at the end of the affected chapters.

2 TEMPERATURE MEASUREMENT

2.1 Theoretical Background

Temperature measurement in today's industrial environment encompasses a wide variety of needs and applications.

Since most other industrial measurements are sensitive to temperature changes, temperature measurement is the most important application in laboratory and industrial environments.

To meet this wide array of needs for measuring temperature the process controls industry has developed a large number of sensors and devices to handle this demand. Temperature is a very critical and widely measured variable for most mechanical engineers. Many processes must have either a monitored or controlled temperature, whether the temperature of process fluids, process support applications, or the temperature of solid objects such as metal plates, bearings and shafts in a piece of machinery.

2.2 Measured parameter

Measured parameter is the environmental temperature. Its engineering unit is °C. In mathematical calculations we need to change the °C to °K.

2.3 Target parameter

The purpose of the temperature measurement is to record the current time-stamped environmental temperature for compensation.

2.4 Measuring methods

Categories of temperature measurement

There are a wide variety of temperature measurement probes in use, depending on what are we trying to measure, how accurately we need to measure it, and on the purpose of measurement (control or monitoring). Devices of temperature measurement will be reviewed in two general categories:

- Thermometers
- Probes

2.4.1 Thermometers: Glass Tube Thermometers

Thermometers are the oldest of temperature measurement devices. Some highly precise measurements are still done with glass thermometers. There are a wide variety of thermometers available on the market today. Since the properties of fluids, and in particular, mercury are well known, the only limitation to accuracy and resolution come in the form of how well we can manufacture a glass tube with a precision bore.

Many thermometers use fluids other than mercury due to the environmental and health hazards and because mercury is banned within EU today. These newer devices use other fluids that have been engineered to have specific rates of expansion. The drawback to these fluids is that they typically are not suitable for measuring wide temperature ranges. Another major drawback of the glass thermometer is the limited environmental pressure range.

Ranges and accuracy

The range of a thermometer and its reading accuracy is dependent on the length of the tube, bore diameter of the tube and the fluid in the thermometer. Typically the smaller the reading increment, the

less range it will have. As an example, a 0.1° C accuracy mercury thermometer with a range of 100°C will typically be about 600 mm long.

Advantage

Some highly precise measurements are still done with glass thermometers.

Disadvantage

Disadvantages of simple glass tube thermometers are the missing electrical output, and also the fragility of glass tubes in challenging environments.

2.4.2 Probes

The next step in the evolution of temperature measurement was the development of temperature probes. They are of three general categories:

- Resistance elements (thermistors, RTD)
- Thermocouples
- Semiconductors

We can easily integrate these elements into an analog or digital electrical measurement system (DAQ). Most of them are non-linear elements; most devices have standard tables or calibration curves that allow users to transform electrical readings that the probe produces to the ambient temperatures.

a) Resistance elements

The thermistor and the Resistance Temperature Detector (RTD) is a thermal resistance element that changes resistance with temperature. The amount of resistance change is defined by

$$\Delta R = k \cdot \Delta T$$

where

- ΔR - the resistance change,
- k - the resistance coefficient of the material
- ΔT - the temperature change.

The temperature is measured by passing a small DC current throughout the device and the voltage drop produced indicates the temperature.

a1) Thermistors

A thermistor is a device that changes its electrical resistance with temperature. The original thermistors were made of loops of resistance wire, but typical thermistors in use today are a semiconductor material with capability of large changes in resistance for a small temperature change.

Thermistors exhibit a negative temperature coefficient, meaning that the resistance of the element decreases as the temperature increases. The most precise ones have extremely good precision, ranging around 0.1° to 0.2°C over working range between 0 and 100°C. Thermistors are non-linear in response. This requires additional work – and equipment - to create a linear output, furthermore adds to the error of the final reading. A new generation of thermistors are called Linear Response elements. These elements actually consist of two elements that are both sensing the same temperature. This layout will allow for a linear voltage output from the probe.

Range and accuracy

Thermistors have very high accuracy and precision. The accuracy is limited and influenced by a number of factors. These factors are also noteworthy for other types of instruments and measurements. One significant factor is the material quality. Manufacturing tolerances can create thermistors with accuracy and repeatability of 0.1°C.

Another major factor is the selection of the electronic interface and powering method. If insufficient current is passed through the device, the signal/noise ratio of the measurement will be very poor. If the current is too high, the probe will start dissipating heat, adding offset to the temperature reading.

The third significant factor is the linearization of the scale. The thermistor is not a linear device, and most units will use some type of polynomial curve to create a calibrated formula for temperature calculation.

Temperature ranges of thermistors are typically from about -80°C to +150 °C. There are some special units that have ranges below and above. The usable range is dependent on its capability to give quite enough resistance changes over a wide temperature change.

The range of the output resistance runs from around 0 to few kΩs. In some cases it can be difficult to create a measurement system to read such a wide range of values. Thus a thermistor is particularly useful in small temperature change environments only.

Figure 1 shows the resistance curve of a typical thermistor.

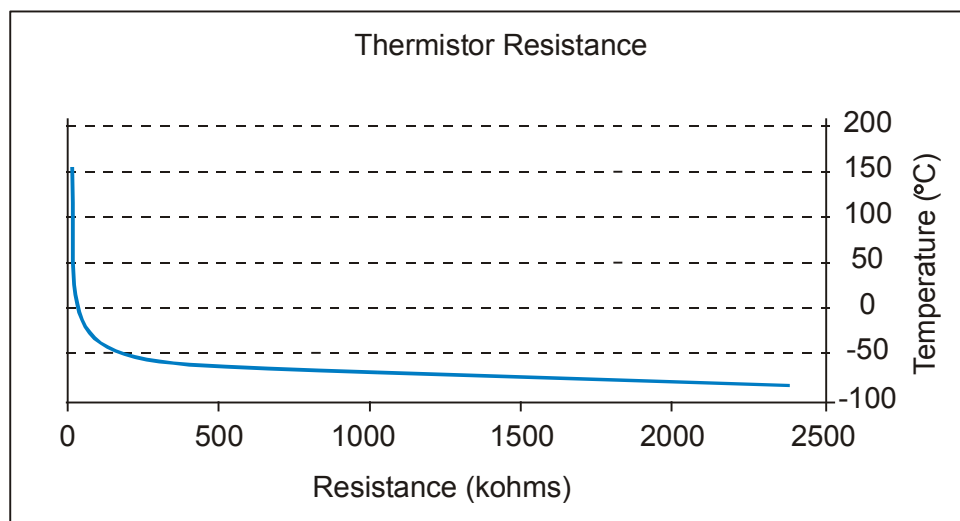


Figure 1. Typical thermistor resistance changing

a2) RTD

The second type of temperature measurements is the RTD (Resistance Temperature Detector). The RTD was developed to obtain greater accuracy than the thermistor. The Resistance Temperature Detector is one of the most accurate temperature measuring devices available. The response is slower and the sensors are much more costly, but these sensors are much more robust, more linear and accurate than thermocouples.

Unlike the thermistor, the Platinum RTD is a linear device, its resistance changes linearly proportionally to temperature change.

RTD operates on the basis of changes of the resistance of metals. The standard for high accuracy measurement elements is the Platinum RTD. Precious metal devices have high precision, and they are accurate and stable over long periods of time.

The simple RTD sensor consists of fine platinum wire wrapped around a ceramic core. Since this element itself is very fragile it is usually placed inside a sheath material. The wire coil is made of material as pure as possible, since the purity of the metal determines its accuracy. Standard metals for building RTDs are: platinum (this is the standard); nickel, copper, Balco (nickel-iron alloy) and tungsten are also used.

Range and accuracy

The temperature range of a Platinum RTD is a much wider range than that of a thermistor, it typically runs from about -270 °C to +850 °C.

The IEC (International Electrotechnical Commission) or DIN (Deutsche Institute for Normung) standard specified a resistance of 100 Ω at 0 °C and a temperature coefficient of 0.00385 $\Omega/^\circ\text{C}$.

There are two classes in the standard, class A and class B in term of accuracy and deviation. The Table 1 shows these two classes.

Temperature and resistance deviation of Platinum RTD				
Temperature °C	Class A		Class B	
	$\pm\Omega$	°C	$\pm\Omega$	°C
-200	0.24	0.55	0.56	1.3
-100	0.14	0.35	0.32	0.8
0	0.06	0.15	0.12	0.3
100	0.13	0.35	0.30	0.8
200	0.20	0.55	0.48	1.3
300	0.27	0.75	0.64	1.8
400	0.33	0.95	0.79	2.3
500	0.38	1.15	0.93	2.8
600	0.43	1.35	1.06	3.3
650	0.46	1.45	1.13	3.6
700	Not used		1.17	3.8
800			1.28	4.3
850			1.34	4.6

Table 1. RTD Classifications.

The RTD – like the thermistor - is a resistance based device. In order to get the resistance, it is necessary a known DC current to flow through the device. The voltage drop across the resistance serves the proper temperature value. But too large current flow can cause self-heating and affect the measured temperature. Modern, factory produced electronics handle this issue.

The RTD can be connected to the transmitter by 2-, 3- or 4-wire connections. The 2-wire connection is the simplest and used where precision is not a major issue. Usually the distance between the sensor and the transmitter is not too large.

The 3-wire system is an advanced solution and improving accuracy. It is often used in a bridge measurement layout.

The 4-wire system is used where long wires need to be employed. Separation of power and measuring lines helps to eliminate the parasite resistance of the long leads.

b) Thermocouples

We do not use thermocouples in a low temperature range with narrow bandwidth and high resolution and precision. Characteristic applications of thermocouples are in the steel industry.

c) Semiconductor Probes

Semiconductor probes are the third main category of probes. Like a resistance probe, they require a current (or voltage) supply to create a reading. This is where there is a similarity with thermistors. Semiconductor probes are created from a semiconductor wafer that contains a number of active circuits.

2.4.3 Notes

Before we draw conclusions, the following definitions are noteworthy for any kinds of measurements.

Accuracy

The accuracy is a difference: amount of uncertainties of the measurement. It shows the proximity of measurement results to the true value. Basically the accuracy is determined by the quality of the sensor and signal conditioner system and their electric parameters: attenuation, gain, bias, offset error, etc.

Precision

The precision gives the repeatability, or reproducibility of the measurement. The smaller the proximity of the measured values the better the precision. It is not necessarily true that good precision means excellent accuracy, e.g. a simple circuit with huge (uncompensated) offset or bias can be precise but will not be accurate.

Resolution

The resolution of the measurement is a unit. This is the smallest, objectively detectable part of the actual measuring range ("span"). It is generally determined by the number of bits of the A/D converter of the system. Unfortunately, the values of other factors also play a role by determining the resolution. The most important of these is noise, it has an impact, which increases the numerical value of the resolution.

Response time

The response time is the (dead) time of a system or functional unit, which reacts to a given input. It has importance in terms of expected frequency of the measurement. This means display and processing of measured values will be delayed. The response time of some sensors can be significant.

2.5 Conclusion

Measuring the temperature is important to make post correction of temperature sensitive measurement methods. Temperature measurement is a simple and reliable method of measuring the environmental condition in flooded mines. Several industrial temperature probes are available. In flooded mine environment it is critically to have high accuracy instrument with sufficient resolution in order to determine small temperature changes in the mine environment. Generally ± 0.1 °C detectable change is feasible. Since the equipment will move during the measurement the second critical requirement is short response time of the temperature sensor.

Suggested/Suggested with comment (suggested in 2.2)/Unsuggested method

The temperature measurement method and available RTD equipment can be used as in-situ measurement considering compromises respect with accuracy.

2.6 References

- [1] Analog Devices AN-892 Application Note, 2006

3 HYDROSTATIC LEVEL MEASUREMENT

3.1 Theoretical Background

Hydrostatic level measurement is a simple and reliable method of measuring water level or depth of the water column. Hydrostatic pressure measurement is suited for level measurement due to the hydrostatic effect of non-flowing fluids. Differential pressure sensors are used for the measurement of the level of a liquid column. This physical principle describes the effect of the weight force of a stationary liquid at the measuring depth. The weight force is described as "hydrostatic pressure". In continuous level measurement, hydrostatic level measurement is the principal sensor technology.

Measuring principle: a standard or submersible pressure transmitter is mounted at a specific depth (zero level). The transmitter measures the pressure caused by the weight of the liquid on top of this level.

The most important condition for hydrostatic level measurement is the "hydrostatic paradox": regardless of the shape and volume of the tank, the hydrostatic pressure at the measuring point of a tank is proportional only to the height of the liquid column. The hydrostatic pressure at the measuring point is proportional to the absolute filling height. If the specific gravity of the liquid is known, the pressure measurement can be calibrated to measure the distance from the surface of the liquid to the zero level, where the transmitter is mounted.

Hydrostatic level transmitter does not only allow measurement of the current height of the surface level. It allows to monitor changes in level from any chosen reference point within the media, anywhere in between the bottom of the resource and its surface.

Hydrostatic level transmitters are unaffected by any disturbances of the liquid's surface like overflow, flood or spill.

3.2 Measured parameter

The pressure transmitter measures the pressure caused by the weight of the liquid column directly on top of the selected zero level where the transmitter is mounted. The hydrostatic pressure at the measuring point is proportional to the water column height.

3.3 Measuring method

3.3.1 Level measurement in open vessels

Measuring liquid level in open vessels by using hydrostatic pressure level sensors is the most popular and the cheapest solution for level measurement applications. It is simple to install and easy to use. It is easy to calculate the filling height of an open vessel from the hydrostatic pressure measured at the bottom of the vessel.

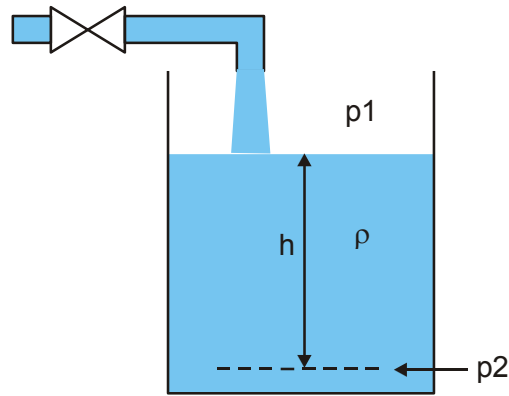


Figure 2. Level measurement in open vessel

The filling height of an open tank or vessel is calculated using the following equation:

$$h = p_2 / (\rho g)$$

where

h - height of the liquid column [m]

p_2 - hydrostatic pressure [bar (relative)]

ρ - density of the liquid [kg/m^3]

g - gravitational force or gravitational acceleration [9.8066 m/s^2]

As a simple rule of thumb for water as a medium: a pressure of 1 bar (relative) corresponds to a filling height of 10 m.

3.3.2 Level measurement in covered vessels

The level measurement in closed vessels requires a pressure compensation in term of the pressure of the enclosed gas phase above the liquid. Measuring the pressure of the gas phase by another individual sensor or via an integrated differential pressure transmitter can help to do the compensation. For the measurement we can use either relative sensors with ambient pressure compensation, or absolute pressure variants with sealed vacuum reference.

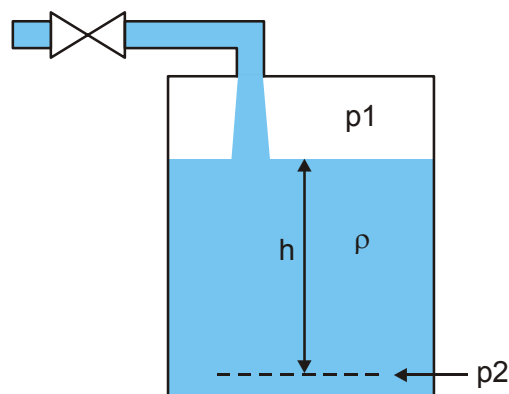


Figure 3. Level measurement in sealed vessel

The filling height of a sealed vessel is calculated using the following equation:

$$h = (p_2 - p_1) / (\rho g)$$

where

- h - height of the liquid column [m]
- p_2 - hydrostatic pressure [bar]
- p_1 - pressure of the enclosed gas in the vessel [bar]
- ρ - density of the fluid [kg/m³]
- g - gravitational acceleration [9.8066 m/s²]

3.4 Target parameter

Determining the submersible's depth.

3.5 Applicability

A standard or submersible pressure transmitter is mounted at a specific depth (zero level). The transmitter measures the pressure caused by the weight of the liquid column on top of it. The hydrostatic pressure at the measuring point is proportional to the water column height / actual depth of immersion.

3.6 Accuracy

The accuracy should be chosen according to the needs of the application. Standard accuracy of <0.5 % will give a possible error of maximum 5 mm per meter (500 mm per 100 meters, 2.5 m per 500 meters). This accuracy corresponds to a military GPS. Highest accuracy variants with <0.1% will be as accurate as max. 1 mm per one meter of level.

3.7 Increasing the accuracy

In measuring the hydrostatic level by pressure sensors, we have to be aware that the level measurement is influenced by several factors, e.g. the specific gravity of the medium and the medium temperature. The temperature also affects the specific gravity of the medium and it may not be stable. If the medium changes in its composition it will also change its specific gravity.

In flooded mines the ion concentration and the specific gravity may rise with depth. Therefore the hydrostatic pressure will show a higher reading, thus over-estimating the depth . If we do not detect changes in the composition of the medium, we can ignore this effect.

The specific gravity can also change due to varying temperature. If the temperature increases, the specific gravity of the medium will decrease and the apparent level will increase. The hydrostatic pressure measurement may not reflect this change in level accurately.

To increase the accuracy of the hydrostatic level measurement we have to compensate for the temperature effects and for the change of specific gravity of the medium.

3.8 Compensation

It is easy to compensate for the temperature effects of the medium, if we know how the density changes due to increasing or decreasing temperature, e.g. by using a standard table for the medium, indicating the specific gravity for each degree of temperature.

A simple additional temperature sensor within the pressure transmitter can provide the needed temperature measurement. If we know the temperature behavior of the medium and how it changes its specific gravity, we can easily compensate for these effects in the control system and correct the level calculation by using the proper specific gravity according to the standard table.

If the medium is changing its composition, a temperature measurement cannot provide sufficient data for the depth correction.

The specific gravity is calculated as follows:

$$\rho = (p_1 - p_2) / g(h_1 - h_2)$$

where

- ρ - density of the fluid [kg/m³]
- p_1 - hydrostatic pressure of the lower sensor [bar]
- p_2 - hydrostatic pressure of the upper sensor [bar]
- g - gravitational force or gravitational acceleration [m/s²]
- $h_1 - h_2$ - distance between the two sensors [m]

3.9 Response to disturbances

Submersible or standard pressure transmitters are positioned in direct contact with the medium at a measuring point below the surface level. Therefore they are not affected by any disturbance above the surface level such as foam, dust or water splashes.

This sensor is in direct contact with the medium. If it is allowed to dry on the pressure sensor, it can easily be cleaned or rinsing it with water as part of the scheduled maintenance.

3.10 Advantages of the method

- Simple installation and operation of submersible pressure transmitters or differential pressure meters.
- Proven and established, field-tested measuring principle, high reliability.
- Robust measuring process. It is not affected by any disturbance above the surface level such as foam, dust, vapour, etc.
- The measurement unaffected by many physical characteristics, e.g. conductivity, viscosity, etc.
- Unaffected by tank geometry
- Direct contact with the medium by flush diaphragm.

3.11 Disadvantages and limitations of the method

- Accurate measurement requires either media with constant density or continuous density measurement of the medium.
- Requires correct mounting. Faulty mounting position is a common source of inaccuracy in the level measurement. The height difference of the measuring points to the differential pressure transmitter lead to an additional hydrostatic pressure between the transmitter inputs.

3.12 Industrial solutions—Purchasable instruments

3.12.1 Types of hydrostatic level sensors

In hydrostatic level measurement, there are three main types of level sensors:

- Conventional pressure transmitters
- Process pressure transmitters
- and submersible pressure transmitters.

They are available in relative, absolute and differential pressure variants.

Conventional pressure transmitters (Figure 4) are the most commonly employed; their price/performance ratio is excellent. They are simple to install and operate, available with a range of accuracies up to < 0.1 %.



Figure 4. Conventional pressure transmitter with pressure port

Process pressure transmitters are primarily used in industrial applications with special demands on the measurement technology. Issues like communication via bus systems, scalability, integrated tank linearization, etc. ensure suitability for the industry. The extensive adjustability and high intelligence of these SMART pressure transmitters is also reflected in their higher price level, typically five to ten times the cost of a conventional pressure sensor.



Figure 5. Process pressure transmitter

Submersible pressure transmitters are frequently used to measure the water level in reservoirs, wells or other open water bodies, specifically in the water and waste-water industry. These pressure transmitters are designed to operate while continuously submerged in liquids. They mainly differ from conventional pressure sensors in their media resistance, pressure tightness, cable quality and ingress protection.

3.12.2 Process connection, membranes, cleaning

Conventional and process pressure transmitters can both be equipped with flush mounted diaphragms for use on fluids that have low viscosity, contain coarse grained particulates or can crystalize. The flush mounted diaphragm prevents plugging of the pressure transmitter's port to maintain accurate readings.



Figure 6. Flush mounted diaphragm

3.12.3 Differential pressure transmitters

Differential pressure transmitters offer the ability to measure and eliminate the effect of the gas phase in gas-tight sealed tanks. This ensures to display correctly the level of the liquid column inside the tank without the need of any additional compensation or additional sensors. The sophistication of this measurement technique is however reflected in the costs of both the instrument itself as well as the corresponding installation.

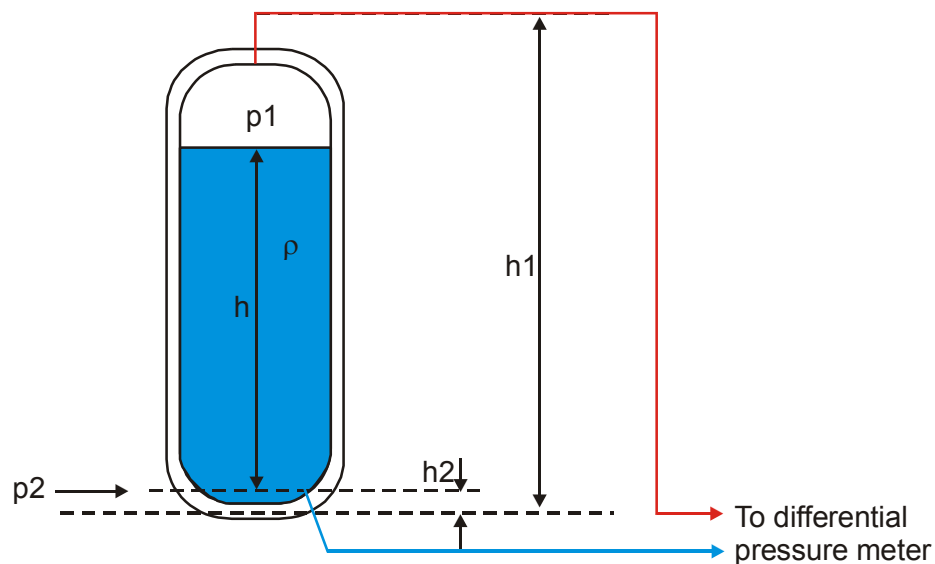


Figure 7. Level measurement by differential pressure transmitter

3.13 Purchasable instrument: Hydrostatic level meter WIKA S-11 pressure transmitter

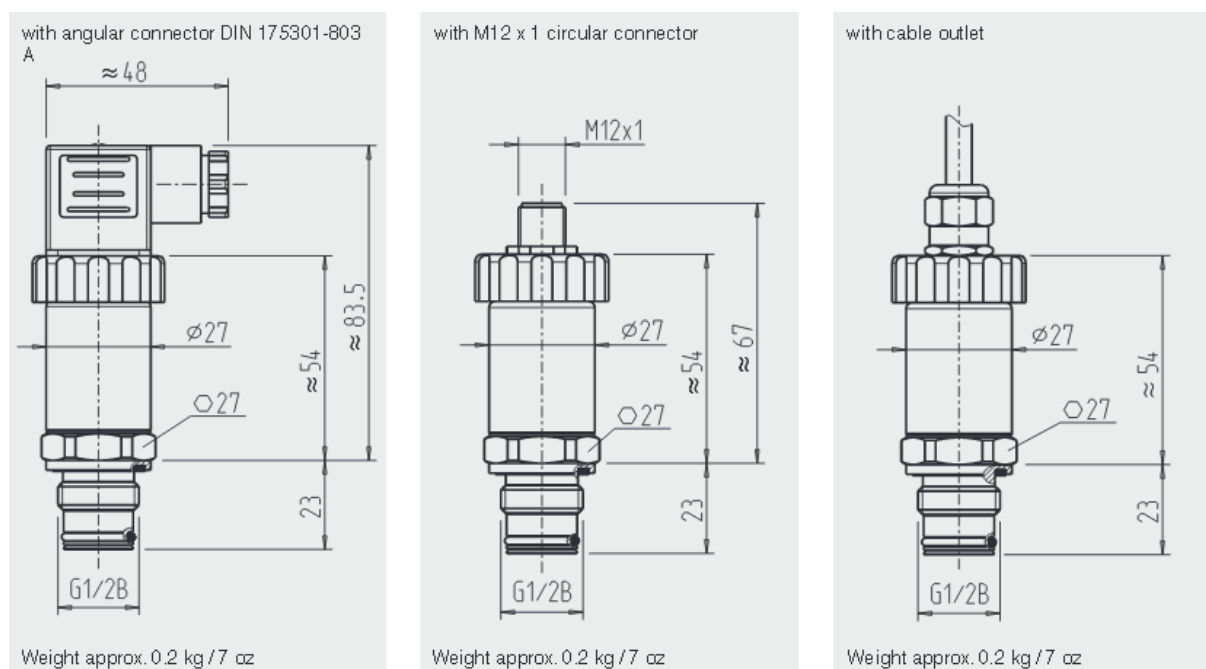
3.13.1 Specifications

- for general industrial applications
- operating in medium temperatures of up to 150 °C
- measuring range: 0...60 bar
- overpressure limit: 120 bar
- accuracy: $\leq \pm 0.5\%$ of span (standard), $\leq \pm 0.25\%$ of span (optional)
- operating temperature: -30...+100 °C without cooling (standard)
- process connection: G1/2 B flush, 0 to 600 bar

Output Signal Type	Required Power Supply
Current, 2 wire, 4-20 mA	DC 10-30V / 20 mA
Current, 3 wire, 0-20 mA	DC 10-30V / 20 mA
Voltage, 3 wire 0-5 V 0-10V	DC 10-30V / 1 mA DC 14-30V / 1mA

Table 2. WIKA S-11 output signal types

3.13.2 Dimensions



3.14 Conclusion

Hydrostatic level measurement is a simple and reliable method of measuring liquid level and the submarine's actual depth of immersion. Changes in specific gravity of the medium and the temperature effects the accuracy so compensation might be required.

Suggested/Suggested with comment (suggested in 2.2)/Unsuggested method

The hydrostatic level measurement method and available equipment can be used as in-situ measurement considering compromises respect with accuracy.

3.15 References

- [1] VDC Research Group, Inc. **What's driving the process level measurement & inventory tank gauging markets**
2011
- [2] WIKA brochure, **Fundamentals of Hydrostatic Level Measurement**
2014 April

4 PH MEASUREMENT

4.1 Theoretical Background

The pH electrode technology hasn't changed much in the past 50 years. With all the technological advancements of the last 30 to 40 years, pH electrode manufacturing remains as a sort of art. The special glass body of the electrode is blown to its configuration by glass blowers. The thickness of the glass determines its resistance and affects its output.

Accurate determination of pH is done by potentiometric method. The potentiometric electrochemical analytical method is based on the measurement of the potential of an electrode submerged into an electrolyte. A submerged electrode will change its potential depending on the physical properties of the medium. An electrode potential can always be determined only in the relation to a second electrode. It is necessary to form a "galvanic battery" with a reference electrode. Measured voltage between reference and pH electrodes gives a response proportional to the pH.

The simplest way to measure pH is to use combined electrodes. A combined pH measuring probe consists of two electrodes in one body. One of them is called the measuring electrode and the other one is the reference electrode. Both electrodes are introduced to the solution where we want to measure the pH.

Since free hydrogen ions are present in solution electrical potential will be generated between the measuring electrode and the reference one.

The electrical potential of the reference electrode is constant. It is originated by the contact with the reference fill solution. The reference electrode delivers this constant potential to the meter and the measuring electrode delivers a varying potential, which will vary linearly with the pH of the solution in a broad pH range.

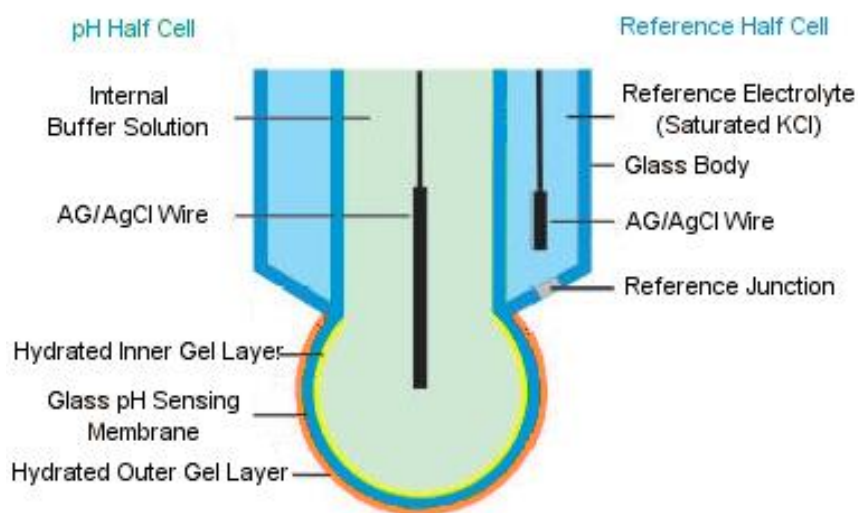


Figure 9. Combined glass pH electrode

The glass pH electrodes are specially formulated, high electrical resistance glass devices. The glass typically contains alkali metal ions. The reference electrode is put into a pH 6-7 Ag/AgCl based buffer solution. The membrane potential of the measuring electrode is determined by the ratio of $[H^+]$ concentration on each side. Inside the glass bulb the $[H^+]$ concentration is constant, so the external electrode will determine the $[H^+]$ concentration.

The emerging potential of a glass electrode can be calculated by the Nernst equation:

$$E = (RT/F) \ln [H_3O^+]$$

where

E - the probe potential in V

R - the gas constant, $8.314472 \text{ J mol}^{-1} \text{ K}^{-1}$

T - the temperature in K

F - the Faraday constant, the number of coulombs per mole of electrons:

$F = 9.64853399 \times 10^4 \text{ C mol}^{-1}$

$[H_3O^+]$ - the concentration of hydronium ions

The simplified Nernst equation at 25 °C:

$$E = 0.0591 \text{ pH}$$

In other words the electrode will produce 59 mV change for each 1.0 pH change, at 25 °C.

4.2 Measured parameter

The concentration of the $[H^+]$ ions. The electrode potential varies linearly with the pH of the solution in broad pH range.

4.3 Measuring method

Most accurate determination of pH is done by potentiometric method.

4.4 Aimed parameter

Determining acidic or alkaline environment.

4.5 Applicability

The voltage signal produced by the pH electrode is a very small signal with high output impedance. The high output impedance requires that it can only be interfaced to any electric equipment with significantly higher input impedance. The input impedance required is of the order of 10^{12} ohms. This is the reason why pH electrodes do not interface directly to any equipment.

4.5.1 Advantages of the method

- The method serves directly the pH log of concentration of $[H^+]$ ions.

4.5.2 Disadvantages of the method

- Requires special electrode handling.
- There are several adverse effects on the accuracy.
- Limited environmental conditions (temperature, pressure)
- Limited numbers of commercial types pH meters for high pressures. High quality, accurate sensors with good precision have mechanically sensitive glass electrodes.
- The pH sensor must be placed vertically or almost vertically.

4.6 Handling electrodes

The glass electrode is mechanically sensitive, it must be protected from any mechanical damage. Taking glass membranes out of service or when stored in dry condition their quality deteriorates within a year. For the correct operation the glass membrane of the electrodes must be swollen. This is achieved by the initial acid usage (0.1 mol/l KCl) activation (conditioning), and is maintained by storage in clean water.

4.7 Effects on the accuracy

Accurate pH measurement has been a long-standing problem due to different effects. There are several effects, which adversely affect the pH measurement process and the final result. For example, temperature changing has a number of significant effects on the measurement. Any variation of Temperature Coefficient effects on the material being measured by the sensor, whether it be calibration buffer or sample.

Further sub-classification is necessary for each of these categories in order to understand the mechanism and to determine the optimal action.

4.7.1 Real pH electrodes are not ideal

- Real pH electrodes have a temperature related drift from actual pH.
- Electrodes have offset error. An ideal electrode produces 0.0 mV when placed in a solution with a pH of 7.00 at 25 °C. A real electrode have different reading which varies from 0 mV.
- Slope error: the ideal mV/pH relation is a straight line with a slope factor of 0.592 V. Any variation from this ideal value is specified as the electrode's span error or slope error. It necessary to compensate the effect of slope error during the calibration procedure.

4.7.2 Effects of Temperature on pH measurements

- Temperature affects electrode slope, there is a variation in Nernst slope with temperature change.
- Calibrated Isothermal point: the isothermal intersection is not at the zero point (0 mV at pH 7) and not at the same point with constant or varying temperatures.
- The response time of the electrode varies with temperature.
- The glass membrane impedance varies with temperature.

4.7.3 Effects of concentration change on pH measurements

- The response time of the electrode varies with concentration change.

4.7.4 Effects of Liquid Temperature Coefficient Variation on the calibration buffer and the sample

Both the Temperature Coefficient Variation of the calibration buffer and the sample lead to inaccurate measured values.

When the temperature is above 25 °C the temperature compensation lowers high pH and raises low pH, resulting in values closer to neutral. Below 25 °C the temperature compensation raises high pH and lowers low pH resulting in values further away from neutral.

Temperature compensation must be used for pH accuracy. If the accuracy requirement is ± 0.1 pH, at a pH of 6 and a temperature of 45 °C, the error is small (0.06), well within the accuracy requirements. Further away from neutral, operating at pH 10 and 55 °C with the same ± 0.1 pH accuracy requirement, would give an error of 0.27 pH. Compensation should be used.

To reduce the potential errors, using water bath should perform instrument calibration and sample measurement at the same temperature, ideally. As the pH of solutions is temperature dependent, the measurement temperature should be recorded.

4.8 Industrial solutions—Purchasable instruments

4.8.1 Cylindrical, high pressure glass membrane pH electrode - IDRONAUT, Italy

Technical specifications:

Membrane type:	uranium glass membrane (500Mohm @ 20° C).
Null point:	7 pH.
Range:	1 .. 13 pH.
Drift:	0.05 pH/month.
Response time:	3 s.
Operating pressure:	600 bar.
Maximum pressure:	700 bar
Output connections:	shielded wire and LEMO plug.
Mounting:	through 12 mm hole with two 0-ring seals (Parker 2-12).
Weight:	35 gr. (including the hydrating cap).
Body:	titanium.

Note: complete with hydrating cap half-filled with
pH 7 Buffer Solution.

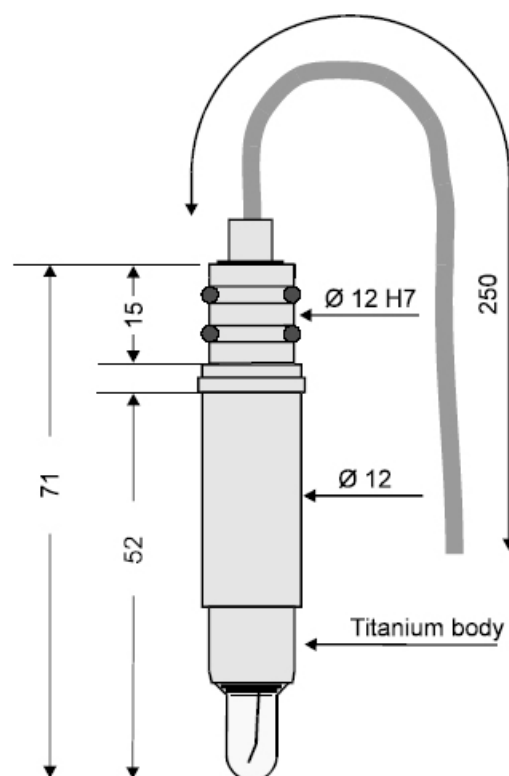


Figure 10. High pressure pH probe

This product is not available in OEM format.

4.8.2 Ocean Seven 305 Plus CTD - IDRONAUT, Italy

<i>Real-time and logging (CTD):</i>	8 Hz.
<i>Interfaces:</i>	RS232C (up to 200m), RS485 (up to 1 km), Telemetry (up to 2 km). Bluetooth® Class 1, SPP compliant range of over 100 m.
<i>Wireless Data memory:</i>	2 Gbytes.
<i>A/D converter:</i>	16-bit SAR.
<i>Supply Voltage (Battery):</i>	3 x size "AA" Alkaline 1.5V battery assembled in a single pack 4.5V. 1 x size "AA" Lithium non rechargeable battery, 3.6V, 2.4Ah. 7.0 - 18 V DC.
<i>RS232C and USB cable</i>	Running: 70 mA at 3.6V; Sleep: 0.008 mA at 3.6VDC.
<i>Telemetry</i>	PTP - proprietary byte oriented binary and plain message protocol.
<i>Supply Current:</i>	Friendly menu driven user interface.
<i>Communication protocol:</i>	
<i>Operator interface:</i>	

Table 3. Electric specifications of Ocean Seven 305 Plus CTD

	1000 dbar	2000 dbar	7000 dbar
<i>Dimensions: diameter</i>	43 mm	75 mm	48 mm
<i>total length (including hanging rod)</i>	715 mm	660 mm	660 mm
<i>weight</i>			
<i>in air</i>	1.3 kg	2.6 kg	2.1 kg
<i>in water</i>	0.7 kg	0.6 kg	1.3 kg
<i>material</i>	AISI316L/POM	White POM	Titanium



Table 4. Physical characteristics of Ocean Seven 305 Plus CTD

Parameter	Range		Accuracy		Resolution		Time Constant
Pressure	0.. 2000	dbar ^(*)	0.05	%full scale	0.0015	%full scale	50 ms
Temperature	-3.. +50	°C	0.005	°C	0.001	°C	50 ms
Conductivity							
Salt water	0.. 70	mS/cm	0.007	mS/cm	0.001	mS/cm	50 ms (at 1 m/s flow rate)
Fresh water	0.7000	uS/cm	5	uS/cm	0.1	uS/cm	50 ms (at 1 m/s flow rate)
Oxygen	0.. 50	ppm	0.1	ppm	0.01	ppm	3s (from nitrogen to air)
	0.. 500	% sat.	1	% sat.	0.1	%sat.	3s (from nitrogen to air)
pH	0.. 14	pH	0.01	pH	0.001	pH	3s (**)
Redox	+/-1000	mV	:	mV	0.1	mV	3s

^{*}Other standard pressure transducers : 10, 40, 100, 200, 500, 1000, 4000, 7000 dbar ranges.

^{**}Differential pH preamplifier, $10^{13} \div 10^{14}$ ohm in

Table 5. Sensor specifications of Ocean Seven 305 Plus CTDput impedance.

4.8.3 Glass pH sensor - Corr Instruments, USA

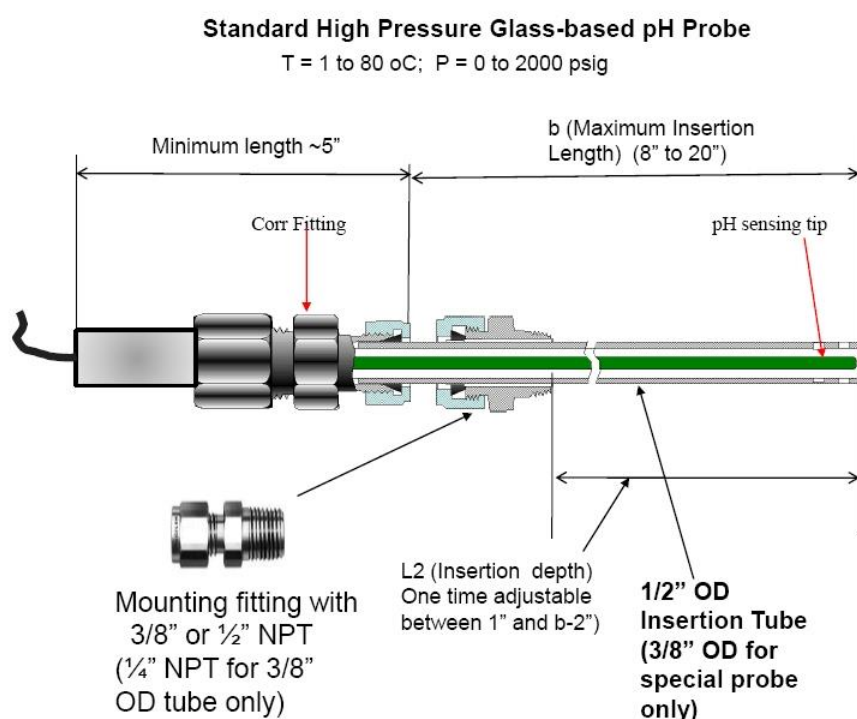


Figure 11. High pressure pH probe

The Lo (Overall Length) value for the shortest probe would be about 10" after the factory reduce the b (Maximum Insertion Length) value to about 5"

Electrical output: BNC, standard.

This probe requires an additional reference electrode. Full warranty is only 3 months because the glass sensing membrane of the probe can be easily broken if it is dropped to hard floor. Partial warranty is 1 year. The probe's life should be good for 2 years, but this life depends on the medium in which it is used.

4.8.4 Reference electrode - Corr Instruments, USA

High Temperature and High Pressure Reference Probes

Internal Probe: $b_2 < 6"$ (recommended for **long-term** use at $T < 100^\circ\text{C}$ and for **short-term** use at $T = 100$ to 310°C)

External Probe: $b_2 > 12"$ (recommended for **long-term** use at T up to 310°C)

P = Water saturation pressure to **2000 psig** (or higher for certain models)

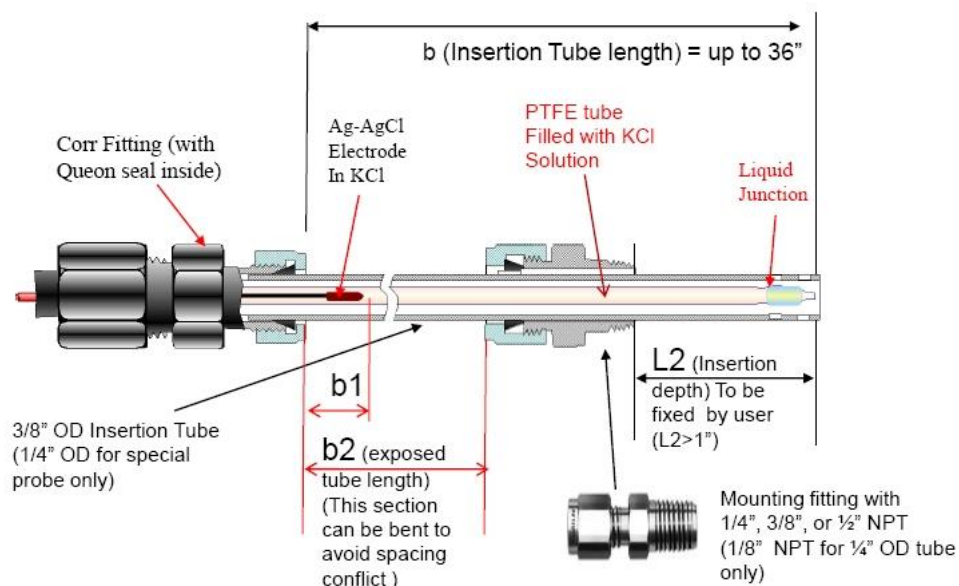


Figure 12. High pressure reference electrode

4.8.5 Analog pH Meter Kit - DFRobot

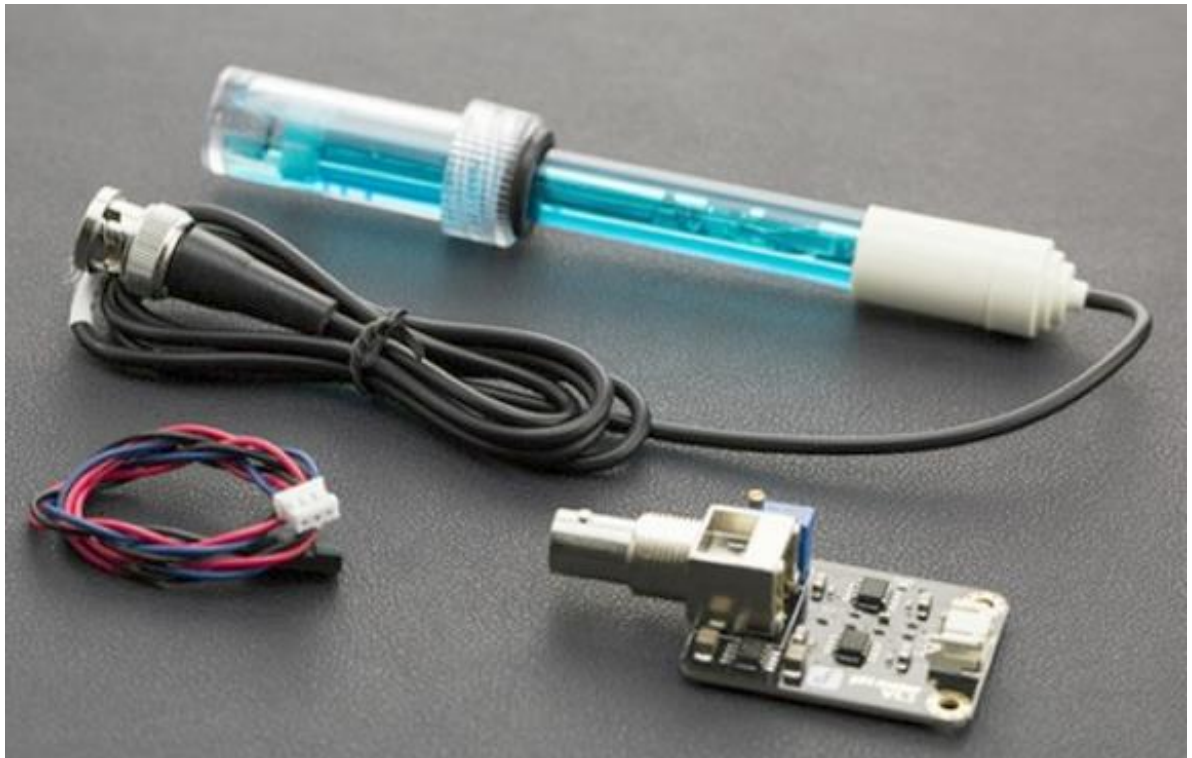


Figure 13. Analog pH meter kit [6]

Specifications

- Module Power : 5.00V
- Module Size : 43 x 32mm(1.69x1.26")
- Measuring Range :0 - 14PH
- Measuring Temperature: 0 – 60 °C
- Accuracy : $\pm 0.1\text{pH}$ (25°C)
- Response Time : $\leq 1\text{min}$
- pH Sensor with BNC Connector
- pH2.0 Interface (3 foot patch)
- Gain Adjustment Potentiometer
- Power Indicator LED

4.9 Case Study

The Research Institute of Applied Earth Sciences developed a small pH interface for a national competition project of a freshwater quality monitoring system. Five devices were manufactured, of which one device is continuously operating near the university at Sajo river.

4.10 Conclusion

The measurement method is simple potentiometry applied with very high input impedance interface amplifier. The method measures pH directly: log of concentration of $[H^+]$ ions. There are limitations in applications especially connected to the environmental conditions (temperature, pressure). Applied sensors requires careful electrode handling and systematic cleaning and calibrations.

Suggested/Suggested with comment (suggested in 2.2)/Unsuggested method

The method and available equipment can be used as in-situ measurement considering compromises respect with accuracy.

4.11 References

- [1] H. Galster: **pH Measurement: Fundamentals, Methods, Applications, Instrumentation**
VCH Publishers Inc., 1991, p21. F.
- [2] **J. J. Barron C. Ashton, L. Geary: The Effects of Temperature on pH Measurement**
- [3] E. Pungor, K. Toth: **Ion-Selective Sensors**
- [4] P Franco, D. Finke, P. Hail: **Improvements in pH Measurement**
- [5] Izquierdo-Ruiz, L.J.Bonales, V.Munoz-Iglesias, O.Prieto-Ballesteros: **Measurements of pH under extreme conditions**
- [6] https://www.dfrobot.com/index.php?route=product/product&keyword=pH&product_id=1110#.V3OKXrVpzTr

5 CONDUCTIVITY MEASUREMENT

5.1 Definition of Conductivity

Conductivity (Electrical Conductivity) is the ability of a material to conduct electric current.

5.2 Measured parameter

Measured parameter is the electrical conductivity (G or EC) the inverse of the resistance (R). Since the object of the measurement is any (liquid) material, the measured value is a specific value, with respect to unit length of the particular material.

5.3 Target parameter

Electrical conductivity is a good indicator of Total Dissolved Solids (TDS). Total dissolved solids (TDS) is a measure of the combined content of all inorganic and organic substances contained in a liquid in molecular, ionized or micro-granular suspended form.

5.4 Theoretical Background

The principle by which instruments measure conductivity is simple—two plates are placed in the sample, a potential is applied across the plates (AC needed), and the current that passes through the solution is measured. Electrical Conductivity is determined from the voltage and current values according to Ohm's law.

$$EC = G = 1/R = I/U$$

where

- EC* or *G* - the Electrical Conductivity, measured in Siemens (S)
- R* - the resistance (impedance) of the actually tested material, (ohms, Ω)
- U* - the applied excitation voltage between probes, (V)
- I* - the resultant electrical current (A).

Since the charge on ions in solution facilitates the conductance of electrical current, the conductivity of a solution is proportional to its ion concentration. However, in some situations conductivity may not correlate directly to concentration: the relationship between conductivity and ion concentration is not linear. Different ionic interactions can alter the linear relationship between conductivity and concentration in some highly concentrated solutions. For example the graph is linear for sodium chloride solution, but not for highly concentrated sulphuric acid.

5.5 Measuring method

Since the object of the measurement is any (liquid) material, the measured value is a specific value, with respect to unit length of the particular material.

There are two main methods to measure EC:

- by inductive loops
- with AC excited electrodes

5.5.1 Inductive loops

Inductive conductivity sensors generate a current in the medium using a primary coil, and measure the current with a secondary coil.

Due to the non-contact measurement principle, inductive conductivity sensors lack the problems connected with electrode sensors, like uncontrollable contamination and polarization effects. A disadvantage of practical inductive conductivity sensors is the reduced sensitivity and the relatively high initial measurement limit (approx. 100 $\mu\text{S}/\text{cm}$).

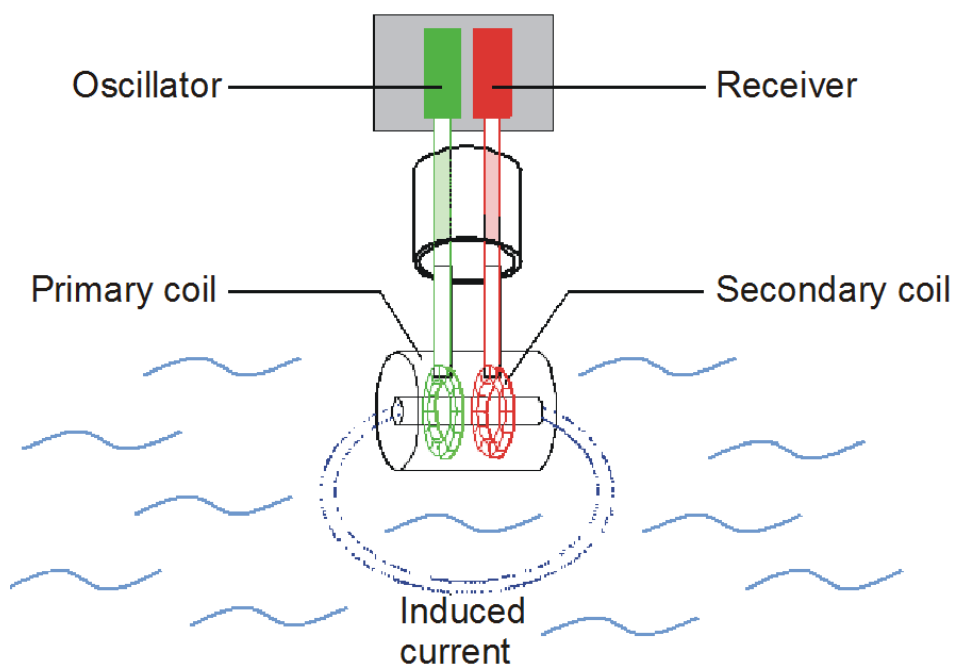


Figure 14. Inductive EC measurement

5.5.2 Measurement by AC excited electrodes

Generally the EC is measured by two electrodes (plates), which are fixed at a determined distance. Geometry of electrode plates may vary. The distance between the electrodes / area of electrode plates is known as the K constant of the measuring cell. An electrode with $K=1$ has 1 cm distance between plates with 1 cm^2 squared area of both plates.

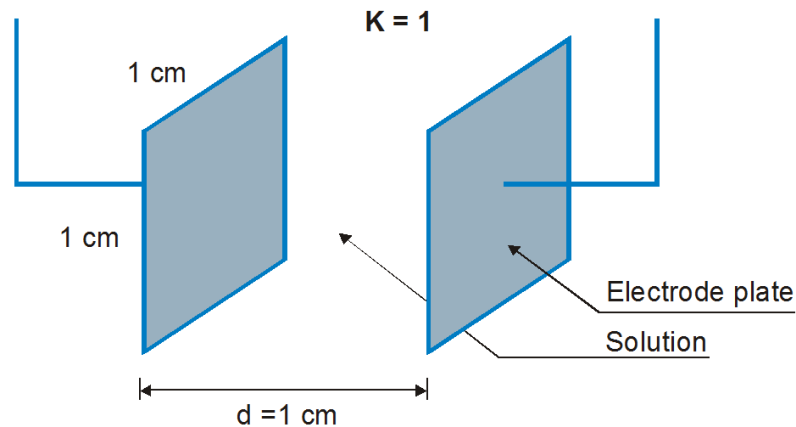


Figure 15. EC electrodes with K=1

Shorter distance between the plates results in smaller K value and an electrode with smaller K factor will amplify the incoming signal and therefore gives better (higher) readings (and narrower measuring span). The final measured value is the specific EC:

$$EC = \text{distance between the electrodes (cm)} / \text{area of electrode plates (cm}^2\text{)} \cdot \text{conductivity}$$

Since the distance between measuring plates appears in the equation, the measuring unit of the specific conductivity is S/cm, mS/cm or $\mu\text{S/cm}$.

The conductivity is calculated by the measuring electronics. The measured sample is listed as a determining factor for the gain of the signal-processing instrument. Therefore the electronics converts the conductivity into millivolt readings.

5.6 Electronic interface

The conversion between conductance and voltage output requires special interface electronics, which is based on quite a simple measuring method.

Since the measured sample becomes a passive electrical component of the interface it needs only small amounts of electrical power.

On the front of the interface there is an AC sine (or square) wave generator – sine oscillator - as measuring signal source, which is connected to an amplitude stabilizer.

DC excitation of the plates is not suitable because it passes DC current through the probes and the medium. We cannot measure conductivity of solutions with DC current because polarized electrodes attract or repel positive and negative ions. The presence of the positive and negative ions means that the solution would conduct electricity and we would get a constantly changing reading that is useless. We overcome this by using an AC signal. If the frequency of the oscillator is high enough (e.g. 10 kHz) charge carriers do not have time to move before they are pulled in the opposite direction.

The sine or square signal – after permanent attenuation - is passed to the next stage, which is a simple amplifier. Its gain is varied by the measured conductivity. The output is a different amplitude AC wave proportional to the conductivity and resistivity according to Ohm's law.

The final stage of the circuit is a precision rectifier, which forms a constant DC level from the rectified AC wave and feed that to the DAQ system.

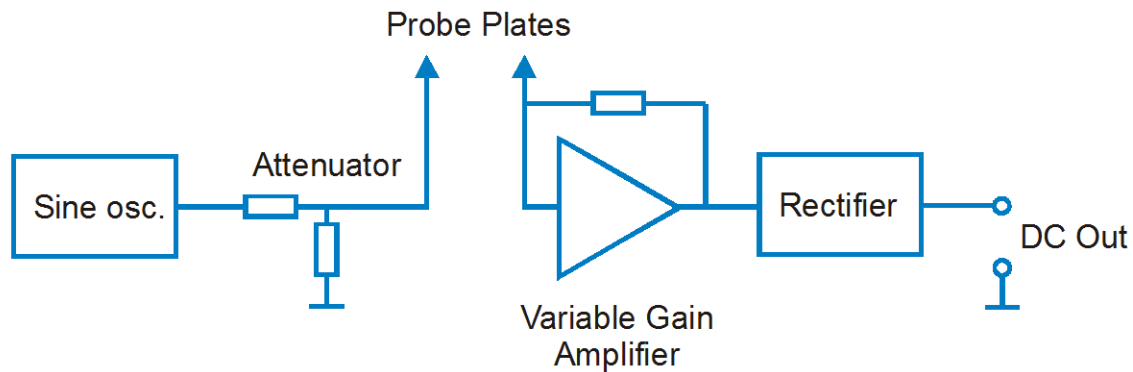


Figure 16. Analog Electrical Conductivity Meter block scheme

5.7 Applicability

Measuring by AC excited plates is suitable for applications in flooded metal mines. The EC gives information about the changing dissolved ions in the water and about spatial changes of Total Dissolved Solids.

5.8 Advantages of the method

- This method and the electronics is quite simple and supplies direct information about total ion content.
- No special orientation needed for the EC probes.
- Low power consumption: ≈ 10 mA at 5 V

5.9 Disadvantages of the method

- Mechanical problems with commercial EC probes at high pressure.
- Not too difficult, but special electronics needed.
- Industrial equipment is too robust and has large dimensions for an underwater application.
- Labour equipment is consisted of usually hand-held gadgets with LCD, without electric signal output, or large 230V AC powered desktop devices.
- Temperature will affect the conductivity; compensation is needed.
- Long term problems with uncontrollable contamination and polarization effects in case of multiple days of continuous measurement. These effects can influence the repeatability.

5.10 Industrial solutions—Purchasable instruments

5.10.1 EC sensor - Corrinstruments, USA

High Pressure Conductivity Probe (Cell Constant >3 1/cm)

(0 To 305 oC; 0 to 2000 psi)
(Pt-(2)-1*10mm-30"-T-Tube375-NPT375A-C276)

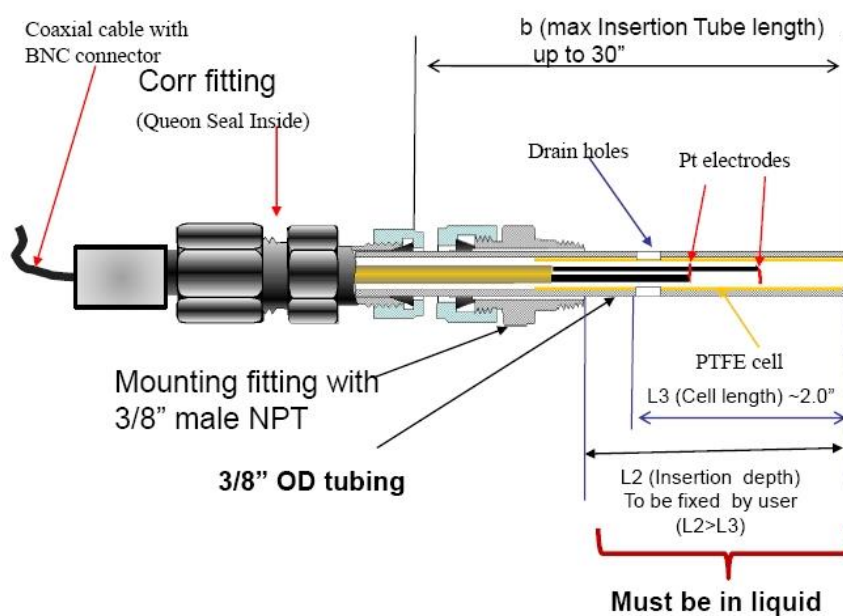


Figure 17. High Pressure EC probe

We cannot determine the exact K (Cell Constant) value now; it can only be known after the factory have made the probe. It will be approximately 1 cm^{-1} . It should be good for solutions with average EC 3 - 4 mS/cm.

5.10.2 Analog Electrical Conductivity Meter with Temperature Compensation – DFR0300 - DFRobot



Figure 18. Analog Electrical Conductivity Meter with Temperature Compensation – DFR0300

Specification

- Operating Voltage: +5.00 V
- PCB Size: 45 × 32mm (1.77x1.26")
- Measuring Range: 1ms/cm -- 20ms/cm
- Operating Temperature: 5 - 40 °C
- Accuracy: < ±5% F.S (using Arduino 10 bits ADC)
- PH2.0 Interface (3-pin SMD)
- Conductivity Electrode (Electrode Constant K = 1, BNC connector)
- Cable Length of the Electrode: about 60 cmDS18B20 Temperature Sensor (Waterproof)
- Power Indicator

5.11 Case Study

The Research Institute of Applied Earth Sciences developed a small EC interface for a national competition project of a freshwater quality monitoring system. Five devices were manufactured; one device is continuously operating near the university at Sajó river (Hungary).

5.12 Conclusion

Simple EC measurement method is suitable for applications in the underground flooded mines. The EC gives information about the changing dissolved ions in the water and about spatial changes of Total Dissolved Solids.

Suggested/Suggested with comment (suggested in 2.2)/Unsuggested method

The method and available equipment can be used as in-situ measurement considering compromises respect with stability and accuracy.

5.13 References

- [1] J.. J. Barron, C. Ashton, **The Effect of Temperature on Conductivity Measurement**
- [2] Karlsruhe Institute of Technology, **Inductive conductivity measurement in industrial metrology**
- [3] DfRobot.com: **Analog EC Meter SKUDFR0300**
- [4] **Mosaic Conductivity Sensing Wildcard**
- [5] US Patent: **High pressure electrical conductivity probe**, US 4507521 A
- [6] <http://www.octiva.net/projects/ppm/>: **EC/TDS/PPM Meter On Limited Budget**

6 ISE MEASUREMENT

6.1 Basic theory of ISE measurements

Ion-Selective Electrodes (ISEs) are relatively simple and inexpensive analytical devices. They have been widely used for more than thirty years.

These electrodes are used in a wide variety of applications for determining the concentrations of various ions in aqueous solutions.

The most well-known and characteristic member of this group is the pH electrode and can represent the basic principles of ISEs.

Like the pH electrode the most essential component of an Ion-Selective Electrode is a special, sensitive glass membrane, which permits the passage of specified ions of the test solution.

The potential difference developed across the membrane is directly proportional to the Logarithm of the ionic concentration of the external solution.

In order to measure the electrode potential developed at the ion-selective membrane the ISE electrode must be immersed in the test solution together with a separate reference source and these two probes must be connected via a millivolt measuring system.

The relationship between the ionic concentration (activity) and the electrode potential is given by the Nernst equation:

$$E = E^{\circ} + (2.303 RT/nF) \text{Log}(A)$$

where

E - the total potential (in mV) developed between the sensing and reference electrodes.

E° - is a constant which is characteristic of the particular ISE/reference pair.

2.303 - the conversion factor from natural to base 10 logarithm.

R - the Gas Constant (8.314 J/K/mol).

T - the temperature (K).

n - the charge on the ion (with sign).

F - the Faraday Constant (96,500 coulombs).

$\text{Log}(A)$ - the logarithm of the measured ion content.

The basic working principles are exactly the same for both ISE and pH electrodes.

As we can see the $2.303 RT/nF$ is the slope of the line. This is an important diagnostic parameter of the electrode - generally the slope is lower as the electrode becomes old or contaminated. The lower the slope the higher are the errors on the sample measurements.

6.2 Differences Between pH and Other Ion-Selective Electrodes

- The pH membrane is a H^+ ion-specific membrane. In contrast, ISE membranes are not entirely ion-specific and can permit the passage for other ions, which may be present in the test solution. This causes ionic interference.
- Most ISEs will only work effectively over a narrow pH range.
- ISEs have smaller linear range and higher detection limit (narrower range) than the pH electrode. Generally we can calibrate them at the region between 10^5 to 10^7 moles/l, and only few probes can be used below this range. For low concentration samples, it may be necessary to construct an individual calibration graph because this range is not linear also.
- The calculation of ionic concentration is strongly dependent on a precise measurement of the potential difference. Only 1 mV inaccuracy can cause significant difference from the true value.
- Variation of ion concentration affects the result of the ISE measurement.

6.3 Types of Ion-Selective Electrodes

Manufacturers give very few details about the internal construction of the electrode or composition of the ion-selective membranes. These are the most important factors, which ensure the performance of the electrode, and are kept as closely guarded trade secrets.

Ion selective electrodes come in various shapes and sizes, nevertheless, there are certain features that are common to all. All consist of about a pen size cylindrical tube, generally made of a plastic material. The ion-selective membrane is fixed at one end so that the external solution can only come into contact with the outer surface. The other end is fitted with a low noise cable or gold plated pin for connection to the millivolt-measuring device. In some cases the internal connections are completed by a liquid or gel electrolyte, but there are all-solid-state ion-selective systems (ISFETs).

Ion-selective membranes are currently only available for a limited number of commonly occurring ionic species.

For measuring cations and anions the most common are:

Cations: Ammonium (NH_4^+), Barium (Ba^{++}), Calcium (Ca^{++}), Cadmium (Cd^{++}), Copper (Cu^{++}), Lead (Pb^{++}), Mercury (Hg^{++}), Potassium (K^+), Sodium (Na^+), Silver (Ag^+).

Anions: Bromide (Br^-), Chloride (Cl^-), Cyanide (CN^-), Fluoride (F^-), Iodide (I^-), Nitrate (NO_3^-), Nitrite (NO_2^-), Perchlorate (ClO_4^-), Sulphide (S^-), Thiocyanate (SCN^-).

There are two main types of membrane material. The first type is based on a solid crystal matrix, either a single crystal or a polycrystalline compressed pellet, and the second type on a plastic or rubber film impregnated with a complex organic molecule.

The manner in which these different membranes select and transport the particular ions is highly variable and in many cases highly complex.

a) Impregnated-PVC-Membrane Electrodes

This type - e.g. Potassium, K^+ - electrode was one of the earliest developed and simplest examples of the first type. The membrane is usually in the form of a thin disc of PVC

Unfortunately this type is not 100% selective and can also conduct small numbers of sodium (Na^+) and ammonium (NH_4^+) ions, thus these can cause errors in the potassium determination if they are present in high concentrations.

b) Crystal-Membrane Electrodes

The typical example of the second type is the Fluoride electrode.

The bulk resistivity of the crystal is reduced. It is 100% selective for F^- ions and is only interfered with by OH^- but this interference can be eliminated by adding a pH buffer to the samples to keep the pH in the range between 4 to 8 and hence ensure a low OH^- concentration in the solutions.

6.4 Handling Ion Selective Electrodes

It is most important that care should be taken to avoid damaging the membrane surface. The glass electrode is mechanically sensitive, it must be protected from any mechanical damage. Like the pH electrodes, for the correct operation the glass membrane of the electrodes must be swollen. An initial acid bath (in 0.1 mol/l KCl solution) and storage in clean water help to keep good condition of the electrode.

Washing with alcohol and/or gently polishing with fine emery paper can regenerate crystal membranes. After the regeneration, they may require soaking in a concentrated standard solution for hours before a stable reading can be re-established.

6.5 Reference electrodes

In order to measure the change in potential difference across the ion-selective membrane as the ionic concentration changes, it is necessary to include in the circuit a stable reference voltage. The most common and simplest reference system is the Ag/AgCl single junction reference electrode.

The problem with reference electrodes is that it is necessary to develop a stable voltage. To ensure this, advanced types of reference electrodes were developed e.g. Double Junction Reference Electrodes, Liquid Junction Potentials, etc.

6.6 Combination Electrodes

Combination Electrodes produce simple, compact units for immersing in the test solution and have the added advantage that the two cells are in a common housing.

The membranes and internal construction of ISEs are generally far more expensive than a simple or combined pH sensors. It is much more cost-effective to have separate units in which the reference probe can be replaced independently from the ISE.

6.7 Advantages

- Ion-Selective Electrodes are relatively inexpensive and simple to use and have a wide range of applications.
- Measuring with IS techniques, we can detect both positive and negative ions.
- The plastic-bodied all-solid-state or gel-filled models are very robust. They are ideal for use in either field or laboratory environments.
- where interfering ions are not a problem, they can be used very rapidly and easily.
- With careful use, frequent calibration, and an awareness of the limitations, they can achieve accuracy and precision levels of ± 2 or 3% for some ions and thus compare favourably with analytical techniques, which require far more complex and expensive instrumentation.
- They are unaffected by turbidity.
- ISEs can be used in aqueous solutions over a wide temperature range, up to 80 °C.

6.8 Disadvantages

- High concentrations of measured solutions cause a problem.
- Most ISEs will only work effectively over a narrow pH range.
- ISE membranes have cross sensitivity: they are not entirely ion-specific and can permit the passage of other types of ions also.
- Requires careful handling, use, cleaning, regeneration and frequent calibration.
- No high pressure product or application exists. All of products can operate only below 5-6 bars.

6.9 Industrial solutions—Purchasable instruments

No high pressure product and application.

A variable gain pH amplifier with reference electrode input can be suitable for ISE applications.

6.10 Case Study

The Research Institute of Applied Earth Sciences developed a small ISE interface for a national competition project of a freshwater quality monitoring system. Ten devices were manufactured; one device is continuously operating near the university at Sajo river.

6.11 Conclusion

The measurement method is potentiometry applied with high input impedance interface amplifier. The method measures concentration of selected ions directly. There are limitations in applications especially the environmental conditions (temperature, pressure). Applied sensors require careful electrode handling and systematic calibrations.

Suggested/Suggested with comment (suggested in 2.2)/**Unsuggested method**

The method and available equipment can be used as in-situ measuring method considering compromises respect with accuracy.

6.12 References

- [1] A. W. Biel, **Introduction to Ion-selective Measurement**
HACH Brochure
- [2] Chris C Rundle, **A Beginners Guide to Ion-Selective Electrode Measurements**
Nico2000 Ltd
- [3] E. Pungor, K. Toth, **Ion-Selective Sensors**

7 SPONTANEOUS POTENTIAL, SELF POTENTIAL

7.1 Theoretical Background

Spontaneous potential (SP) is the naturally occurring electrical potential of the earth resulting from geologic, geochemical, and hydrologic interactions which cause electric potentials to exist in the earth in the vicinity of the measurement point. The SP method has been employed in the search for minerals. Since spontaneous potentials are usually caused by charge separation in clay, they are often measured down boreholes for formation evaluation in the oil and gas industry, and they can also be measured along the Earth's surface for mineral exploration or groundwater investigation.

Spontaneous potential is also called "self potential" and it originates from naturally occurring electric potential difference in the Earth. It can be measured by an electrode pair, and the result is relative to a fixed reference electrode.

7.2 Measured parameter

Measured parameters are potential differences. These potentials are measured in millivolts relative to a "survey base" or reference electrode, where the potential is arbitrarily assigned to be zero volts. Amplitudes of SP values in mineralized areas range from a few millivolts to one or more volts. The potentials are always negative above a mineralized body relative to a point outside the mineralization.

The basic equipment required is simple, consisting of a pair of electrodes connected by wire to high input impedance millivolt meter capable of a reading resolution of 100 μ V.

7.3 Target parameters

Anomalous surface potentials are commonly measured in the vicinity of pyrite (marcasite), chalcopyrite, pyrrhotite, sphalerite, and graphite.

7.4 Limitations

There are two restrictions on the electrodes and voltmeter which are most important. They are:

- no spurious potentials can be introduced by the measurement technique,
- the reference or base electrode must be placed outside the system, above the wet layer, and out of any reducing environment such as a bog or swamp.

7.5 Components and types of Self Potential

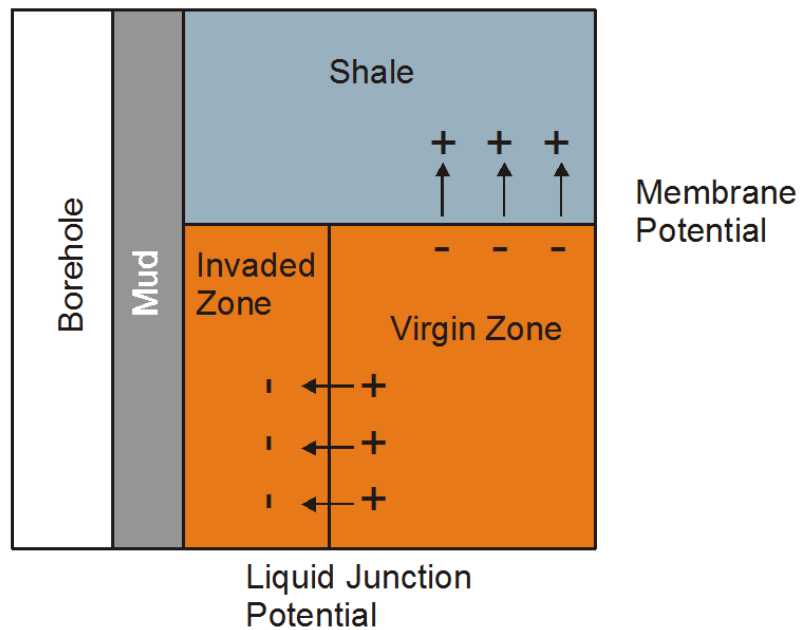


Figure 19. Potential between solid layers

The "Electrochemical Potential" (EC) is the sum of Liquid Junction Potential or Diffusion Potential (EJ), and Membrane Potential (EM).

The "Liquid Junction potential" is established at the direct contact of the mud filtrate and formation water at the edge of the invaded formation.

$$E_J = K_1 \log_{10}(a_w/a_{mf})$$

where

K_1 - 11.6 mV at 25 °C

a_w - formation water ionic activity

a_{mf} - mud filtrate ionic activity

Membrane Potential develops when two electrolytes of different ionic concentrations, such as mud and formation water, are separated by shale.

$$EM = K_2 \log_{10}(a_w/a_{mf})$$

where

$K_2 = 2.3 RT/F$, where:

R - ideal gas constant

T - absolute temperature in kelvins

F - Faraday constant

a_w - formation water ionic activity

a_{mf} - mud filtrate ionic activity

The total electrochemical potential is thus summarized as

$$EC = EM + EJ = K \log_{10}(a_w/a_{mf})$$

7.6 Applicability in water or any aqueous solutions of ion compounds

The same electrodes are dipped into any liquid - whether they are made of metal, precious metal (platinum) or graphite – named "first kind" conductors (metals). "Second kind" conductors are aqueous solutions of ion compounds. When a conductor of a first kind submerges into a second kind conductor, they form an electrode together.

Without power coupling of the electrodes, a chemical change occurs at the interface between the liquid and solid, the electrons can travel from the metal into the electrolytes (and vice versa). When ions form or dissolve, the ion charge number changes.

At the contact surface of the electrolytic solution and the immersed metal an equilibrium state is achieved after a certain time. A potential difference appears between the solution and the metal. This potential difference is the electrode potential.

Two pieces of metal or carbon electrodes are almost the same. However:

- Due to manufacturing, their sizes are different
- Due to the difference between the positions they occupy in the solution, they also have different environment (the ion concentrations there).

Thus the potential of one would be a little larger than the other. But these potentials would be formed with the same direction.

The change in electrical potential follows the direction of the change of ion concentration in the liquid, where higher concentration changes results in greater voltages. Therefore, if we submerge a pair of electrodes to greater depths, we would see that larger voltages would be obtained.

This measuring method would give information about the change of concentration (direction) only.

There would be one more problem: the question of the extent of electrode potentials.

The absolute value of the electrode potential cannot be determined. In practice a standard electrode potential was arbitrarily chosen to be zero, and the other electrode potential is measured by comparison. The Standard Hydrogen Electrode (SHE) was chosen for basis of measurement.

The design of the SHE is quite difficult. It can only be possible to create under laboratory conditions: it is a compound electrode, wherein the pressure of a hydrogen flow is 0.1 MPa, which is in contact with 1 mol / dm³ H₃O⁺ ion concentration solution at 25 °C. Finally a platinum electrode submerges into this solution as electric junction.

The processes taking place in electrodes results in interconversion between chemical energy and electric energy.

Electrode processes include:

- Formation or neutralization of cations at the anode, for example. $\text{Cu} \leftrightarrow \text{Cu}^{2+} + 2\text{e}^-$
- Formation or neutralization of anions on the cathode $4\text{OH}^- \leftrightarrow \text{O}_2 + \text{H}_2\text{O} + 4\text{e}^-$
- Changes in charge of ions on both electrodes: $\text{Fe}^{2+} \leftrightarrow \text{Fe}^{3+} + \text{e}^-$

The process is in equilibrium after a certain time, when the same number of ions is generated and broken up per time unit.

Since the oxidation and reduction occurs at the same time the name of this type of reaction is redox reaction.

The effect of oxidation or reduction of water can be determined more efficiently by measuring ORP (Oxidation-Reduction Potential).

Since the charge of ions in solutions facilitates the conduction of electrical current, the conductivity of a solution is almost always proportional to ion concentration. The relationship between conductivity and ion concentration is linear if the concentration is quite low.

Therefore the Electric Conductivity (EC) measurement is the method, which can be recommended to get any information of aqueous solutions of ion compounds.

Classic SP (Spontaneous Potential, Self-potential) measurements would not work if submerged into any aqueous solutions.

7.7 Case Study

We performed SP test measurements of the mineral lake of Rudabánya, which has high concentration of ions. The electric conductivity of the water is 3-4 mS/cm.

The test equipment was a DIAPIR-18 SP measurement device.

Measuring the soil SP provided average values and by changing the electrode direction (swapping them) the polarity of the measured electric potential was altered.

Measuring in the water as the instrument was lowered deeper, larger voltages are obtained. By pulling the electrode pair back the voltage decreased. Change of direction in the water during the measurement was not observed.

The value of electric potential depended on the measuring depth e.g. the ion concentration only.

Since none of the electrodes were Standard Hydrogen Electrode (SHE), the measured voltage values were inadequate. Therefore more information on the ion concentrations could not be established.

7.8 Advantages of the method

Self-Potential measurement is a very simple, passive analogue measuring method. It requires only two pieces of metal electrodes (per orientation) and a high input impedance amplifier. Observed potential values are in mV ranges.

7.9 Disadvantages of the method

Self-Potential measurement works only in solids e.g. soil, boreholes, earth surface, etc. The reference or base electrode must be placed outside the system, above the water table, and not in a reducing environment such as a bog or swamp.

In the UNEXMIN application electrodes should touch the wall and be insulated from the water.

7.10 Conclusion

Logging the SP is useful in detecting permeable beds and to estimate formation water salinity and formation clay content, identifying the path of groundwater flow in the subsurface, or seepage from an earthen dam. However, classic SP measurements would not work with both electrodes submerged into any aqueous solutions.

The Electric Conductivity (EC) measurement is better method, which can be recommended to get any information of aqueous solutions of ion compounds, e.g. water total salinity.

Suggested/Suggested with comment *Unsuggested method*

Classic SP (Spontaneous Potential, Self-potential) measurements is not recommended to use under water.

7.11 References

- [1] C. E. Corry, G. T. DeMouly, M. T. Gerety, 1980 **Field Procedure Manual For Self-Potential Surveys** Zonge Engineering & Research Organization, Tucson, Arizona
- [2] Corwin, R. F., 1990, **The self-potential method for environmental and engineering applications** Ward, S. H., editor, Geotechnical and Environmental Geophysics, Volume I: Review and Tutorial, Society of Exploration Geophysicists, Tulsa, OK
- [3] M.Gondouin, M.P.Tixier, G.L.Simard, Journal of Petroleum Technology, February 1957, **An Experimental Study on the Influence of the Chemical Composition of Electrolytes on the SP curve**
- [4] Guyod, H., Oil Weekly, 1944, **Electrical Potentials in Bore Holes**
- [5] Pirson, S.J., The Oil and Gas Journal, 1947, **A Study of the SP Curve**

8 NATURAL GAMMA RAY MEASUREMENTS

8.1 Theoretical Background

Natural gamma ray surveys can be used in geological, structural investigations and in exploration for the ores of radioactive metals or minerals.

The method based on the phenomenon of radioactivity. Gamma ray emission is a natural phenomenon. Radioactive elements, uranium (U), thorium (Th) and potassium (K) naturally emit gamma rays which are distinctive in both number and energy. Potassic alteration is commonly associated with many types of volcanic-associated massive-sulfide, base-metal and gold deposits.

When gamma rays collide with atoms, they cause the emission of high energy electrons which collide with other atoms and liberate many more electrons. This charge is collected, either directly or indirectly to detect the presence of the gamma ray and measure its energy.

Table 6 shows the mean natural radioelement content of sedimentary rocks.

Rock type	Thorium [ppm]	Uranium[ppm]	Potassium[%]
Evaporite	0.4	0.1	0.1
Carbonate	1.6	1.6	0.3
Sandstone	5.7	1.9	1.2
Shale	11.2	3.7	2.7

Table 6. Mean natural radioelement content of sedimentary rocks

Gamma-rays have long half-lengths, which property allows the gamma-rays to penetrate far enough via the media to be detected by airborne or field work. The interaction of the gamma ray with matter is detected and the final result is an electrical pulse. Its voltage is proportional to the energy deposited in the detecting medium.

The gamma-ray activity can be measured in spectral or integral mode. In integral mode the total gamma ray spectra is measured. In spectral mode the energy spectrum is recorded.

The result depends on the decay series disequilibria, topographical errors, water content and atmospheric influence during surveying. These factors, not representative of the underlying rock, influence the results.

8.2 Measured parameter

The ionizing action of the gamma radiation is detected (counts per channel) via an electrical pulse whose voltage is proportional to the energy deposited in the detected medium. The range of the measurement: 0-2000 cps.

8.3 Measuring method

The most common gamma measuring and logging technique is the “total gamma” detection. In this case the whole gamma radiation energy spectrum is registered. Spectral gamma technique detects count rates within the scintillation system with certain specific energy windows of the gamma radiation spectrum in order to quantify the amount of the isotopes of Uranium, Potassium and Thorium. This type of measurement of gamma-ray is useful in identifying the presence of Uranium over Thorium or vice versa. Filtered gamma records can be used also to detect thin layers of a range of metals (typically lead, copper or brass or combinations) around the scintillation detection system.

A complete Gamma Spectroscopy System consists of detector, cooling system (if it is needed), electronics and analysis software.

The following basic types of gamma ray detectors can be used to measure the radiation. Ionization chambers, Geiger-Mueller detectors, proportional counters (used only in neutron activation measurements) operate on the general principle of gas ionization caused by incident gamma rays. The fourth instrument is the scintillation counters that are composed of sodium iodide (NaI) crystals, which emits a tiny flash of light when struck by a gamma ray. The flash of light is amplified by a photo-multiplier tube, which in turn generates an electrical pulse, counted by appropriate electronics.

Gas-Filled Detectors have a sensitive volume of gas between two electrodes. The thin inner electrode is placed at the center of the cylinder. The outer electrode can be found in the cylindrical wall of the gas pressure vessel.

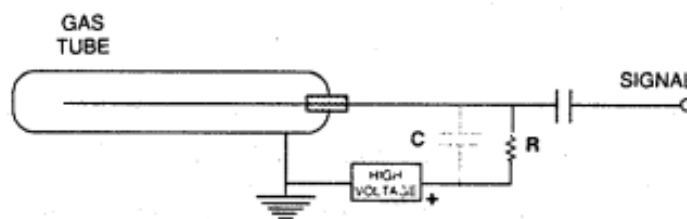


Figure 20. The scheme of a gas-filled detector

The *ionization chamber* is a gas-filled counter that collects only the primary ionization charge. The electrical output signal is proportional.

The *proportional counter* is a type of gaseous ionization detector instrument which works as a combination of a Geiger–Müller tube and an ionization chamber. It is a specific application that changes the gas pressure and/or the operating voltage. The output signal in this case is also proportional. The energy resolution between NaI scintillation counters and germanium (Ge) solid-state detectors is intermediate.

Geiger-Mueller (GM) detector - the amount of ionization saturates is not depend on the initial energy deposited in the gas. The Geiger-Mueller tube gas counter is not suitable identifying different kinds of particles or their energies. It counts only the number of particles entering the detector.

The proportional counter is used to measure particles of ionizing radiation. It is commonly used in those cases when only the energy levels of incident radiation need to be investigated. Proportional counters can detect high energy photons including gamma-rays.

Scintillation Detectors record the gamma-ray-induced light emissions. When gamma rays arrive and interact with scintillator material the ionized atoms “relax” from the excited state that is produced. Their energy-level decreases and they emit photons of light that can be detected. The scintillation material (solid, liquid, or gas) can be organic or inorganic. Organic scintillators can be anthracene, plastics, and liquids. Inorganic scintillation materials could be sodium iodide (NaI), cesium iodide (CSI), lithium iodide (LiI) or zinc sulfide (ZnS). Bismuth germanate ($\text{Bi}_4\text{Ge}_3\text{O}_{12}$) is a new luminescent material.

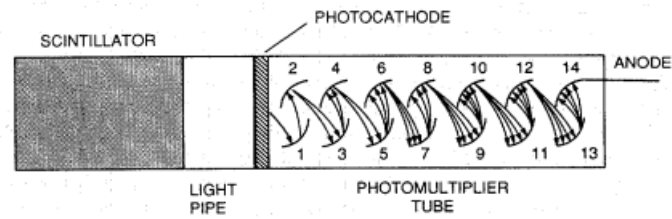


Figure 21. Typical arrangement of components in a scintillation detector

The most common scintillation detectors are solid, and made from inorganic crystals (the most favorable is NaI). This type of detector can be used for spectroscopy and total radiation measurement.

Solid-state detectors collect directly the charge produced by the photon interactions. The sensitive volume in a semiconductor material is an electronically conditioned region in which liberated electrons and holes move freely.

Germanium is used as a solid-state proportional counter. The ionization charge appears directly at the electrodes by the high electric field in the semiconductor and produced by the bias voltage that is collected.

Earlier the detectors contained lithium-doped germanium [Ge(Li)] as the detection medium, but nowadays the preferred material is hyperpure germanium (HPGe) crystals. The new n-type HPGe crystals are less vulnerable to neutron damage.

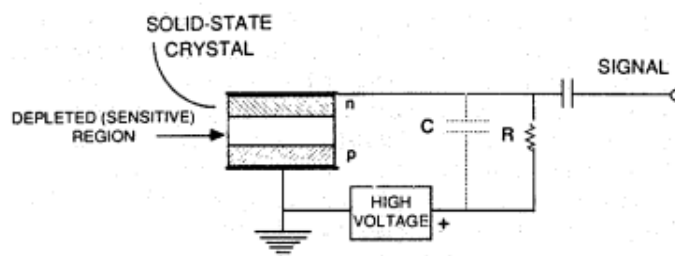


Figure 22. Typical arrangement of components in a solid-state detector

Semi-conductor detectors can determine greater spectral details than the previously introduced ones.

These detectors are available with planar and coaxial configurations.

In case of planar configuration the electric field for charge detection is mainly radial with some axial component in the closed-ended configuration.

The planar detector contains a crystal or circular cross section and sensitive semiconductor detectors.

The germanium solid state detector needs cooling (typically with liquid nitrogen) to reduce natural electrical noise.

New solid-state detection media are CdTe, Hg12, and GaAs which operate on room-temperature.

Scintillation and solid-state detectors are preferred to be used in spectroscopic studies. Gas counters are used for neutron detection or total activity measurement.

The final result of detection is an electrical pulse. The voltage is proportional to the energy deposited in the detecting material.

The pulse can be recorded in digital and analog form. The following Figure 23 shows these two possibilities:

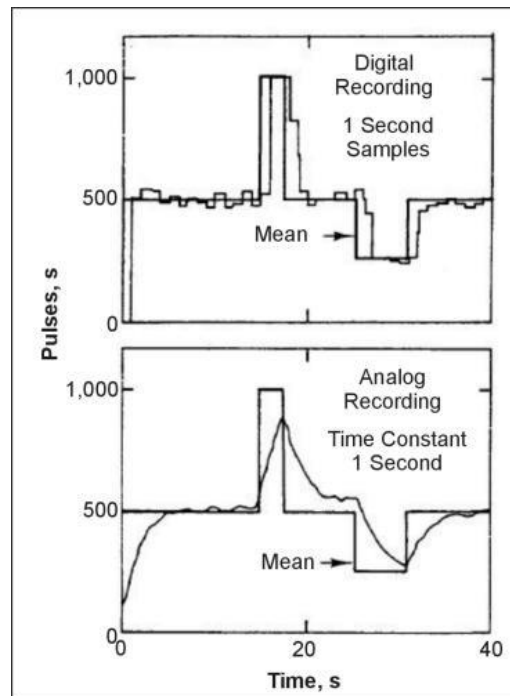


Figure 23. Analog and digital recording

8.3.1 Measurement in field

During surface GR spectral measurements the detector is placed on the ground or above the surface (max. 20 cm). Counting time is about 4 min at each station to detect a statistically adequate number of counts. The total count and the number of counts in each of the windows (potassium, uranium, and thorium) are recorded at each station. The windows are usually centered on the following photopeaks: 2.26 Mev for thorium, 1.76 Mev for uranium, and 1.46 Mev for potassium.

Figure 24 shows schematically the method of gamma-ray measurement on the ground with a portable gamma-ray detector. Gamma-rays penetrate through the rock or air more effectively than alpha or beta radiation.

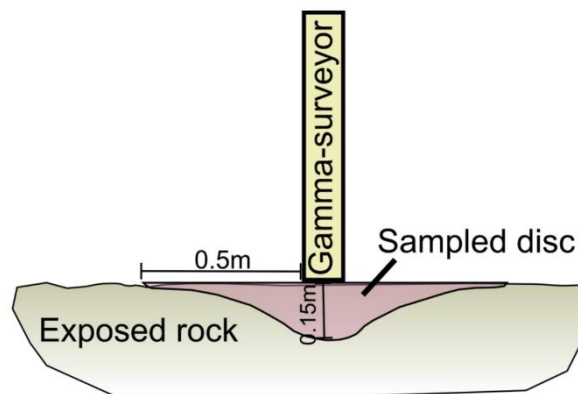


Figure 24. Gamma-ray detection with portable gamma detector that is placed on rock surface

The penetrating ability of the gamma-rays makes this method useful for detecting radioelement concentrations within rock. The gamma rays penetrate up to 0.5 m through rock which makes it possible to detect the local concentration heterogeneity. Penetration of gamma-rays through air could be up to several hundreds of metres thus the aerial surveys are recorded 30–300 m above the surface.

8.3.2 Aerial measurement

When we measure from the air the measured data is from a mixture of bare rock, water courses and peat cover. Another difficulty is the weather that influences the concentration of uranium, thorium and potassium at the surface. These issues can be compensated with calibration by testing samples in the laboratory. The concentrations of specific radioelements is determined. The ^{40}K isotope emits photons with energy of 1.46 MeV. The thorium and uranium are detected via their daughter products, thus these concentrations are determined as equivalent uranium (eU) and equivalent thorium (eTh). We make aerial surveys from an airplane or helicopter (Figure 25).

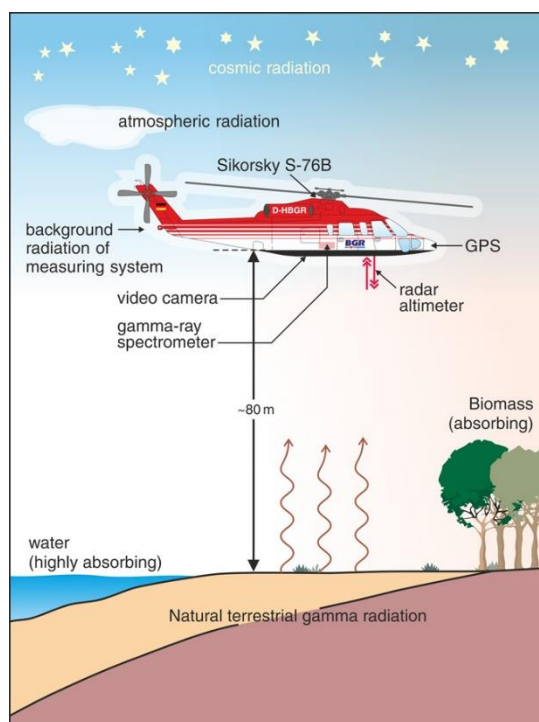


Figure 25. Gamma-ray measurement in the air

During the data processing several corrections are needed: removing aircraft background radiation, compensating for atmospheric radon, correcting for cosmic radiation, correcting for higher energy contributions to lower energy windows by spectral stripping, correcting for altitude. Compton Scattering affects gamma-rays as they penetrate rock because of the gamma-rays interacting with electrons which absorb some of the energy from the gamma-ray. When a photon is detected it shows much less energy than when it was created during decay. These effects can be corrected for in spectral analysis. At the end the corrected data needs to be converted to ground concentrations.

8.3.3 Measurement in marine environment

Before field measurement, calibration of the detector (energy, energy resolution and efficiency) is needed. Furthermore in situ continuous monitoring of radioactivity in the water environment has several difficulties. For example the continuous work of a photomultiplier tube results in a shift in the measured spectrum towards lower energies so re-calibration of the detector is regularly needed. Vlachos (2004) [8] dealt with measuring radioactivity in seawater and proved that a photo peak around 50 keV is always present in the measured spectrum, thus it can be used for the continuous calibration of the detector. As an example from Osvath et al. (2001) [3] about the underwater gamma-spectrometer application is shown on Figure 26 and Figure 27.

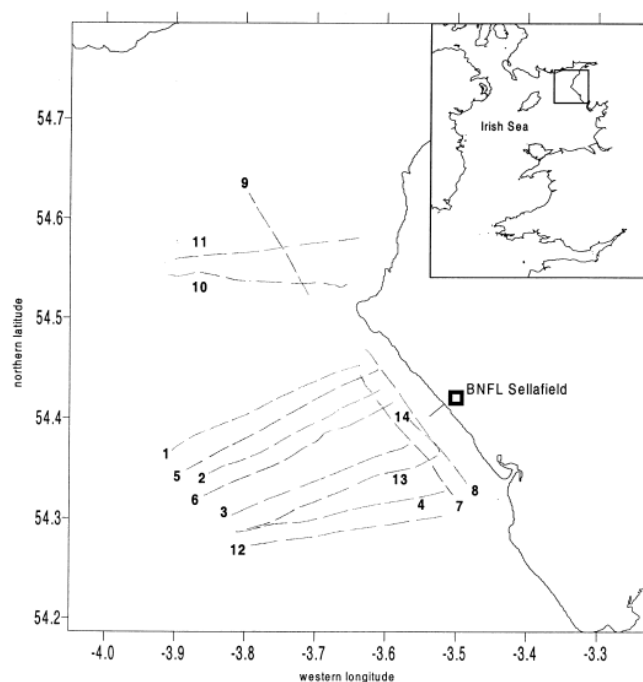


Figure 26. Profiles of gamma-ray survey in the Irish Sea seabed

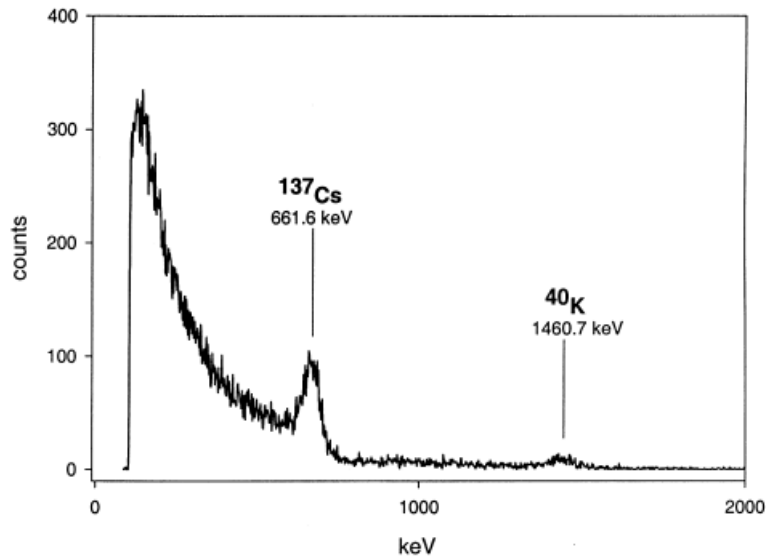


Figure 27. Typical 1-min spectrum recorded with the NaI(Tl) detector on the seabed offshore of Sellafield

Measurements were taken on the seabed at water depths up to 45m along an array of 14 transects (Figure 26) totaling almost 300km (160Nm). During the survey the speed of the ship was between 2.5 and 4 knots and over 1800 individual 1-min spectra were recorded. The spectrum- logging computer's clock was synchronized with the ship's radio-clock periodically, and any differences were recorded and the corrections were applied at the time of data processing as required. The sequence of spectrum recording and data storage was managed through batch computing. The time interval between two successive spectrum records was on average 72 s, out of which 60 s were dedicated to spectrum recording and the remaining time to data storage and spectrometer re-initialization. Additional data back-up operations were required periodically.

8.3.4 Measurement in borehole

For borehole measurements a gamma ray sonde is applied which contains the detector that could be Geiger Muller counters or scintillation counters.

The calibration of gamma probes is needed to produce a depth based profile of uranium ore grade. An example log can be seen in Figure 28.

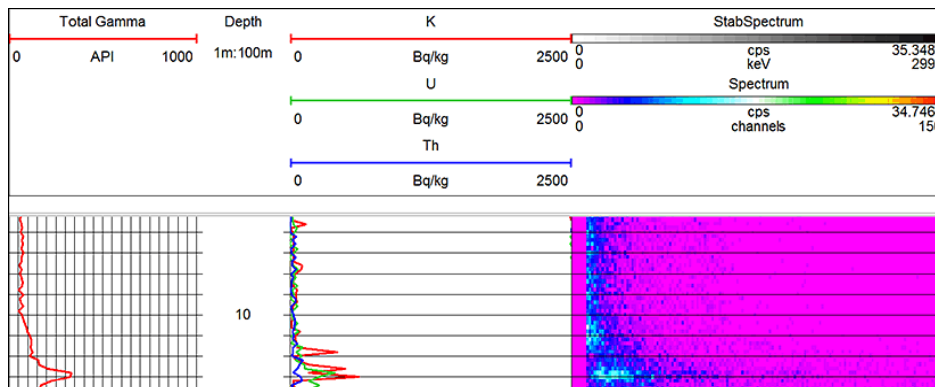


Figure 28. Logging result with gamma ray sonde

8.4 Target parameter

In multichannel analysis the histogram of the detected output pulses is the result that shows the values sorted by magnitude.

8.5 Applicability

- Clay/Mudstone Wayboard detection
- Petrophysical parameters
- Delimiting specific geological formations
- Reconnaissance of radiogenic chemical species

8.6 Advantages of the method

It is a passive method, thus there is no need to apply a radiation source.

8.7 Disadvantages of the method

Wall contact is preferred. Water influences the result. Several corrections are needed.

8.8 Industrial solutions—Purchasable instruments

Several instruments are available in the market, some of them is detailed below as examples.

8.8.1 NP4-2 Gamma-ray Energy Spectrometer



Figure 29. NP4-2 Gamma-ray Energy Spectrometer

Main applications of the NP4-2 Gamma-ray Energy Spectrometer (Figure 29):

- Searching for uranium, thorium and potassium ores;
- Gamma-ray intensity analysis of habitable rooms and building materials;

Features of the spectrometer:

- Large LCD display
- Use rechargeable Ni-MH batteries as the power source
- High sensitivity, high stability, low noise spectrum
- Photomultiplier Response

Other technical specifications:

- Energy Discriminating window Peak: Potassium (1.46MeV), Uranium (1.76MeV), Thorium (2.62MeV), total counts (all energy higher than 0.5MeV);
- Content Analysis Sensitivity: Potassium channel (3000~5000 ppm), uranium channel (≤ 2 ppm), thorium channel (≤ 3 ppm);
- Instrument Outline Dimension: 290×110×290mm;
- Probe Outline Size: $\phi 102 \times 432$ mm;
- Weight: 5 Kg;
- Temperature Range: -10°C~ +60°C.

8.8.2 FD-908 Portable γ Spectrometer



Figure 30. FD-908 Portable γ Spectrometer

Main applications of this spectrometer (Figure 30):

- Prospecting of uranium, thorium, potassium, oil, coal and gold and other minerals.
- Radioactive geological mapping
- Radiation environment detection
- Construction materials radioactive environment detection

Main characteristics of the instrument:

- Low power consumption, digital, intelligent, portable, easy to operate
- 2 μ s latency time, digital pulse technology
- High stability, with backlight LCD display, keyboard input, menu operations
- Measuring result: shows counting rate (S-1) or content (Ur)
- Parameters can be set. It can store 2 million groups of measuring data
- Standard RS232 port, dump data can satisfy geological mapping request

Technical parameters:

- Detector: $\phi 75\text{mm} \times 75\text{mm}$ sodium iodide crystal
- Energy resolution: $\leq 8\%$ (for ^{137}Cs)
- Content measurement range:
 - eU : $2 \sim 1000 \times 10^{-6}$ (Ur)
 - eTh : $3 \sim 1000 \times 10^{-6}$ (Ur)
 - eK : $0.5 \sim 100 \times 10^{-2}$ (%)
- Channel width measurement:
 - U : 1.60 ~ 1.90 MeV ;
 - Th : 2.40 ~ 3.0 MeV ;
 - K : 1.30 ~ 1.60 MeV ;
 - Σ : 0.5 ~ 3.00 MeV
- Accuracy accord with the requirement of relative deviation in the verification regulation: eU、eTh : $E \leq 7\%$; eK : $E \leq 12\%$
- Weight: 3.6kg
- Power Supply: rechargeable 2.4Ah lithium battery, overall power consumption ≤ 200 mW
- Environmental conditions: Temperature $0^\circ\text{C} \div 50^\circ\text{C}$; relative humidity $\leq 90\%$ ($+50^\circ\text{C}$)

8.8.3 FD-3022 microcomputer four channel γ Spectrometer



Figure 31. FD-3022 microcomputer four channel γ Spectrometer

Main features of the instrument (Figure 31):

- 4 channels to count at the same time, and display counting rate of 4 channels by turns, also can display content of U, Th, K and total amount.
- Do U and Th to Cs to affect revision and enhance signal quality of reference source. - Use micro PC to seek peak and track spectrum shift automatically, then can stable the spectrum.
- Equipment can deduct background value automatically.
- Counting rate output of 3 channels like U, Th and K is all normalized to the value of 100s, and total counting rate will be all normalized to the value of 10s.
- Self-stable status will be indicated on table head.
- Have radioactive abnormal noise alarm, which can choose among 15×10^{-6} -200-6 in abnormal alarm switch according to uranium content in all.
- Set alarm when batteries invalid and probe without signal.
- High sensitivity, portable, light weight, firm and reliable, fit for field work.

Main parameters of the spectrometer:

- Content sensitivity threshold: uranium: 1×10^{-6} , thorium: 2×10^{-6} , Potassium: 0.2%
- Content measuring range: uranium: $1 \times 10^{-6} \sim 1000 \times 10^{-6}$, thorium: $2 \times 10^{-6} \sim 1000 \times 10^{-6}$, Potassium: 0.2%~100%, Total channel: $2 \times 10^{-6} \sim 1000 \times 10^{-6}$

Usage environment:

- It can operate normally in the temperature of $-10^{\circ}\text{C} \sim +55^{\circ}\text{C}$ or temperature $+40^{\circ}\text{C}$ and relative humidity 95%. Comparing to each channel counting rate in normal climate condition and limit condition, the relative error is no more than $\pm 15\%$.
- Repetition: under the same measurement condition, if you do continuous 20 times measurement to the same component, the relative standard deviation is no more than $\pm 10\%$.
- Stability: stable for 8 hours, the relative error is no more than $\pm 10\%$.
- Power and consumption: six 1# batteries, currency is $\leq 90\text{mA}$
- Equipment dimension and weight:
- Operation desk: volume: $220 \times 105 \times 175\text{mm}$,
- Weight: 2.6kg (batteries not included)
- robe:
- length: 490mm,
- max. diameter: 100mm,
- weight is about 3.0kg

8.8.4 Geometrics GR-101 Scintillometer



Figure 32. Geometrics GR-101 Scintillometer

The GR-101A is a rugged, gamma ray scintillometer for uranium prospecting and all total count gamma ray reconnaissance surveys (Figure 32). It provides high accuracy and stable measurements of all naturally occurring gamma radiation above 0.05 Mev.

This is older, analogue technology, but works perfectly well for reconnaissance work. The GR101 has been used for mapping all over the world.

Technical details:

- Large internal 1.5" x 1.5" NaI(Tl) crystal.
- Audio alarm triggered at selectable setting.
- Hands-free, eyes-free operation while carried in belt pouch.
- Full-view, 250 degree rate meter calibrated directly in cps.
- Wide dynamic range, switch selectable from 100 to 10,000 cps full scale

8.8.5 NaI(Tl) Gamma spectrometer for iPhone\iPad\Android AtomSpectra 3



Figure 33. NaI(Tl) Gamma spectrometer



Figure 34. NaI(Tl) Gamma spectrometer in use

The scintillation detector assembly consists of 16*40 mm (0.63"*1.57") NaI(Tl) monocrystal, micro photomultiplier tube, low-noise regulated adjustable power supply, low-noise preamplifier and Li-ion battery with protection and charging circuits.

16*40 mm NaI(Tl) detector is effective for gamma-spectrometry in more than 20 Kev – 1.5 Mev energy range. Typical energy resolution is 8% for 662 Kev peak of Cs137 source. Light output of NaI(Tl) crystals depends on temperature, so after temperature change calibration is recommended. It is not recommended to change temperature of the detector faster than 1°C\minute.

Scintillation crystal is optically matched with 8-stage spectrometric photomultiplier tube.

16*40mm NaI(Tl) scintillation detectors have very high sensitivity: around 11 000 pulses per minute to microsievert per hour. It is normal that in typical gamma radiation background (0.1 uSv/h) you will see 16-20 counts per second, or 1000 – 1200 counts per minute. ADC sampling rate is most devices is limited to 48000 Hz, so more than 1000 counts per second load is not recommended.

8.8.6 IH-99DNC dose rate meter for high dose rate measurement



Figure 35. IH-99DNC Dosimeter

This dosimeter (Fig. 35) has been selected to be built into the autonomous robot.

The instrument is a nuclear radiation measuring device with two operational modes. It operates as a gamma radiation dose and dose rate meter.

Features of this instrument:

- Detector: energy-compensated GM-tube.
- Effective gamma dose-rate measurement range:
- Range: 1μGy/h ... 1Gy/h
- Indication range: 20nGy/h ... 100 Gy/h
- Energy range: 60keV...1,5Mev
- Measurement time: 2s ... 4min, automatic
- Power supply: 12 V, max. 25mA
- Temperature range: -30 ... + 50°C
- Communication: RS-485
- β-radiosensitivity: 0.3%
- Energy dependency: +/-20%
- Contingency: The instrument cannot be damaged till 100 Gy/h

8.9 Case Study

We have made laboratory studies to test the applicability of the method in an underwater environment. The following steps summarized the research:

- minerals with higher gamma ray activity were selected with the Geiger Muller counter from the Department of Mineralogy. These minerals were juxtaposed in a 50cm*50 cm square on the laboratory table then the instrument was placed in the middle of the set of the selected minerals without any shade.
- A plastic PP pail was placed in the middle of the set of minerals of the 1st measurement then the distance of the GF Instrument Gamma Surveyor instrument was changed compared to the bottom of the pail.

- A plastic PP pail was placed over the set of the minerals of the 1st measurement. It was filled with 30-20-10 cm tap water the measurement was performed by touching the water surface with GF Instrument Gamma Surveyor scintillation detector.
- Two minerals from the set were selected with extremely high radioactivity. They were placed into a 8 cm thick leaden cylinder. The bottom of the cylinder was also closed so the emitted gamma photons could leave the minerals only upwards. At first we had measured the emission without shade, then we cover the minerals with a small sized PP plastic pail and measured the natural gamma ray activity over the opened-end of the leaden cylinder.
- The measurement was carried out according to the parameters of the 4th measurement supplemented with a big sized pail filled with 30-20-10 cm tap water.

Figures 36-Figure 38 show the concentration of the isotopes along the distance of the “wall”.

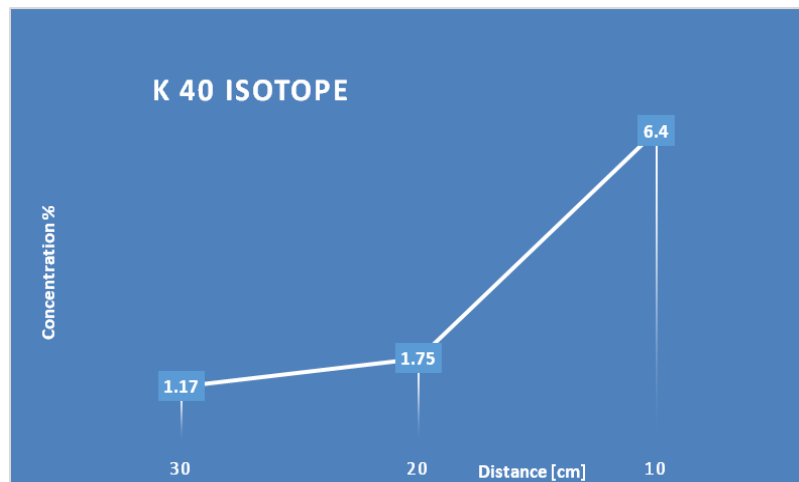


Figure 36. Concentration of K40 Isotope

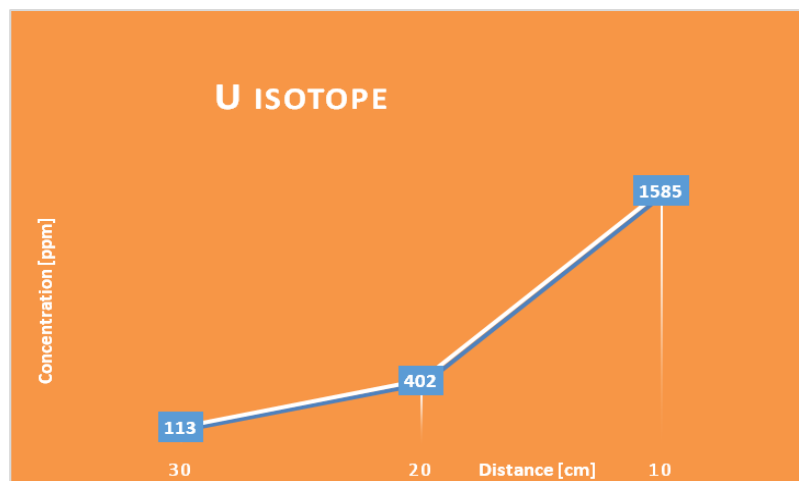


Figure 37. Concentration of U Isotope

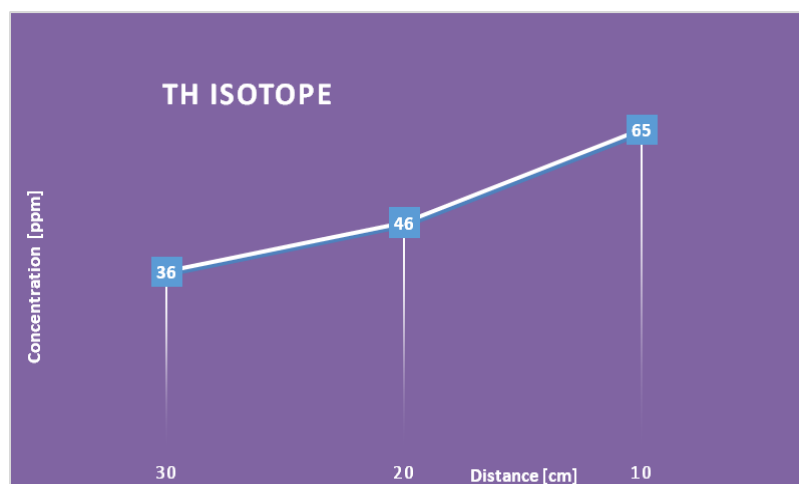


Figure 38. Concentration of Th Isotope

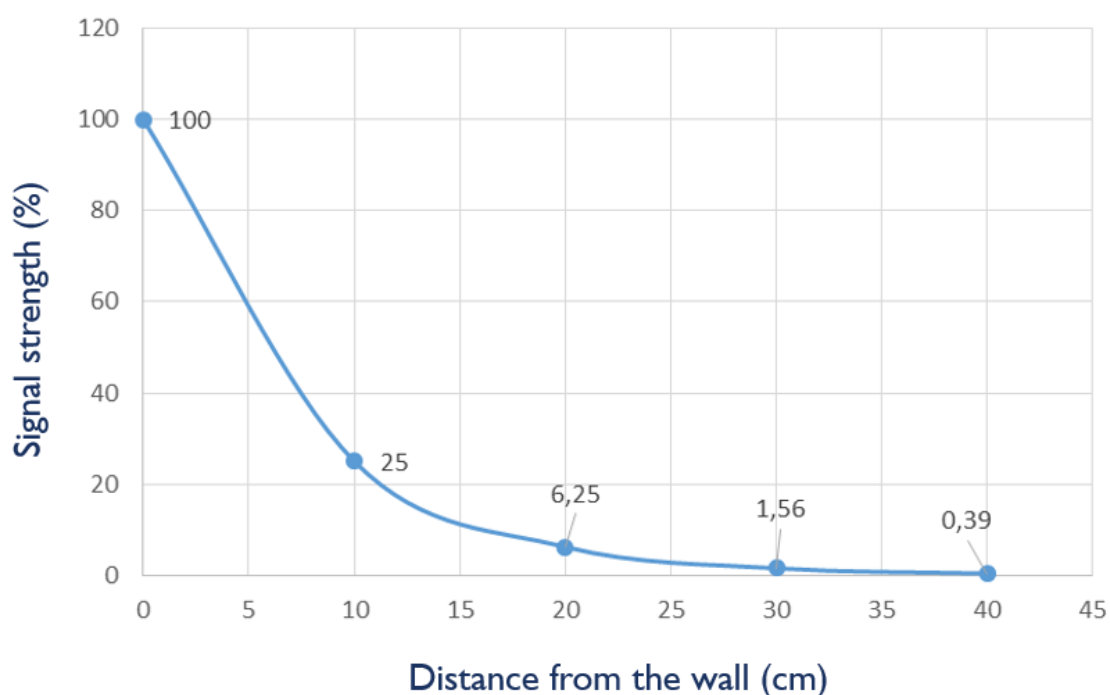


Figure 39. Signal strength in the function of the distance from the wall

The sensitivity decreases quickly with increasing thickness of water. As a result of our analyses, we measured $\frac{3}{4}$ signal absorption in every 10 cm of water (Figure 39). It has two effects:

- measurements can only be performed close to the wall. According to the results detection from 30 cm is poor. The precise distance depends on ore concentration, water chemistry and the detector casing solution.
- The K does not have enough natural radiogenic isotope to be able to detect the signal of even the most potassic-rich natural stone farther than a few cm under water. Only Th and U can be effectively in sufficient concentration to be successfully detected.

8.10 Conclusion

The method is useful for detecting radioactive ores and distinguishing them from the environment. The laboratory tests show that K isotope detection decreases quickly in water, due to its low radiogenic isotopic ratio (intensity), we advise to use only the integral gamma ray spectrometry in the first trials and we suggest using this method in Urgeiriça. According to the calculations, the method will only be sensitive to the Th and U content of the rock. We do not advise to use this method to detect fractured zones filled with clay in non-radioactive rock, potassic-altered zones or reconnaissance of radiogenic chemical species in underwater environment far from the mine wall.

Suggested/*Suggested with comment* (wall contact gives better results)/Unsuggested method

8.11 References

- [1] Alistair T. McCay 1,* , Thomas L. Harley 1, Paul L. Younger 1, David C. W. Sanderson 2 and Alan J. Cresswell: **Gamma-ray Spectrometry in Geothermal Exploration: State of the Art Techniques** Energies 2014, 7(8), 4757-4780; doi:10.3390/en7084757
- [2] Lovborg, L.: **The calibration of portable and airborne gamma-ray spectrometers—Theory, problems, and facilities** Rise Natl. Lab. 1984, 2456, 3–207.
- [3] Osvath I., Povinec P.P.: **Seabed gamma-ray spectrometry: applications at IAEA-MEL** Journal of Environmental Radioactivity 53, pp.:335-349, 2001
- [4] Parasnis D.S.: **Principles of Applied Geophysics** ISBN 0-412-28330-1. Chapman and Hall, 1986
- [5] Schwarz, G.: Klingelé, E.; Rybach, L. **How to handle rugged topography in airborne gamma-ray spectrometry surveys** First Break 1992, 10, 11–17.
- [6] Sharma P.: **Environmental and Engineering Geophysics** ISBN 0-521-57632-6. Cambridge University Press, 1997
- [7] Tsabarisa C., Bagatelasb C., Dakladasc Th., Papadopoulosb C.T., Vlastoub R., Chronisa G.T.: **An autonomous in situ detection system for radioactivity measurements in the marine environment** Applied Radiation and Isotopes 66, pp.:1419–1426, 2008
- [8] Vlachos D.S.: **Self-calibration techniques of underwater gamma ray spectrometers** Journal of Environmental Radioactivity 82, pp.:21-32, 2005
- [9] <http://www.gammatech.hu/>
- [10] <http://www.expins.com/item/gr-101>
- [11] <http://www.aidush.com/en/index.php/default/content/13220.html>
- [12] <http://mountsopris.com/items/2ghf-1000-triple-gamma-probe/>
- [13] <http://www.ebay.com/itm/Nal-Tl-Gamma-spectrometer-for-iPhoneiPadAndroid-AtomSpectra-3-Resolution-8-/222153622949?hash=item33b96345a5:g:UDsAAOxyOMdS36cp>
- [14] http://www.bgr.bund.de/EN/Themen/GG_Geophysik/Aerogeophysik/Bilder/prinzip_gamma_spektrometrie_g.html
- [15] <http://borehole-wireline.com.au/2015/05/gamma-logging-techniques-for-uranium/>

9.1 Theoretical background

Hyperspectral or multispectral imaging combines digital image processing and spectroscopy. The purpose of the method is to find objects, identify materials or detect processes by obtaining the spectrum for each pixel in the image of the scene.

The human vision sees the colour of visible light in three bands (red, green and blue). Spectral imaging divides the spectrum into many more bands and the processed spectrum can be extended beyond visible light, to the ultraviolet and infrared wavelength range.

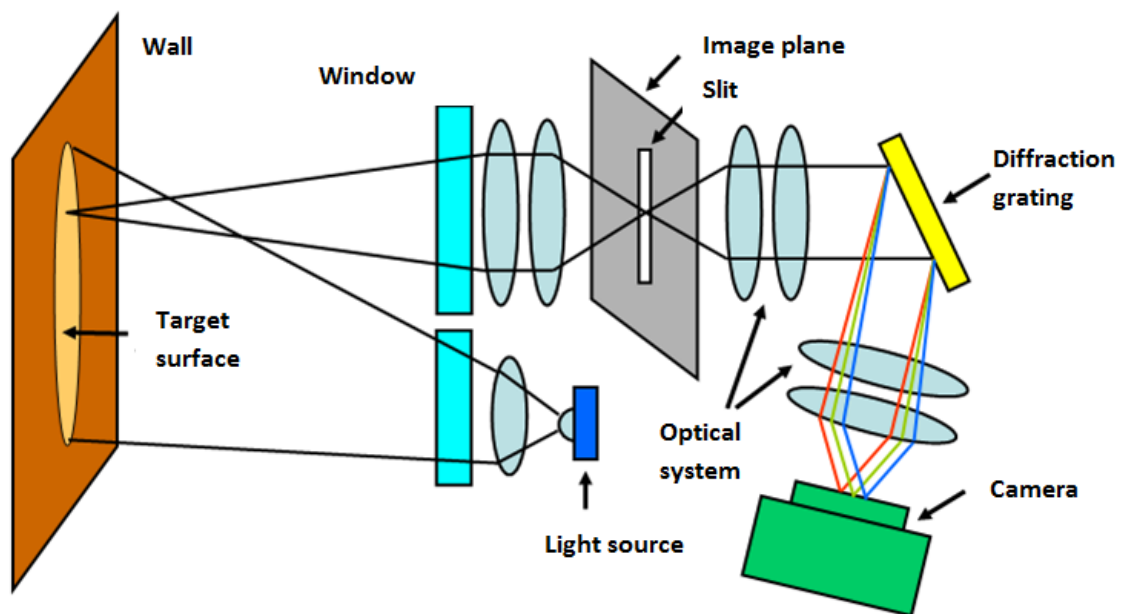


Figure 40. Hyper/Multispectral imaging system

Traditional hyperspectral cameras are based on the method shown in Figure 40. It is possible to build more energy efficient device, which is more robust and less expensive based on the method shown in Fig. 41. A very important advantage of the LED method, it can easily be performed from 2D areas, till the first method allows only line imaging with pixel thickness. The principle of the operation is to illuminate the surface with different monochromatic light sources (LEDs) from 400 nm to 1000 nm (one wavelength at a time) and to detect the reflection with a monochrome image sensor. Since we know the wavelength (because there is only one at a time) we only have to detect the brightness. Because this method detects a single wavelength on the image the pixels can be larger which produces better sensitivity.

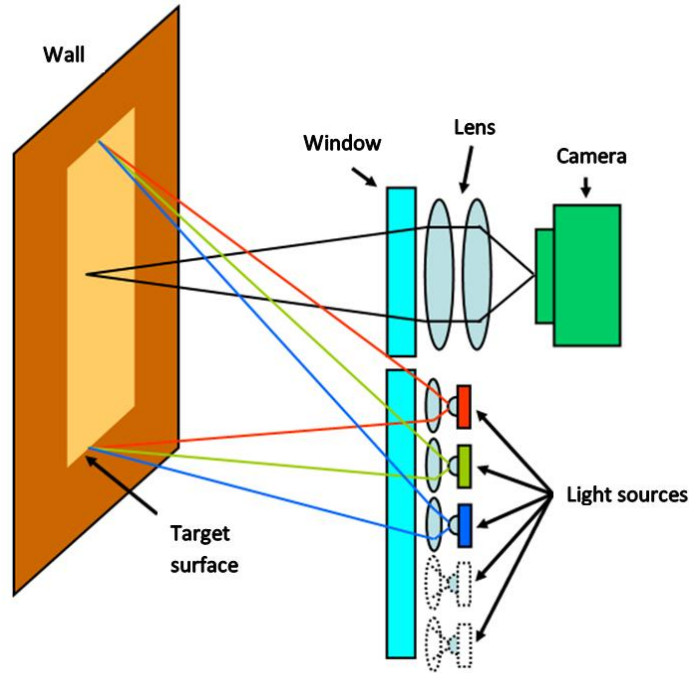


Figure 41. Hyper/Multispectral imaging system with monochrome camera

9.2 Measured parameter

With the hyperspectral imaging system we get spectral images of the wall in the 400nm - 1000nm (visible + near infrared) spectral range. With appropriately selected frame size and frame rate - depending on the travelling speed - we can map the whole mine wall at about 1-5 mm resolution.

9.3 Aim

By using hyperspectral image analysis we can detect minerals on the mine walls. Collating the hyperspectral data with spectral mineral databases [1], [2] we can map the mineral content of the entire mine wall. The development of a robust method for automatic analysis and database search is required.

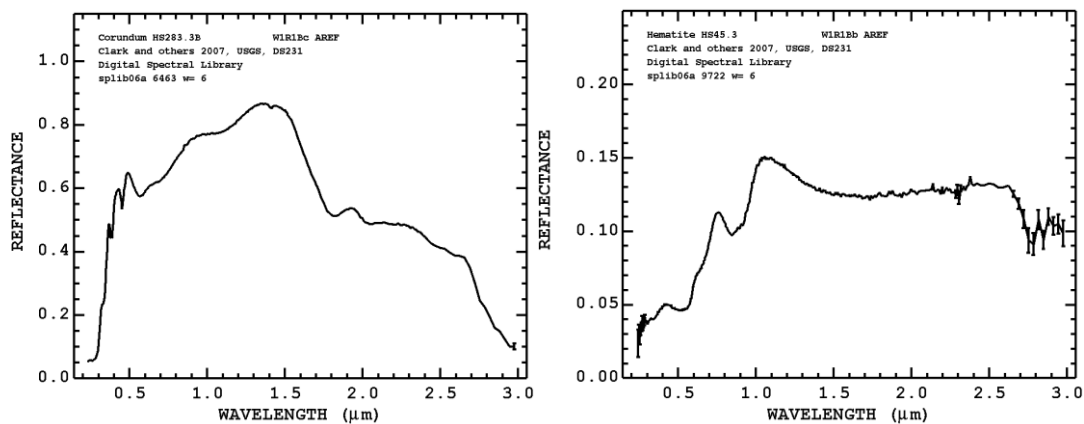


Figure 42. Spectral diagrams of minerals from USGS Digital Spectral Library

9.4 Hyper/Multispectral camera type

Traditional hyperspectral cameras are large (more than 300 mm in length) and heavy (3-5 kg or more) because of the complex optical system. In our application size is a critical parameter so we need the most compact camera available.

Over the last few years IMEC, a Belgian research institute, has developed a process to integrate the optic system with the surface of the CMOS image sensor (Figure 43). This technique allows them to build a very compact camera without moving parts or an easily damaged optical system. This type of cameras has a drawback: the 2D image is divided to lines and columns, the columns are the spatial dimension and the lines are the spectral. That is, we can see spectral distribution of different lines of the image plane (Figure 43) which means we need accurate synchronization between movement of the explorer and the imaging system.

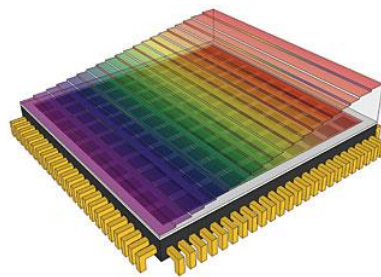


Figure 43. Linescan hyperspectral sensor

A possible solution is to develop a special camera which fulfils our needs. The team of the Dept. of Atomic Physics, Budapest University of Technology and Economics, has a concept (as shown in Figures 40 and 41), which seems suitable for our application because it integrates the optics, the camera and the lighting system.

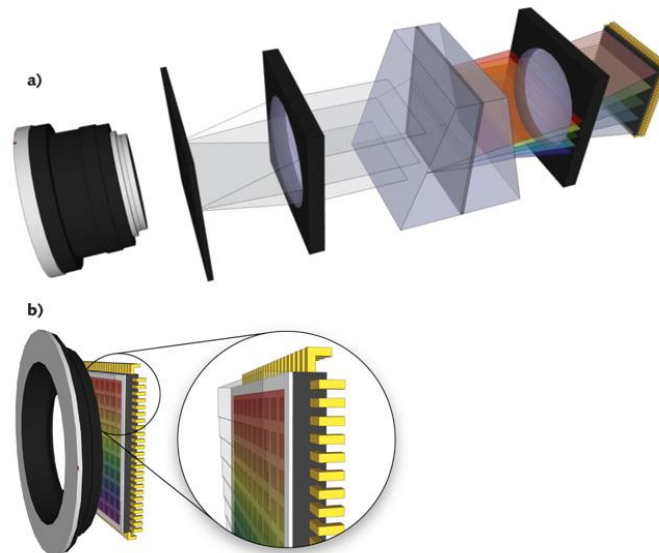


Figure 44. Traditional HSI camera (a) versus Imec's solution (b): a) Focusing objective - Slit - Collimator - Dispersive element - Focusing lens – Detector; b) Spectral filter integrated to the CMOS image sensor

9.5 Spectral range considerations

HSI cameras are available with a spectral range from 250 nm to tens of micrometers. In our application the most important region is the 400 nm to 3000 (or even 10000) nm wavelengths, which means the visible (400-700 nm) through to near infrared (NIR, 700-1400 nm), shortwave infrared (SWIR, 1400-3000 nm) to the mid wavelength infrared (MWIR, 3-8 μm). The importance of, and limitations on, spectral regions are listed here:

- **Ultraviolet (10 to 400 nm):** According to mineral spectral databases ([USGS](#), [ASTER](#)) the UV range is not so important. Few available cameras can handle this range, thus we need a separate device to sense this. The available UV-capable camera ([Headwall Hyperspec-UV](#), 250-500 nm) is large and expensive. In addition, it needs a special lighting solution. On the other hand, there is a phenomenon called *photoluminescence*, which means some minerals emit visible light under ultraviolet lighting. As well as hyperspectral imaging we can use standard digital cameras built to the front of the robot to detect photoluminescence of the mine wall. By analysing the colour images we can detect some minerals which are known to produce photoluminescence [4].
- **Visible (400-700 nm):** important range and most of the cameras can sense this. Lighting is simple.
- **Near infrared (NIR, 750-1400 nm):** important, most of the cameras can sense this. Lighting is not difficult, but water absorption is a problem.
- **Infrared (SWIR-MWIR, 1400-8000 nm):** important range, but we cannot use it. Lighting is easy, but needs infrared radiation which uses a lot of power. Sensing the IR range above 1500 nm needs MCD (HgCdTe) sensor element and those types of sensors need cooling. The operating temperature of IR imaging MCT sensors is below 150 K. In our application this cooling is impossible because of the limited power source and we cannot deal with the heat inside the underwater explorer.

9.6 Problem with underwater infrared imaging

The light absorption of water is an important limiting factor. We have to do the imaging through 10-50 centimetres (or even more) of water, and the water absorbs almost everything except visible light as can be seen on Figure 45. According to preliminary calculations, we can sense the range where absorption coefficient is below 0.01 cm^{-1} , this means, approximately, in the 200-750 nm range. Detecting reflected infrared light needs very powerful lighting and cooling system, which, again, is not possible in our project because of the limited power source.

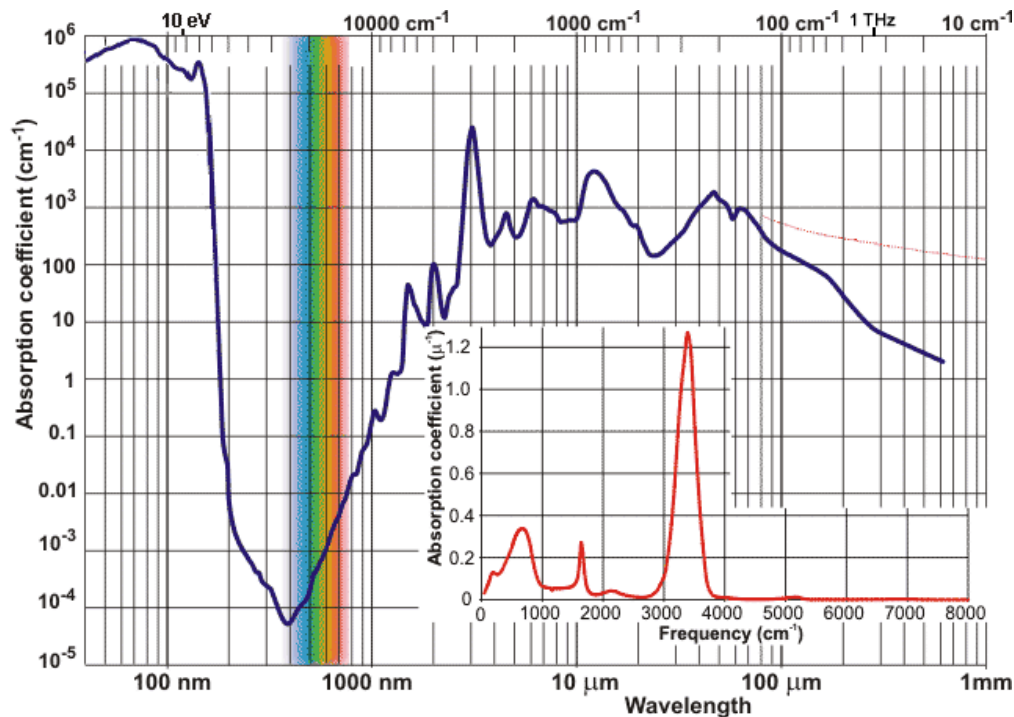


Figure 45. Absorption coefficient of water according to wavelength [3]

9.7 Advantages of the method

We can map the whole mine wall on spectral images with reasonably high resolution so, assuming all scanned material has a recognizable “spectral fingerprint” in the above mentioned spectral range, we can detect even the smallest traces of minerals.

9.8 Disadvantages of the method

- The imaging system is expensive
- The necessary lighting system is expensive, needs a lot of power and we have to take care not to interfere with other instruments (cameras, optical measurement equipment)
- We cannot see the surface of the wall if it is covered with sediment, therefore cleaning or grinding might be needed (but it’s not impossible)

9.9 Industrial solutions – Purchasable instruments

Table 7 shows the parameters of suitable HSI cameras available on the market. All cameras are linescan models with VIS, VISNIR or NIR spectral range. According to the circumstances above, VIS range (400-700 nm) is required, thus we have two contenders: The Ximea xiSpec VISNIR and the BaySpec OCI-F models. The price of the OCI-F is lower, but it’s a bit limited on both spatial and spectral resolution. Prices are shown without VAT, other taxes and S&H costs and without lenses. The cost of lenses, cables and other accessories are about 2000 EUR.

The Ximea xiSpec VISNIR model can sense the spectral range our project needs, has suitable spatial (2048 pixel) and spectral (150 bands) resolution. In addition, the xiSpec is the software compatibility lists for: OpenCV, DirectShow, GeniCam GenTL, MathWorks Matlab, NI LabView, Matrox MIL, etc.

Manufacturer	Ximea	Ximea	Photonfocus	BaySpec	Headwall
Type	MQ022HG-IM-LS100-NIR	MQ022HG-IM-LS150-VISNIR	MV1-D2048*1088-HS1	OCI-F	Hyperspec
Sensor type	Linescan				
Spect. range (nm)	600-975	450-960	600-1000	400-1000	250-500
Spatial resolution	2048		2048	800	1392
Spectral resolution	100+ bands	150+ bands	100 bands	60 bands	961 bands
Interface	USB3	USB3	GigE	USB3	USB2
Dimensions (mm)*	26*26*31	26*26*31	55*55*52	110*70*30	? (3.2 kg)
Price	12500 EUR	16500 EUR	8873 EUR (?)	15980 USD	?

Table 7. Available HSI cameras on the market

9.10 Conclusion

Suggested/Suggested with comment (suggested in 2.2)/Unsuggested method

The method is definitely suggested, but accurate consideration of the equipment to be used and system design is needed. The solution shown in Figure 41 is small, robust and simple and so we plan to perform the measurement using this method.

9.11 References

- [1] R. N. Clark, G. A. Swayze, R. Wise, K. E. Livo, T. M. Hoefen, R. F. Kokaly, and S. J. Sutley, 2007, **USGS Digital Spectral Library** splib06a
U.S. Geological Survey, Data Series 231.
- [2] **ASTER Spectral Library**
Jet Propulsion Laboratory, California Institute of Technology
- [3] M. Chaplin, **Water Structure and and Science**
Water Absorption Spectrum, 2016.
- [4] G. Barmarin, **Complete list of luminescent minerals**, 2010.

10 INDUCED POLARIZATION (IP)

10.1 Theoretical Background

IP is a geophysical technique used to identify mainly the electrical chargeability of subsurface materials. Induced polarization is well known as an effective geophysical method in ore prospecting. Among geoelectric methods, the Induced Polarization (IP) method yields excellent results [1], [3]. However, the metal content in an observed sample is not the only factor resulting in polarizability of the medium: filtration- and membrane effects as well as electrochemical (redox) properties can also lead to similar responses. Induced Polarization is a very useful geophysical method also in the detection and characterization of environmental hot-spots, particularly to detect waste sites.

The RCI (resistive, capacitive and inductive) model can be used to describe the electrical and electromagnetic properties of materials (solid, liquid and gas). We must take resistive (R), capacitive (C) and inductive (I) components into the model, where R is the resistance in ohms, C is the capacitance and I is the inductance of the material. We get the so-called ohmic model, if the capacitive and inductive components have been eliminated. The ohmic model is unsuitable to describe the phenomena of capacitance and inductance in the soil. This model is good only for model characterization using ohmic resistivity. However in the heterogeneous and anisotropic media, the boundaries are filled (capacitive effect) and the inductive effects can occur too. Describing these effects are suitable only for the RCI models. In case of RCI models electrical resistivity of polarized media will be frequency-dependent. This is the basic phenomenon of frequency-domain IP. The time-domain basic phenomena is that the media are charging up gradually in time due to field current and a quasi-exponential decay curve can be measured between the potential electrodes after turning off the current.

The TAU-transform method was introduced by Turai [4], [5] for the interpretation of IP curves. This method was applied first near Offheim in a TEMPUS project [6] and it was demonstrated several times successfully above contaminated areas in Hungary [8], [9], [10].

10.2 Measured parameters

This chapter summarizes the main static and dynamic parameters in both the time domain and the frequency domain. The static parameters are measured at fixed frequencies (frequency domain) or at fixed reference times (time domain). The dynamic parameters are measured in a large frequency range (frequency domain) at many frequencies or in a large time interval (time domain) at many time reference points.

10.3 In Frequency Domain

10.3.1 Static parametres

Percent frequency effect

$$PFE = \frac{\rho_a(f_1) - \rho_a(f_2)}{\rho_a(f_2)} \cdot 100 [\%],$$

where

f_1 -the first frequency (usually 0,5 Hz),

f_2 -the second frequency (between 1 Hz and 10 Hz),

$\rho_a(f_1)$ -apparent resistivity measured at first frequency,

$\rho_a(f_2)$ -apparent resistivity measured at second frequency.

IP phase parametre

$$PIP = \frac{f_2 \varphi_{U,I}(f_1) - f_1 \varphi_{U,I}(f_2)}{f_2 - f_1},$$

where

$\varphi_{U,I}(f_1)$ -phase shift between the voltage and the current measured at the first frequency,

$\varphi_{U,I}(f_2)$ -phase shift between the voltage and the current measured at the second frequency.

Metal factor in frequency domain

$$FDMF = k \frac{PFE}{\rho_{dc}},$$

where

PFE -percent frequency effect,

ρ_{dc} -direct current resistivity,

$k=2\pi 10^5$ -mineralization constant.

10.3.2 Dynamic parametre

Cole-Cole spectrum

$$\rho_a(f) = \text{Re}[\rho_a(f)] + j \text{Im}[\rho_a(f)],$$

where

j -the imaginary unit ($j = \sqrt{-1}$),

$\text{Re}[\rho_a(f)]$ -real part of the measured frequency-dependent apparent resistivity,

$\text{Im}[\rho_a(f)]$ -imaginary part of the measured frequency-dependent apparent resistivity.

10.4 In Time Domain

10.4.1 Static parametres

Apparent polarizability

$$\eta_a(t) = \frac{\Delta U_{M,N}(t)}{\Delta U_{M,N}(TG)} 100[\%],$$

where

t - an arbitrary fixed time reference point of the decay curve,

$\Delta U_{M,N}(t)$ -the electrical potential difference at the time reference point (t) after turning off the field current measured between M and N electrodes,

$\Delta U_{M,N}(TG)$ -the electrical potential difference before turning off the field current measured between M and N electrodes.

Apparent chargeability

$$M = \frac{\int_{t_1}^{t_2} \Delta U_{M,N}(t) dt}{\Delta U_{M,N}(TG)},$$

where

t_1 - the first time reference point of decay curve,

t_2 -the second time reference point of decay curve,

Apparent chargeability M defined as the area beneath the decay curve over a certain time interval (t_1 - t_2) normalized by the potential difference $\Delta U_{M,N}(TG)$.

Metal factor in time domain

$$TDMF = k \frac{\eta_a(t)}{\rho_{dc}},$$

where

$\eta_a(t)$ -the apparent polarizability value,

ρ_{dc} -direct current resistivity,

$k=2\pi 10^5$ -mineralization constant.

10.4.2 Dynamic parametres

Time constant spectrum

$$\eta_a(t) = \int_0^{\infty} w(\tau) e^{-\frac{t}{\tau}} d\tau,$$

where

t -the independent time variable of the decay curve,

τ -the time constant,

$\eta_a(t)$ -the measured IP decay curve,

$w(\tau)$ -the time constant spectrum.

Weighted Amplitude Value (WAV)

$$WAV(\tau) = \tau \cdot w(\tau),$$

where

τ - the time constant,

$w(\tau)$ - the time constant spectrum.

We can raise the effect of higher time-constants of the waste site (connected with harmful components - chemical and metallic) and similarly we can reduce the lower time-constant effect (no dangerous components - water and dispersed clay) using a simple weighting procedure [7] multiplying the amplitude value of the time constant spectra by the time constant. The main components of the material in a contaminated site are connected to the main types of polarizations (see in Table 8.).

Polarization type	Source of polarization
filtration	porous soil and rocks with conductive fluid
membrane	porous soil and rocks with dispersed clay and water
electrochemical or redox	chemical agent with high reactivity for oxidation or reduction
metallic	metallic components in porous rocks with conductive fluid
dielectric	poorly conducting or non-conductive materials (dispersed plastic materials, aromatic dispersed hydrocarbons, electrically non-conductive organic materials) in porous rocks with conductive fluid

Table 8. Environmental reason of polarization

Based on the WAV maps or sections the grade of ores and contamination can be given:

- very high grade of ores or contamination- WAV is higher than 0.2 (20%),
- high grade of ores or contamination - WAV is between 0.1 (10%) and 0.2 (20%),
- medium grade of ores or contamination - WAV is between 0.05 (5%) and 0.1 (10%),
- low grade of ores or contamination- WAV is between 0.02 (2%) and 0.05 (5%),
- no mineralization or contamination- WAV is lower than 0.02 (2%).

Corrected apparent conductivity of the media

$$\sigma_{corr}(\tau) = \sigma_a \cdot w(\tau),$$

where

τ - the time constant,

σ_a - the apparent direct current conductivity,

$w(\tau)$ - the time constant spectrum.

Contamination level of soil can be estimated using the corrected apparent conductivity parametre for estimation (Turai, 2012a). If the σ_{corr} value is approximately 50-100 milliSiemens/metre (mS/m) the soil has a medium ion contamination or medium polarizable ore concentration.

10.5 Measuring method

The capacitive and inductive properties of the ground cause both the transient decay of a residual voltage and the variation of apparent resistivity as a function of frequency. The IP effects are representations of the same phenomenon in time and frequency domains. These two manifestations of the capacitive and inductive properties of the ground provide two different survey methods for the investigations of the effect (Kearey et al, 2002).

The measurement of a decaying voltage curve over a certain time interval is known as time domain IP surveying. Measurement of apparent resistivity at two or more low AC frequencies is known as frequency domain IP surveying.

10.6 Aimed parametre

Using both static and dynamic IP parameters in both time and frequency domains we can calculate IP parameter profiles and maps. These profiles and maps will show us the areas containing metal ore bodies or enrichments of some contaminant(s) in ionic form.

10.7 Applicability

10.8 Advantages of the method

IP methods are suitable for surveying metallic ore minerals (pyrite, chalcopyrite, magnetite, etc.) clay content determination of the rocks and for solving environmental problems, ground and water base contamination detection and characterization because of the metallic, membrane and redox polarizations.

10.9 Disadvantages of the method

The main disadvantages of this method are its very high sensitivity to electric and electromagnetic noise and the relatively long measuring time. Specifically, so-called non-polarized electrodes should be used for measurements especially in the time domain.

10.10 Industrial solutions—Purchasable instruments

Several types of IP instruments are available. IRIS time domain IP instruments are listed below with their details.

10.10.1 SYSCAL Junior (2 channels - 100 W resistivity meter) [19]



Figure 46. SYSCAL Junior Ro&IP instrument

Main features

- Compact
- Measurement of electrical resistivity & chargeability (IP)
- 2 simultaneous reception channels
- Outputs : 400 V – 100 W – 1.25 A.

Outstanding features

- Microprocessor controlled measurement of electrical resistivity and chargeability
- LCD display with 4 lines of 20 characters
- Display of voltage, intensity, SP, standard deviation
- Computation of resistivity for most electrode arrays: Schlumberger, Wenner, Gradient, Dipole-Dipole, Pole-Dipole, Pole-Pole...
- Internal memory for more than 44 800 readings, and data transfer to PC through USB or serial link
- Capability to drive automatic multi-electrode switching system (Switch Plus and Switch Pro).

Output current specification

- Intensity up to 1250 mA
- Voltage up to 400V (800V peak to peak)
- Power up to 100 W
- Selectable cycle time of 0.25, 0.5 , 1, 2, 4 or 8s and Current measurement precision: 0,5% typical.

Input voltage specification

- 2 simultaneous reception channels
- Measuring process: automatic ranging and calibration
- Input impedance : 100 M Ω
- Input voltage protection up to 1000V, range from –15 V to +15 V
- Rejection filters for 50 Hz and 60 Hz
- Voltage measurement precision: 0.5% typical
- Noise reduction: continuous stacking selectable from 1 to 255 stacks.
- SP compensation through linear drift correction

- Resistivity accuracy: 0,5% typical
- Induced polarization (chargeability) measurement over 20 predefined windows
- Chargeability a.: 1% of measured value for input voltage higher than 10 mV.

Accuracy and reliability

- Noise monitoring before injection
- SP compensation including linear drift
- Digital stacking for noise reduction
- Standard deviation computation
- Weather proof
- Wide operational temperature range from -20°C to +70°C
- Shock resistant fibre-glass case.

General specifications

- Dimensions : 31 x 21 x 21 cm
- Weight: 10 kg
- Operating temperature : -20 to +70 °C
- Data flash memory : more than 44 800 readings
- USB and serial link RS-232 for data download
- Possibility of data storage on external SD card: 7 000 000 readings (option)
- Power supply: internal rechargeable 12V, 7 Ah battery or external 12V car battery
- Autonomy with internal battery: more than 6000 readings at 20 mA output current and 10 kΩ electrode resistance with 10 seconds injection time for each reading
- Emergency push button for security.

10.10.2 SYSCAL R1 Plus (2 channels - 200 W resistivity metre) [20]



Figure 47. SYSCAL R1 Plus Ro&IP instrument

Main features

- Compact
- Measurement of electrical resistivity & chargeability (IP)
- 2 simultaneous reception channels
- Outputs : 600V/1200Vp-p-200W-2.5A.

Outstanding features

- Power source, transmitter and receiver in a single unit
- Fully automatic measurement controlled by a micro-processor: automatic self-potential correction, automatic ranging, digital stacking, error display in case of procedure troubles
- Display of noise level before measurement
- Measurement and display of ground resistance, current, voltage, self-potential and standard deviation
- Computation of the apparent resistivity for the various electrode arrays: Schlumberger & Wenner (sounding or profiling), Dipole-Dipole, Gradient...
- Measurement and display of the chargeability (IP) through up to 20 predefined windows
- Multi-electrode mode for use with the automatic switching system
- Storage of data in the internal memory (44 800 readings)
- Possibility of data storage on external SD card: 7 000 000 readings (option)
- Communication port for serial or USB data transfer
- Emergency Push button for security

Transmitter specifications

- Maximum output power: 200 W
- Automatic fitting of the current and voltage output values: Maximum output voltage: 600V/1200Vp-p
- Maximum output current: 2500 mA
- Output current specifications
- Resolution: 10 μ A
- Accuracy: Standard 0.3%
- Max 1% from -20°C to 70°C
- Waveforms: choice of [ON+, ON-] or [ON+, OFF, ON-, OFF] (for IP measurements), with a selectable pulse duration (0.25, 0.5, 1, 2, 4 or 8s).

Receiver specifications

- 2 simultaneous reception channels

- Input impedance: 100 MΩ
- Input overvoltage protection
- Input voltage range: -15 V to +15 V
- Automatic SP bucking (± 10 V) with linear drift correction
- 50/60 Hz power line rejection
- Voltage measurement specifications:
 - o Resolution: 1 μ V after stacking
 - o Accuracy: Standard 0.3%
 - o Max 1% from -20°C to 70°C
- Continuous digital stacking up to 255 stacks
- Chargeability accuracy: 1% of value for input voltage higher than 10 mV value for input voltage higher than 10 mV.

Accuracy and reliability

- Noise monitoring before injection
- SP compensation including linear drift
- Digital stacking for noise reduction
- 1 μ V resolution after stacking
- Standard deviation computation
- Weather proof
- Wide operational temperature range from -20°C to +70°C
- Shock resistant fibre-glass case.

General specifications

- LCD display with 4 lines of 20 characters
- Power supply (battery):
- Internal 12 V / 7.2 Ah rechargeable, External 12 V
- Operating temperature range: -20°C to 70°C
- Storage temperature: -40°C to 80°C
- Dimensions: 31x21x31 cm
- Weight: 11 kg (including battery).

10.10.3 SYSCAL R2 (Resistivity and IP system for sounding and profiling) [21]



Figure 48. SYSCAL R2 Ro&IP instrument

Main features

- Powerful system
- 800 V – 2.5 A
- Easy to use / Accurate.

Outstanding features

- Powerful: The SYSCAL R2 uses an external DC source for energizing the ground (800 V maximum output voltage):
 - 250 W DC/DC converter supplied by a 12V battery
 - 1200 W AC/DC converter supplied by a standard motor generator
- Automatic: The SYSCAL R2 is controlled by a microprocessor for:
 - o automatic Self-Potential compensation
 - o automatic gain ranging for both current and voltage measurements
 - o automatic digital stacking to enhance the signal-to-noise ratio and to optimize the acquisition time.
- o Easy to use: The SYSCAL R2 computes and displays the apparent resistivity automatically for the most common electrode arrays (Schlumberger and Wenner sounding and profiling – gradient – dipole-dipole ...)
- o Induced Polarization measurement: The SYSCAL R2 measures and displays the apparent chargeability (Induced Polarization parameter) through up to four chargeability programmable windows. Its Induced Polarization parameter completes the information given by the classical DC electrical parameter.

Transmitter specifications

- Maximum output voltage: 800 V (1600 V peak to peak)
- Maximum output current 2.5 A supplied by an external DC source (DC/DC or AC/DC converter).
- Output current specifications:
 - o Resolution: 10 μ A
 - o Accuracy: standard 0,3 % - max. 1% from - 20°C to +70
- Output current waveform:
 - o Frequency domain [ON+, ON-] for resistivity.
 - o Time domain [ON+, OFF, ON-, OFF] for resistivity and chargeability.
 - o Pulse duration (ON time) programmable from 0.25 to 10 s, with preset values of 0.5 s - 1 s or 2 s.
- Thermal circuit breaker for overheating protection.

Receiver specifications

- Input impedance: 10 Mohms min.
- Input over voltage protection.

- Input voltage range:
 - o Standard: -5 V to +5 V
 - o With a Multi-electrode system: -10 V to +10V
- Automatic SP bucking
- 50 Hz and 60 Hz power line rejection.
- Ground resistance measurement: from 0.1 to 1000 k Ω .
- Voltage measurement specifications:
 - o Resolution: 1 μ V after stacking.
 - o Accuracy: standard 0,3 % - max. 1 % from - 20°C to +70°C.
- Chargeability measurement specifications:
 - o Resolution: 0.1 mV/V.
 - o Accuracy: 1 % of displayed value for a voltage greater than 10 mV.
- Continuous digital stacking up to 250 stacks.

Accuracy and reliability

- A noise monitoring system for pre-injection control, consisting of a DC digital voltmeter function.
- A line check/ground resistance measurement which permits to check that the electrodes are properly connected to the resistivity-meter.
- A low-pass analog filter, which reduces the effect of higher frequency natural and cultural noises (50-60 Hz).
- A resolution after stacking of 1 μ V allowing to measure some low-amplitude signals; the standard deviation is displayed to give an indication of the noise level during the measurement.
- high-latitude cold countries
- dusty and hot desert areas
- high-humidity tropical forests
- Its field-conditioning specifications include:
 - A shock and vibration resistant fibre-glass case.
 - A large operating temperature range (-20°C to +70°C).
 - A weather-proof design for operation up to 100% humidity.

General specifications

- LCD display of 2 lines of 20 characters.
- Weather-resistant case.
- Dimensions: 31 x 21 x 21 cm.
- Weight: 6 kg including dry cells.
- Power supply:
 - o Internal six 1.5 V D size dry cells (over 300 hours operation autonomy at 20°C) and External DC source for ground energization (DC/DC or AC/DC converter).
- Operating temperature range: -20°C to +70°C (-40°C to +70°C in option).
- Storage temperature: -40°C to +80°C.

10.10.4 SYSCAL Pro (10 channels - 250W resistivity metre) [22]



Figure 49. SYSCAL Pro Ro&IP instrument

Main features

- Ten simultaneous channels: for high speed data acquisition, up to 1 000 rdgs/mn
- Up to 800 - 1 000v, 2.5a outputs: for penetration & data quality
- Automatic switching capability: for 24, 48, 72, 96, 120, up to 1 300 electrodes
- Resistivity & induced polarization: twenty ip chargeability windows

Outstanding features

- The SYSCAL Pro Switch is a versatile electrical resistivitymetre which combines a transmitter, a receiver and a switching unit in one single casing. It is supplied by a 12V battery.
- The measurements are carried out automatically (output voltage, stacking number, quality factor) after selection of limit values by the operator, and are stored in the internal memory.
- The output specifications are 800V (1 600V peak-to-peak) in switch mode, 1000V (2 000V peak-to-peak) in manual mode, 2.5A, and 250W with the internal converter and a 12V battery.
- The SYSCAL Pro Switch uses multi-core cables for controlling a set of electrodes connected in a line or in several lines. The standard number of electrodes: 24, 48, 72, 96, 120, can be increased through Switch Pro units for 2D or 3D ground images.
- The ten channels of the system permit to carry out up to 10 readings at the same time for a high efficiency.
- The Induced Polarisation chargeability (IP) is also measured through 20 windows for a detailed analysis of the decaying curves displayed on the graphic LCD screen.
- The SYSCAL Pro Switch unit can be operated with cables in boreholes, or cables pulled on the ground by a vehicle or on the surface of the water by a boat for continuous acquisition surveys.
- The SYSCAL can be used for time lapse readings (monitoring)

Transmitter specifications

- Max voltage: 800V in switch mode
- Max voltage: 1 000V in manual mode
- Max current: 2.5A, typ. accuracy 0.2%
- Max power : 250W with internal DC/DC converter and 12V external battery; 1200W with external AC/DC and Motor Gene.
- Option 25mA max for readings on samples
- Pulse duration: 0.2s, 0.5s, 1s, 2s, 4s, 8s
- Internal 12V, 7Ah battery, plug for ext. batt.

Receiver specifications

- Automatic ranging, 10 input channels
- Input impedance: 100 Mohm

- Max voltage channel 1: 15V
- Max voltage sum of channel 2 to 10: 15V
- Protection up to 1 000V
- Typ accuracy: 0.2%, resolution: 1 microV
- Digital rejection better than 120 db at power lines 50 and 60 Hz
- Stacking process, SP linear drift correction
- Reading of current, voltage, standard dev.,
- 20 IP windows (preset or selectable).

General specifications

- Memory: 40 000 readings USB & SD card link
- GPS input for coordinates
- Fibre glass casing, weather proof
- Temperature range: -20 to +70°C
- SYSCAL Pro Switch 48: 31x23x36cm,
- Weight: 13kg, Cable w/ 24 take-out: 23kg.

10.10.5 SYSCAL Pro Deep Marine (10/20 channels - 2500W resistivity metre) [23]



Figure 50. SYSCAL Pro Deep Marine Ro&IP instrument

Main features for salt water environment

- 13 graphite floating nodes (A – B – P1... P11) - 4 metres spaced
- GPS input on the Syscal Pro for an accurate location of the profile
- Array type: Reciprocal Wenner array (AB at the centre and MN apart from AB)
- Data acquisition speed: 10 resistivity data points each 2 s (minimum time required by GPS)
- Boat speed during acquisition: 3-4 km/h
- About 3000 data points acquired in the section below
- $V_{ab} \approx 50 \text{ V}$ - $I_{ab} \approx 2.5 \text{ A} \Rightarrow$ Grounding resistance $\approx 20 \Omega$
- Water resistivity given by a conductivity-metre: $0.20 \Omega\text{m}$ (good correlation with the resistivity computed with the first reception dipole)
- Water layer thickness: between 1 and 3 metres

10.10.6 SYSCAL Junior Switch 72 (2 channels - 100 W resistivity metre 72 electrodes string) [24]

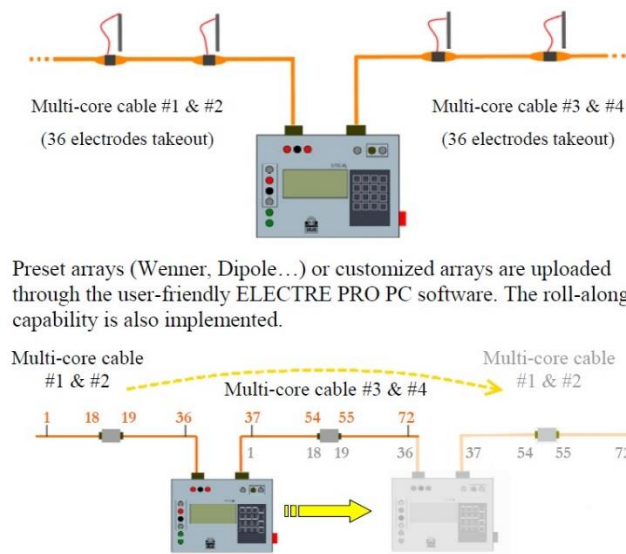


Figure 51. SYSCAL Junior Switch 72 Ro&IP System

Main features

- Compact, easy to use
- Automatic ranging
- Automatic switching
- 2 measuring channels
- Outputs: 400 V- 100 W- 1.25 A

Outstanding features

- Aim: imaging the underground geological structures through surface electrical measurements
- Principle: transmitting a current I through two electrodes and measuring a voltage V with two other electrodes
- Apparent resistivity: $\rho = K \cdot V/I$, K depending on the chosen electrode array and the electrode separation
- Resistivity and IP pseudo-section: contoured plot of the apparent resistivity data, using the electrode distance as a pseudo-depth parameter
- True resistivity and IP section: contoured plot of the resistivity distribution obtained through the inversion of the measured data (using a nonlinear parameter fitting scheme)
- Applications: environmental studies, groundwater investigation, civil engineering, archaeology.

General specifications

- Weight: 13.8 kg
- Dimensions: 31 x 23 x 38 cm
- Weather proof
- Shock resistant fibre-glass case
- Operating temperature: -20 to +70 °C
- LCD display with 4 lines of 20 characters
- Data flash memory : more than 44 800 readings
- USB and serial link RS-232 for data download, possibility of data storage on external SD card with a capacity of 7 000 000 readings (option)
- Power supply: two internal rechargeable 12V / 7.2 Ah batteries ; optional external 12V backup car battery for transmitter power
- Autonomy with internal battery: several thousands of readings
- Weight of a 18 takeout multi-core cable on a reel: about 15 kg (for 5m spacing)
- Emergency push button for security

10.10.7 SYSCAL Pro Switch (10 channels - 250W resistivity metre 48 to 96 electrodes string) [22]

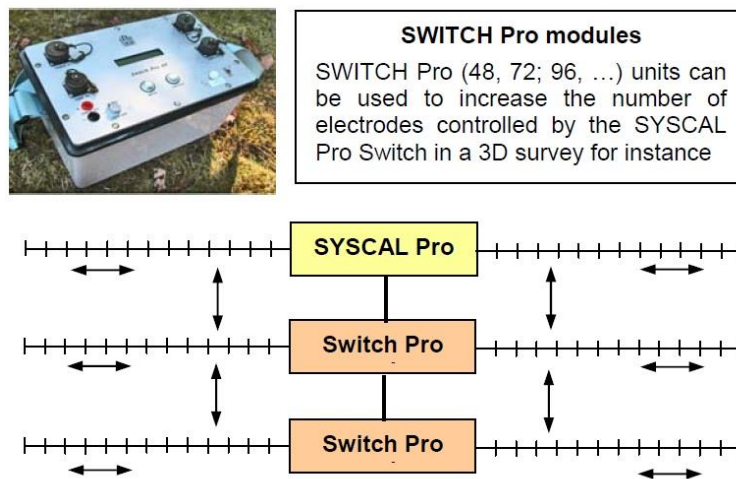


Figure 52. SYSCAL Pro Switch Ro&IP System

Main features

- The SYSCAL Pro Switch units use segments (seg) of multi-core cable which are reversible and interchangeable.
- For instance, the SYSCAL Pro Switch 48 with 10m spacing has 4 segments of cable a, b, c, d, with 12 electrodes each, for a total line length of 480m. The SYSCAL is placed in the middle of the line, between segments b and c.
- If the profile to measure is longer than the linelength, a ROLL ALONG technique can be applied where, after a first set of readings with (a, b, c, d), segment a is placed after segment d to form a new (b, c, d, a) combination etc.

10.10.8 SYSCAL Pro for continuous land survey [22]

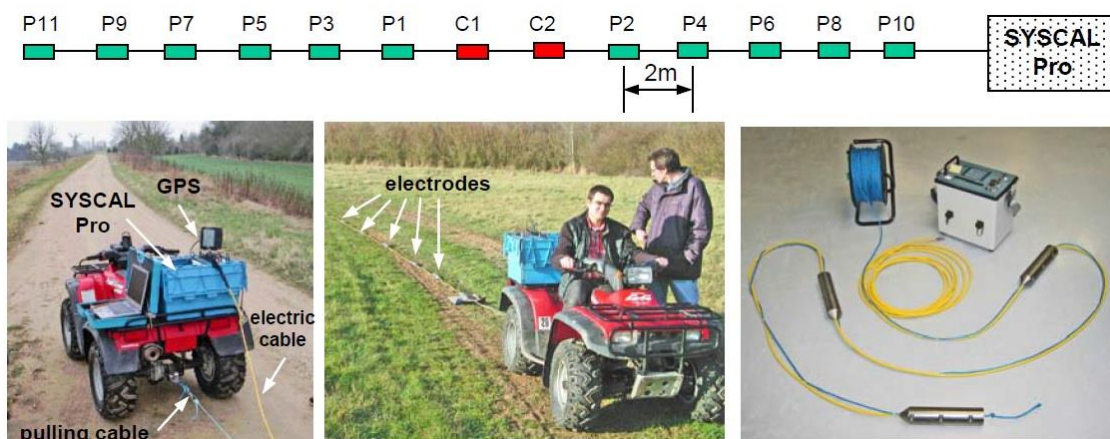


Figure 53. SYSCAL Pro for continuous land survey Ro&IP System

Main features

- The SYSCAL Pro can be used with a specific cable pulled on the ground by a light vehicle, for a continuous acquisition of resistivity readings.
- The cable features 13 cylindrical stainless steel electrodes (8cm diameter 25cm length, 4.2kg) at 2m spacing:
- 2 for transmitting the current,

- 11 for simultaneously measuring
- ten potential channels.
- A PC continuously records the 10 resistivity values and the GPS data, displays profiles in real time
- Recommended electrode array: reciprocal Wenner Schlumberger
- Penetration depth: about 5m
- Best conditions: wet grounds
- Acquisition speed: typ. 3km/h.

10.10.9 SYSCAL Pro for river and sea survey [22]

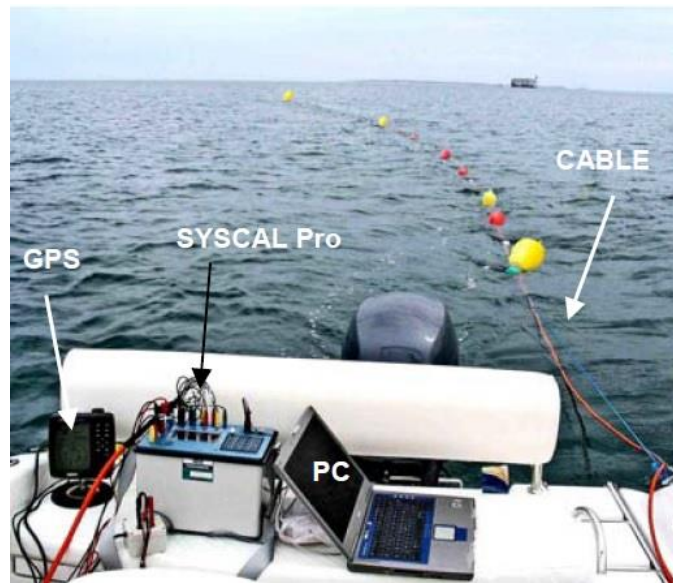


Figure 54. SYSCAL Pro for river and sea survey Ro&IP System

Main features

- The SYSCAL Pro can be used with a specific cable pulled on the ground by a light vehicle, for a continuous acquisition of resistivity readings.
- The cable features 13 cylindrical stainless steel electrodes (8cm diameter 25cm length, 4.2kg) at 2m spacing:
 - 2 for transmitting the current,
 - 11 for simultaneously measuring ten potential channels.
- A PC continuously records the 10 resistivity values and the GPS data, displays profiles in real time
- Recommended electrode array: reciprocal Wenner Schlumberger
- Penetration depth: about 5m
- Best conditions: wet grounds
- Acquisition speed: typ. 3km/h.

10.11 Case Study Examples

10.11.1 Geotechnical Study

Figure 55 shows a characterization of the slope formations overburden lying over the shales bedrock measured for a tunnel project.

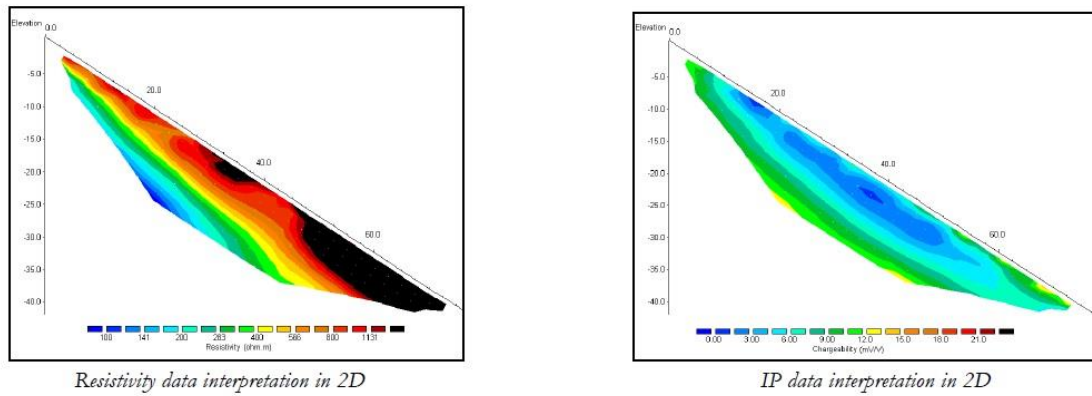


Figure 55. 2D resistivity and IP chargeability sections showing the bedrock in a tunnel project

10.11.2 Mineral Exploration Study

Induced Polarization is a phenomenon which occurs with some types of minerals such as sulphide particles (Figure 56).

Over a massive sulphide ore body the resistivity parameter is low and chargeability is high (on the left side of Figure 56) but over disseminated ore body both parameters are higher than average (on the middle and right sides of Figure 56).

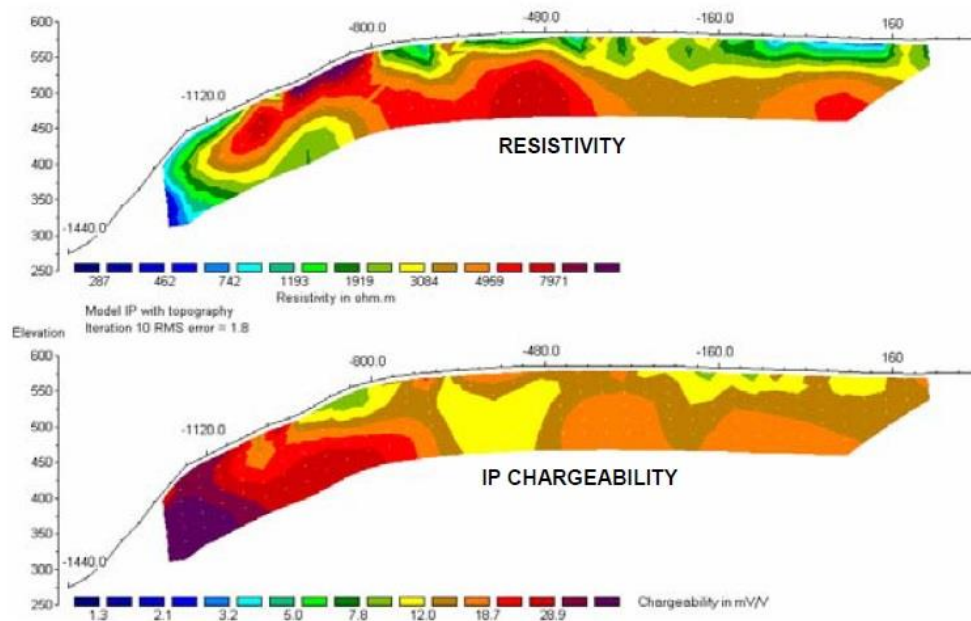


Figure 56. 2D resistivity and IP chargeability sections over a massive and disseminated [28]

10.11.3 Gold Exploration Study

A dyke with sulphide and gold minerals appears in Figure 57 with very low resistivity and high chargeability.

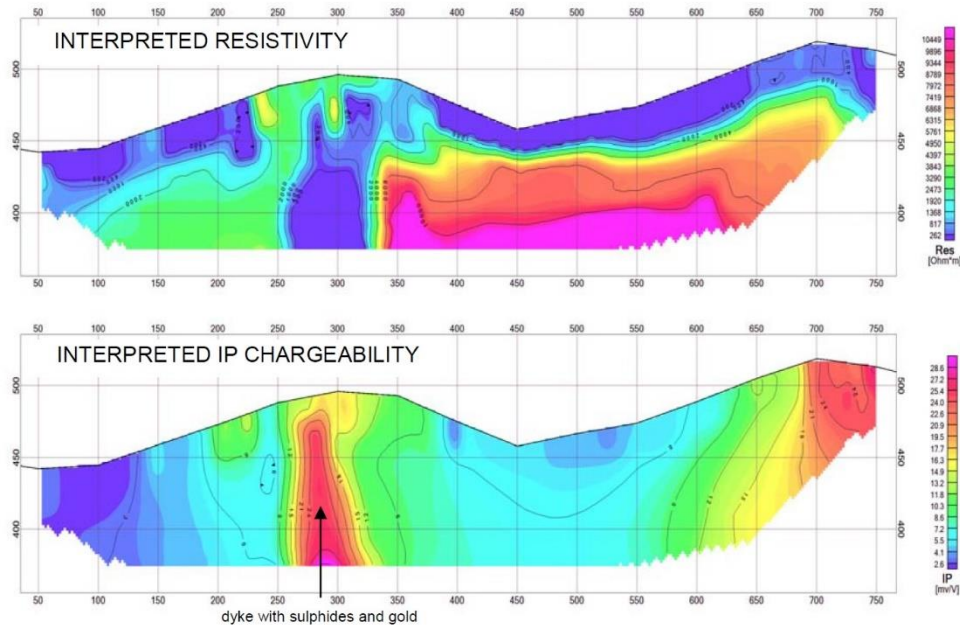


Figure 57. 2D resistivity and IP chargeability sections over a dyke with sulphide and gold minerals [31]

10.11.4 Refuse Dump Study

Figure 58 shows the vertical WAV section over a Hungarian refuse dump near Felsőtelekes. As can be seen, there are weighted amplitude values (WAV) over ten percent, indicating high and very high contaminated areas under the surface caused by metallic and redox polarization effects. The corrected apparent conductivity vertical section is presented in Figure 58. The thick black contour line shows the points of the section where the corrected conductivity value is the critical 100 mS/m. The WAV map (Figure 56) calculated at a 10 m reference depth inform about the lateral distribution of the polarizable ore concentration in the Felsőtelekes waste rock body.

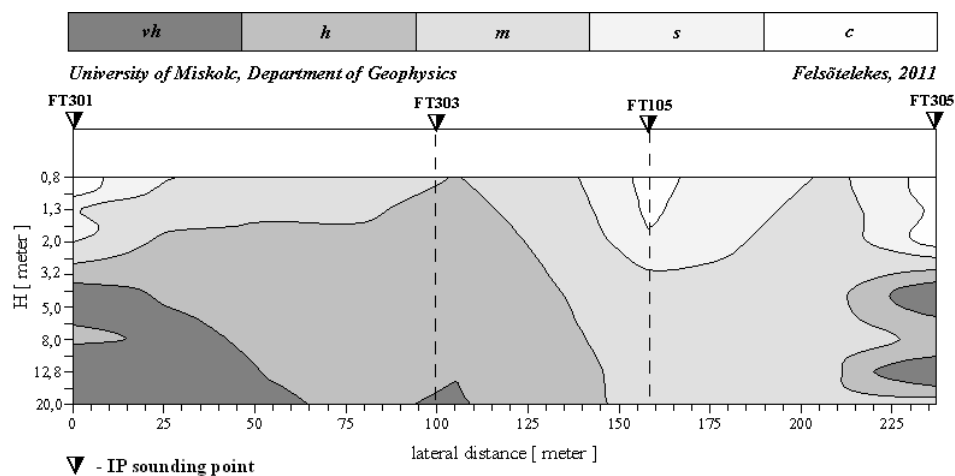


Figure 58. Vertical WAV section over a refuse dump (WAV levels: > 0.2 – very high; 0.1-0.2 – high; 0.05-0.1 – medium; 0.02-0.05 – small; < 0.02 – clean) [11]

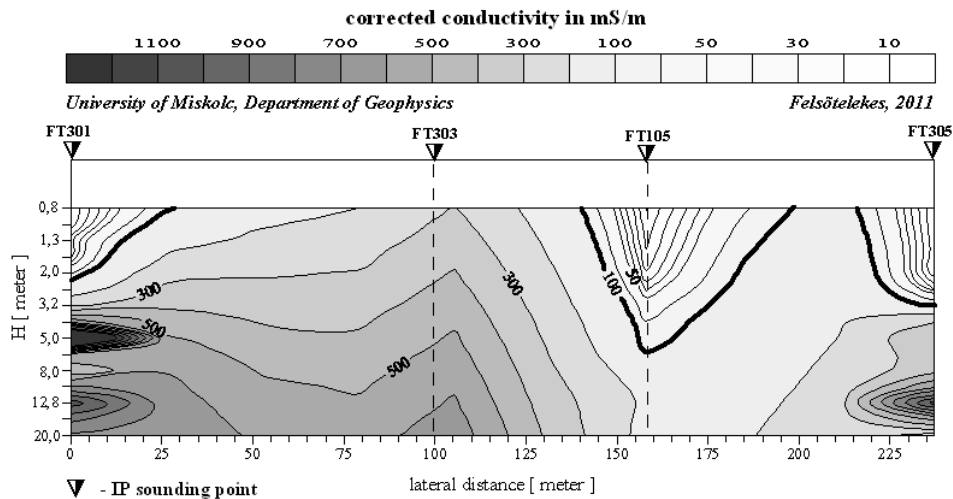


Figure 59. Vertical section of the corrected apparent conductivity over a refuse dump [11]

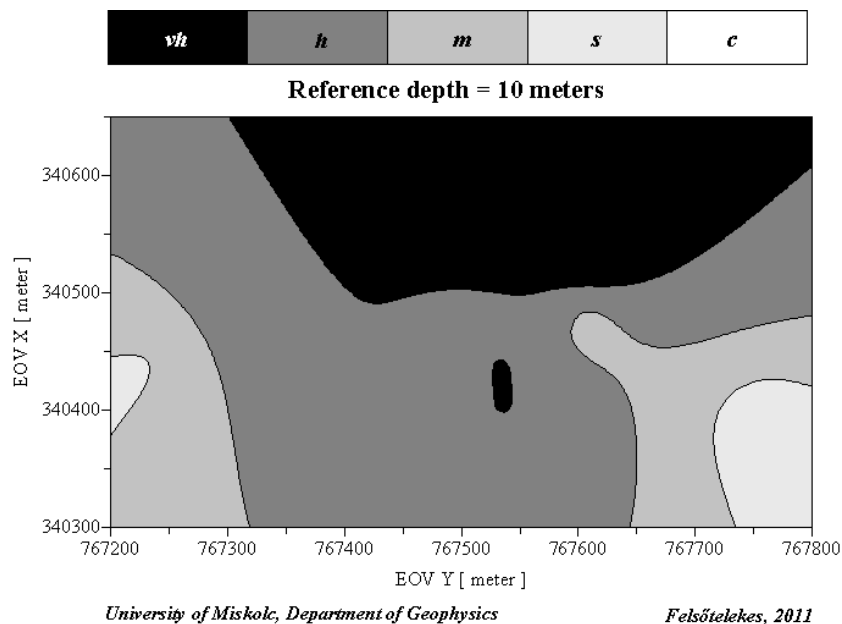


Figure 60. WAV map at 10 m reference depth over a refuse dump [11]

10.11.5 Waste Site Study

The vertical WAV section calculated from IP data measured above the Nagytétény (Hungary) communal waste site indicates very high level of contamination is presented in Figure 61. The vertical section of corrected conductivity is presented in Figure 62, where the lighter contour lines show the corrected conductivity value of 50 mS/m, indicating medium level of contamination.

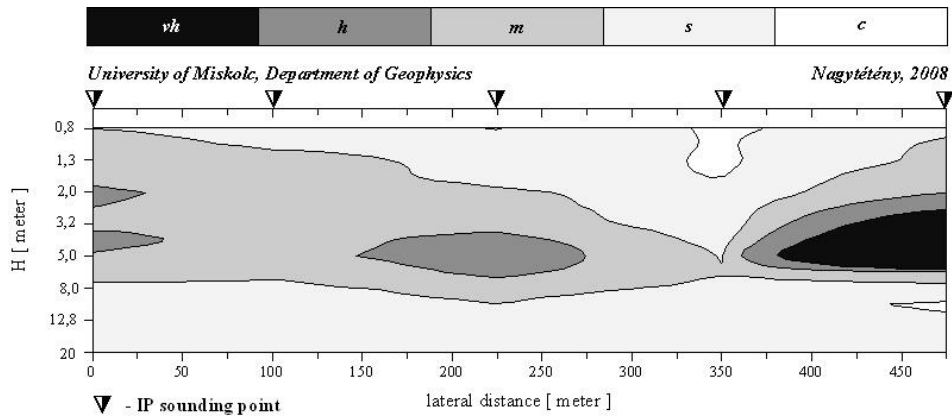


Figure 61. Vertical WAV section over Nagytétény waste site (WAV levels: > 0.2 – very high; 0.1-0.2 – high; 0.05-0.1 – medium; 0.02-0.05 – small; < 0.02 – clean) [11]

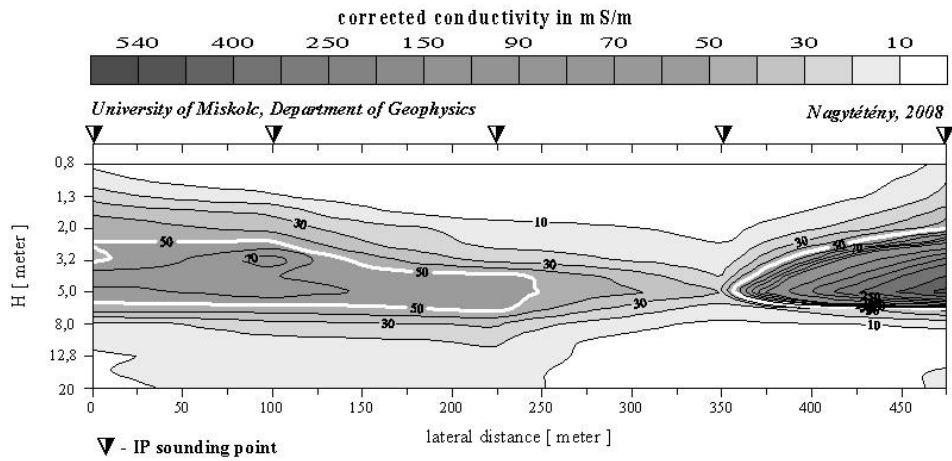


Figure 62. Vertical section of the corrected apparent conductivity over Nagytétény waste site [11]

10.11.6 Oil Contaminated Site Study

As shown in Figures 63 and 64 (see red colour tones) the oil contaminated bodies under the surface appear in high chargeability interval.

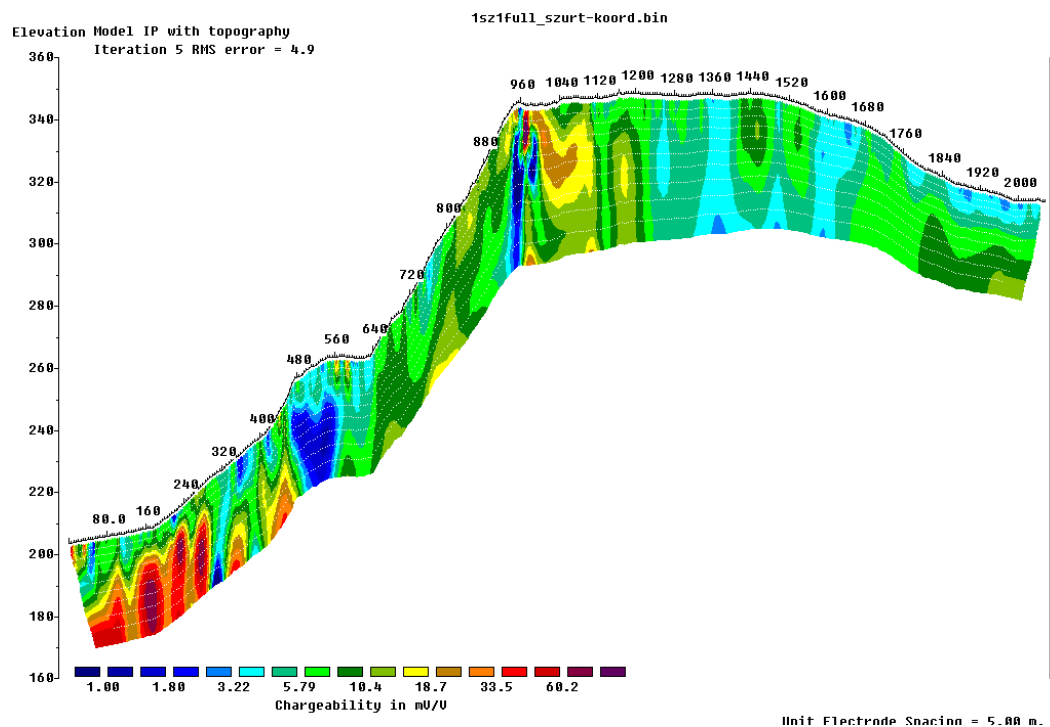


Figure 63. 2D IP chargeability section in dip direction over a Hungarian oil contaminated site [12]

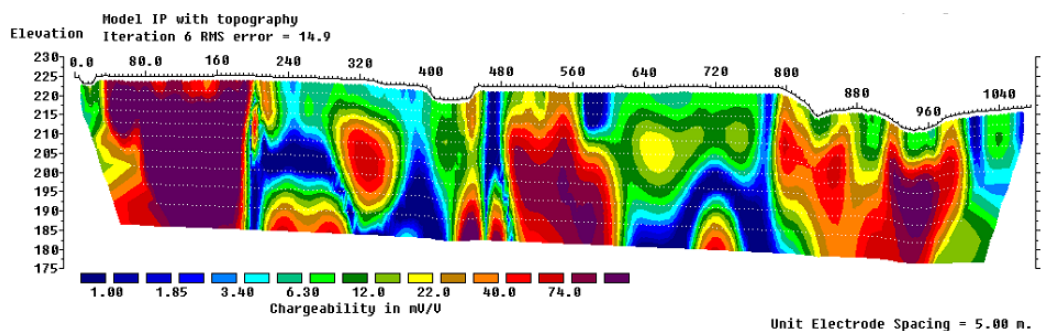


Figure 64. 2D IP chargeability section in strike direction over a Hungarian oil contaminated site [12]

10.11.7 Red Sludge Tailings Study

Both parameters, the WAV and corrected conductivity parameter have a very high sensitivity to the contaminations. We checked the parameter sensitivity around a red sludge tailings cassette has been tested, where the REF1 sounding point was situated on the red sludge. In both figures below (Figures 65 and 66) the contamination plumes escaping from the cassette are clearly visible.

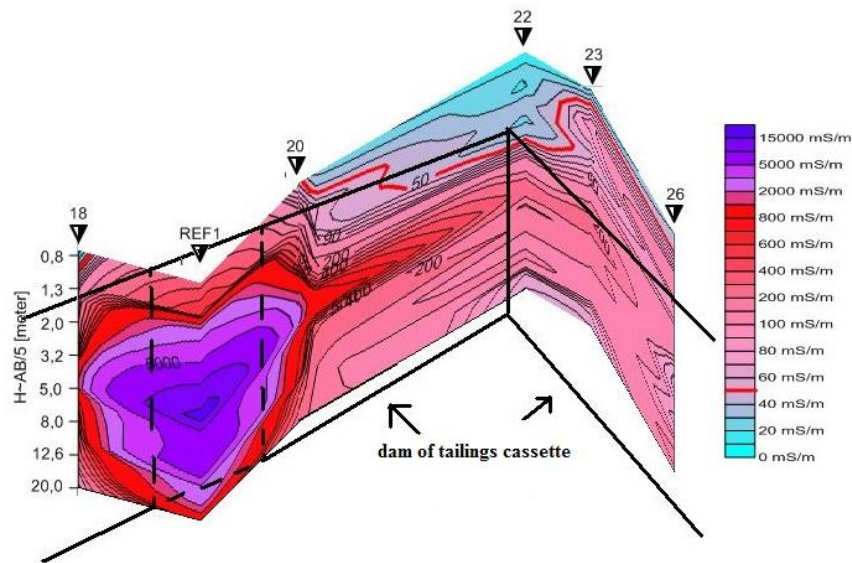


Figure 65. Vertical polyline section of the corrected apparent conductivity around a red sludge tailings cassette [12]

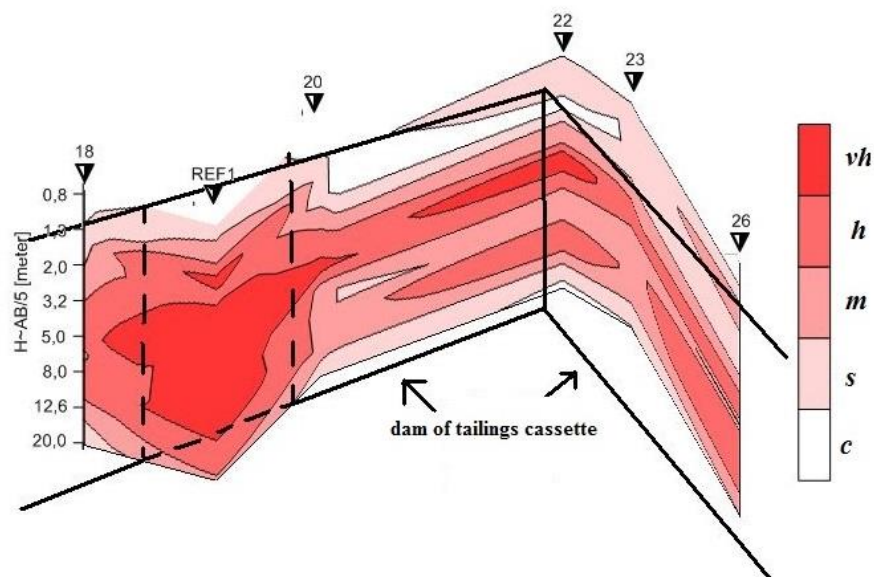


Figure 66. Vertical polyline section of the WAV parametre around a red sludge tailings cassette[12]

10.12 Conclusion

It can be concluded, that the IP method is a very useful method for mineral exploration and contamination detection in both time and frequency domains, respectively. However, the measurement of the IP parameters in water can be achieved only in case of a contact robot.

Suggested/Suggested with comment (suggested in 2.2)/Unsuggested method

10.13 References

- [1] Keller, G. W., Frischknecht F. C. 1966: **Electrical Methods in Geophysical Prospecting** Pergamon Press, Oxford.
- [2] Kearey, P., Brooks, M., Hill, I. 2002: **An Introduction to Geophysical Exploration** Blackwell Publishing Company, Oxford.
- [3] Sumner, J. S. 1976: **Principles of Induced Polarization for Geophysical Exploration** Elsevier Scientific Publishing Company, Amsterdam.
- [4] Turai E. 1981: **GP time-domain görbék TAU-transzformációja** Magyar Geofizika XXII/1, 1981, 29-36. (in Hungarian)
- [5] Turai, E. 1985: **TAU-Transformation of Time-Domain IP Curves** ANNALES Univ. Scien. Budapestinensis de Rolando Eötvös Nom. I-II, pp. 182-189.
- [6] Turai, E., Elsen, R., Limbrock, K. 1992: **Analysis of IP time-domain data measured above a waste site near Offheim using TAU-transformation of IP chargeability curves** TEMPUS pr. Report, DMT Institute for Applied Geophysics, Bochum.
- [7] Turai, E. 2004: **IP Data processing results from using TAU-transformation to determine time-constant spectra** Geophysical Transactions 44, pp. 301-312.
- [8] Turai, E. 2011: **Data Processing Method Developments using TAU-transformation of time domain IP data** Acta Geodaetica et Geophysica Hungarica 46(4), pp. 391-400.
- [9] Turai, E. 2012a: **Application possibilities of IP method in the fields of environmental protection, ore- and direct hydrocarbon exploration** GEOSCIENCES AND ENGINEERING 1(2), pp. 161-166.
- [10] Turai, E. 2012b: **Some field measurement results of IP method** GEOSCIENCES AND ENGINEERING 1(2), pp. 167-172.
- [11] Turai, E., Nádas, E. 2014: **In Field Classification of Waste Site Material Using Tau-Transformation of IP Data** 18th International Conference of Waste Recycling, Paper wr18-paper-Turai
- [12] Turai E., Nádas E., Szilvási M. 2016: **New results of the field geoelectric geophysical methods applied in environmental assessments** Technical Sciences in the North East Hungarian Region 2016 Conference, Conference Proceedings, pp. 1-10. (in press in Hungarian)
- [13] Wait, J. R. 1959: **Overvoltage Research and Geophysical Applications**, Pergamon Press, London.
- [14] <http://www.expins.com/item/ultra-minires>
- [15] http://www.iris-instruments.com/Product/Brochure/brochure_geophy.html
- [16] <http://www.iris-instruments.com/Product/Brochure/syscal.html>
- [17] <http://www.iris-instruments.com/Product/Brochure/vip-elrec.html>
- [18] <http://www.iris-instruments.com/Product/Brochure/FullWaver.html>
- [19] http://www.iris-instruments.com/Pdf_file/Junior_Gb.pdf
- [20] http://www.iris-instruments.com/Pdf_file/R1Plus_Gb.pdf
- [21] http://www.iris-instruments.com/Pdf_file/R2_Gb.pdf
- [22] http://www.iris-instruments.com/Pdf_file/SyscalPro_Gb.pdf
- [23] http://www.iris-instruments.com/Pdf_file/MarineSurvey.pdf
- [24] http://www.iris-instruments.com/Pdf_file/Junior_72_Gb.pdf
- [25] http://www.iris-instruments.com/Pdf_file/Res6.pdf
- [26] http://www.iris-instruments.com/Pdf_file/Induced_Polarization/operation_transmitters.pdf
- [27] http://www.iris-instruments.com/Pdf_file/ELREC_Lite_ELREC_Lite_G_GB.pdf
- [28] <http://www.gddinstrumentation.com/ip-transmitter>
- [29] <http://www.gddinstrumentation.com/i-p-receivers>
- [30] <http://www.aidush.com/en/index.php/default/content/13189.html>
- [31] <http://www.iris-instruments.com/mineral-exploitation.html>

11 WATER SAMPLER AND STORAGE

11.1 Theoretical Background

Water quality refers to the biological, chemical, radiological and physical characteristics of water. The many types of measurements of water quality indicators show the complexity of water quality. Water exists in equilibrium with its surroundings, which is why the most accurate measurements of water quality are made on-site. Measurements commonly made on-site and in direct contact with the water source in question include temperature, dissolved oxygen, pH, turbidity, conductivity and so on. Complicated measurements are often made in a special laboratory requiring a water sample to be collected, preserved, transported, and analyzed at another location. So water sampling is the process of taking a portion of water for analysis or other testing, which can be drinking water to check that it complies with relevant water quality standards, or bathing water to check that it is safe for bathing, or river water to check for pollutants, or intrusive water in a building to identify its source. One objective of surveillance is to assess the quality of the water supplied by the supply agency and of that at the point of use. Any significant difference between the two has important implications for remedial strategies. Samples have to be taken from locations that are representative of the water source, storage facilities, treatment plant, distribution network, points at which water is delivered to the consumer, and points of use. [27], [28]

11.2 Theoretical summary of possible design

High pressure storage units and water sampler are used in the deep-sea environment around the world. The features of commercially available, in situ sensors are not able to meet the requirements of deep-sea applications, thus offshore or onshore laboratories are used for analysis of water samples. Most of the research has been performed in recent decades, where water storage and sampling units were used. This report contains a short overview which can be found in oceanic studies.

The intake process of the water sampling and the sampler capacity play a key role in classifying the four main categories of water sampling units (Table 9). [7]

Sample intake	Sample capacity	
	Fixed	Variable
Passive	Fixed Passive	Variable Passive
Active	Fixed Active	Variable Active

Table 9. Sample capacities

Two types of sampler container capacity can be distinguished: variable or fixed. Variable capacity sampler containers include bag and syringe. These are created from glass, plastic and other materials. Fixed capacity sampler containers obtain samples using valves and other similar apparatus. [1], [7]

In some papers two kinds of sample intake methods are described. These methods are active and passive. The active intake method usually uses actuators like pumps. In case of passive types, the sampler is sent to the target fluid depth with lid open. [1], [7]

Other systems like BoWaSnapper, that correspond to passive fixed sampling which can conduct 21-layer water sampling at 200 mm intervals, include the Fine Scale Sampler, and the multi-horizon bottom water sampler which specializes in multilayer fluid sampling just above the sea bottom. Active fixed capacity water sampling like WHATS-II includes Water and Hydrothermal-fluid Atsuryoku Tight Sampler which uses a pump for high temperature sampling. [2], [3], [4], [5], [7]

Passive variable capacity water samplers have not been used yet in seawater. The active variable capacity samplers sometimes attach a bag-, syringe water sampler. [1], [8], [9]

There are some other publications, dealing with variable samplers. In some cases these samplers are used in high temperature conditions, e.g. Mat Sampler which use syringes and a manipulator. [10], [11], [12], [13], [14], [15], [16], [17], [18], [7]

11.3 Processes with the stored samples

Different investigations can be conducted with stored samples in accredited laboratories. Typically mass spectrometry and chromatography methods can be considered. The following list (Table 10 and Table 11) shows available packages at the international laboratory station of the Australian Laboratory Services Ltd. The minimum sample volume is 60 ml for the investigation in the ALS laboratory, but usually similar element detections can be reached in similar European laboratories from smaller amounts like 10-20 ml volume.

The different analyses are summarised in the Table 10 and Table 11.

11.3.1 Hydrogeochemistry Package ME-MS14HR

Analysis for:

- trace metals
- total dissolved solids
- conductivity
- alkalinity
- pH
- anions

200 USD/sample (whole package only)							
<i>det. lim. in µg/l</i>		<i>det. lim. in µg/l</i>		<i>det. lim. in µg/l</i>		<i>det. lim. in µg/l</i>	
Ag	0.005	Fe	0.03 mg/L	Re	0.005	Y	0.005
Al	0.9	Ga	0.05	Sb	0.01	Zn	0.9
As	0.05	Hg	0.05	Se	0.2	Zr	0.05
B	5	K	2 mg/L	Si	0.05 mg/L	TDS	3 mg/L
Ba	0.1	Li	0.2	Sn	0.2	Conductivity	2 µS/cm
Be	0.005	Mg	0.1 mg/L	Sr	0.05	Alcalinity	1 mg/L
Bi	0.05	Mn	0.2	Te	0.01	pH	0.1 units
Ca	0.05 mg/L	Mo	0.05	Th	0.005	Br	0.05 mg/L
Cd	0.005	Na	2 mg/L	Ti	0.2	Cl	0.5 mg/L
Co	0.05	Ni	0.2	Tl	0.002	F	0.02 mg/L
Cr	0.5	P	0.3 mg/L	U	0.002	NO2	0.001 mg/L
Cs	0.005	Pb	0.05	V	0.05	NO3	0.005 mg/L
Cu	0.5	Rb	0.02	W	0.01	SO4	0.5 mg/L

Table 10. Determination limits for ME-MS14HR package code

11.3.2 Hydrogeochemistry Package ME-MS14L

Analysis for:

- trace metals
- total dissolved solids
- conductivity
- alkalinity
- pH
- anions by chromatography

56.50 Eur/sample (ME-MS14L)							
<i>det. lim. in µg/l</i>		<i>det. lim. in µg/l</i>		<i>det. lim. in µg/l</i>		<i>det. lim. in µg/l</i>	
Au	0.002	Cu	0.1	Ni	0.2	Ta	0.01
Ag	0.005	Fe	0.003mg/L	P	0.005mg/L	Te	0.01
Al	3	Ga	0.05	Pb	0.05	Th	0.005
As	0.05	Hf	0.005	Pd	0.005	Ti	0.2
B	3	Hg	0.05	Pt	0.005	Tl	0.002
Ba	0.05	In	0.01	Rb	0.01	U	0.002
Be	0.005	K	0.01mg/L	Re	0.002	V	0.05
Bi	0.01	La	0.005	S	0.2mg/L	W	0.01
Ca	0.02mg/L	Li	0.1	Sb	0.01	Y	0.005
Cd	0.005	Mg	0.005mg/L	Sc	0.01	Zn	0.5
Ce	0.005	Mn	0.05	Se	0.05	Zr	0.02
Co	0.005	Mo	0.05	Si	0.03mg/L		
Cr	0.5	Na	0.01mg/L	Sn	0.05		
Cs	0.005	Nb	0.005	Sr	0.05		
16.50 Eur/sample (MS14L-REE)							
<i>det. lim. in µl</i>		<i>det. lim. in µl</i>		<i>det. lim. in µl</i>		<i>det. lim. in µl</i>	
Dy	0.005	Gd	0.005	Nd	0.005	Tb	0.005
Er	0.005	Ho	0.005	Pr	0.005	Tm	0.005
Eu	0.005	Lu	0.005	Sm	0.005	Yb	0.005
40 Eur/sample (MS14L-ANPH)							
Br	0.05mg/L	NO3	0.005mg/L	pH	0.1	Conductivity	2µS/cm
Cl	0.5mg/L	SO4	0.5mg/L	TDS	3 mg/l	Alkalinity	1 mg/l
F	0.02mg/l						

Table 11: Determination limits for ME-MS14L package code

11.4 Industrial solutions – Purchasable instruments

In this part of the report some commercially available, deep ocean sampler will be detailed. These constructions can give ideas for later investigation.

11.4.1 Aqua Monitor

This device, called Aqua Monitor, was originally designed to collect versatile water and phytoplankton sampler as a part of an AUV. The device could be programmed for autonomous sampling or operated as a slave unit within an integrated system. Aqua Monitor equipment is able to collect 50 samples of up to 1000 ml each. The Figure 67 shows the equipment. [29]



Figure 67. Aqua Monitor device [29]

The construction can be divided to three parts. The first part is a high integrity syringe mechanism, which is used to capture the samples. The second part is a multiport valve, which distributes the samples to flexible bags. The sample store unit is the third main part, which includes flexible bags. The distributor multiport-valve has 50 outlets and one inlet and electrical motor to actuate it to the required position. The construction of the sampler unit permits programmability via a macro language which can be used for creating of unique, in situ sampling tasks. The reference says a special deep ocean version of Aqua Monitor is available, but the website of the manufacturer is not available. The system was used in the Denmark Strait at a depth of 1200 m sampling once per week for a year. [29]

11.4.2 AquaLab

AquaLAB is a water sampler which can collect 50 samples in deep ocean exploration projects. The volume of the collected samples is up to 1000 ml each. This construction uses high integrity 50-port rotary valve which injects the sample into titanium foil bags. These samples can store for post analysis. The equipment operates automatically in a time-series mode using a user pre-set interval or a master device which controls the time of sampling of the system. Package of AquaLAB includes the ESM-1 Plus controller/datalogger, which can be used for simple control tasks and is ideal for other external sensors. The system can program via a script based programming language, called Eco-Script programming language. Eco-Script has been designed to provide the user with maximum control and flexibility in implementing sampling times. Scripts can be used to include extra flushing, sample preservation, rejection or even in-situ sampling processing. [29]



Figure 68. AquaLab [29]

11.4.3 BallTrap

BallTrap is a compact and light-handling multisampler system, where the feature of a high number of samples is combined with minimum weight and volume. The main principle is to use tubes for water samples, blocked at each end by a sphere acting as a ball valve. The two spheres include a nipple. The tube is completely clear before the sampling process, the two spheres being out of the way of the water flow. When water sampling is over, the two spheres are released and they seal the tube. When the equipment is brought back on the deck, the air inlet nipple and the water outlet nipple are cleaned. To get the samples air or nitrogen is injected at the upper part of the tubes and sampled water is collected at the bottom part. [30]



Figure 69. BallTrap [30]

11.4.4 BoWa_Snapper - Multihorizon-Bottom Water Sampler K/MT 421

The BoWaSnapper is Multihorizon-BottomWaterSampler, which is suitable for deep-sea deployment and used for the investigation of the sediment-water interface such as particles, organisms or geochemical tracers. It has been developed in the Alfred-Wegener-Institute, Bremerhaven, Germany at the beginning of 2000. The equipment can be used at water depths between 20 m and 5500 m and has six vertically adjusted water bottles. The BoWaSnapper is equipped with an autonomous bottom releaser that closes the water bottles some minutes after the touch-down on the sea bed. [31]



Figure 70. BoWa_Snapper [31]

11.4.5 Bottom Water Sampler K/MT 420

The Bottom Water Sampler (K/MT 420) is designed for collecting water samples above the sea floor, especially taken from different water depths. The equipment includes 5 Niskin sample bottles each with a volume of 5 litres. The tanks are horizontally attached to the revolvable middle axis of the frame of the system and adjustable between 10 and 120 cm above the bottom. The axis of the Sampler is revolvably fixed to the outer frame and aligned with a current vane. The outer rack is also equipped with two current vanes for turning the whole instrument in the direction of flow. [31]



Figure 71. Bottom Water Sampler K/MT 420 [31]

11.4.6 NWS-11C5

The principle of operation of this water sampler is completely different from others. In general other samplers use valves or pumps to connect sampling lines to the sampling bags. In this system the water is taken into sampling bag by depressurizing the outside of the bag with a pump. Each sample line is independent from others and the tip tube is clamped until sampling time. The sampling unit can do automatic water sampling with unlimited clean condition. The unit can be used in the shallow sea, the apparatus has been made small and lightweight so that a small control vessel can easily install and collect it. [32]



Figure 72. NWS-11C5 [32]

11.4.7 Niskin Bottles

This bottle can be a part of a bigger sampler system, but it can work alone. It is a non-metallic, free-flushing sampler tank, which is recommended for general purpose water sampling. The main manufacturer of the bottles is Richter and Wiese. They can be used individually or serially attached on a hydrocable and activated by messenger or placed in any kind of multisampling system and activated by remote or pre-programmed command. The Standard PVC Niskin Type Sampler is made of grey PVC (RAL 7011) and features a spring closure made of latex tubing with optional stainless steel spring closure, clamp bolts for attachments on a cable and mounting blocks for Multisampling System attachment. All metal parts are made out of special V4A-stainless steel. [33]



Figure 73. Niskin Bottles

11.4.8 SBE 32 Carousel Water Sampler

SBE 32 Carousel Water Sampler is an innovative design, which has no problems associated with motor-driven types. In this construction each bottle has its own magnetically-activated lanyard release latch, so there are no moving-shaft seals that can bind up at low temperatures or under pressure. The heart of every Carousel is the magnetically-actuated lanyard release. A pressure-proof electromagnet at each bottle position is energized on command to release the latch holding the bottle lanyard. Titanium, acetal plastic, and other corrosion-resistant materials are used in the latch and magnet assembly. [34]

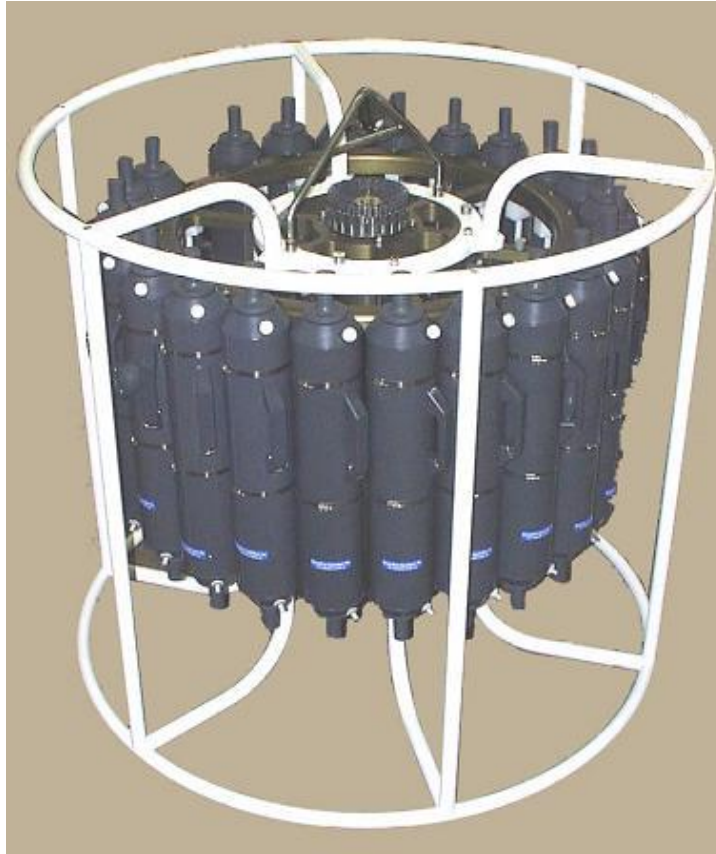


Figure 74. SBE 32 Carousel Water Sampler [34]

11.4.9 SBE 55 ECO Water Sampler

The ECO is a small-boat water sampler construction for coastal, estuarine, and large lake ecological monitoring. The ECO is a light and economical system including three or six bottles with 4-litre ECO sample bottles. The ECO can operate autonomously using internal batteries as power supply. During the operation process it closes bottles at selected depths, allowing deployment using nonelectrical wire or line. The closing mechanism of bottles is a magnetically actuated lanyard release latch derived from the SBE 32 Carousel Water Sampler, which has a long history of reliability and ease-of-use. A pressure-proof electromagnet is used to close the bottles, thus the magnets are energized and the lanyard released. The ECO can be configured with different modules fitted to actual scenario. Main control system is called Electronics Control Module (ECM) which controls the magnets and executes the data acquisition of the connected sensors. The systems includes an ECM, one or two lanyard release modules, three or six 4-liter ECO sample bottles mounted in saddle brackets and fastened with band clamps, stainless steel guard frame with integral lifting bail, and mesh panels for mounting the ECM, CTD, and other sensors that may be integrated with the CTD (e.g., dissolved oxygen sensor, fluorometer, turbidity sensor, etc.). [34]



Figure 75. SBE 55 ECO Water Sampler [34]

11.4.10 Water Sampler with CTD

This water sampler is ideal for autonomous sampling techniques. The system is based on Chlorotech CTD control. The device can store maximum 10 sampling bottles. Five parameters, eg., temperature, depth and salinity can be measured by the unit. The data of the measurements are stored in the memory unit of the system. Furthermore the unit is equipped with a rechargeable battery. Real-time communication is not necessary, because of the pre-programming ability of the system, thus the sampling bottles can be closed at the desired depths. The water sampler with CTD has a small and light design and can be operated by a small boat, equipped with a winch if the weight is greater than 150 kg. [35]



Figure 76. Water Sampler with CTD [35]

11.4.11 KIPS – Deep Sea Water Sampling

In situ samples can be guaranteed by the Deep Sea Water System. The system is useable in marine environments and also in extreme conditions. The unit is well suited for a wide range of platforms, e.g., ROVs and long term benthic stations. A modular construction can provide a flexible setup. The system is suitable for use in challenging environments, e.g., hot fluids in water depths up to 5000 m. The materials of the unit have been chosen carefully to ensure proper operation in extreme conditions. [36]



Figure 77. KIPS – Deep Sea Water Sampling [36]

11.5 Comparison of some available water samplers

The design process of the pressure-free cell has been aborted, because of the listed disadvantages, mentioned before. Therefore an autonomous sampler system is required, which will be able to collect liquid samples. Many water sampling systems have been built over the past 40 years, mainly for use in oceanography. The main parameters of some sampler constructions are given in Table 12.

The specifications of some samplers have been evaluated. A total of 6 parameters have played a key role in preparation of the comparison. It is important that the dimension and the weight of the water sampling system should be minimized in the UNEXMIN project. The parameters of the examined samplers have been listed in Table 12. The comparison was extended to include the number and capacity of samples. The usage intervals of these systems have been filled to get some information about the opportunities. The types of the communications have been also mentioned.

In some publications, the weight of the sampler systems are measured in air and in water, these values are given in Table 12. In some cases the sampling storage dimensions have been added, but in others only the dimension of the whole sampling unit is given. The usage intervals are written in meters. The number of samples can be modified. There are some water sampler systems, which can collect liquid and solid/gas samples equally. One sample capacity is added in millilitres. The main communication type used was the RS232 standard.

Literature cited	Weight (System)	Sampling storage dimensions	Usage interval	Number of samples	One sample capacity	Communication
[20]	600 g (max. payload)	-	0-100 m	3	20 ml	2.4 GHz 802.15.4 radios
[12]	56 kg in air	Ø165x580 [mm] (System)	0-4961 m	12-36	140 ml (1 syringe) → Mat material, 100 ml → water samples	RS232
[7]	40 kg in air, 20 kg in water	Ø10x500 [mm]	0-5000 m	128 (4x32)	40 ml	RS232C
[21]	12,25 kg in air, 2,27 kg in water	Ø120x850 [mm] (System) Ø15,875x114 [mm]	0-2000 m	8	20 ml	Serial Interface
[22]	23 kg	Ø180x670 [mm] (System)	0-1600 m	49	400 ml sample bags were fitted	Serial Interface
[16]	-	Ø120x680 [mm] (System)	0-1800 m	1	1000 ml → maximum value	-
[23]	2,5 kg in air, 1,55 kg in water	Ø70x300 [mm] (System)	Test in: 1374 m	1 sample/1 module	100 ml, dead volume 25 ml	-
[17]	10 kg in air, 6 kg in water	450x170x70 mm LxHxW (System)	0-4500 m	1	150 ml (but it can be modified), dead volume 4 ml	-
[24]	1,2 kg	-	0-10 m	2	-	Master/Slave, CMD/ACK hand-shaking protocol
[25]	38,6 kg in air, 46,7 kg in air	Cage is: 495x460x560 [mm] (WxDxH)	0~3000 m	6 independent samples	(before store the samples are passed through a filter) 75 ml → Field testing	RS232
[3]	approx.: 200 kg	2400 mm High, Bottom frame: 800x800 mm	0-6000 m	6 Niskin type sample bottles	6000 ml	-
[26]	40 kg without samplers	Ø555/650x830x880 mm	0-3000 m	6	1000-3500 ml	RS232
[18]	-	Ø120x500 [mm] (System)	0-4000 m	2 sample/ 2 modules	1300 ml → 1,6 km of tubing	

Table 12. Comparison of water samplers

The carousel type water sampler construction type seems to be the best solution. The samples can be placed to the peripheral surface, e.g., [22] and [26]. Some available constructions are shown in Figure 78.

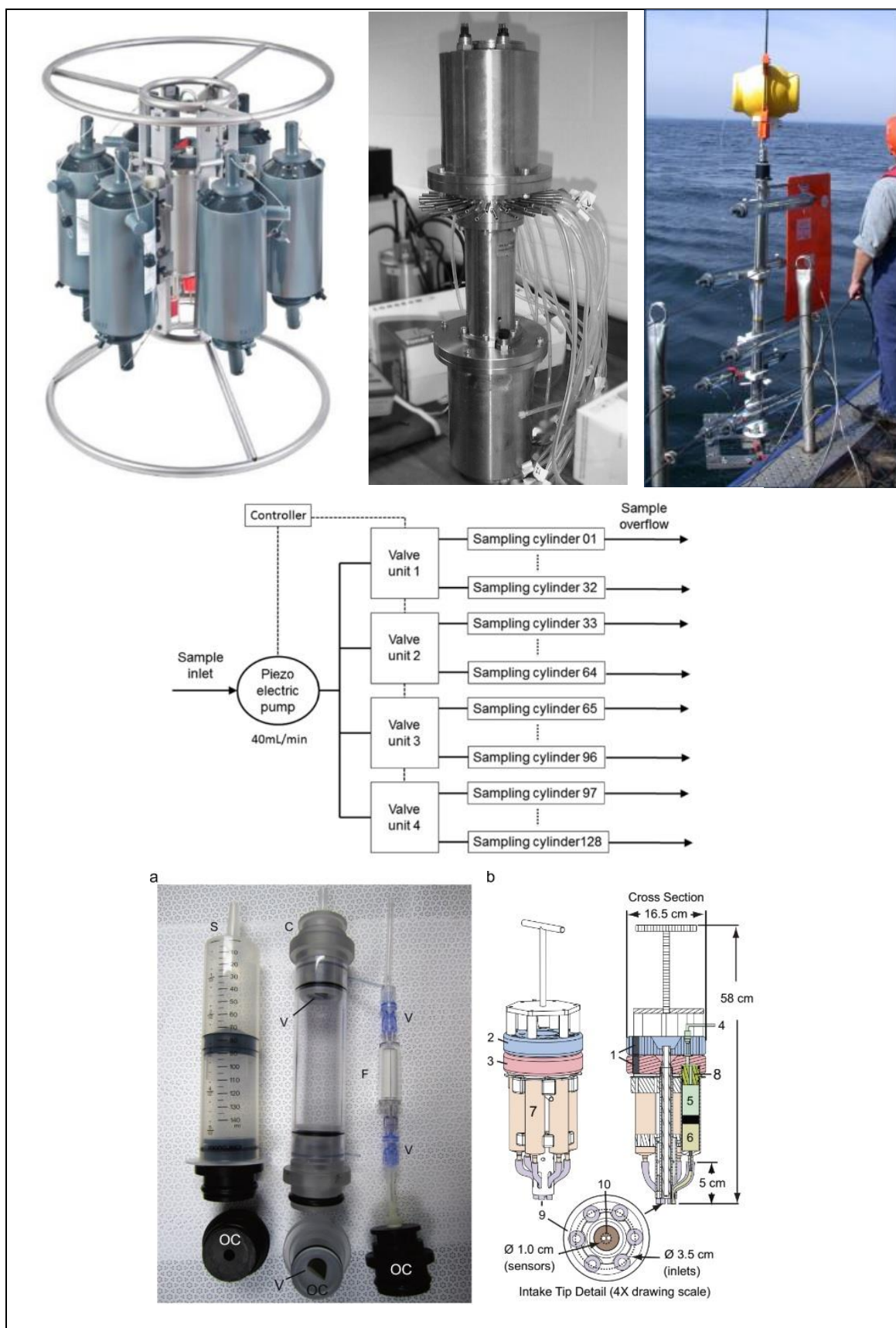


Figure 78. Water sampler constructions [26], [22], [3], [7], [12]

11.6 Development of water sampler

Using the experience of the literature and scientific papers, a new water sampler will be developed using wherever possible commercial components, from different manufactures.

Figure 79 shows the potential structure of the sampler unit. The unit can be divided into 4 main structural parts. These are the electronics, water pump, valve unit, and tank unit.

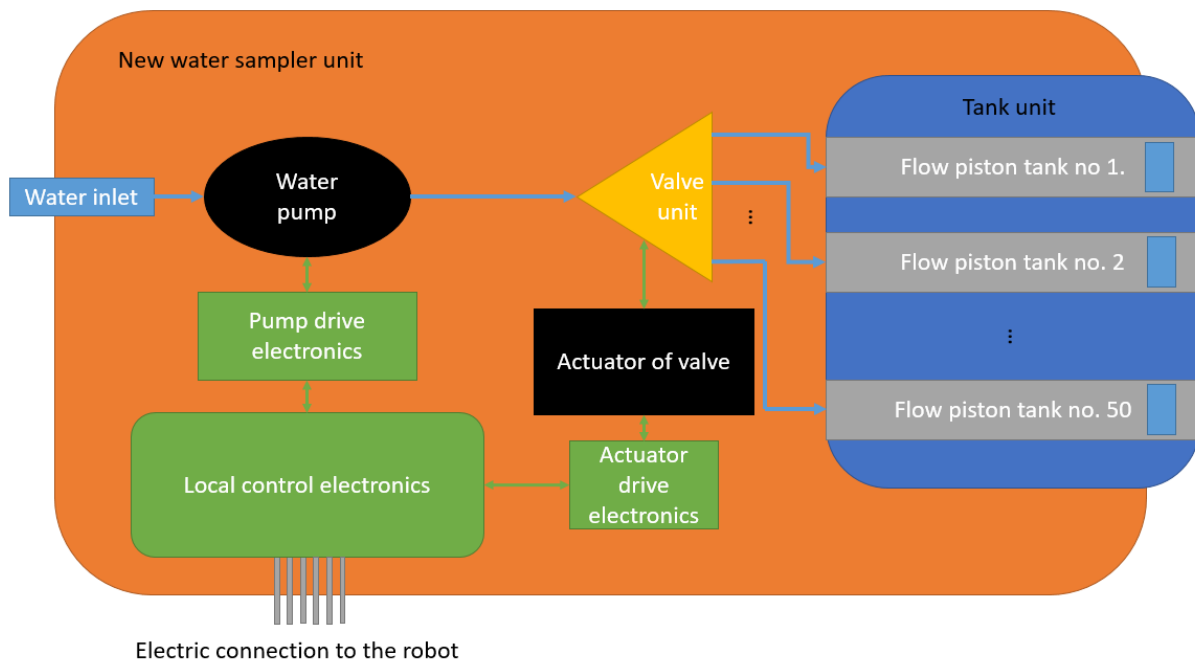


Figure 79. Potential structure of the sampler unit

The electronics need to have several different tasks and features:

- control the water pump
- control the position of the valve
- manage communication with the main control system of the robot
- fault determination
- alarm generation

The next main component is the water pump, which collects the sample water from the environment and forwards the water to the valve. The electronics controls the start and stop of water sampling using the pump.

The valve unit is responsible for setting the sampled water into the next empty tank. This unit must be controlled with one or more actuators and drive electronics. The drive of the actuator is controlled by the local control electronics so some communication is needed between them. During the development process we shall endeavour to find and use suitable commercial valves.

The last main part is the tank unit, which includes small tanks for the water samples. Every tank includes a small sealed piston to solve the pressure problems during the storage process.

11.7 Conclusion

Instead of in-situ measurements, it is much easier to use water samples and analyse them in special laboratories.

Suggested/Suggested with comment (suggested in 2.2)/Unsuggested method

11.8 References

- [1] D.J. Baker Jr. **Ocean instruments and experiment design**
B.A. Warren, C. Wunsch (Eds.), *Evolution of Physical Oceanography*, MIT Press, Cambridge (1980), pp. 396–433
- [2] M. Lunven, J.F. Guillaud, A. Youénou, M.P. Crassous, R. Berric, E. Le Gall, R. Kérouel, C. Labry, A. Aminot **Nutrient and phytoplankton distribution in the Loire River plume (Bay of Biscay, France) resolved by a new Fine Scale Sampler**
Est. Coast. Shelf Sci., 65 (2005), pp. 94–108
- [3] E.J. Sauter, M. Schlüter, J. Wegner, E. Labahn **A routine device for high resolution bottom water sampling**
J. Sea Res., 54 (2005), pp. 204–210
- [4] J. Bell, J. Betts, E. Boyle **MITESS: a moored in situ trace element serial sampler for deep-sea moorings**
Deep Sea Res. I, 49 (2002), pp. 2103–2118
- [5] S. Saegusa, U. Tsunogail, F. Nakagawa, S. Kaneko **Development of a multibottle gas-tight fluid sampler WHATS II for Japanese submersibles/ROVs**
Geofluids, 6 (2006), pp. 234–240
- [6] K.L. Von Damm, J.M. Edmond, B. Grant, C.I. Measures, B. Walden, R.F. Weiss **Chemistry of submarine hydrothermal solutions at 21°N, East Pacific Rise**
Geochim. Cosmochim. Acta, 49 (1985), pp. 2197–2220
- [7] Kei Okamura, Takuro Noguchi, Mayumi Hattaa, Michinari Sunamurab, Takahiko Suzuec, Hideshi Kimotoc, Tatsuhiro Fukubad, Teruo Fujiie **Development of a 128-channel multi-water-sampling system for underwater platforms and its application to chemical and biological monitoring**
Methods in Oceanography (2013), pp. 75–90
- [8] M.C. Honda, S. Watanabe **Utility of an automatic water sampler to observe seasonal variability in nutrients and DIC in the Northwestern North Pacific**
J. Oceanog., 63 (2007), pp. 349–362
- [9] J.P. Cowen, D.A. Copson, J. Jolly, C.-C. Hsieh, H.-T. Lin, B.T. Glazer, C.G. Wheat **Advanced instrument system for real-time and time-series microbial geochemical sampling of the deep (basaltic) crustal biosphere**
Deep Sea Res. I, 61 (2012), pp. 43–56
- [10] J.B. Corliss, J. Dymond, L.I. Gordon, J.M. Edmond, R.P. von Herzen, R.D. Ballard, K. Green, D. Williams, K. Crane, T.H. van Andel **Submarine thermal springs on the galapagos rift**
Science, 203 (1979), pp. 1073–1083
- [11] U. Tsunogai, J. Ishibashi, H. Wakita, T. Gamo, K. Watanabe, T. Kajimura, S. Kanayama, H. Sakai **Peculiar features of Suiyo Seamount hydrothermal fluids, Izu-Bonin Arc: differences from subaerial volcanism**
Earth Planet. Sci. Lett., 126 (1994), pp. 289–301
- [12] J.A. Breier, D. Gomez-Ibanez, E. Reddington, J.A. Huber, D. Emerson **A precision multi-sampler for deep-sea hydrothermal microbial mat studies**
Deep Sea Res. I, 70 (2012), pp. 83–90
- [13] P.S. Tabor, J.W. Deming, K. Ohwada, H. Davis, M. Waxman, R.R. Colwell **A pressure-retaining deep ocean sampler and transfer system for measurement of microbial activity in the deep sea**
Microb. Ecol., 7 (1981), pp. 51–65
- [14] K.L. Von Damm, J.M. Edmond, B. Grant, C.I. Measures, B. Walden, R.F. Weiss **Chemistry of submarine hydrothermal solutions at 21°N, East Pacific Rise**
Geochim. Cosmochim. Acta, 49 (1985), pp. 2197–2220

- [15] T. Naganuma, M. Kyo, T. Ueki, K. Takeda, J. Ishibashi **A new automatic hydrothermal fluid sampler using a shape-memory alloy**
J. Oceanog., 54 (1998), pp. 241–246
- [16] H.W. Jannasch, C.O. Wirsen, C.L. Winget **A bacteriological pressure-retaining deep-sea sampler and culture vessel**
Deep Sea Res. Oceanog. Abst., 20 (1973), pp. 661–664
- [17] J.S. Seewald, K.W. Doherty, T.R. Hammar, S.P. Liberatore **A new gas-tight isobaric sampler for hydrothermal fluids**
Deep Sea Res. I, 49 (2001), pp. 189–196
- [18] H.W. Jannasch, C.G. Wheat, J.N. Plant, M. Kastner, D.S. Stakes **Continuous chemical monitoring with osmotically pumped water samplers: OsmoSampler design and applications**
Limnol. Oceanog. Methods, 2 (2004), pp. 102–113
- [19] C.R. German, D.R. Yoerger, M. Jakuba, T.M. Shank, C.H. Langmuir, K. Nakamura **Hydrothermal exploration with the Autonomous Benthic Explorer**
Deep Sea Res. I, 55 (2008), pp. 203–219
- [20] John-Paul Ore, Sebastian Elbaum, Amy Burgin, Baoliang Zhao, Carrick Detweiler: **Autonomous Aerial Water Sampling**
- [21] C. Roman, R. Camilli: Design of a Gas Tight Water Sampler for AUV Operations
- [22] P. A. Dodd , M. R. Price , K. J. Heywood, M. Pebody: **Collection of Water Samples from an Autonomous Underwater Vehicle for Tracer Analysis**, 2006
- [23] Takeshi N., Masanori K., Tatsuhiko U., Kazuhiko T., Jun-Ichiro I.: **A New Automatic Hydrothermal Fluid Sampler Using a Shape-Memory Alloy**, 1998
- [24] S. Dhull, D. Canelon, A. Kottas, J. Dancs, A. Carlson, N. Papanikolopoulos **Aquapod: A Small Amphibious Robot with Sampling Capabilities**
- [25] C. D. Taylor, K. W. Doherty, S. J. Molyneaux, A. T. Morrison, J. D. Billings, I. B. Engstrom, D. W. Pfitsch, S. Honjo: **Autonomous Microbial Sampler (AMS), a Device for the Uncontaminated Collection of Multiple Microbial Samples from Submarine Hydrothermal Vents and Other Aquatic Environments**
- [26] Hydro-Bios: **Multi Water Sampler SlimLine 6**
- [27] Diersing, Nancy: **"Water Quality: Frequently Asked Questions."** Florida Brooks National Marine Sanctuary, Key West, FL. (2009)
- [28] GUIDELINES FOR DRINKING-WATER QUALITY: **Water sampling and analysis**
- [29] EnviroTech Instruments LLC homepage: <http://envirotechinstruments.com>
- [30] Technicap homepage: <http://www.technicap.com>
- [31] K.U.M. Umwelt-und Meerestechnik Kiel GmbH homepage: <http://www.kum-kiel.de>
- [32] Nichiyu Giken Kogyo Co., Ltd. homepage: <http://ocean.nichigi.com>
- [33] OSIL homepage: <http://www.osil.co.uk>
- [34] Sea-Bird Electronics, Inc. homepage: <http://www.seabird.com>
- [35] JFE Advantech Co., Ltd. homepage: <http://ocean.jfe-advantech.co.jp>
- [36] Emma Technologies homepage: <http://www.emma-technologies.com>

12.1 Theoretical Background

Side-scan sonar devices produce acoustic pulses (conical-shaped or fan-shaped pulses) that travel through the water column, strike objects in the water or the bottom, and these acoustic pulses are reflected back to the transducer device. The time and strength of the returning acoustic pulses (like the backscatter) are compiled by the sonar system into sequential rows of shaded pixel elements that together produce a flat picture of the underwater environment. As an active remote sensing system, the installation (swimming boat) must be moving through the water surface in order to create an image that can be evaluated. The evaluation procedure is similar to the image scanning of any document. The boat and sonar equipment act as the light bar that moves over the surface of a document in a scanner machine [Robinson, 1988].

The intensity of the acoustic wave reflections from the bottom of the sea of this fan-shaped beam of pulses is recorded in a series of cross-track segments. When concatenated together along the direction of motion, these slices create an image of the seafloor within the order (coverage width) of the pulse. The acoustic audio frequencies applied in side-scan sonar commonly range between 100 to 500 kHz. The higher frequencies (close to 500 kHz) yield better resolution but lower range [4].

Single channel wave reflection profiling systems (occasionally described as sub-bottom profiling sets) are frequently operated together with an accurate echo-sounder, for precise bathymetric information. The side-scan sonar method is a sideways scanning acoustic survey technique wherein the bottom of the sea to one or both sides of the survey boat is scanned by a high frequency acoustic beam (like a ping), transmitted by transceivers fixed to the side of the boats hull or in independent towed units (called tow fish) as shown in Figure 80 (a) and (b). Ocean or lake bottom features facing towards the survey boat, such as a bottom inhomogeneity or sedimentary bed shapes, reflect acoustic wave energy back towards the transducer elements. In the case of features facing away from the boat or a featureless ocean bottom, the acoustic wave energy is reflected onward from the transducer elements. The same type of data recorder is used to create seismic profiling datasets. The resulting signal shape of the returned acoustic energy is well known as a sonar. Scale distortion is created by the skew incidence of the sonar, resulting from the changing wave path lengths and angles of incidence of returning rays, as shown in Figure 80 (b). This wave distortion can be automatically repaired prior to displaying so that the sonar gives an isometric map view of ocean or lake bottom features.

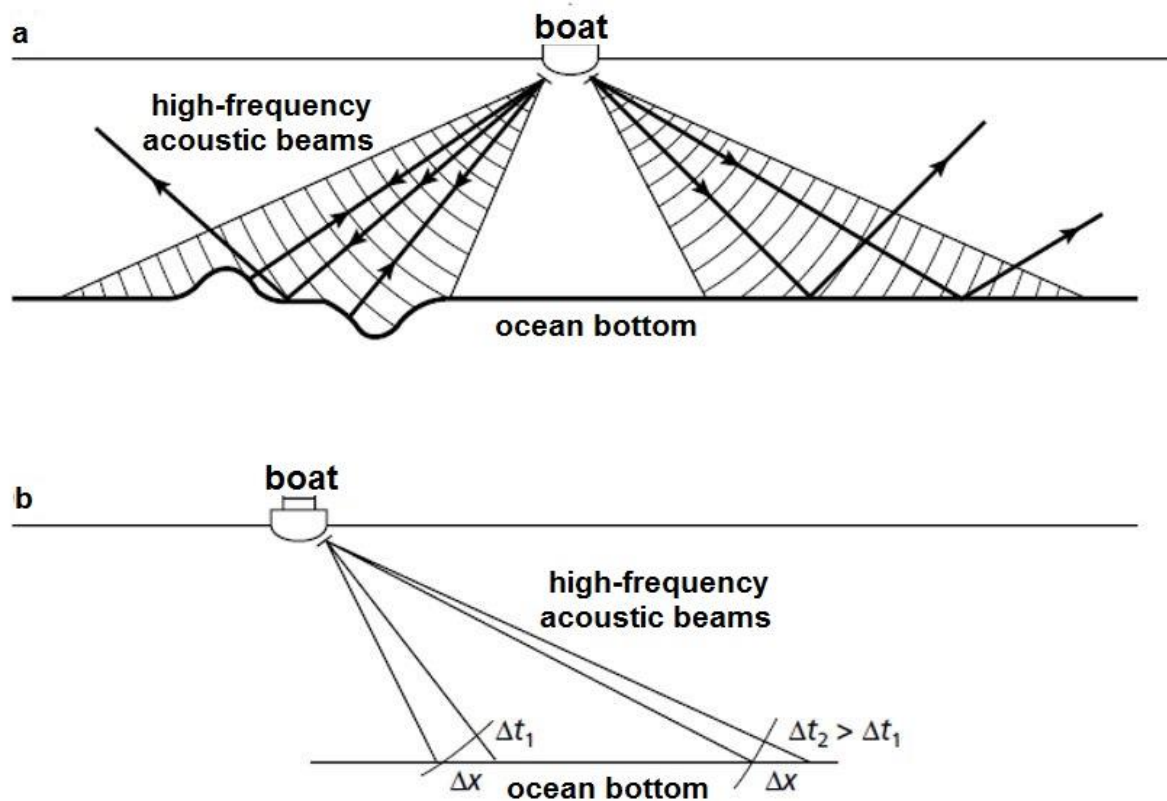


Figure 80. Sketch of the side-scan sonar

- Individual reflected beam paths within the transmitted units, showing signal return from ocean bottom inhomogeneities.
- Scale distortion resulting from skew incidence: the same widths of ocean bottom Δx are represented by different time intervals Δt_1 and Δt_2 at the inner and outer edges of the sonar (from left to right).

Initially side-scan type sonar equipment utilized only a solo conical-beam transducer. Over time sonar devices were developed with double transducers to cover both of the sides of the surveying boats. The transducers were either contained in a boat's single side-fixed package or with two packages on both sides of the ship [Waters, (1978)]. Later the transducers advanced to fan-shaped type beams which generate a better interpreted sonar image. In order to get closer to the bottom of the ocean in deep water the side-scan transducers were installed in a swimming unit, the so called *tow fish*, which is pulled by a towing line from the boat.

12.2 Measured parameter

The amplitude, or strength of the reflected acoustic ray, plays a critical role in ability of side-scan sonar to create imagery that illustrates differences among features. The return ray amplitude is influenced by several parameters [6]. Ray amplitude can be affected by the density of the ocean's floor objects or surface that reflects the signal. Dense, hard objects like large rocks, bridge base elements or sunken ships reflect more sonar energy than soft surfaces like a sandy or muddy bottom.

The acoustic waves can travel far in the water of oceans or lakes. Acoustic waves travels in saline or fresh water in a moving series of pressure zones because acoustic waves are compressional waves. The acoustic waves and pressure zones propagate at a specialized speed in water. The section specific speed of acoustic

waves can change depending on the salinity, temperature and pressure of water. The speed of acoustic wave is measured in meters per second (m/s). Generally the average acoustic wave speed is around 1500 m/s and depends on the above detailed water parameters.

The distance between two pressure zones gives the wavelength. The SI unit of wavelength is the metre (m). The frequency of acoustic waves measured in Hertz (Hz). These two parameters are strongly related to each other.

$$\text{Speed of acoustic waves} = \text{Wavelength} * \text{Frequency}$$

The acoustic power (energy) of the sound wave per unit time is proportional to the square of its amplitude. Figure 81 shows diagrammatically the components of a sound wave.

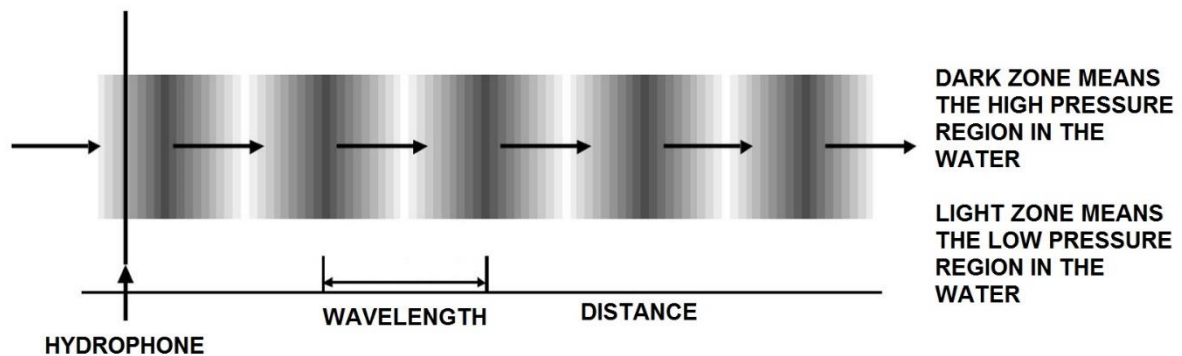


Figure 81. Components of acoustic waves (measurable by hydrophones) [14]

12.3 Measuring method

12.3.1 Survey Speed

In any kind of geophysical surveying time is equal to money in a very real sense. A single-beam echo sounder is not time-efficient enough. If the purchased sonar equipment has a very narrow beam, which gives high precision locations for depth direction measurements, the measuring process will require many individual cycles and take a really long time. The method can be speeded up by using sonar equipment with a greater beam that maps a greater area with each measuring cycle, but at the cost of much more poorer sea or lake bottom resolution.

12.3.2 The Multi-beam Solution

A multi-beam sonar is an instrument that can measure more than one site on the sea or lake bed with a single ping and with higher resolution than traditional echo sounders. The work of a narrow single acoustic beam echo sounder is performed at many different locations on the seabed at once. With this arrangement the instrument can continuously map the sea or lake bottom. This area name is swath. The dimension of the swath is called the swath width, and it can be scanned either as a fixed angle. The physical size of the swath width changes with depth. The multi-beam acoustic sonar swath showed in Figure 82. [14]

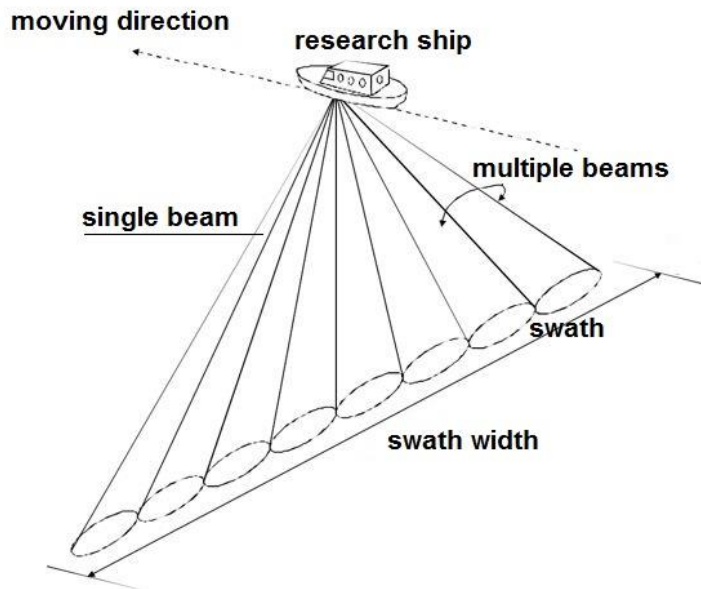


Figure 82. Multi-beam acoustic sonar swath

12.4 Range and resolution

A fundamental relationship exists between the range of acoustic sonar and image resolution. Acoustic range is the widest distance that will be screened in a sonar image (Figure 83). Acoustic range and image resolution are highly proportional as acoustic range increases, image quality declines in the distant space portions of the image. Sonar range is a setting that can be manipulated by the device operator during the measurement [1].

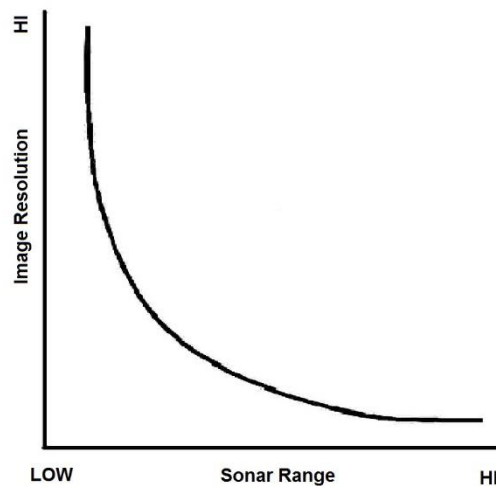


Figure 83. Acoustic sonar range vs. image resolution

Acoustic sonar frequency and image resolution are directly proportional. Higher frequencies produce higher image resolution (Figure 84).

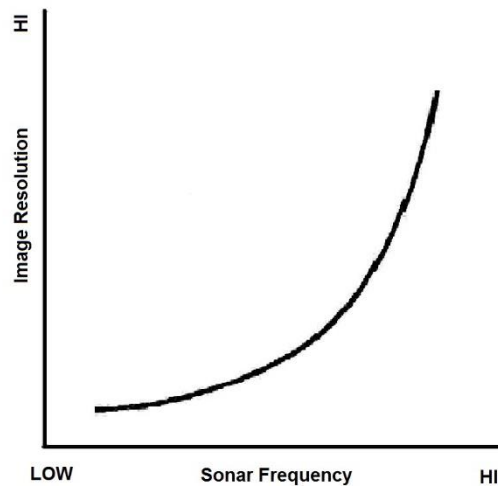


Figure 84. Acoustic sonar frequency vs. image resolution

Higher frequency signals attenuate quicker than lower frequencies as they are scattered and absorbed more easily by water elements. With this fact, an inverse relationship exists between acoustic sonar frequency and sonar range (Figure 85). Lower sonar frequencies have a higher operating range than higher frequencies. The application of higher frequency may improve the ability to find small elements of the bottom. This relation between frequency and range is often utilized during exploration and recovery operations. When a huge area of open water must be scanned in search of a sunken ship, a lower sonar frequency will be used at high range, thereby covering a large swath in each round. The operator will investigate the recorded data set for anomalous targets, anything that appears out of the screen. The lower frequency may not be sufficient to create a very detailed image of the sunken object, but may still identify the target object as something different from the surrounding area. When anomalous elements on the screen are encountered, a return process close to the object can be made using higher frequency to create a further detailed view of the object in question.

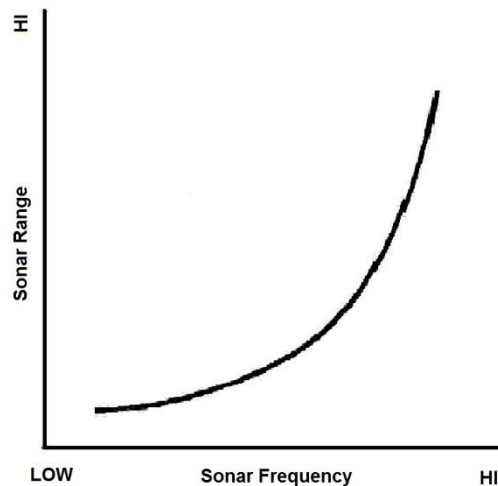


Figure 85. Acoustic sonar frequency vs. sonar range

12.5 Target parameters

The frequencies of sonars range from infrasonic to above a megahertz. Generally, the lower frequencies have longer range, while the higher frequencies offer better resolution, and smaller size for a given directionality. To achieve reasonable directionality, frequencies below 1 kHz generally require large size, usually achieved as towed arrays. Low frequency sonars are loosely defined as 1–5 kHz, albeit some navies

regard 5–7 kHz also as low frequency. Medium frequency is defined as 5–15 kHz. Another style of division considers low frequency to be under 1 kHz, and medium frequency at between 1–10 kHz.

12.6 Applicability

Today's side-scan sonar technique may be utilized to conduct research for subaqueous bottom profiling, archaeology, geological structure imaging, in conjunction with ocean or lake bottom samples it is able to give an understanding of the discrepancies in material and texture type of the bottom. The imagery of the side-scan sonar technique is also a generally utilized method to catch detritus items and other impediments on the bottom of the river that may be hazardous to shipping or to seafloor installations by the oil and gas lines. In addition, the position of pipelines and electric cables on the bottom of the sea or ocean can be investigated using side-scan type sonar. The sonar datasets are often acquired along with bathymetric sounding profiles and sub-bottom profiler datasets, thus providing a glimpse of the seabed. Side-scan type sonar is also utilized technique for fishing practice and environmental investigations. It also has military applications including UXO detection [10], [2].

12.7 Advantages of the method

Initially side-scan sonar was the only available instrument for mapping underwater environment and began with the development of submarine technology.

- Wide area of coverage allows for few survey profiles
- Provides very high resolution (under favourable conditions)
- With sufficient experience and instrumentation the side-scan sonar is a fast technique

Further advantages of the sonar technique [15]:

- Sometimes can be used in very shallow water
- Really small objects (in centimetre range) can be detected
- High resolving detail
- Is easy to use in the marine environment

Disadvantages of the method

Many side-scan sonar image suffered from numerous features because of a number of reasons such as the transversal scale, a function of the skew range, is different from the longitudinal scale.

The longitudinal scale varies as it is function of the boat's speed, the survey line not being exactly straight and the position of the towfish (pitch setting, heading, roll) is not constant.

Further disadvantages of the sonar method:

- Relatively expensive method,
- Wirelines might catch on underwater inhomogenities,
- Depends on well-trained on-line operators for good results,
- Demands precise transportation for multi-beam units,
- Requires the latest interpretation and processing skills,
- Backscatter technique is a new "unknown" to much of the survey community.

12.8 Industrial solutions—Purchasable instruments

12.8.1 EdgeTech 2200 and 2205 [12]

The EdgeTech 2200 and 2205 are compact, highly flexible and applicable sonar systems (Figure 86). These units are specially planned for installation and application on Underwater Vehicles, Submarines (UUVs / AUV), Remotely Operated Submarines and Boats (ROVs), Unmanned Surface Ships (USVs),

and other hosted platforms. This modular equipment can be organized, based on the users' application, to collect sub-bottom track analyses, side-scan sonar imagery, and bathymetric data sets. The EdgeTech system is provided as a complete package where the 2200/2205 electrical units are enclosed in a pressure tank, or alternatively the electronical control units can be provided as boards equipped onto a frame so the customer can integrate the sonar system into the AUV or ROV pressure housing. In both cases the transducer units are provided for the side-scan sonar. The system can operate independent of the fixed platform by storing the data or it can be configured to independently operate with the boat during its survey. Deep water units can be depth rated from 0 to 6000 meters. The sturdy design and modular units of 2200/2205 system includes EdgeTech's unique and exciting deep water imaging technologies: Full Spectrum® CHIRP Processing, Multi-Pulse technology (special opportunity), Dynamic Array Focusing (optional feature) and Dynamic Aperture Sonar Arrays. This technique provides long range resolutions through improved signal-noise ratios. The Multi-Pulse technique sends up to 4 pulses in the water simultaneously thereby enabling a 4 times imaging speed increase over conventional side-scan sonar systems. EdgeTech's exclusive Dynamically Focused Arrays provide better resolution in the far zone and enable better target determinations at longer ranges. The Dynamic Aperture of the sonar array increases the resolution imagery possible in near and far zone ranges.



Figure 86. Different type of sonars from of EdgeTech (2200 and 2205 AUV / UUV / ROV / ASV / USV) [12]

Features:

- Simultaneous Dual Frequency operations,
- Sub-bottom Frequencies from 500Hz to 24 kHz,
- Multi-Pulse operation,
- Side-scan Frequencies from 75 kHz to 1600 kHz,
- NEW Tri-Frequency option: 230 kHz, 540 kHz and 1600 kHz,
- On-line self-test and status reporting,
- Bathymetry capabilities with full swath coverage and no nadir gap.

Applications:

- Pre/Post Dredging Surveys,
- Scour/Erosion Investigation,
- Cable and Pipeline Surveys,
- Sediment Classification,
- Route Surveys,
- Geological/Geophysical Surveys,
- Shallow Water Hydrographic Surveys,
- Mine Counter Measures (MCM),
- **Archaeological Surveys,**
- Marine Construction Surveys,
- Geological/Geophysical Surveys,

- Military Rapid Environmental Assessments (REA),
- Port & Harbour Security,
- Dredging Operations,
- Marine Debris Search,
- Benthic Habitat Mapping.

12.8.2 Marine Sonic Technologie's Sea Scan® PC AUV/ROV

The Marine Sonic Technologie's Sea Scan® PC AUV/ROV systems have been designed and built to the exacting standards of today's AUV/ROV market. Every AUV/ROV system consists of the Sea Scan® PC system electronics card (Installed in the PC), a Sea Scan® PC transducer electronics card/module, a pair of Sea Scan® PC transducers, and connecting cables. The AUV/ROV system components use the same proven technology found in the towed systems but have been redesigned to make them smaller and more energy efficient. All four components work together and each works only with Sea Scan® PC components (Figure 87). Technical details are listed in the Table 13. [13].

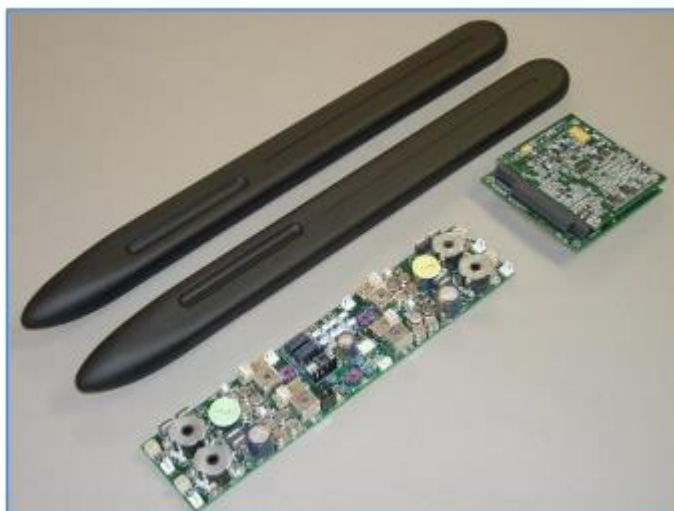


Figure 87. Elements of Dual Frequency Transducer Electronics Board, SPC PC Acquisition Board, Streamlined 900/1800 kHz

Frequencies	150, 300, 600, 900, 1200, 1800 kHz (single frequency or in combination for dual frequency)
Transducer Dimensions	Dimensions vary based on frequency and transducer configuration. Transducers are custom designed for the specific platform (included in system cost). Please contact us for more information.
Operating Range (maximum*)	400m @ 150 kHz, 200m @ 300 kHz, 75m @ 600 kHz, 40m @ 900 kHz 25m @ 1200 kHz, 15m @ 1800 kHz
Data Collection Speed	5.28 knots max. (4.68 knots @ 100 meters range to meet NOAA Survey Standards)
Horizontal Beam Width	0.8 ° @ 150 kHz, 0.4° 300kHz and above (one-way), < 0.6° @ 150 kHz, < 0.3° 300kHz and above (two-way)
Vertical Beam Width (one-way)	20° @ 150 kHz, 20° @ 300 kHz, 40° @ 600 kHz, 40° @ 900 kHz, 40° @ 1200 kHz , 40° @ 1800 kHz
Transducer Material	PVC (Standard – other materials available upon request)
Maximum Operating Depth	600 meters (1,968 ft.) Standard / 1000 meters (3,281 ft.) Optional (other depths available upon request)
Transducer Depression Angle	10° down from horizontal
Transmission Pulse	Tone Burst, 26.67us @ 150 kHz, 20us @ 300 kHz, 10us @ 600 kHz, 6.67us @ 900 kHz, 5us @ 1200 kHz, 4.44us @ 1800 kHz
Temperature	0°C to 70°C
Digital Across Track Resolution	~1 cm @ 5m range (512 Samples Divided by Range)
Digital Along Track Resolution	~2 cm @ 5m range and 2 Knots SOG (range and SOG dependent)
Acoustic Across Track Resolution	4cm @ 150 kHz, 3cm @ 300 kHz, 1.5cm @ 600 kHz, 1cm @ 900 kHz, 0.75cm @ 1200 kHz, 0.67cm @ 1800 kHz
Acoustic Along Track Resolution (two-way) @ end of near-field	30.5cm @ 150 kHz, 30.5cm @ 300 kHz, 15.24cm @ 600 kHz, 10.16cm @ 900 kHz, 7.62cm @ 1200 kHz, 5.08cm @ 1800 kHz
End of Near-field	9.3 m @ 150 kHz, 18.6 m @ 300 kHz, 9.3 m @ 600 kHz, 6.2 m @ 900 kHz, 4.6 m @ 1200 kHz, 3.1 m @ 1800 kHz
Power Consumption	< 5 Watts Max. (not including CPU)
Operating System	Windows™ 9X, Windows™ 2000, Windows™ XP
Aux. Data Inputs	NMEA-0183 (Latitude, Longitude, SOG, COG, Heading, Depth, Altitude)

Table 13. Sea Scan® Specifications type of PC AUV

Sea Scan® PC AUV PC system electronics card (installed in the PC) is available in two configurations: Full size, full length, ISA card and a compact PC-104 card for embedded installations. System Electronics ISA Card: Size 340mm x 100mm x 19mm Weight: 361 g, Power consumption is 6-10 watts (Consumption is dependent on scanning speed and selected range scale). System Electronics PC-104 Card: Size 97mm x 92mm x 17mm, Weight: 142 g, Power consumption is 4.8 watts maximum (Consumption can be lower depending on scanning speed and selected range).

12.8.3 Other manufacturers:

Side-scan sonar systems include Furuno, Sonardyne, Lowrance, Simrad, Raytheon, Northrop Grumman (formerly Westinghouse), EdgeTech (formerly EG&G), C-MAX Ltd., L-3/Klein Associates, J.W. Fishers Mfg. Inc., Imagenex Technology Corp., RESON A/S, Sonatech Inc., Benthos (the sonar formerly produced by Datasonics), WESMAR, Marine Sonic Technology, Kongsberg Maritime, Geoacoustics, EDO Corporation, Ultra Electronics, Hummingbird (Techsonic Industries Inc), and Deep Vision Technologies. Shallow-water side-scan systems, Trittech and deeper rated side-scan systems.

12.9 Case Study

A similar use of side-scan sonar is in shallow sea floor mapping with a good example in this paper: Lazar et. al. (2013) Side-Scan Sonar Mapping of Anthropogenically Influenced Seafloor: A Case-Study Of Mangalia Harbor, Romania. Geo-Eco-Marina 19/2013 [5].

In this utilization the side-scan sonar is a valuable tool in investigating harbour areas and traffic fairways, for its capability of imaging the seafloor objects and features, as well as offering information regarding their position and dimensions. Debris and other traces of human activity were inventoried and monitored much more easily using underwater acoustics than with conventional techniques. The scanned area of the Mangalia Harbour shows intense human activity signs, such as various debris, traces of dragged anchors and dredging areas, all of them being clearly visible on the sonograms. Most objects pose no threat to the intense navigation in the harbour, as no high object was identified in the area where large ships manoeuvre. There is still the danger of shipwrecking in case of large ships moving outside of the main channel, as a mound of rocks lies on the floor near the harbour entrance. There is a comparison of images of the same objects scanned at different frequencies, in an attempt to underline the advantages of both high and low frequencies. Considering the relation between resolution and range, high frequencies are more suitable for shallow waters, where they can provide better details. However, in deeper waters, as the frequencies have a very limited range, they tend to have less coverage, as the nadir blind area gets wider, thus requiring a lowering of the tow fish. Therefore, we recommend the use of the highest frequency available for practical applications in harbor areas.

Other many good examples of the application of side-scan sonar technique for seafloor sediment investigations and analyses see at website of <https://www.chesapeakeotech.com/case-studies/>.

12.10 Conclusion

This method can be applicable conditionally in the project, because the side-scan sonar technique able to provide information about cracked and loosened zones. Also, the method can give information about the thickness of sediment. The sonar technique also applied for the robot control system of orientation. For this reason it is not worth using two similar systems built in the same robot.

Suggested/Suggested with comment/Unsuggested method

12.11 References

- [1] Adam, J. K. (2013) **An Illustrated Guide to Low-cost, Side-Scan Sonar Habitat Mapping** (<https://www.fws.gov/panamacity/resources/An%20Illustrated%20Guide%20to%20Low-Cost%20Sonar%20Habitat%20Mapping%20v1.1.pdf>).
- [2] Bates, C. R. et al. (2011) **Geophysical Methods for Wreck-Site Monitoring: The Rapid Archaeological Site Surveying and Evaluation (RASSE) programme**
The International Journal of Nautical Archaeology, Vol. 40 (2), pp. 404–416.
- [3] Camina, A. R. and Janacek, G. J. (1984) **Mathematics for Seismic Data Processing and Interpretation**
Graham & Trotman, London.
- [4] Dobrin, M. B. and Savit, C.H. (1988) **Introduction to Geophysical Prospecting** (4th ed.)
McGraw Hill, New York.
- [5] Lazar A. A., Bugheanu A. D., Ungureanu G. V., Ionescu A. D.. (2013) **Side-Scan Sonar Mapping Of Anthropogenically Influenced Seafloor: A Case-Study Of Mangalia Harbor, Romania**
Geo-Eco-Marina 19/2013
- [6] McGraw, H. (1983) **Principles of Underwater Sound** by Robert J. Urick (3rd ed.)
[ISBN13: 9780070660878].
- [7] Robinson, E. S. and Çoruh, C. (1988) **Basic Exploration Geophysics**
Wiley, New York.
- [8] Sakellariou, D. (2007) **Searching for Ancient Shipwrecks in the Aegean Sea: The Discovery of Chios and Kythnos Hellenistic Wrecks with the Use of Marine Geological-Geophysical Methods**
The International Journal of Nautical Archaeology, Vol. 36.2, pp. 365–381.
- [9] Waters, K. H. (1978) **Reflection Seismology-A Tool for Energy Resource Exploration**
Wiley, New York.
- [10] Quinn, R. et al. (2005) **Backscatter Responses and Resolution Considerations in Archaeological Side Scan Sonar Surveys: A Control Experiment**
Journal of Archaeological Science, Vol. 32, pp. 1252- 1264.
- [11] <https://www.chesapeakeotech.com/case-studies/>
- [12] www.edgetech.com/products/auv-rov-sonar/2200-2205-auv-rov-sonar/
- [13] www.marinesonic.com/products/SSPCAUV/
- [14] <https://www.ldeo.columbia.edu/res/pi/MB-System/sonarfunction/SeaBeamMultibeamTheoryOperation.pdf>
- [15] www.vliz.be/imisdocs/publications/113831.pdf

13 MAGNETIC METHOD

13.1 Theoretical Background

Conventional utilization of geomagnetic methods contains such tasks as spatial imaging of volcanic extrusive and intrusive rocks and identifying the depth of crystalline basement below sedimentary cover. Volcanic rocks usually contain large amounts of ferromagnetic material. Unconsolidated sediments and sedimentary layers generally are poorly magnetized. For shallow investigations, today's highly sensitive instruments easily detect buried faults, structures of igneous rocks, iron pipelines, former walls of buildings, etc. [11]. This method is a rapid and affordable technique in geophysical engineering practice [10].

Magnetizable rocks include many types of ferromagnetic and other kind of minerals like para-, dia-, ferri- and antiferro-magnetic. Magnetizable minerals are capable of acquiring remanent magnetization which is useful for paleomagnetic studies. Samples that are poor in magnetizable substances, or contain diamagnetic minerals, will yield lower or negative magnetic values [8].

There is only a limited applicability of magnetic method in mapping of structural geology [1].

13.2 Measured parameter

In the applied geophysical magnetic method, volume susceptibility is a physical quantity which describe the observed material properties in the external magnetic field. In geophysical engineering practice the magnetic volume susceptibility is denoted by κ , and can defined by the equation of $\kappa = M/H$, where M means the volume magnetization induced, H denote the external magnetic field. Volume susceptibility (κ) is a unitless quantity. The susceptibility value depends on the utilized unit system: $\kappa \text{ (SI)} = 4\pi \kappa \text{ (cgs)} = 4\pi$. The Tesla is the unit of the force of a magnetic field. The specific susceptibility is defined as $\chi = \kappa/r$, where r means the rock density. The dimensions of specific susceptibility are therefore cubic meters per kilogram.

13.3 Measuring method

Systematic magnetic surveys can be used to searching for mineralogical conditions or locating magnetizable objects. With systematic grid the typical utilizations of the magnetic method include:

- Aeromagnetic survey,
- Ground exploration,
- Borehole investigation,
- Marine survey.

Magnetometers in engineering practice can be divided into two basic types:

- Scalar magnetometers, which are measure the total force of the magnetic field,
 - Proton precession magnetometer, sensitivity ~ 0.1 nT.
 - Overhauser magnetometer, sensitivity ~ 0.1 nT.
 - Cesium vapour magnetometer, sensitivity ~ 0.01 nT
- Vector magnetometers, which can measure magnitude of the total magnetic field and the components of the total magnetic field in X, Y, Z directions.
 - Fluxgate magnetometer, sensitivity ~ 1 nT

The magnetograph is a special magnetometer that continuously records magnetic data. Magnetometers can also be classified as "Alternate Current, AC". This type of magnetometer measures field values rapidly in time (more than 100 Hz). There are also "Direct Current, DC" magnetometers. This type of equipment measures the total magnetic field almost statically. The AC type of magnetometers find utilization in electromagnetic surveys (magnetotelluric methods). The DC type of magnetometers are used in the practice of mineral exploration and imaging of geological structures.

13.4 Target parameter

The aim of geomagnetic measurements is to explore subsurface geology. Generally the magnetic susceptibility of minerals is highly variable depending on the different type of rocks and the geological background. Generally the Earth's total magnetic field and many times also the vertical magnetic gradient is measured. Horizontal and vertical gradient magnetic measurements can also be carried out [18].

In near surface engineering practice gradiometry is the generally used method. Magnetic gradient method is a commonly used technique to increase the signal/noise ratio. With the technique of magnetic gradiometry the geophysicist can separate relatively shallow magnetic bodies from large distant magnetic sources associated with geological formations. Gradiometers are pairs of magnetometers with vertically or horizontally separated sensors, with fixed distance. The general distance between the magnetic sensors is 1m. Magnetic gradiometry is applicable for archaeological work, site investigation and unexploded ordnance location. With this method, both along-line and across-line gradients can be computed.

Magnetic, just like gravity, methods are potential field methods [6]. Anomalies on the surface or in the subsurface of the Earth are caused by induced or remanent magnetism [12].

In mines, magnetic applications can detect magnetic anomalies (faults, veins) and presence of magnetizable minerals. The main magnetizable minerals are listed in Table 14:

Magnetic Properties of Minerals

Mineral	Composition	Magnetic Order	T _c (°C)	σ _s (Am ² /kg)
Oxides				
Magnetite	Fe ₃ O ₄	ferrimagnetic	575-585	90-92
Ulvospinel	Fe ₂ TiO ₂	AFM	-153	
Hematite	αFe ₂ O ₃	canted AFM	675	0.4
Ilmenite	FeTiO ₂	AFM	-233	
Maghemite	γFe ₂ O ₃	ferrimagnetic	~600	~80
Jacobsite	MnFe ₂ O ₄	ferrimagnetic	300	77
Trevorite	NiFe ₂ O ₄	ferrimagnetic	585	51
Magnesioferrite	MgFe ₂ O ₄	ferrimagnetic	440	21
Sulfides				
Pyrrhotite	Fe ₇ S ₈	ferrimagnetic	320	~20
Greigite	Fe ₃ S ₄	ferrimagnetic	~333	~25
Troilite	FeS	AFM	305	
Oxyhydroxides				
Goethite	αFeOOH	AFM, weak FM	~120	<1
Lepidocrocite	γFeOOH	AFM(?)	-196	
Feroxyhyte	δFeOOH	ferrimagnetic	~180	<10
Metals & Alloys				
Iron	Fe	FM	770	
Nickel	Ni	FM	358	55
Cobalt	Co	FM	1131	161
Awaruite	Ni ₃ Fe	FM	620	120
Wairauite	CoFe	FM	986	235

FM = ferromagnetic order

AFM = antiferromagnetic order

T_c = Curie or Néel Temperature

σ_s = saturation magnetization at room-temperature

Table 14. Main magnetizable minerals [17]

13.5 Applicability

Magnetometric surveys can be useful in locating magnetic anomalies which indicate the presence of ore bodies (direct magnetic detection), or sometimes gangue minerals associated with magnetizable ore deposits (indirect detection). These types of deposits include magnetizable iron ore, like hematite, magnetite and often pyrrhotite which is a reddish-bronze iron sulfide mineral. Today's developed countries invest huge amounts of money in systematic airborne magnetic exploration of their territory and surrounding oceans, to assist with geological mapping and in the discovery of magnetizable mineral deposits. The magnetic field of magnetizable ore bodies falls off proportional to inverse distance cubed (dipole magnetic target), or at best inverse distance squared (magnetic monopole target). Generally, the combination of multiple magnetic sources is measured on the surface of the Earth [Macintyre, Steven, 2014]. Airplane mounted magnetometers record variations of the Earth's magnetic field. Different types of magnetometers often can detect metallic explosive devices. The location of the geomagnetic measurements are determined by GPS units.

The magnetic method is generally adaptable for the following themes:

- Locate ditches and pits including buried ferromagnetic debris,
- Locate deserted steel well casings,
- Locate buried steel pipes and tanks,
- Investigate former waste dumps and landfill bodies,
- Detect covered unexploded ordnance (UXO),
- Imaging basement geology and fault structures,
- Explore archaeological sites.

13.6 Advantages of the method

The total magnetic field surveys are capable of discovering massive sulphide mineral layers, especially when utilized the magnetic method in conjunction with electromagnetic measurements. Nevertheless, the main target of magnetic measurements is iron ore. The magnetite/haematite ratio must be high to produce significant anomalies, as haematite is generally non-magnetic.

13.7 Disadvantages of the method

Ground magnetic measurements are generally performed over not so large areas on a formally detected target. Reasonably, the spacing between two stations is generally of the order of 1–100m or continuous measurements (with overhauser type magnetometer). Of course smaller distances can be employed where magnetic gradient values are high. Measurements cannot be taken in the vicinity of ferromagnetic objects such as automobiles, metallic pipelines, roads, iron fences, barbed wire, buildings..., which can disturb the local magnetic field. For similar reasons, users of magnetometers should not wear ferromagnetic clothing.

Base station readings are necessary for monitoring the diurnal variations of the total magnetic field.

13.8 Industrial solutions—Purchasable instruments

Mapping Marine Ferrous Targets Using the SeaQuest Gradiometer System. Figure 88 show the results of a target survey conducted by the United States Naval Undersea Warfare Centre (NUWC) – Keyport, WA. The images show the striking contrast between conventional magnetometer (total field) data and the high resolution gradient data obtainable with SeaQuest. See at <http://www.marinemagnetics.com>. Figure 88 shows the total magnetic field data collected by the top sensor of the SeaQuest platform.

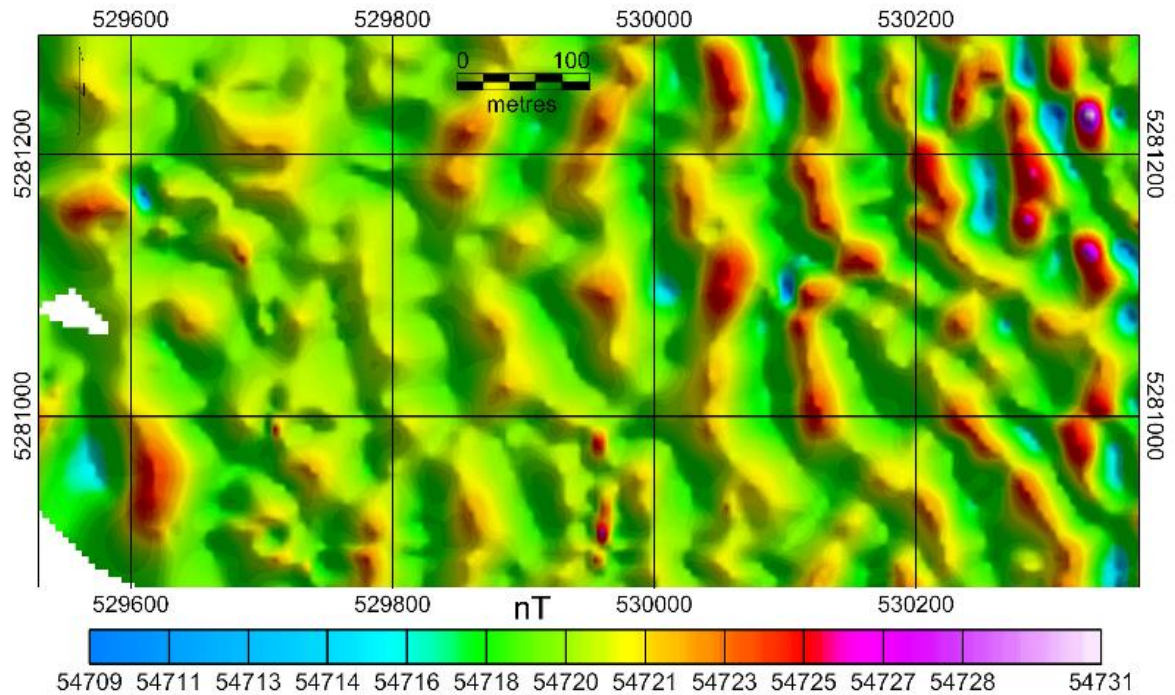


Figure 88. Total magnetic field map of the NUWC survey site. The image is dominated by North-South trending curvilinear anomalies related to buried geology [16]

Only a few ferro-magnetic targets are identifiable. The Eastern part of the survey block is dominated by geological noise. This image shows data that would be obtainable by a conventional total field survey. North-south trending curvilinear anomalies dominate the total field image. These anomalies are related to the magnetic susceptibility variations in the bedrock. It is hard to quickly identify anomalies associated with ferrous objects because of the strong background magnetic response [14]. Presenting the total field grid with a 'stretched' colour-scale allows identification of at least four potential ferrous targets in the western half of the survey site. In contrast, the total gradient map (Figure 89) allows easy identification of at least 12 (high-confidence) ferro-magnetic objects within the survey block.

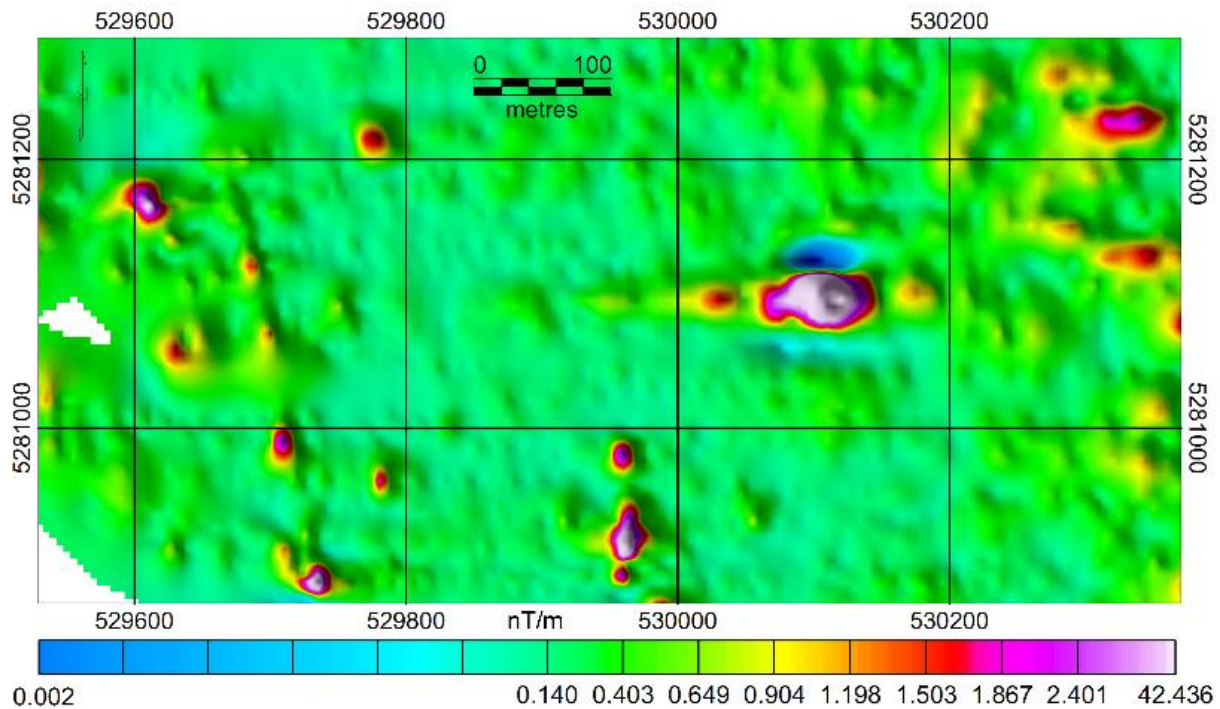


Figure 89. Total Magnetic Gradient (analytic signal) map of the NUWC survey site. The deep geological signal is eliminated, and extremely small targets can be easily resolved, including a faint linear feature in the west that was invisible in the total field data [

The wavelengths associated with the geological magnetic effects are effectively suppressed in this image in comparison to the total field image. Targets are defined by simple 'bulls-eye type' positive anomalies, which are centered over the target position. In the western part of the survey block, a low amplitude NNW-trending linear anomaly is present. This anomaly corresponds to a known pipeline marked on the marine charts of the area. It is worth noting that the amplitude of the pipeline anomaly is less than 0.5nT/m, and yet it is clearly visible in the total gradient map. Also of interest is the large anomaly east of the center of the map. Despite its size, the anomaly is obscured by geology in the total field data, yet it shows up prominently in the total gradient data. It is easy to see that the total gradient (Analytic Signal) directly measured by SeaQuest provides the clearest results, effectively creating an intuitive magnetic 'image' of the sea bottom. While the single axis gradient results enhance only certain types of anomalies based on their geographic direction, the total gradient is effectively a direction independent result, enhancing all near-surface anomalies equally, and suppressing deep geology evenly. Magnetic gradient is commonly used to enhance the signals from small, relatively close sources typical of iron manmade objects, and to suppress the signals from large distant sources associated with geological variation. The total gradient technique goes even further by eliminating the directional dependence of conventional gradiometer methods. This produces an easily interpreted magnetic 'image' of the sea floor, with target positions unambiguously marked by 'bulls-eye' type anomalies (Figure 90). Also, the total gradient anomalies are expressed with a higher signal-to-background-noise ratio than with conventional techniques, enabling the identification of tiny targets that would otherwise be invisible. The SeaQuest gradiometer platform enables the acquisition of high quality total gradient data because of its hydrodynamic stability and the high absolute accuracy of its sensors, producing clean results free from heading errors and offsets. Despite high currents and demanding conditions, SeaQuest provided consistent results that did not require the filtering or level-shifting that is necessary steps, yet large sources of calculation error, for other gradiometer instruments.

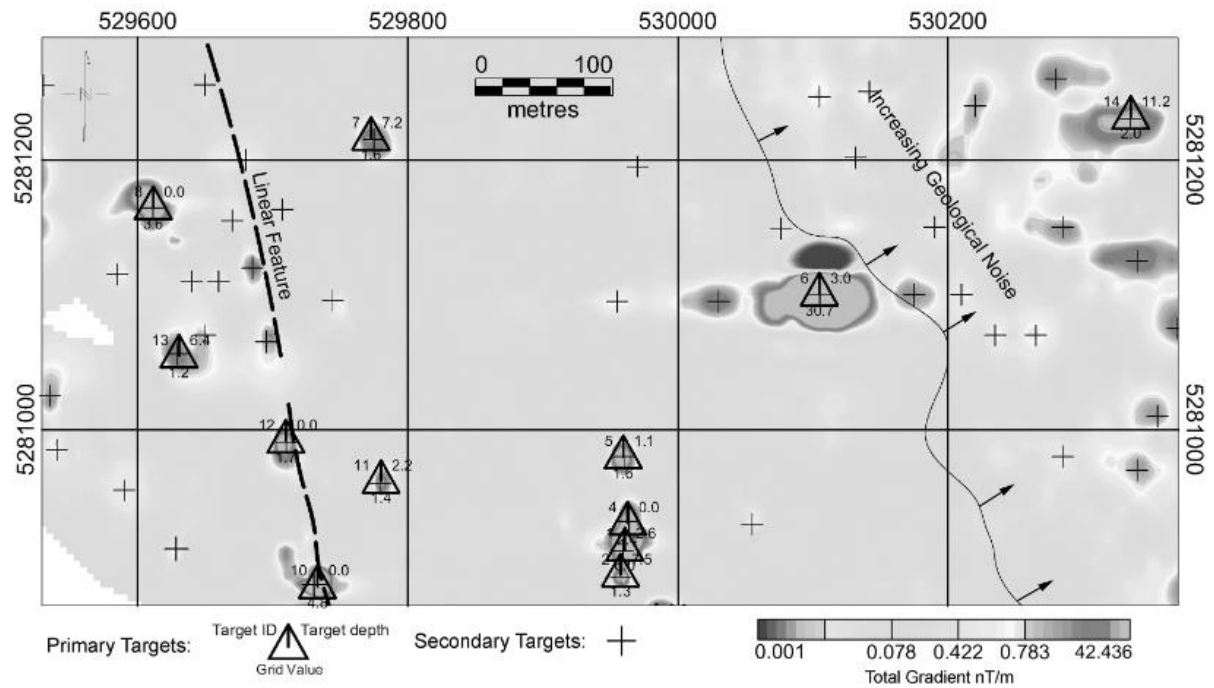


Figure 90. Interpretation of data products overlaid on grayscale total gradient map. Primary target depth estimates (see triangle symbols) obtained from Euler Deconvolution of the measured gradients. Total gradient grid values of the target position provide an estimate of the relative target [16]

13.9 Conclusion

The method may yield misleading results because of iron objects in the mines (as with the pipeline in the example above). Magnetizable objects can interfere with the measurements.

Though it is important to point it out that with the short-time stoppage of the trusters of the UX1 robot (a few seconds), the flux-gate sensors to be installed can provide useful information about the crossing position of the layers of the unexploited magnetic ore bodies, and about the archeologic information regarding mining processes.

Suggested/Suggested with comment (suggested in 2.2)/Unsuggested method

13.10 References

- [1] Arnaud Gerkens, J. C. (1989) **Foundations of Exploration Geophysics**
Elsevier, Amsterdam.
- [2] Bloom, A. L. (1962) **Principles of operation of the rubidium vapor magnetometer**
Applied Optics, Vol. 1, pp. 61–68.
- [3] Budker, D. and Romalis, M. (2007) **Optical magnetometry**
Nature Physics, Vol. 3, pp. 227–234.
- [4] Campbell, W. H. (2003) **Introduction to Geomagnetic Fields**
2nd ed. Cambridge: Cambridge University Press.
- [5] Everett M. E. (2013) **Near-Surface Applied Geophysics**
Cambridge University Press
- [6] Kanasewich, E. R. & Agarwal, R. G. (1970) **Analysis of combined gravity and magnetic fields in wave number domain**
Journ. Geophys. Res., Vol. 75, pp. 5702–12.
- [7] Macintyre, Steven A. (2014). **"Magnetic field measurement."** (PDF)
ENG Net Base (2000). CRC Press LLC.
- [8] Nettleton, L. L. (1971) **Elementary Gravity and Magnetism for Geologists and Seismologists**
Monograph Series No. 1. Society of Exploration Geophysicists, Tulsa.
- [9] Nettleton, L. L. (1976) **Gravity and Magnetism in Oil Exploration**
McGraw-Hill, New York.
- [10] Paterson, N. R., and Reeves, C.V., (1985) **Applications of gravity and magnetic surveys - The state-of-the-art in 1985**
Geophysics Vol. 50, pp. 2558-2594.
- [11] Sharma, P. (1976) **Geophysical Methods in Geology**
Elsevier, Amsterdam.
- [12] Stacey, F. D. & Banerjee, S. K. (1974) **The Physical Principles of Rock Magnetism**
Elsevier, Amsterdam.
- [13] Swindt, P. D. D., Svenja, K., Vishal, S., Hollberg, L., Kitching, J., Liew, Li-A. , Moreland J. (2004) **Chip-scale atomic magnetometer**
Appl. Phys. Letters, Vol. 85, Num. 26. [DOI: 10.1063/1.1839274].
- [14] Tarling, D. H. (1983) **Palaeomagnetism**
Chapman & Hall, London.
- [15] Telford, W. M., Geldart, L. P., and Sheriff, R. E. (1990) **Applied Geophysics (2nd ed.)**
Cambridge: Cambridge University Press
- [16] http://seatronics-group.com/files/4714/1820/5717/Marine_Magnetism_SeaQuest_-_Datasheet.pdf
- [17] http://www.irm.umn.edu/hg2m/hg2m_b/hg2m_b.html
- [18] <http://www.os.is/gogn/unu-gtp-sc/UNU-GTP-SC-11-24b.pdf>

14 MICROGRAVIMETRY SURVEYING

14.1 Theoretical Background

Gravity is a basic attribute of matter. Gravity surveys are based on the different bulk density of the rocks and use the natural field to study the geological situation for ore and oil exploration, environmental purposes, and locating cavities.

Microgravimetry studies the g variations, to detect density anomalies underground and is expressed in μGal ($1\mu\text{Gal}=1\times 10^{-8}\text{m/s}^2$).

Gravity anomalies arise from natural or artificial sources (for example voids, cavities, dense material/rock). The average gravitational pull is 980,000,000 μGals . Variations caused by voids generally involve up to 200 μGals of change.

Gravimeters have been developed for measuring gravitation in land or marine environment.

The gravity signal involves a direct Newtonian attraction, and a contribution because of the flexure of the Earth's crust which modifies the gravimeter altitude. Furthermore several types of noise complicate the observed signal.

When a gravimeter is placed above a dense material it records a relative high gravity value. When it is positioned over a low density feature (for example: cave) a relative low gravity value is recorded. See an example of negative anomaly below in Figure 91.

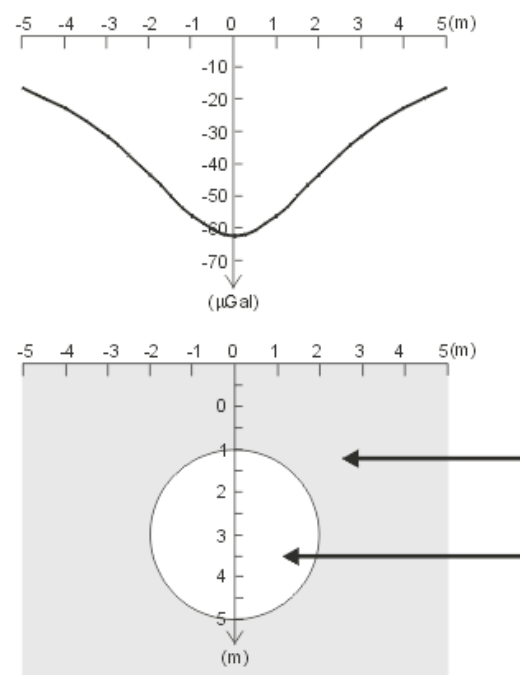


Figure 91. Diagram about a negative anomaly over a void

The modern generation of field gravimeters allows to register promptly or digitally anomalies.

A density anomaly can be detected only if the produced gravimetrical anomaly is higher than the significance level. The significance level can be approx. 15 or even 10 μgals in good measuring conditions but in extreme conditions it can increase significantly, decreasing the efficiency of the method.

Microgravity surveys are particularly sensitive to the data collection methodology so careful data acquisition and processing is required.

Readings are recorded at stations of different distances depending on the situation. An example can be seen in Figure 92.

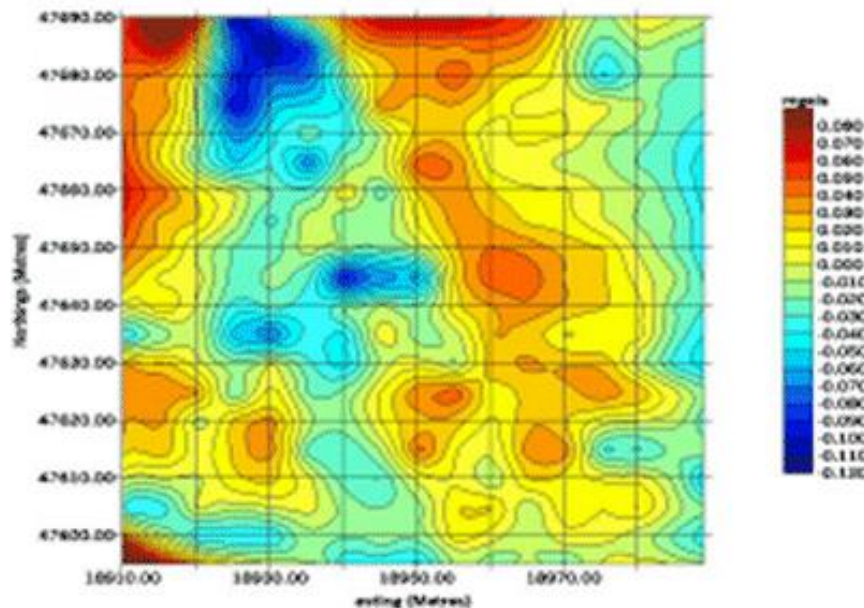


Figure 92. Example of Microgravity Results

Butler investigated the gravity and gravity-gradient determination and the interpretation process of microgravity. Debeglia & Dupont studied the types of noise in the microgravity surveys. Styles et al. dealt with corrections in microgravity under complicated environments. Nind et al. [9] studied the application of gravimetry in boreholes.

14.2 Measured parameter

In gravimetry the changes of the gravitational acceleration have been detected. The measured parameter could be the potential or the derivative of the potential.

14.3 Measuring method

Gravimeters are based on either the free-fall method or the rise & fall method. The fundamental method used by both of them is the movement of a sensor in a vacuum chamber. For the required accuracies of gravimeters the observation is needed within two or three days.

The observation time in case of new generation of miniaturized, transportable absolute gravimeters is reduced to 10 minutes in an undisturbed area.

In exploration studies relative gravimeters are used to determine the observed differences in gravity. The gravity differences (Δg) caused by local density inhomogeneities that show small variances from the undisturbed gravitational acceleration. The construction of relative gravimeters only enables the observation of the vertical component of Δg . Relative gravimeters can operate in dynamic mode or static mode. The gravimeters that work in dynamic method observe the oscillation time of the sensor. Those based on the static method have the sensor held in a null-position and the change of equilibrium between two observations is a function of the gravity change.

Before the gravitation survey the data collection methodology has to be carefully tailored to the site and environmental conditions, as well as to the survey target. Calibrations are needed before measurement.

We have two base stations, the relative and the absolute one. The hand held instrument could be brought into the field and the gravity changes can be recorded in discrete data points. At each point, the exact elevation have to be determined. The calculation process could be very slow because of the several corrections and records.

The accuracy of corrected gravity measurements is influenced by inadequate corrections of tidal effects and by a poor estimation of ocean loading effects. In field studies the residual tidal effects are usually integrated into an experimental terrain drift estimated on the basis of frequent repeated measurements. Correction of the measured data with a mobile gravimeter could be carried out with the records of a fixed gravimeter.

Gravity surveys in boreholes are carried out with Gravilog sonde. The probe is deployed inside the hole and left there overnight and the measurements are collected on the next day.

At each station the probe is secured by a clamp. The pressure is detected, the gravity sensor was levelled, and recordings are taken twice per minute. Then the clamp is disengaged and the probe is moved to the next station. At each station the whole process takes about 5 minutes.

Figure 93 shows a residual gravity log as an example:

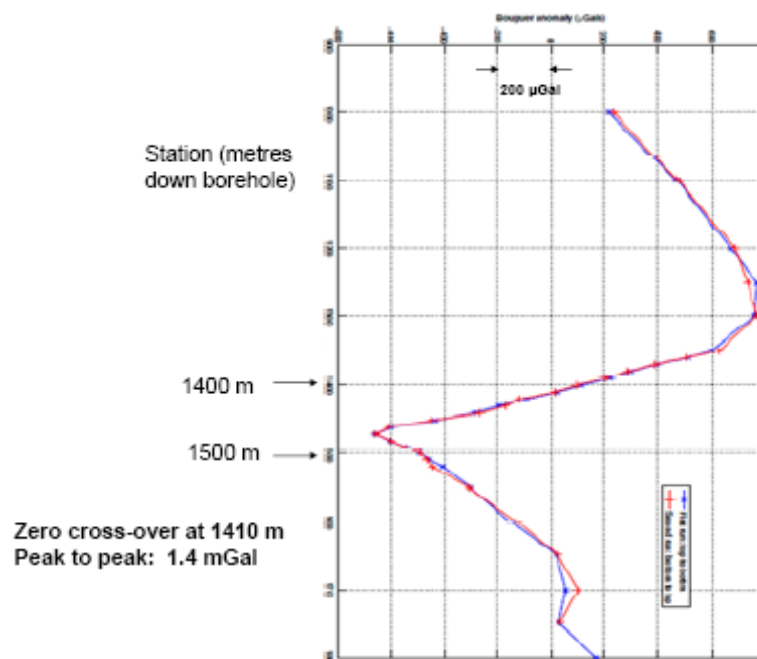


Figure 93. Residual anomaly in Norman Township test [9]

After the gravity measurements several corrections (for example instrument drift, earth tides etc.) are needed. The Data Processing consists of correcting measurements of all disruptive gravimetrical effects and filtering. The Figure 94 shows 3D gravity effects along profiles.

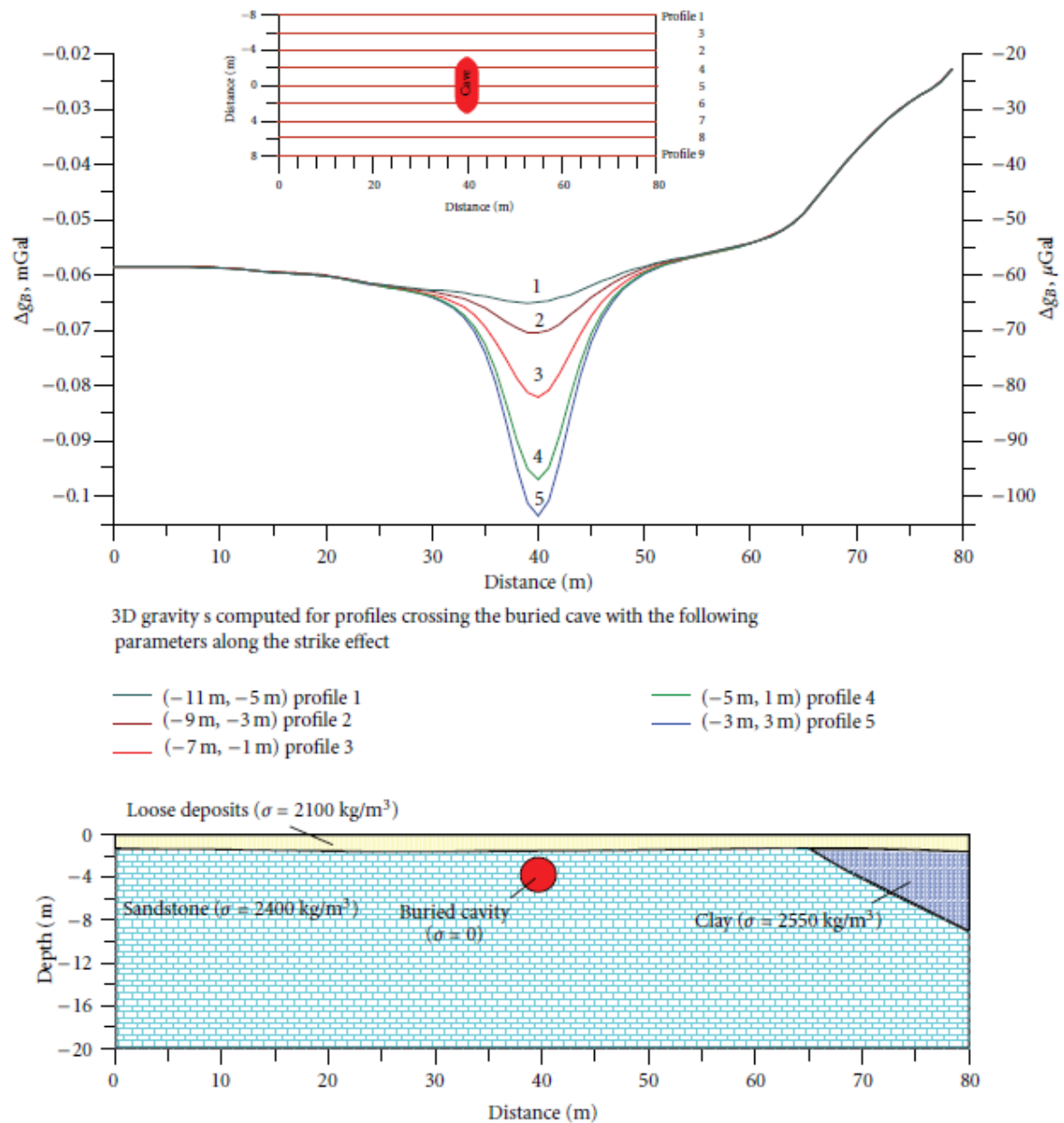


Figure 94. 3D gravity anomalies over a prehistoric cave. In the upper part of the figure the profiles and the position of buried cave can be seen, below it the 3D computed gravity effects is visible, and at the bottom the picture shows the geological-archaeological sequence

The bulk density in a borehole is shown in the Figure 95:

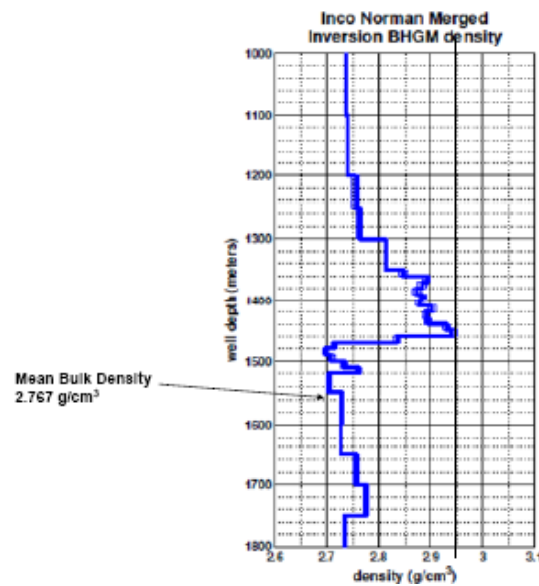


Figure 95. The bulk density in a borehole [9]

The outcome of data processing is the Bouguer anomaly that represents the variations of g due to geological effects. Based on the Bouguer anomaly, the residual anomaly has been determined which is represented on profiles and maps. The negative anomalies correspond to voids or decompressed zones. The positive anomalies can be caused by geological structures (faults, volcanic intrusions, etc.). The example Figure 96 shows a residual anomaly map.

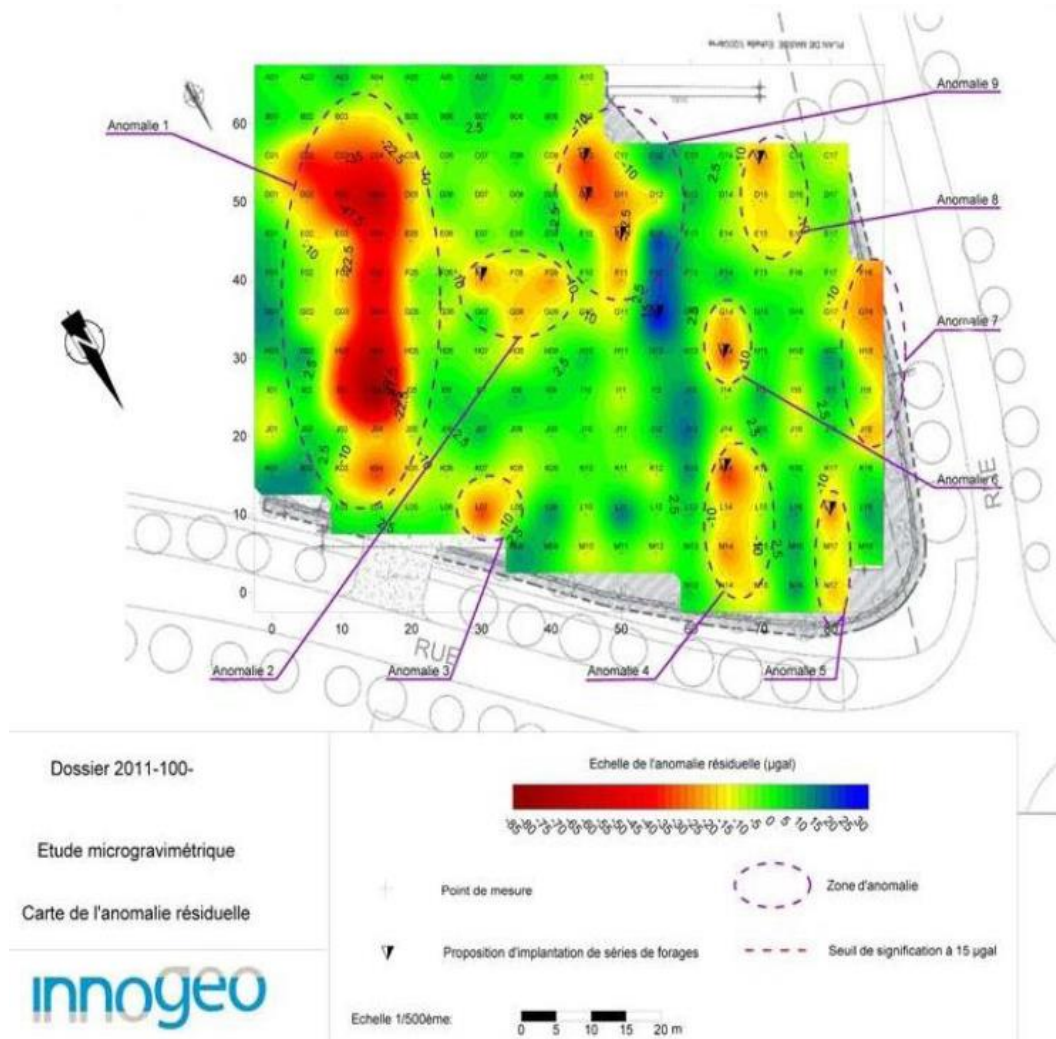


Figure 96. Residual anomaly map of a site in the North of France

14.4 Target parameter

The result is Bouguer anomaly map or gravity effects along profiles.

14.5 Applicability

Microgravity can be applied:

- determining the depth to bedrock
- investigating Bedrock Channels
- situation of abandoned mines
- location of void spaces that contain air and/or water
- detection of bedrock anomalies
- strike direction of the structure and big changes can be detected
- detect different aspects in a soil profile
- determine voids and the void depth and size

14.5.1 Advantages of the method

- It is a passive geophysical method, so there is no needed induction.
- The main advantage of microgravity is that it is not an intrusive technique.
- There are no residual effects of a microgravity investigation.

14.5.2 Disadvantages of the method

- The main disadvantage from the project view is that we need to wait hours/minutes stationary at one measurement point to get correct data.
- Microgravity is a highly sensitive method; any vibrations can invalidate the data.
- The data analysis could take a lot of time.
- Several corrections are needed during the data processing.
- It is not applicable to search horizontal layers.
- Several rocks have similar bulk density.
- The effect of the source depends on the distance between the source and the gravimeter.

14.6 Industrial solutions – Purchasable instruments

Several types of Gravimeters are available in the market. Some of them are introduced below. Commonly in use are gravimeters from LaCoste & Romberg, Scintrex, and Worden.

14.6.1 Worden gravimeters

The measurement with this gravimeter restricted to about 200 mGal, but it can be extended to about 6600 mGal by resets. The precision is about 10 μ Gal.

The gPhoneX gravitimeter

The gPhoneX gravity meter is based upon the G-Meter of the LaCoste and Romberg technology. It has a low drift so that it can be used to integrate periodic signals (like earth tides) for very long time periods (years). The gPhoneX can be coarse-ranged over 7000mGal and it has a ± 50 mGal dynamic range during measurement.

It has a sophisticated data acquisition system synchronized by a rubidium clock that can be locked to GPS. It has 0.1 μ Gal resolution.

LaCoste & Romberg has several gravimeters and microgravimeters.

LaCoste & Romberg gravimeters Model G

It is about 7000 mGal.

LaCoste & Romberg gravimeter Model D

It is restricted to 200 -300 mGal. For surveys of larger gravity differences it must be reset to the requested measurement range. It has a precision of $\pm 10\mu$ Gal.

Micro-g LaCoste Absolute Gravimeters are summarized in the following comparison Table 15:

Meter	Accuracy	Precision	Repeatability	Temp Range	DC	AC	Outdoor Operation
	μGal	$\mu\text{Gal}/\sqrt{\text{Hz}}$	μGal	$^{\circ}\text{C}$			
FG-L	10	100	10	15 to 30		×	
A-10	10	100	10	-18 to +38	×	×	×
FG5-X	2	15	1	15 to 30		×	

Table 15. Comparison table of the Micro-g LaCoste Absolute Gravimeters

From our point of view the A-10 could be interesting, thus this instrument is detailed below.

LaCoste A10 Outdoor Absolute Gravimeter

The A10 (Figures 97 and 98) is an absolute gravimeter optimized for fast data acquisition and portability in outdoor applications. In harsh field conditions (in outdoor sites, in the sun, in snowy and windy conditions) it can also be applied. It has automated leveling, battery operated, temperature controlled sensor, ideal roadside operation from a vehicle. It is based directly on international standards of time and distance.

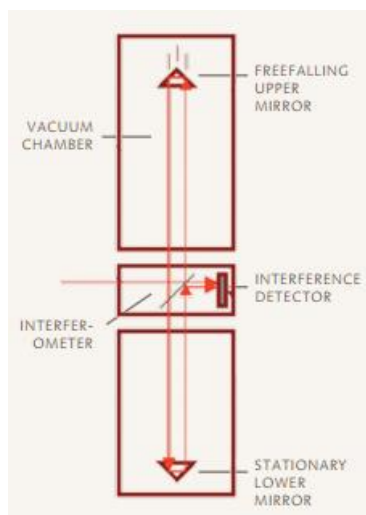


Figure 97. Inside of the LaCoste A10 Outdoor Absolute Gravimeter



Figure 98. LaCoste A10 Outdoor Absolute Gravimeter in use.

Details of the A10:

- Input Power 12-14 DC (vehicle or from lab based 100-240VAC supply –included)
- Full load 25A (300W)
- Average load 16A (200W)
- Total Weight 105kg
- Accuracy 10 μ Gal (Absolute)
- Precision 10 μ Gal in 10 minutes at a quiet site
- Operating temperature -18°C to +38°C,
- Continuous operation

LaCoste & Romberg has developed a gravimeter for borehole use, but it was impractical because of its size and the operational limitations of the probe.

Scintrex has also several instruments. One of them is the **CG-5 Autograv Gravity Meter** (Figure 99) which is fully automatic including correction for earth tides, tilt, and temperature, etc. Its precision is about 5 μ Gal and it can be operated worldwide without resetting.

This microgravimeter is used to make a recording of the shipboard gravimeter. The gravity is measured both at pier and at the standard point where the absolute gravity is well known. Horizontal installation is only needed, since this gravity meter performs measurement and the compensation by the tide automatically.



Figure 99. Scintrex CG-5 Autograv Gravity Meter

The Scintrex CG-5 delivers superior data repeatability in rough field terrain. Station positions are measured with the integrated GPS capability.

- Internal GPS and precise clock for X-Y positions and earth tide corrections
- External GPS input for Z-position and altitude corrections
- Real time free air and Bouguer corrections
- Online near zone terrain corrections
- R/F On Off

Considering that the target environment of UNEXMIN is underwater mines the following instrument could be interesting too.

14.6.2 INO sea-floor gravimeter

This gravimeter uses the CG-5 Autograv™ fused quartz sensor with electrostatic nulling which is incorporated into a submersible system. It has user-friendly software to provide μGal repeatability on the sea floor. The INO gravimeter is designed for a depth of 600 m with an Aluminum pressure sphere.

Scintrex developed a Gravilog probe for gravity surveys in boreholes based on the probe of LaCoste & Romberg. Scintrex reduced the size of its quartz sensor and developed automatic leveling, temperature control and electronics systems to fit into a small diameter probe suitable for mining and exploration boreholes.

Gravilog Slim Hole Gravity Tool (Figure 100) for Mining and Geotechnical Applications

A borehole gravity survey can provide valuable information such as: bulk density determination, rock properties, verification of surface and airborne gravity anomalies, association of mass with conductors, detection of cavities and voids.



Figure 100. Gravilog Slim Hole Gravity Tool

The following hole requirements are needed to use this tool:

- Maximum depth : 2000m
- Minimum hole dia: NQ drill rods (57.2mm, 2 ¼)
- Sensitivity: $>5 \mu\text{Gal}$
- Deviation of Vertical: < 60 degrees

Table 16 below summarizes the target specifications of the Gravilog system.

	Target specification
Sensitivity	better than 5 μ Gal with a one minute reading time
Operating range	7000 mGal
Max sonde diameter	48 mm
Max sonde length	Approx 3 m
Max. operating depth	3000 m (water filled hole)
Minimum hole diameter	NQ drill rods (57.2 mm)
Max. hole deviation from the vertical	60 degrees
Operating temperature range	0 ⁰ C - +70 ⁰ C (downhole section) -40 ⁰ C - +50 ⁰ C (uphole section excluding PC)
Vertical position determination in borehole	+/- 5 cm between successive stations (depth will be determined with a combination of pressure sensor, winch encoder and inclinometer)

Table 16. Target Specifications of Gravilog System

14.7 Conclusion

This method needs a long stationary positioning time that cannot be ensured in the autonomic robot. The weight and size need of this type of technique is beyond the possibility of the robot considering the currently available instruments in the market. The records would be very noisy so data processing development would be needed.

By the above microgravimetry discussion it is not suggested that this is used in this phase of the project.

Suggested/Suggested with comment (suggested in 2.2)/Unsuggested method

14.8 References

- [1] Brown J. M., Niebauer T.M., Richter B., Klopping F.J., Buxton W.M., Valentine J.: **Minaturized gravimeter may greatly improve measurements**
EOS Online Transactions, 1999
- [2] Castiello G., Florio G., Grimaldi M., and Fedi M.: **Enhanced methods for interpreting microgravity anomalies in urban areas**
First Break, Vol. 28, no. 8, pp. 93–98, 2010.
- [3] Debeglia N. and Dupont F.: **Some critical factors for engineering and environmental microgravity investigations**
Journal of Applied Geophysics, Vol. 50, no. 4, pp. 435–454, 2002.
- [4] Eppelbaum Lev V.: **Review of Environmental and Geological Microgravity Applications and Feasibility of Its Employment at Archaeological Sites in Israel**
Hindawi Publishing Corporation. International Journal of Geophysics, Volume 2011, Article ID 927080, 9 pages doi:10.1155/2011/927080
- [5] Parasnis D.S. : **Principles of Applied Geophysics**
ISBN 0-412-28330-1. Chapman and Hall, 1986
- [6] Seigel H.O., Nind C.J.M., Milanovic A., MacQueen J.: **Results from the Initial Field Trials of a Borehole Gravity Meter for Mining and Geotechnical Applications**, 2010
- [7] Sharma P.: **Environmental and Engineering Geophysics**
ISBN 0-521-57632-6. Cambridge University Press, 1997
- [8] Lalancette-Le Quentrec M.F., Simon B., Orseau D., Florsch N., Llubes M., Amalvict M., Hinderer J.: **Ocean loading and crustal deformation in Bretagne (France): an experiment involving differential GPS, gravimetry and tide gauges**
Bollettino Di Geofisica Teorica ed Applicata, Vol 40, N.3-4, 533-536, 1999
- [9] Nind C.J.M., Seigel H.O., Chouteau M., Giroux B, **Development of a Borehole Gravimeter for Mining Applications**
EAGE First Break v. 25, pp.: 71-77 July 2007
- [10] Torge W (1989): **Gravimetry**
Walter de Gruyter, 465 pp
- [11] http://www.scintrexltd.com/internal.php?storeCategoryID=1&subcatID=9&s_page=Gravity
- [12] <http://www.microglacoste.com/gPhoneX.php>
- [13] https://patentscope.wipo.int/search/docservice_fpimage/WOIB2008000738@@@false@@@
- [14] <http://www.microglacoste.com/index.php>
- [15] <http://www.scintrexltd.com/gravity.html>
- [16] <http://www.microglacoste.com/index.php>

15.1 Theoretical Background

Nowadays the 3-D interpretation method is preferred rather than single 2-D sections to give information about the structure of the subsurface. Seismic reflection tomography gives three dimensional images of the subsurface based on a seismic measurement database. The seismic methods rely on the different bulk densities of the layers and the mechanical properties of geological formations. These properties cause different wave velocity in the rocks. Wave generation can be passive or active. When the geophysicist generates seismic waves in order to collect data from targeted area this is called the active method. This tomography can be acquired either at sea or on land. There are no specific required site conditions to work with it.

In practice the travel time of certain types of seismic energy has been measured by geophones. Seismic energy travels in waves in the subsurface then before the energy arrives at a geophone it is refracted and/or reflected at interfaces between materials with different densities (seismic velocities). The law of refraction and reflection of seismic energy behaviour at density contrasts is the same as for light passing through prisms. When a generated seismic wave strikes a density contrast some part of the energy is refracted into the underlying layer, and the remained energy is reflected at the angle of incidence. The reflected seismic wave is never detected as first arrival (see the Figure 101).

At less than approx. 15 m depth, the reflections from surface of density contrasts arrive at geophones nearly at the same time as the surface waves and the air blast. Deeper targets (more than 15.24 m) can be detected more easily because the reflections from greater depths arrive at geophones after the surface waves and air blast.

Seismic waves are recorded. The results of the measurement are complex databases of overlapping seismic arrivals which contains filtered data. Based on the travel time the structure of the subsurface can be estimated. The vertical resolution of this method is 5 to 10 percent of depth. The lateral resolution is approximately half of the the geophone spacing.

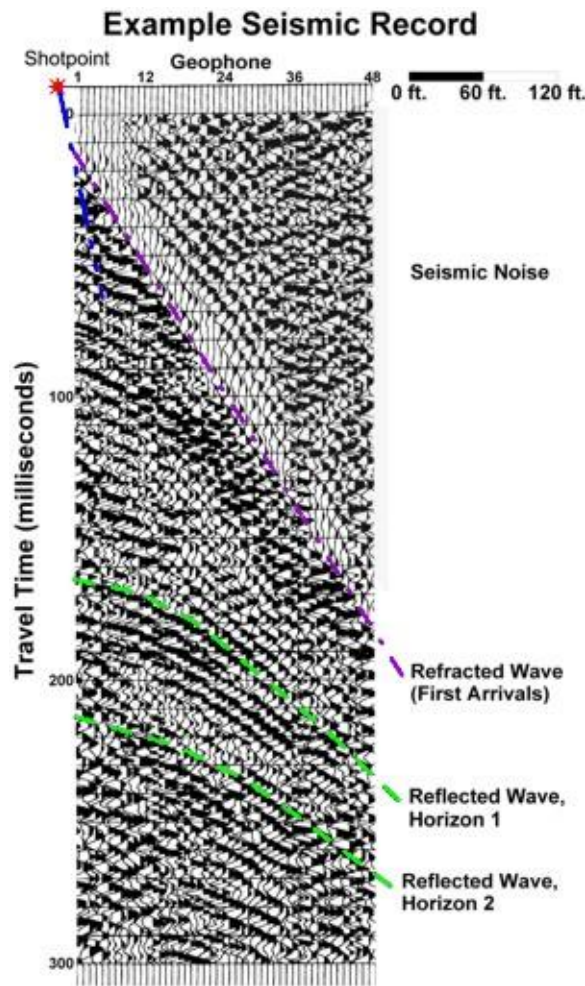


Figure 101. An Example of Seismic Record that is typical ground motion produced by a shot [1]

15.2 Measured parameter

The measured parameter is the time difference that is detected between the shot and the first wave arrival time at the geophone.

15.3 Measuring method

The Reflection Tomography consists of two steps. The first one is the seismic measurements for identification of acoustic discontinuities and determination of relative travel times at different source-receiver positions. The second step is the local velocity model estimations by an iterative inversion procedure. The picking accuracy is limited by various effects. The systematic error of the velocity and the reflection depth points determination is about 3%. The seismic method could be used on land and at sea. The basic concepts of the measurement are the same in both environments but the measuring technique is different.

In case of a submarine survey the measuring method can be seen in Figure 102.

As energy sources we use air guns, which produce noise by using compressed air. The shot point is the place of detonation. Each shot point is uniquely numbered. The sound waves pass through the water column, then the noise penetrates into the sea floor and reflects from the underlying rock formations. An array of hydrophones receives the reflected noise signals. Their exact travel time will depend on the speed

that sound travels through the rock (seismic velocity). Examining the readings the structure of rock strata can be determined.

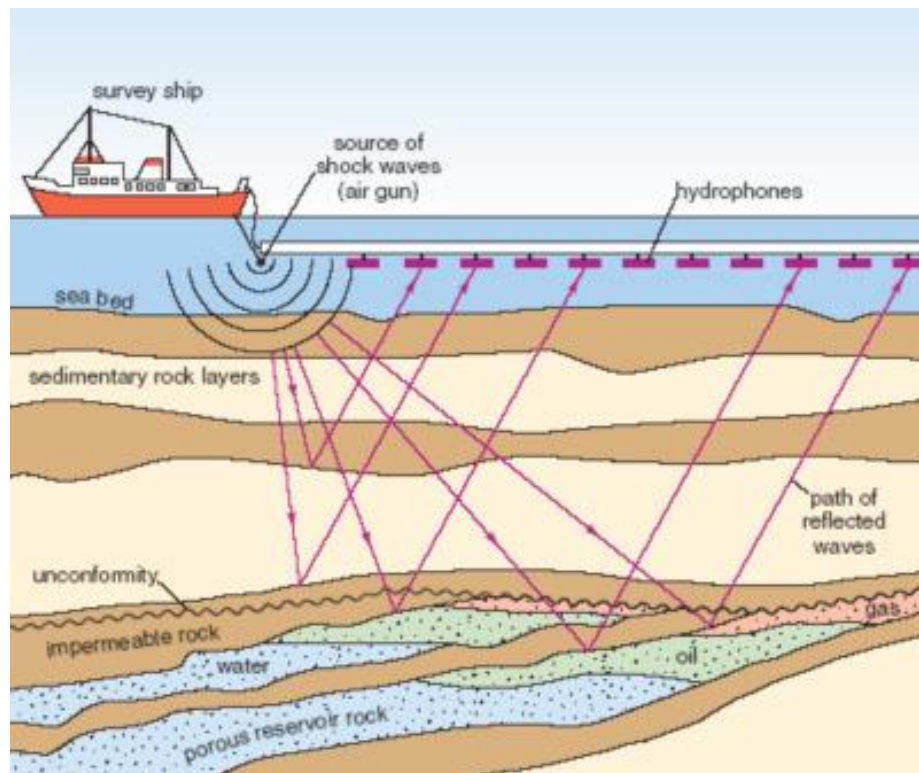


Figure 102. Seismic surveys in marine environment [2]

Computer processing makes it possible to amalgamate the recordings from all the shot points, and filter out unwanted signals of different sorts. The 2-D or 3-D seismic data are displayed in a coordinate-system. The horizontal axis indicate the distance along the profile and the vertical axis shows the time (in seconds). The TWT is usually converted into depth.

In case of ground survey the measuring method is shown in Figure 103.

Vibration can be generated in different ways. The source wave can be generated with hammer, via explosions, etc. then the generated seismic waves are reflected, refracted at interfaces of the ground, and travel times are recorded in the arrays of geophones. The seismic velocities via fragmented material are slower than in more consolidated material. The velocities of P-waves are bigger in saturated than in unsaturated environment.

In practice with the field and data processing procedures the geophysicists try to maximize the energy reflected along near vertical ray paths by subsurface density contrasts.

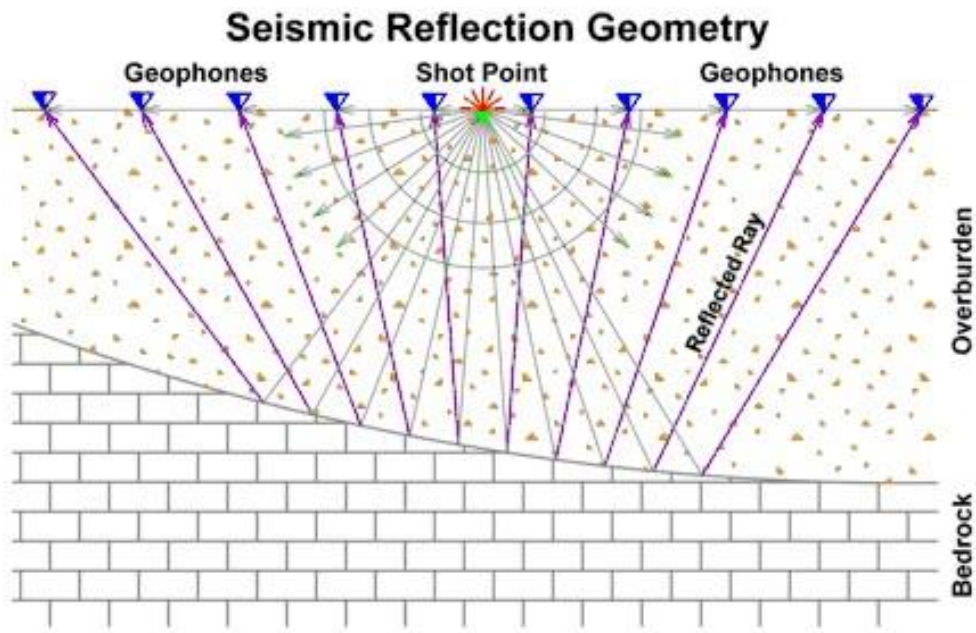


Figure 103. Seismic survey in the ground [1]

The target parameter is the density contrasts. The final result of the seismic method is a 2-D seismic section or a 3-D visualization. See an example in Figure 104. At the outset, interpretation includes tracing continuous reflectors on 2-D sections in order to create a structural representation of the subsurface.

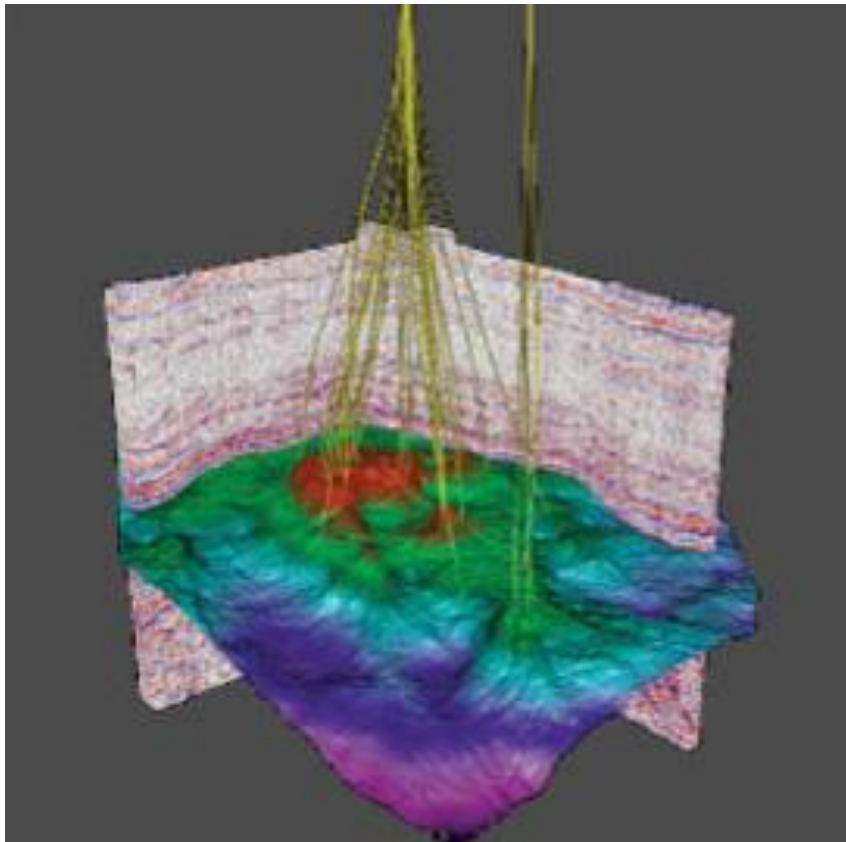


Figure 104. A 3-D view of the Palaeocene reservoir in the Nelson Field, North Sea

15.4 Applicability

This method is most commonly applied for determining the geometry of oil/gas reservoirs, showing the presence of petroleum directly and particularly dispersed gas, surveying rock characteristics, and investigating depositional environments. We can use the method to locate oil and gas deposits beneath the sea floor, and for research on submarine rock structures.

15.4.1 Advantages of the method

It is suitable for marine applications. In marine environment high quality reflection data collection is possible even at very shallow depths because of the inability of water to transmit shear waves. The method could be useful in the case of a very deep environment or small targets.

15.4.2 Disadvantages of the method

The main disadvantages of this technique are its high cost. Other difficulties are the practical limitations. From the point of view of the UNEXMIN project additional energy is needed. Because it is an active method, energy is needed to generate the vibration.

15.5 Industrial solutions—Purchasable instruments

Several types of seismographs are available in the industry. Some examples are listed below with their details.

The **StrataVisor NX** model (Figure 105) from the Geometrics is a Land and Marine application with up to 132 internal channels.



Figure 105. StrataVisor NX Seismograph

This product is available in rugged portable form or rack mount model. It is suitable for all seismic surveys: reflection, refraction, downhole, VSP, marine or monitoring.

ES3000 Seismograph (Figure 106) with 12 channel works perfectly for cross-hole surveys, engineering, construction, road building, and teaching.



Figure 106. ES3000 Seismograph

This instrument is applicable for finding bedrock, depth-to-water, faults and fractures. It gives best quality data with automatic settings, minimum errors. Its interface is easy. There are no complicated drivers, plugs directly into your PC Ethernet port. It is 25 x 20 x 14 inches of size, lightweight (8 lbs/3.5 kg) and low-power.

Geode Seismograph (Figure 107) is ideal for refraction or reflection, downhole or VSP - even tomography surveys.



Figure 107. Geode Seismograph

Geode architecture and Geometrics software let one build seismic recording systems from 3 to 1000 channels with multiple lines and built-in roll capability. The Geode seismic modules house from 3 to 24 channels each, weigh only 3.6 kg and interconnect using inexpensive digital network cable. The Geode will run all day on a small 12V battery and sleeps when not in use.

The last example of seismographs is the **SmartSeis SE 24 Seismograph** (Figure 108).



Figure 108. SmartSeis SE 24 Seismograph

It is a 24-channel integrated seismic exploration system that can provide answers in the field with built-in rugged PC, daylight-visible screen and even a high-resolution plotter. The SE Model is modified with longer record length collection suitable for Surface Wave surveys. It is capable of refraction, reflection and MASW projects.

Applications in this Seismograph:

- Depth-to-bedrock
- Rippability surveys
- Groundwater hydrology
- Foundation investigations
- Landside potential
- Hazardous waste migration
- Dynamic moduli measurements
- Fault Location
- Stratigraphic mapping
- Gravel and aggregate mining
- Thickness of overburden
- Mineral and gold exploration
- Landfill delineation and siting
- IBC Vs30 site classification

This instrument is 23 X 25 X 17 inches of size and 70 lbs weighs.

The other important equipment in underwater environment is the hydrophone.

Hydrophone Singles (Figure 109)



Figure 109. Hydrophone

These are individual pressure transducers (9Hz with piezoelectric crystals) with long leads for connecting to Mueller-type take-outs. They are intended to be used in situations where a stream crossing allows the cable to be suspended above the water and the phones can easily be attached and dropped on the bottom to eliminate gaps in the record. Hydrophone diameter is 0,04 m. Its length is 0,2 m. Each hydrophone has a 0,5 m lead. 0,04 x 0,2 m.

The GEOEEL with up to 480 channels is another type of seismic equipment applied in marine environment. It is a towed hydrophone streamer (Figure 110).

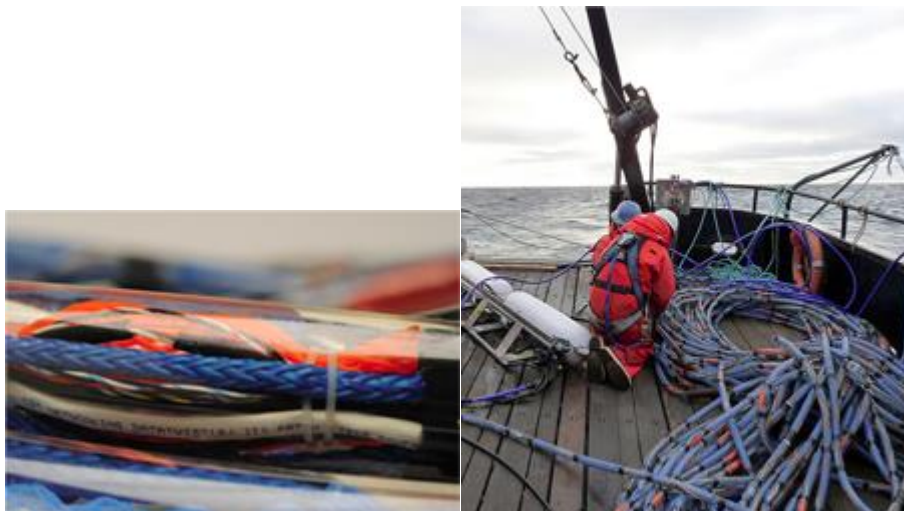


Figure 110. a) GEOEEL b) Digital towed hydrophone streamers

The GEOEEL series of digital towed hydrophone streamers are the first small diameter arrays with the performance of larger systems. With a diameter of only 41mm, the GEOEEL-Liquid is easy to deploy, easy to transport and largely immune from the noise, leakage and ground loops that plague the installation of analog streamers in a marine environment.

The GEOEEL-Liquid is filled with inert silicon oil which makes it environmentally safe. Thick 1/8" abrasion resistant polyurethane keeps the streamer extremely rugged but still flexible enough to be deployed by hand or mount on small winches. And the GEOEEL-Liquid is easy to be repaired – no fragile fiber optics to break or go bad.

Sampling intervals of 2 ms to 1/8 ms make the GEOEEL-Liquid suitable for deep petroleum, high-resolution engineering surveys or even for sub-bottom profiling. Near-zero dead time makes surveys fast and efficient. A built-in digitally controlled oscillator provides calibration test signals for each channel. Other tests include noise, offset, pulse test, timing, leakage and capacitance of hydrophone elements.

The GEOEEL-Liquid transmits data via fast Ethernet to Geometrics CNT-1 controller, running field-proven software.

Features of the equipment:

- configurable with up to 240 channels
- digital Streamer means better quality data, less time deploying system
- comparable in price to analog systems
- light weight, easy to deploy on small boats
- 2 ms to 1/8 ms sampling means suitability for more kinds of surveys
- 24-Bit, 110 dB dynamic range
- automatic configuration and fully self-testing
- small diameter (41 mm, 1.6") means easy deployment by hand or with small winches
- easily shippable, no special environmental requirements, filled with inert silicon oil
- rugged, 1/8" wall thickness, can be used as bay cable, transition zones
- multiple streamer configuration
- works with standard birds
- uses geometrics CNT-1 PC controller
- separate windows display shots, gathers, trigger timing, noise, gun energy, tape status, alarms
- real-time brute stack
- multiple storage devices
- integrates data from sources,
- drives multiple printers

GEOEEL is suitable for wide range of surveys for example high-resolution engineering surveys, sub-Bottom profiling. It uses any impulsive source, and large channels (up to 240) or small channels (hand deployed)

15.6 Conclusion

Since it is an active method additional energy is needed. Furthermore the full reflection seismic system is needed to be created. Wall contact is required for the geophones or the hydrophones series is needed to be pulled by the robot.

For economic reasons and considering the requirements of the project (applying non-invasive methods, autonomous robot without any external cabling, is not recommended method in this project.

Suggested/Suggested with comment (suggested in 2.2)/*Unsuggested method*

15.7 References

- [1] <http://www.enviroscan.com/home/seismic-refraction-versus-reflection>
- [2] <http://www.open.edu/openlearn/science-maths-technology/science/environmental-science/earths-physical-resources-petroleum/content-section-3.2.1>
- [3] <http://www.alpha-geo.com/products/seismic/>
- [4] <http://www.expins.com/item/se-24>
- [5] Böhm G. and Vesnaver A. L.: **The Sampling Problem in Seismic Tomography** 57th EAGE Conference and Exhibition, Extended Abstracts, 1995
- [6] Butler K. D.: **Near-Surface Geophysics. Society of Exploration Geophysicists** Oklahoma, USA, 2005
- [7] De Iaco R., Green A.G., Maurer H.-R., Horstmeyer H.: **A combined seismic reflection and refraction study of a landfill and its host sediments** Journal of Applied Geophysics. Vol 52., pp.: 139-156, 2003.
- [8] Monier-Williams M., Maxwell M., and Schneider G.: **Preparing for waste: geophysics in geotechnical and environmental assessments of proposed mine waste facilities** In Proceedings of Exploration'97, Fourth Decennial International Conference on Mineral Exploration, ed. A.G. Gubbins, pp.: 893-904. Toronto, 1997
- [9] Lanz E., Maurer H.R., Green A.G., 1998. **Refraction tomography over a buried waste disposal site** Geophysics 63, pp.: 1414 – 1433, 1998
- [10] Parasnis D.S. : **Principles of Applied Geophysics** ISBN 0-412-28330-1. Chapman and Hall, 1986
- [11] Sharma P.: **Environmental and Engineering Geophysics** ISBN 0-521-57632-6. Cambridge University Press, 1997
- [12] Upadhyay S.K.: **Seismic Reflection Processing** ISBN 3-540-40-875-4. Springer. 2004

16.1 Theoretical Background

Raman spectroscopy is based on the analysis of the emitted electromagnetic radiation resulted from the interaction between a laser beam and the irradiated material. A monochromatic laser beam irradiating any type of materials will produce scattering = emitted radiation. Similarly to FTIR analysis, the vibration modes and energies of chemical bonds are the basis of investigation. Contrary to FTIR, where only absorption occurs, in Raman spectroscopy scattering is the measured parameter. Three types of scattering have to be taken into account: Rayleigh scattering, Stokes Raman scattering and anti-Stokes Raman scattering (Figure 111). Here, vibrational energy states refer to the naturally occurring vibrations characteristic for the environment in which the given material is stable.

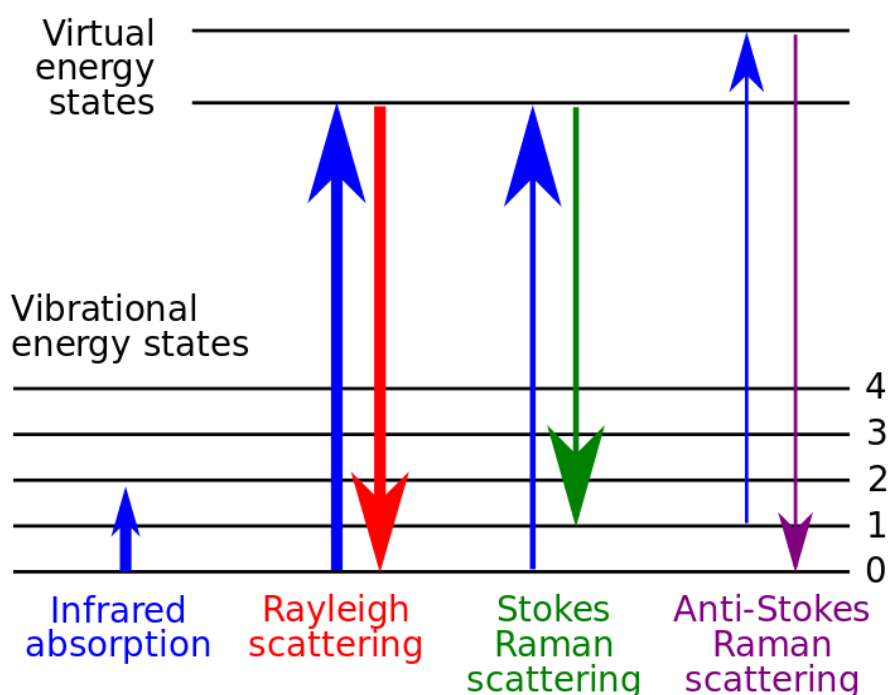


Figure 111. Scattering types as a result of laser excitement [9]

Rayleigh scattering comprises the elastically scattered photons which preserve the frequency of the incident beam. The analytically useful interaction is materialized as excitement of chemically bonded elements, the radiation emitted during neutralization is known as Raman spectra, if plotted as intensity vs. the shift of wavelength from the incident radiation. The Raman scattering, very weak in intensity as compared to the irradiating beam and also the Rayleigh scattering, is produced by inelastic scattering. Inelastic scattering occurs when the incident photon is adsorbed leading to excitation of molecular motion (raising the natural vibration state), thus creating a higher and unstable energy state (Figure 112). The decay from the unstable energy state may result in emission of photons with different energy from that of the incident beam. Regarding the vibrational state before and after excitation, the Stokes and anti-Stokes domains can be delimited in the emitted spectra, as left and right side part in relation to the incident beam energy. Spectral distribution is expressed as frequency of radiation and quantified as reciprocal centimetres ($1/\text{cm}$).

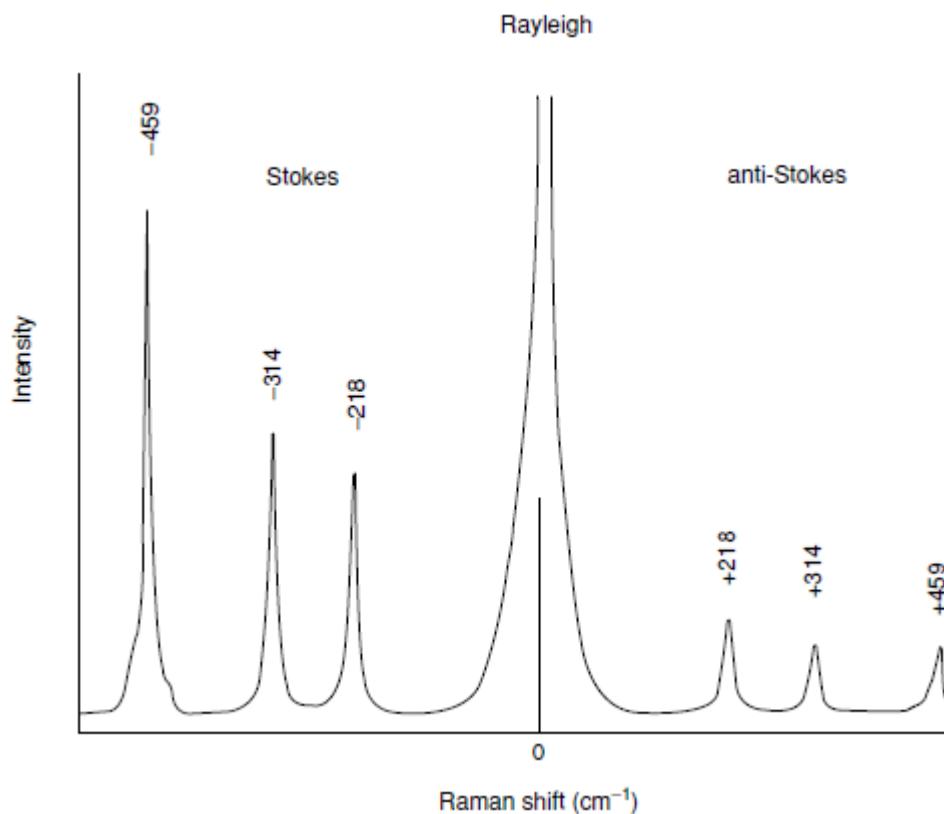


Figure 112. Scattering types and regions recorded on CCl₄ at 488 nm excitation [10]

16.2 Measured parameter

Electromagnetic radiation emitted from the irradiated material volume is collected and analysed by an optical system. Spectra displaying peaks arising from Raman shift due to lattice vibrations are best suited to identify crystalline materials through “finger-print” searching databases. Interaction with solid materials also reveals the non-crystalline state of matter, meaning the total absence of ordered structure. Interaction with molecular materials – solid, fluid or gaseous – also will produce characteristic spectra suitable for materials identification. Figure 113 presents a plot of the frequencies of the asymmetric modes of several anionic groups in minerals versus the bond lengths of the involved atoms. The larger frequency shifts are associated with the shortest bonds, again illustrating the principle that the stronger bonds are short and longer bonds are weak.

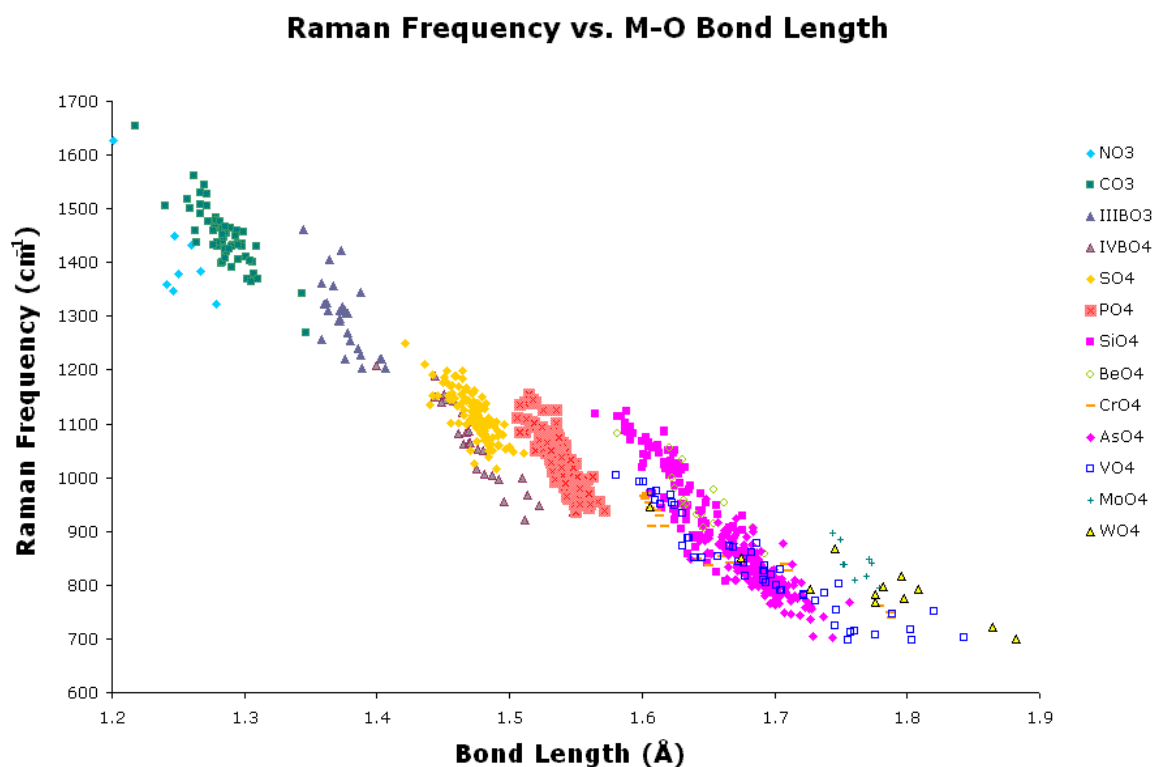


Figure 113. Complex anions detected by Raman spectroscopy [11]

Raman scattering is also sensitive to lattice vibrations, thus materials without complex anionic groups also produce a specific Raman spectrum. Accordingly, a large number of minerals can be easily identified and differentiated if they are chemically (Figure 114) or structurally similar (Figure 115).

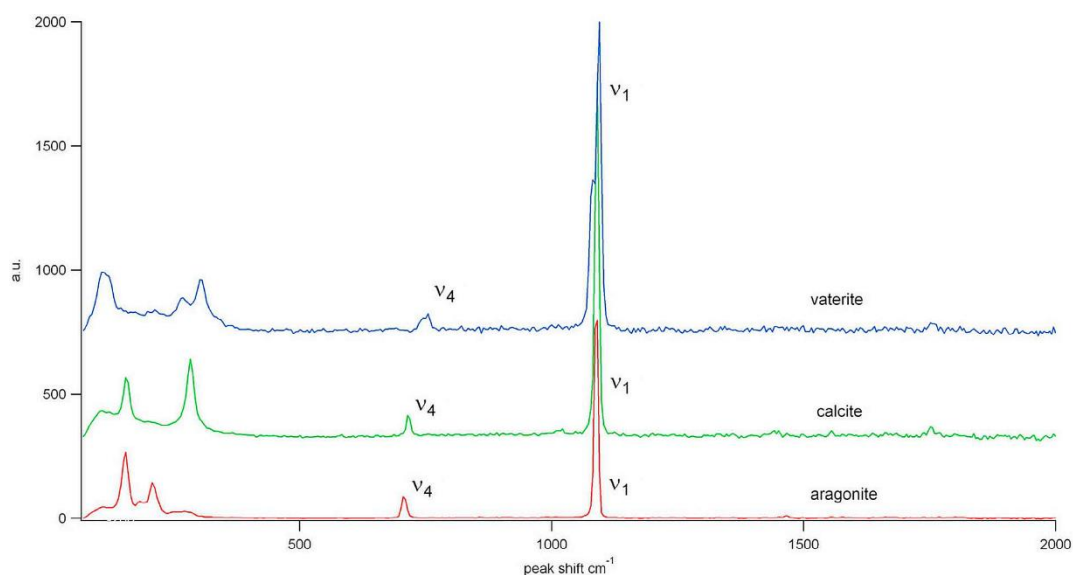


Figure 114. Raman spectra of CaCO_3 varieties [1]

The basis for mineral identification is the position of the peak – usually known as band – maxima on x-axis = Raman-shift and the associated intensity on y-axis. The intensity of peaks may vary depending on crystallographic orientation, which can be deduced from the spectrum analysis. Asymmetry of peaks may also contain structural and chemical information, whereas peak broadening is mainly related to the

crystallinity of the investigated material (broadening indicates a decrease of crystallite/domain size or degradation of ordering in the lattice).

Identification of minerals is usually done by using comparative spectrum, but using band position – intensity data is also suitable. Several type of quantitative information can also be extracted from the spectrum. Abundance of given molecules or groups in the structure of the investigated material can be estimated, or calculated by using calibration. Relative abundances of mineral phases, compounds can also be deduced.

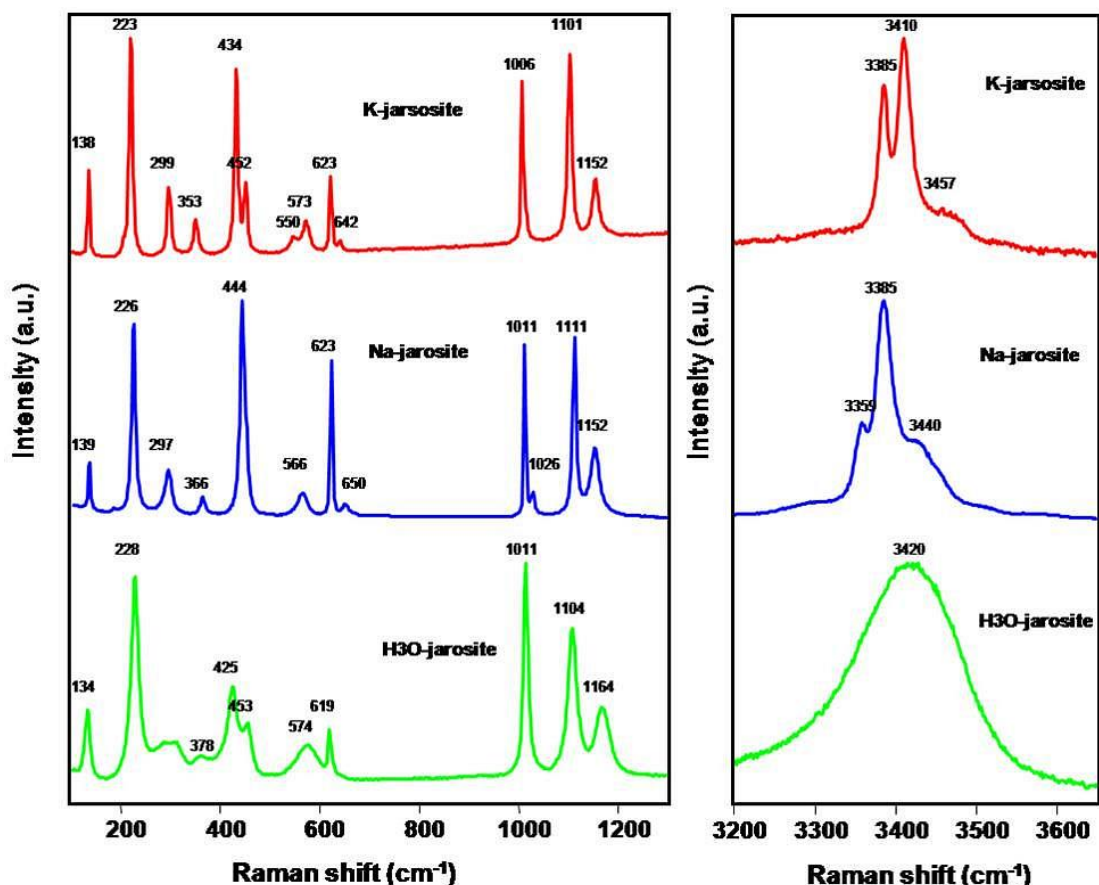


Figure 115. Raman spectra of jarosite varieties [2]

16.3 Measuring method

An instrument capable to function as Raman spectrometer (Figure 116) must comprise (1) a laser source for excitation, (2) a collecting optical system for the emitted radiation, (3) filtering system to cut out the Rayleigh scattering – notch filter, edge pass filter, or a band pass filter, (4) 166pectros grating for Raman spectral decomposition and a (5) detector for photon counting, most suitably CCD devices.

Excitation sources (1) are lasers (diodes or Nd:YAG) in the ultra-violet, visible and near-infrared regions of electromagnetic radiation (wavelengths of 633 nm, 660 nm, 785 nm and 1064 nm).

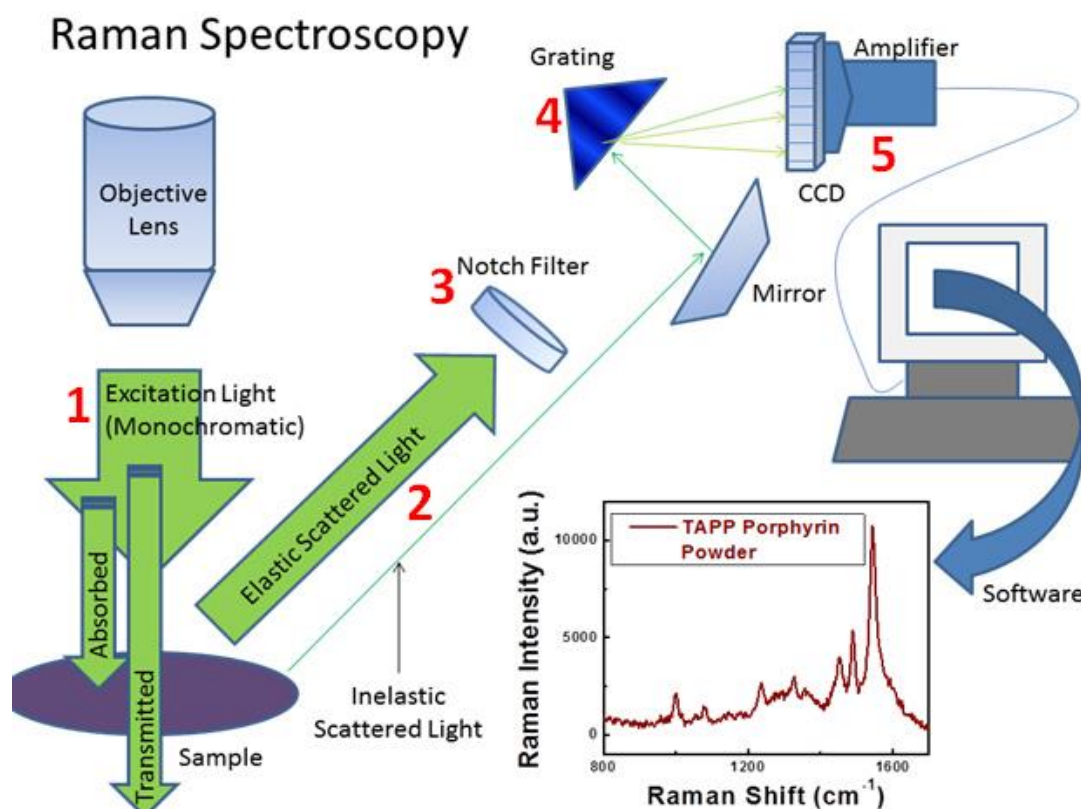


Figure 116. Instrumentation for regular Raman spectrometry – a schematic illustration [12]

Although the method is traditionally applied on solid samples (monoblock and powder also), it is suitable to investigate fluids, gases and immersed solid samples too. As a consequence, it is applicable to investigate geological samples in underwater environments.

16.4 Target parameters

By the use of Raman spectrometry, we aim to identify mineral groups and species building up host-rock (where accessible) and alteration products found in the underwater mining galleries. First proposed at MBARI in 1999 [7] the idea of ROV-deployable Raman spectrometer reached wide scale applications since then. Underwater Raman spectroscopy solutions have been established in the past decades. Applications on large scale are common nowadays in oceanology and sea floor geological exploration. As defined in the key requirements of Deep-Ocean Raman In Situ Spectrometer – DORISS project, analysis of ocean floor mineralogy, pore water chemistry, gas seeps and sea floor vents was developed [4].

16.5 Applicability

Current status of underwater Raman spectrometry allows several key measurements which can be successfully applied in UX1. Systems like DORISS and similar give the advantage to 167pectro the surface of solid materials, composition and content of porous media and the composition of fluids.

16.5.1 Pore water analysis.

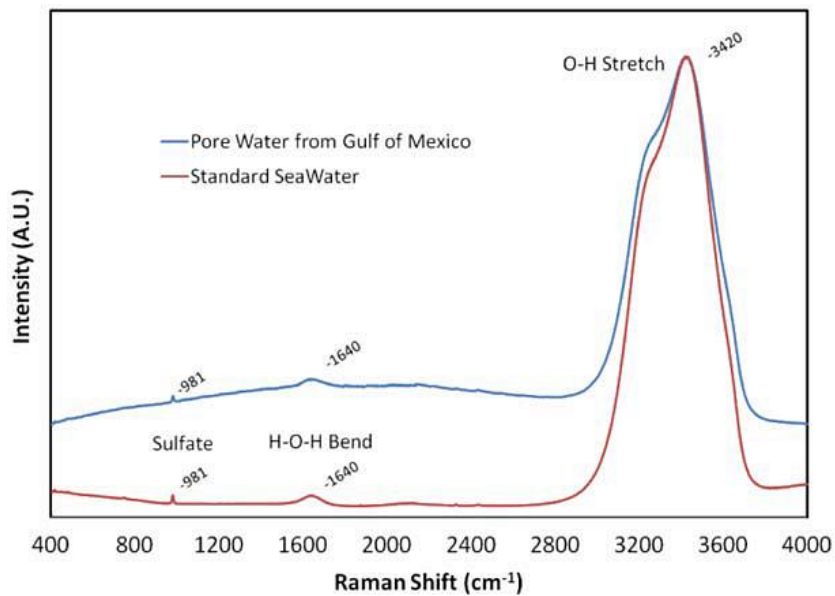


Figure 117. Raman spectra of pore water (Gulf of Mexico) and standard seawater (P-series IAPSO, salinity = 34.992, sulphate=28.9mM, Ocean Scientific International, Ltd.) [3]

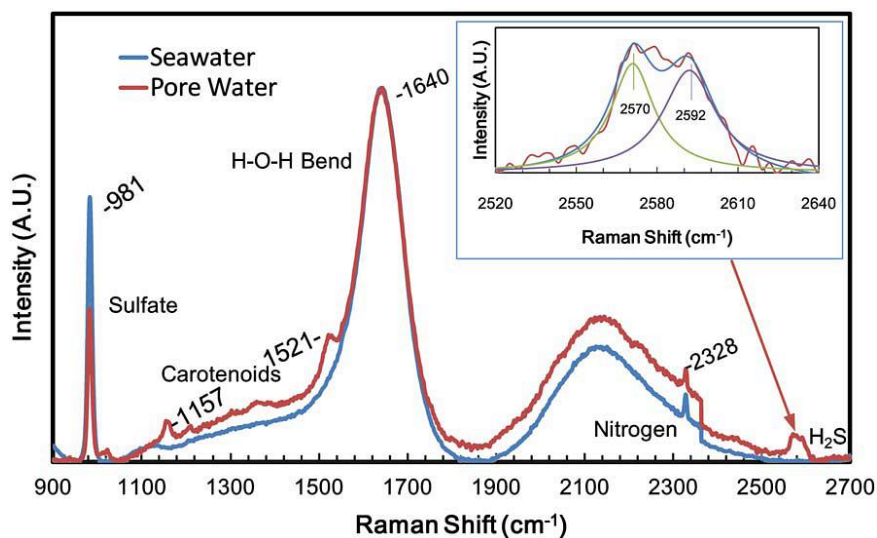


Figure 118. Raman spectra of in situ pore water and the surrounding seafloor seawater in a vesicomyid clam patch at Clam Field [3]

Individual mineral grains of millimetre size were analysed in a seafloor environment, producing clear spectrum for mineralogical identification [5]

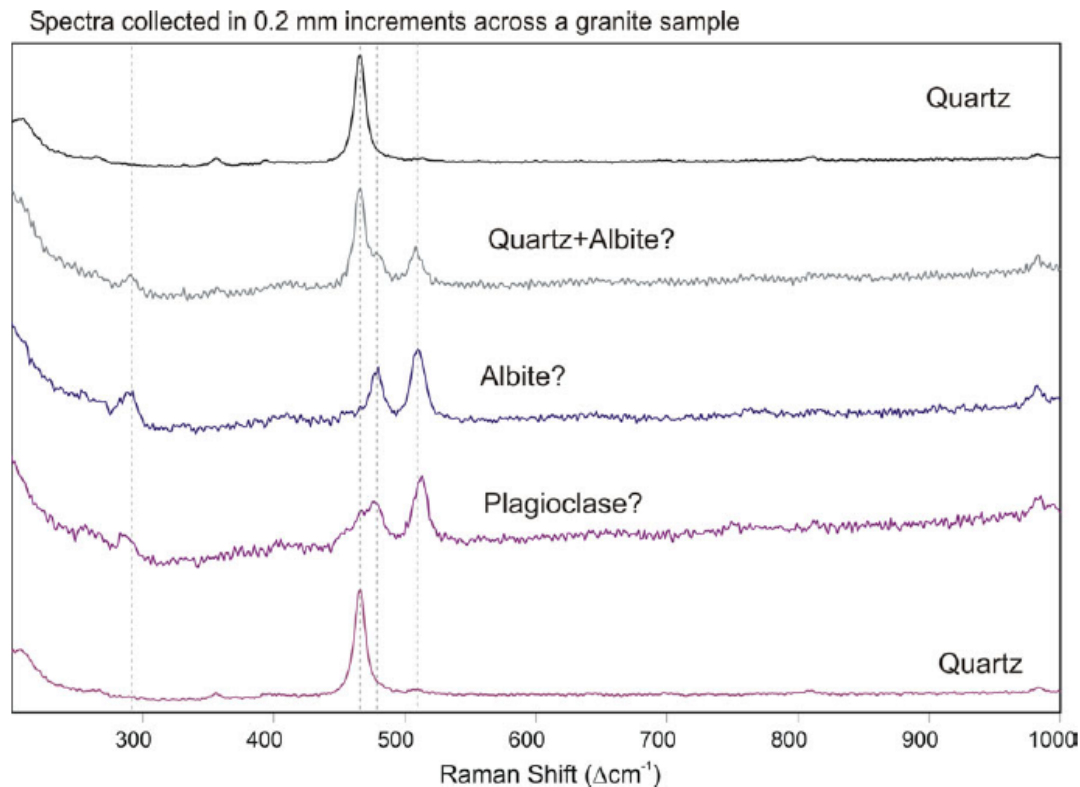


Figure 119. Identification of minerals on a known rock specimen deployed on the seafloor, probing millimetre grains [5]

16.6 Advantages of the method

- Raman spectra of minerals can be used to identify phases by fingerprinting; by the use of databases structural and chemical information can also be extrapolated for the 169 petros materials
- due to the nature of interferences, Raman spectroscopy is more adequate to investigate aqueous systems and dissolved species than IR spectroscopy, which produces more significant interference with water molecules
- since the measured Raman intensities are directly proportional to phase concentrations, good quality quantitative results can be obtained
- for most of the measurements no to little samples preparation is required; for phase identification, rough surfaces are also suitable
- most samples suffer no damage to crystal structure or chemical composition during investigation
- a large variety of transparent materials can be used for laser protection window, e.g. in the case of underwater measurements
- counting times range from fractions of a second to several minutes per measurement point, making it ideal for quick data acquisition

16.7 Disadvantages of the method

- pore water analysis will not be possible with the UX1 configuration, but contributions in the measured spectrum are to be expected
- the Raman scattering intensity is related to transparency of minerals, opaque minerals (like sulphides) will have a lower scattering power – Raman signal – than more transparent (like sulphates, carbonates) minerals [5]

- fluorescence may arise from chemical elements contained as trace elements or impurities in minerals (Figure 120), these fluorescent peaks have to be recognized and excitation adapted to minimize these effects [5].

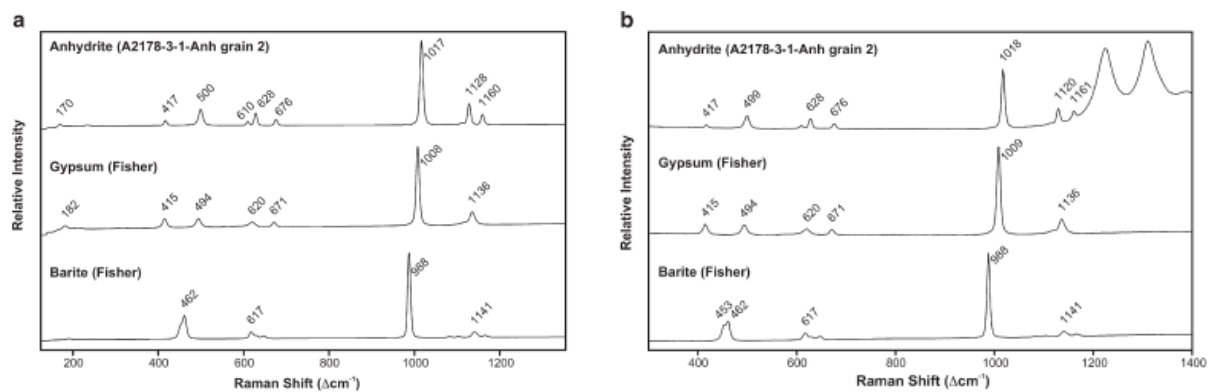


Figure 120. Raman spectra of sulphates obtained with the microprobe (10× objective) and green excitation. The anhydrite spectrum is 10×10 s; the gypsum spectrum is 10×20 s; and the barite spectrum is 10×7 s. b. Raman spectra of sulphates obtained with the In Photote spectrometer using red excitation. All spectra are single exposures of 10 s for anhydrite and barite, and 30 s for gypsum [5]

- presence of microbial organisms (Figure 121) or organic material traces (Figure 122) may also produce interference that creates fluorescence [6]

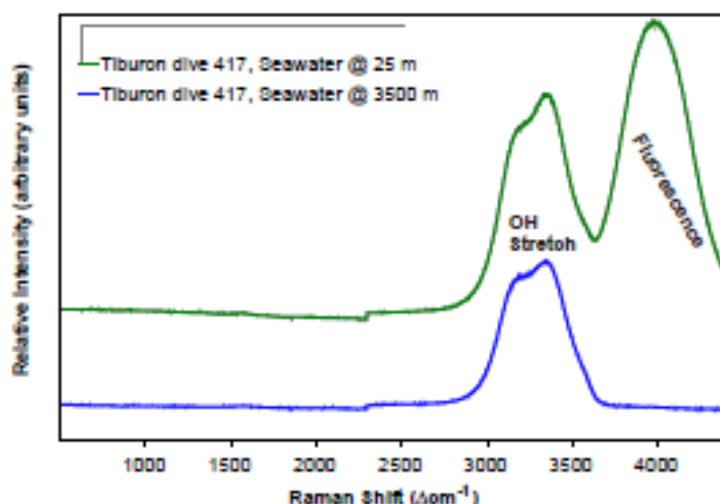


Figure 121. Two spectra taken in situ of natural sea water: upper trace from 25m depth, showing the fluorescence from phytoplankton pigments; and lower trace obtained at 3500m depth with fluorescence absent [6]

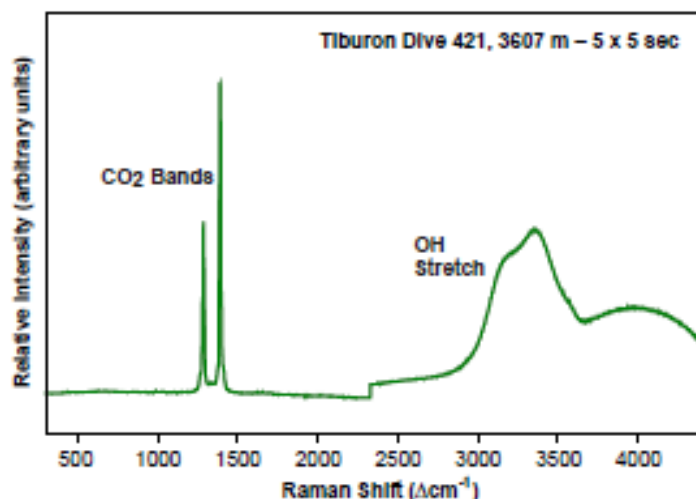


Figure 122. Raman spectrum of a pool of liquid CO₂ on the sea floor, stand-off optic, O–H stretch signal results from sea water in the optical path, the broad hump is fluorescence from organic matter in the surficial marine sediments [6]

16.8 Industrial solutions—Purchasable instruments

Possible solution: DORISS – deep-ocean Raman in situ spectroscope, attached to remotely operated vehicle (frequency-doubled Nd: YAG laser operating at 532 nm was chosen Coherent model DPSS532). The development of DORISS and DORISS2 took a long period, each part being designed and fabricated specifically. Oil-filled optical fibre cable proved to be the best solution for signal transfer [7].

16.8.1 Lasers

- **HORIBA Scientific [13]**

HORIBA Scientific has a program and development and testing of laser excitations for Raman – with many collaborative projects in place with the leading manufacturers of laser systems. All Raman systems from HORIBA Scientific offer the very best in laser technology, and are fully tested and evaluated. Only those lasers which pass our own stringent QC tests are supplied.

UV lasers, HeNe, DPSS 532 nm, Solid-state visible lasers, NIR Diode, High power fibre linked

- **ONDAX Inc. [14]**

All SureLock™ Wavelength Stabilized Laser Diodes and Laser Modules incorporate the Ondax PowerLocker® VHG filter to provide single-frequency or narrowed linewidth spectral performance, stabilized temperature operating characteristics, and low power consumption – delivering affordable, portable, instrument quality performance for a diversity of applications. Available in a wide range of wavelengths, power levels, and form factors, Ondax can also custom-configure a wavelength-stabilized solution to meet your exact application requirements.

16.8.2 Optical fibre, fibre probes

- **HORIBA Scientific SuperHead Fibre Probes [15]**

The SuperHead fibre optic probes are a range of high efficiency Raman sensors which enable in situ, non-invasive chemical analysis to be undertaken. Immersion, high temperature/pressure and integrated camera versions are available.

Each SuperHead probe is connected to an excitation laser source and base Raman 172pectros by fibre optic cables. Its rugged and robust construction means that it is suitable for a wide range of applications including true industrial reaction monitoring.

16.8.3 Filters

- **ONDAX Raman filters and Filter Assemblies [16]**

Ondax's SureBlock™ Ultra-Narrowband Notch Filters are the ideal solution for highly selective wavelength applications like low frequency (low wavenumber) Raman spectroscopy.

Ondax's patented SureBlock™ XLF Notch Filter Systems enable fast, clear capture of Raman spectra in the Low-Frequency (Low Wavenumber/THz regime (~5 cm⁻¹ to 200 cm⁻¹, or 150 GHz to 6 THz), using only a standard single-stage spectrometer.

16.8.4 Benchtop instruments [17]

Horiba Scientific LabRAM HR Evolution is a high resolution microraman spectrometer, which allows laboratory measurements of polished solid state specimens, samples with rough surface, powders and liquids with the aid of quartz cell (cuvette). The system includes an optical microscope on which the laser optical mount is fixed and allows the investigation of grains as low as ~10 micrometres. It can be upgraded with an XYZ stage and mapping, depth profiling and polarization options. Lasers of 532, 633 and 785 nm are available.



Figure 123. Benchtop LabRam HR Evolution system [18]

16.8.5 Handheld spectroscopes and probes [19]

Bravo (Bruker Raman Verification Optics) handheld Raman spectrometer for raw materials identification by Bruker AXS offers reliable solution for quick mineralogical investigations. It's a dispersive Raman spectroscopy system with proprietary fluorescence rejection, with spectral range of 300-3200 cm^{-1} , spectral resolution of 10-12 cm^{-1} with DuoLaser™ solution (700 and 1100 nm source). The size is 27*15.6*6.2 cm with a 1.5 kg weight.



Figure 124. Handheld Raman spectroscope, Bruker Bravo [19]

16.9 Conclusion

For realisation of an underwater Raman measurement it is needed to keep the laser sources and the observer optics in a predefined proper position. Due to the implementation difficulties we do not recommend the Raman methods despite the fact that it is able to give much useful information from the surface of the examined materials.

Raman spectroscopy can be an useful tool in the future UX robots, but the development of a suitable equipment needs more resources (development time, and money) than the capabilities of this recent project.

Suggested/Suggested with comment (suggested in 2.2)/*Unsuggested method*

16.10 References

- [1] Nehrke G., Poigner H., Wilhelms-Dick D., Brey T. & Albele D. (2012) **Coexistence of three calcium carbonate polymorphs in the shell of the Antarctic clam *Laternula elliptica***
Geochem. Geophys. Geosys. Vol. 13. No. 5, Q05014, doi:10.1029/2011GC003996.
- [2] Ling Z., Cao F., Ni Y., Wu Z. Zhang J. & Li B. (2015) **Raman 175 spectroscopic study of the K-Na jarosite solid solutions**
46th Lunar and Planetary Science Conference, 2731.(pdf)
<http://www.hou.usra.edu/meetings/lpsc2015/pdf/2731.pdf>
- [3] Zhang X., Walz P. M., Kirkwood W. J., Hester K. C., Ussler W., Peltzer E. T. & Brewer P. G. (2010) **Development and deployment of a deep-sea Raman probe for measurement of pore water geochemistry**
Deep-Sea Research I, Vol 57, pp. 297-306
- [4] Pasteris J.D., Wopenka B., Freeman J.J., Brewer P.G., White S.N., Peltzer E.T., Malby G.E. (2004) **Raman spectroscopy in the deep ocean: successes and challenges**
Appl Spectrosc. Vol. 58 No. 7, pp. 195-208
- [5] White S. N. (2009) **Laser Raman spectroscopy as a technique for identification of seafloor hydrothermal and cold seep minerals**
Chemical Geology, Vol. 259, pp. 240-252
- [6] Brewer P. G., Malby G., Psteris J. D., White S. N., Peltzer E. T., Wopenka B., Freeman J. & Brown M. O. (2004) **Development of a laser Raman spectrometer for deep-ocean science**
Deep-Sea Research I, Vol. 51, pp. 739-753
- [7] Sherman A. D., Walz P. M. & Brewer P. G. (2007) **Two generations of Deep-Ocean Raman in-situ spectrometers. Lessons learned while optimizing instrument robustness and sensitivity**
Sea Technology, February 2007 issue, pp. 10-13
- [8] White S.H., Kirkwood W., Sherman A., Brown M., Henthorn R., Salamy K.A., Peltzer E. T., Walz P. & Brewer P. G. (2004) **Laser Raman Spectroscopic Instrumentation for in situ Geochemical Analyses in the Deep Ocean**
OCEANS '04. MTTs/IEEE TECHNO-OCEAN '04 Conference Proceedings, Vol. 4, DOI 10.1109/OCEANS.2004.1402901
- [9] <http://www.geo.arizona.edu/xtal/geos306/geos306-12.htm>
- [10] Ferraro J. R., Nakamoto K. & Brown C. W. 2003
- [11] <http://www.geo.arizona.edu/xtal/geos306/geos306-12.htm>
- [12] <https://www3.nd.edu/~kamatlab/images/Facilities/raman%20spectroscopy.jpg>
- [13] www.horiba.com/scientific/products/raman-spectroscopy/accessories/laser-sources/
- [14] <http://www.ondax.com/products/surelock-wavelength-stabilized-lasers>
- [15] <http://www.horiba.com/scientific/products/raman-spectroscopy/raman-spectrometers/modular-and-fibre-coupled-raman/details/superhead-fibre-probes-150/>
- [16] <http://www.ondax.com/products/raman-filters-filter-assemblies>
- [17] <http://www.horiba.com/scientific/products/raman-spectroscopy/raman-spectrometers/raman-microscopes/hr-evolution/labram-hr-evolution-17309/>
- [18] <http://www.horiba.com/scientific/products/raman-spectroscopy/raman-spectrometers/raman-microscopes/hr-evolution/labram-hr-evolution-17309/>
- [19] http://www.bravo-bruker.com/pdf/BRAVO_Specs_EN.pdf

17.1 Theoretical Background

The LIBS is a chemical analytical method, which melts solid materials with short laser pulses, inducing high energy excitation on localized spots. In this regard, it practically resembles a traditional optical emission spectroscopy where a laser source provides the required excitation energy, and all the elements of the investigated material produce characteristic wavelength radiation in the visible spectrum. Analytical procedures involve a laser beam source and excitation effect on chemical elements in the target are measured. In contrast with laser ablation (LA) which is used to evaporate and analyse solid materials, the LIBS method produces a plasma state material, resulting in optical emissions from the chemical elements. LIBS was mainly developed for non-contact in-situ local chemical investigations, also serving as a short distance remote sensing method as long as a free optical path is provided for the laser beam and emitted radiation. Due to the ease of use, it is frequently used and increased number of instruments have been developed in the past two decades. Special field of applications is used for underwater investigations. One of the main advantages is that sample preparation is not required, and surface depositions, crusts of thin layers can be removed by the use of laser beam itself.

17.2 Measured parameter

Depending on the excitation energy (temperature) chemical elements emit characteristic radiation. This radiation can be used for spectroscopy and spectrometry applications, to identify and quantify the chemical elements and their levels in the investigated material (Figure 125).

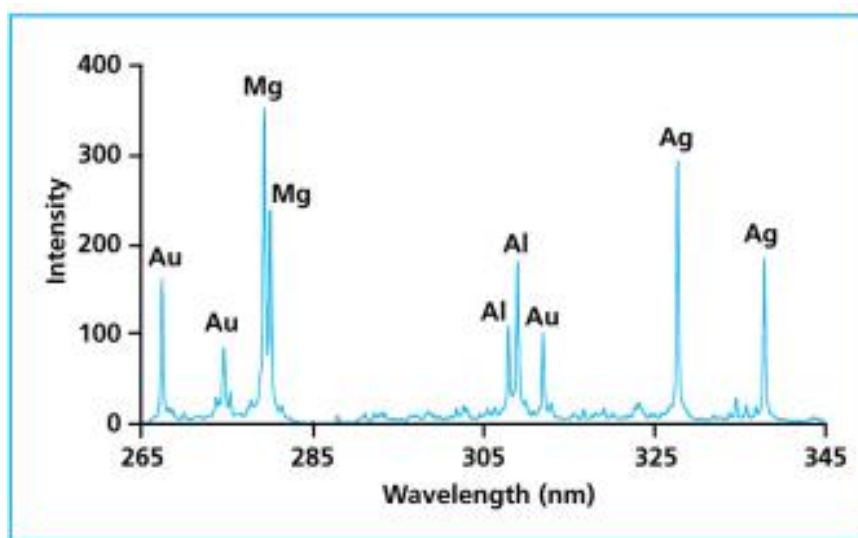


Figure 125. LIBS spectra with chemical elements of various atomic number [5]

17.3 Measuring method

Two main areas of geometrical set-up have been developed: single and dual laser pulse. In the dual pulse set-up two laser sources are applied, with sequential pulses. Dual pulse set-up was developed for underwater applications. Laser sources are Nd:YAG (Nd-doped yttrium garnet), pulses are focused on the sample using an optical assembly. Then, the plasma light (containing the analytical information concerning the sample) is collected and transported to the detector (Figure 126).

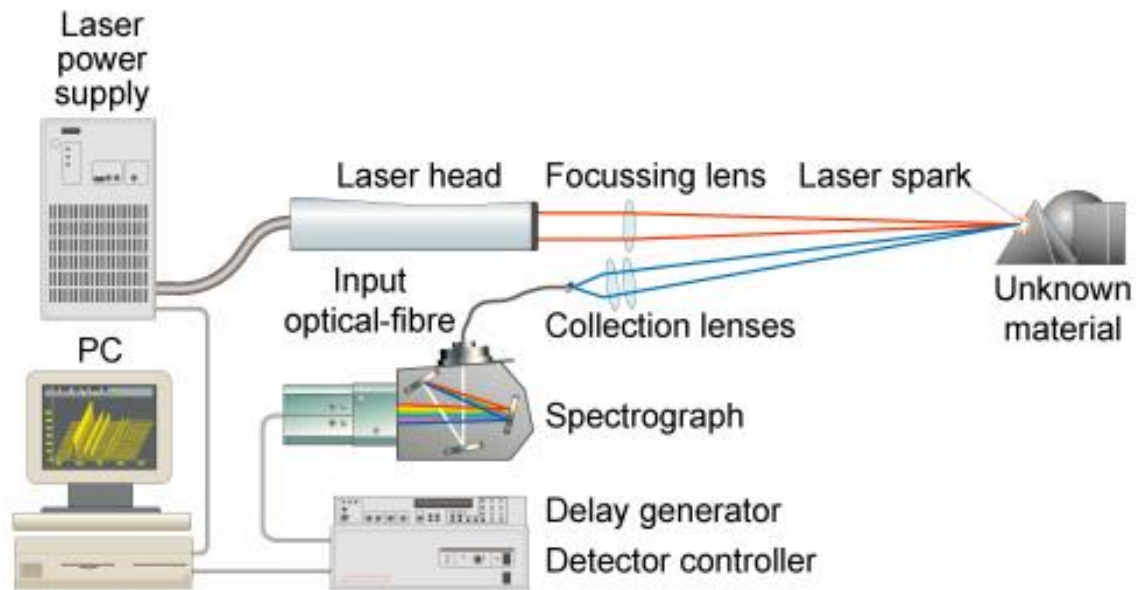
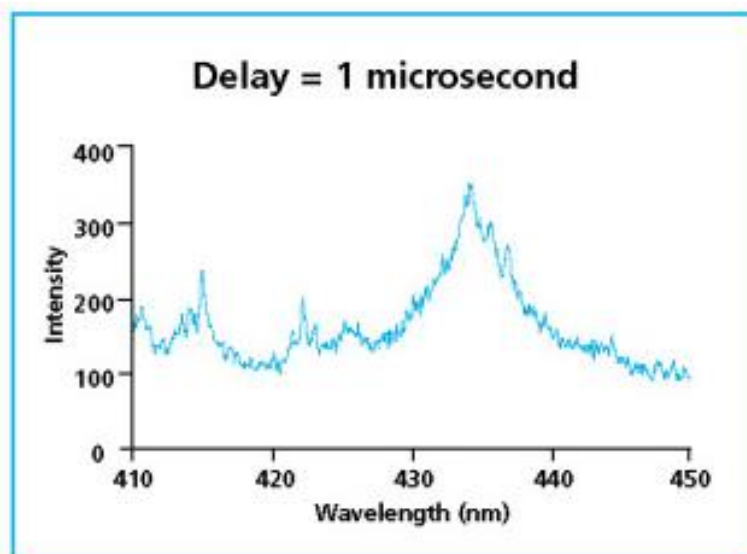


Figure 126. Arrangement of a LIBS instrument [6]

Due to the plasma emission characteristics, time resolved detection is necessary, to exclude the radiation continuum emitted during plasma quenching. Detectors are controlled to have their counting start delayed with microsecond time ranges, the time by which continuous radiation will decay and only characteristics will be measured.



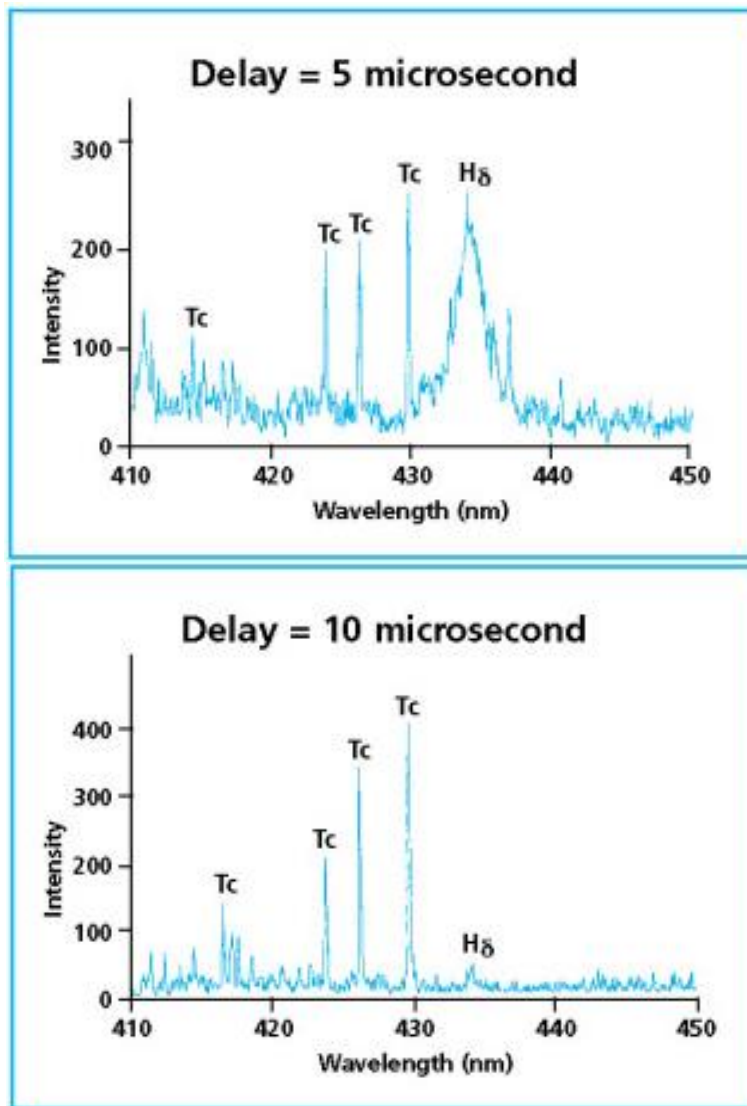


Figure 127. Effect of delayed counting on the quality of characteristic lines [7]

17.3.1 Single-Pulse LIBS

In the traditional SP-LIBS measurements the laser beam which creates the plasma state material in the excitation spot also provides the energy to obtain atomic emissions. The spectrometer records emitted radiation travelling collinearly with laser beam in a back-scatter geometry. In the case of underwater measurements, the plasma generated by the short laser pulse (e.g. 8 ns) will produce a gas bubble and a subsequent quenching results in low atomic emissions [2]. A poor signal is generally obtained with SP-LIBS in underwater measurements, with a suitable results obtained only for dissolved alkali and alkaline earth metals.

17.3.2 Dual-Pulse LIBS

Double pulse, or dual-pulse LIBS (DP-LIBS) has been developed to enhance the applicability of instruments in underwater measurements (Figure 128).

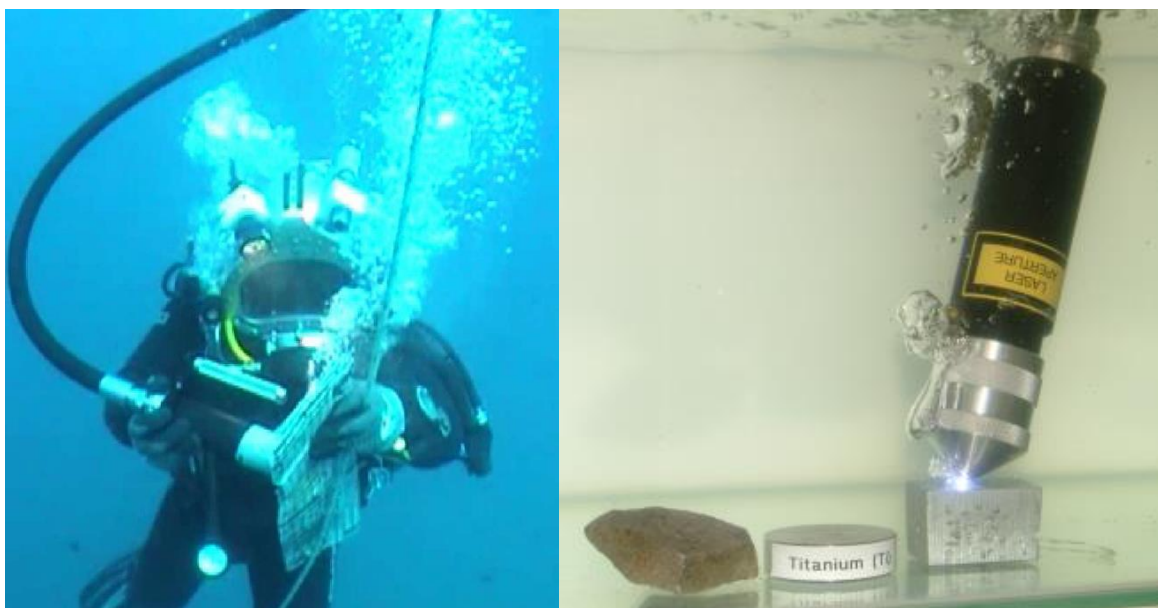


Figure 128. Photo of the LIBS probe taken during a LIBS analysis underwater at 30 m (left) and in the laboratory (right)

Water based DP-LIBS solutions uses two consecutive laser pulses towards immersed objects (Figure 128). The water at the solid interface – in the laser beam focus – is undergoing breakdown, forming high temperature and pressure plasma (6000–15 000 K and 20–60 kBar, respectively) resulting in thermal expansion and gas bubble generation (i.e., thin layers of vapour and diffused gas) around the volume of the excited material. After a few milliseconds of short plasma decay a large vapour bubble is formed. The second laser pulse is focused on the solid surface in the region of the vapour bubble at the point of maximum expansion, creating a plasma of the investigated material.

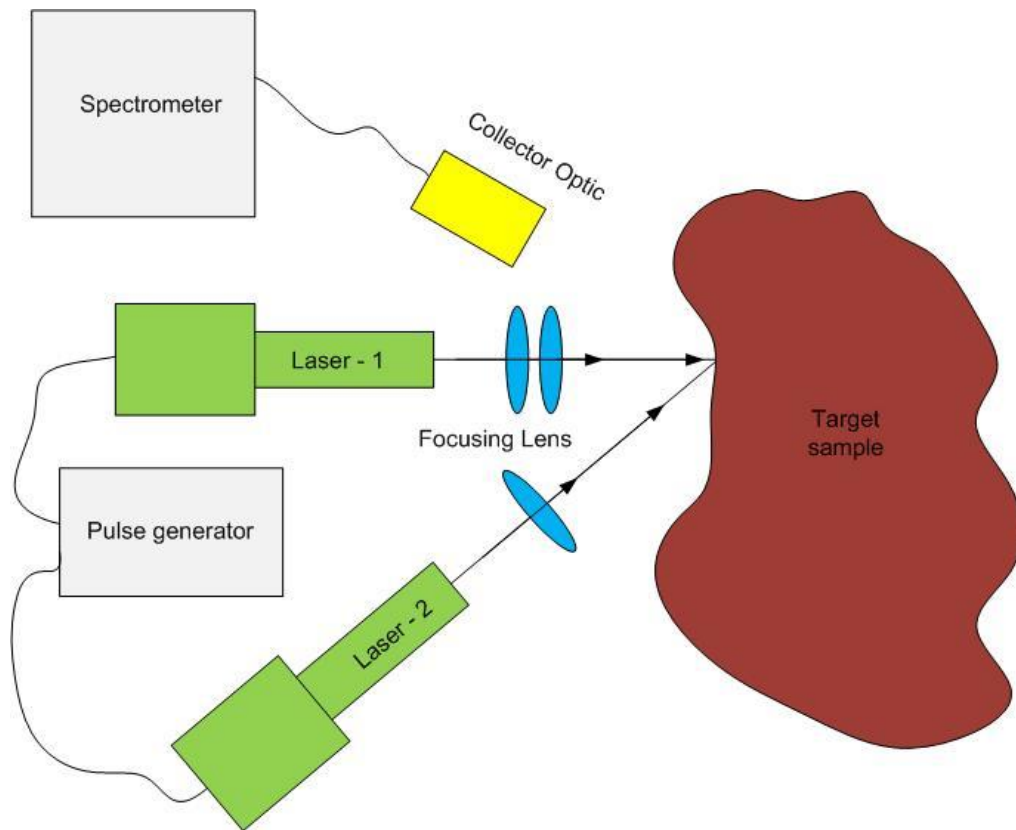


Figure 129. Typical arrangement of DP LIBS measurement

In order to obtain maximum excitation and atomic emissions, the second pulse has to be focused and timed to the maximum expansion moment of the vapour bubble.

DP-LIBS is suitable also for the measurements of large scale dissolved elements, allowing the detection of weaker emission lines, undetected by SP-LIBS. One major characteristic that also has to be considered for underwater exploration is the effect of liquid pressure on the emission rate of excited material. With the increase of pressure a dramatic suppression of all emissions occurs (Figure 130).

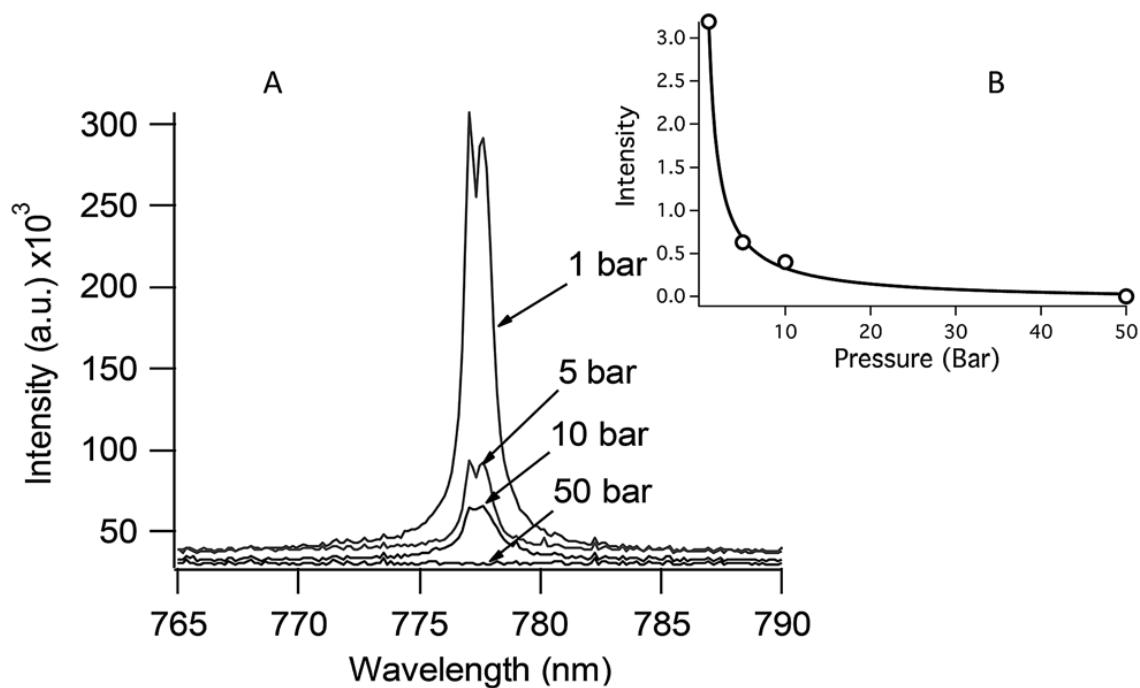


Figure 130. The emission intensity is inversely proportional to the solution pressure [1]

17.4 Target parameter

Exploiting possibilities offered by DP-LIBS, the desired result is to determine chemical elements present in the wall-rock, alteration crusts and products. To the extent of possibilities, quantitative results are also expected.

17.5 Applicability

By building the instrument from parts, it is possible to reach the desired arrangement and operation. Large numbers of handheld solutions exist on the market, and also underwater testing and development is advanced enough for experimentation. According to Lascola et al (2001) [4] underwater exploration using LIBS analysis is difficult also due to the enhanced quenching effect of the water on the excited plasma, suppressing the emissions from atoms.

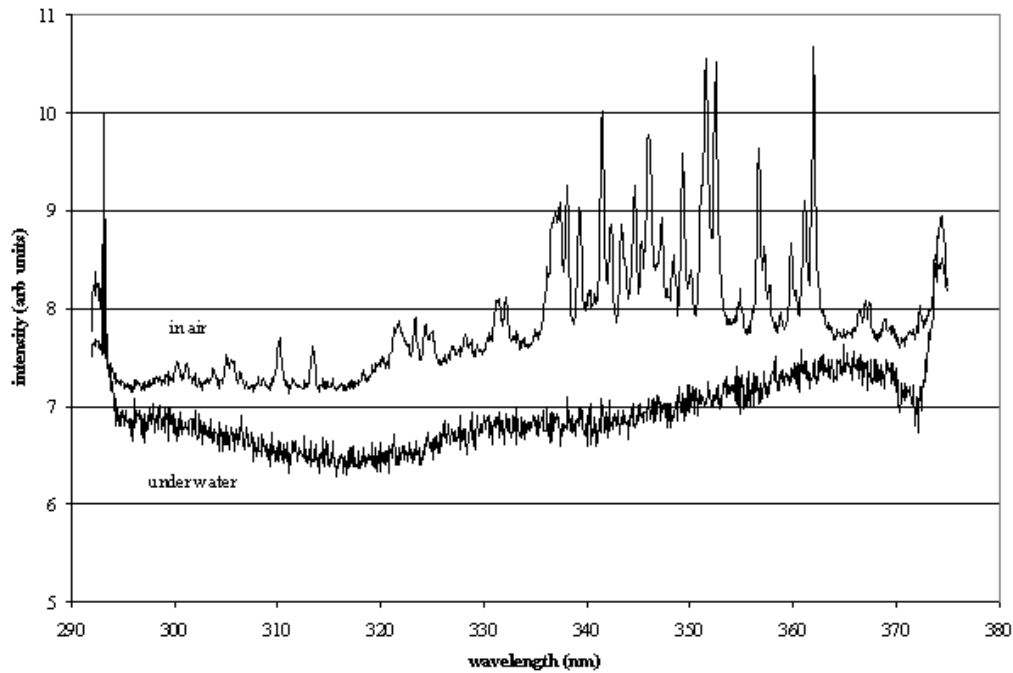


Figure 131. LIBS spectra of Ni sample in air and under water (99 mJ pulse energy at 10 Hz, air sample with 6 seconds, underwater sample with 20 seconds integration time [8])

Thus, a laser-induced cavitation bubble has to be produced with the first laser, and excitation must be created with a second laser source – this is the double-pulse LIBS setting. A study for underwater double-pulse LIBS optimization [12] has found that focusing below the target surface (20 cm focal length, 0.5 mm laser spot) is beneficial for bubble generation and collapse. Pulse energies had to be adjusted to allow corrections for water adsorption. The process has a disadvantage manifested in scarce reproducibility of the cavitation bubble created by the first pulse, since liquid pressure and dimensions of the bubble strongly affect plasma emission.

17.6 Advantages of the method

- LIBS can (in principle) detect all elements
- In-situ method in real environments
- Non-contact
- No sample restriction in size and shape
- Fast analytical response
- Qualitative and quantitative (limited) analysis
- Spot size in the order of a few micrometres in diameter
- Non-destructive analysis (minimal ablation pit)

17.7 Disadvantages of the method

- Emission intensity is inversely proportional to the solution pressure (Figure 130)
- Need to precisely set up and control the laser-to-sample distance and the angle of incidence
- Just a few real underwater experiences exist

17.8 Industrial solutions—Purchasable instruments

There is no commercial LIBS product working underwater. Underwater LIBS solutions are few, and they are only in the development stage. Even if we use available state-of-the-art technology some R&D will be required before it can be applied in UNEXMIN project.

There are numerous industrial solutions and products for LIBS working in air medium. The next three examples show the handheld product line. These are small and lightweight (under 5 kg), possibly light enough to build into an underwater autonomous robot, with R&D.

17.8.1 SciAps Z—High Performance, Handheld LIBS Analyzer [9]

The main features of the Z LIBS (Figure 132) 183luminu are:

- High resolution spectrometer
- OPTi-Purge technology
- Camera and video
- Autofocus
- Auto calibration
- Rastered 2D laser

Emission in the UV, visible and NIR spectral region are detected, including hydrogen (H) to sodium (Na). This includes critical elements like C, Li, Be, B and others. The SciApsZ measures elements like Mg, Si, Al at low detection limits due to the optical nature of the technology.

The SciApsZ's PULSAR technology generates bursts of 5-6 mJ/pulse range, at up to 50 Hz frequencies, with 1 ns wide pulses. It is well established that mJ, rather than μ J laser pulses yield superior analytical results.



Figure 132. Handheld instrument of SciAps [9]

17.8.2 Handheld LIBS Analyzer for Metal Alloys—mPulse [10]

mPulse, is optimised for the rapid sorting of metal alloys.

- Identify a wide variety of metal alloys at the press of the trigger
- Measure elements, light and heavy in only 1 second
- Test large or small samples such as shavings, turnings, granules, cables etc.

- No x-rays and free from the regulatory constraints usually associated with x-ray analysers
- Simple point-and-shoot operation

The mPulse analyser is the fastest device on the market used mainly as alloy sorter. It has been designed for the rapid identification and sorting of heavier alloys such as Stainless Steels, Ni, Cu, Co, Ti alloys and many more.

17.8.3 PMI-analytical EOS Handheld LIBS [11]

It has excellent detection of low atomic number elements (Al, Mg, Si, Li and Na).

The EOS is based on laser excitation of a metal sample followed by quantitative analysis of the light generated in the plume. This technology provides quick (3-5 s) analysis of alloys including Al/Ti/Mg alloys. The EOS is especially well suited to scrap sorting of these alloys because of its quick and user friendly operation. In addition to the normal XRF elements, the EOS is capable of measuring very light elements such as Li, Be and B; as well as laser fast analysis of Mg, Al, Si.

Weight: 2 kg.

17.9 Conclusion

The LIBS method provides very useful and unique information considering the chemical composition of the rock wall and its minerals. It provides bulk chemical information of the measured spot, and, to some extent, spatial chemical analysis is possible. The mineralogical limitation is that it does not give phase analysis (it cannot distinguish among polymorphs, e.g.: diamond/graphite or rutile/anatase/brookite, and also among minerals with similar compositions).

For the underwater application the DP LIBS would be better application because of the better signal to noise ratio of the method, but there are limited number of real solutions and experiences available today.

At the moment this method is not suggested to be integrated in the UX-1 prototype because during the measurement the available equipment must be hold on fixed position (accurate distance and angle). Because the planned UX-1 robot will move constantly, it makes the correct positioning of the spectrometer extremely challenging. For a LIBS measurement it is necessary to localize the point of measurement with stationary platform - this task is complicated for an autonomous, mapping robot. In spite of this LIBS could be an excellent target for future developments, as the LIBS method would give very useful geochemical data about the mine environment, for both water and solid materials.

Suggested/Suggested with comment (suggested in 2.2)/Unsuggested method

17.10 References

- [1] S. Michael Angel,* Joseph Bonvallet, Marion Lawrence-Snyder, William F. Pearman and Janna
Underwater measurements using laser induced breakdown spectroscopy
Register – Royal Society of Chemistry, Published on 17 November 2015.
The Royal Society of Chemistry 2016 J. Anal. At. Spectrom., 2016, 31, 328–336 | 333
- [2] Monica SIMILEANU1, Roxana RADVAN2, Niculae PUSCAS3, **Underwater LIBS Investigations Setup for Metals' Identification**
- [3] **LIBS Analysis of Archaeological Materials Underwater**
U.P.B. Sci. Bull. Series A, Vol. 72, Iss. 4, 2010 ISSN 1223-7027
Laser Laboratory Analytical Chemistry Department University of Malaga Campus de Teatinos s/n 29071 Malaga
- [4] Lascola R. J., Nave S. E. & Spencer W. A. (2001) **Laser induced breakdown spectroscopy of DOE process materials**
WSRC-TR-2001-00486 (source: <http://sti.srs.gov/fulltext/tr2001486/tr2001486.html>)
- [5] [http://www.appliedphotonics.co.uk/images/Graphs/Au-Al-Mg_spectrum\(350x245\).JPG](http://www.appliedphotonics.co.uk/images/Graphs/Au-Al-Mg_spectrum(350x245).JPG)
- [6] [http://www.appliedphotonics.co.uk/images/Schematics/lib_configuration\(500x280\).JPG](http://www.appliedphotonics.co.uk/images/Schematics/lib_configuration(500x280).JPG)
- [7] http://www.appliedphotonics.co.uk/lib/about_libs.htm
- [8] <http://sti.srs.gov/fulltext/tr2001486/fig7.gif>
- [9] <https://www.sciaps.com/lib-handheld-laser-analyzers>
- [10] <https://www.oxford-instruments.com/products/analysers/handheld-analysers/lib-analyzer-mpulse-series>
- [11] <http://www.pmi-analytical.co.uk/handheld-x-ray-spectrometry/eos-handheld-lib/>
- [12] Cristoforetti G., Tiberi M, Simonelli A, Marsili P, Giammanco F., **Toward the optimization of double-pulse LIBS underwater: effects of experimental parameters on the reproducibility and dynamics of laser-induced cavitation bubble**
2012 Mar 1; Optical Society of America 51(7):B30-41

18.1 Theoretical Background

In both, XRD and XRF analytical techniques the investigated materials are irradiated with X-rays, and the results of interactions of matter with x-rays are registered to obtain information. In the case of XRD, the crystal structure is investigated, and the results of XRF reveal the chemical (elemental) composition of the material. The techniques require two different instruments, since the type and nature of interactions is different. XRD is regularly performed with diffractometers: one setting is an X-ray source (Cu or Co target, monochromated to $K\alpha$ lines) and a detector moves in the circle pattern around the inspected sample (goniometer circle); diffraction on crystal lattice planes produce x-ray peaks, allowing the minerals to be identified. XRF measurements require a spectrometer: X-ray source (usually Pd target) and filters, also known as secondary targets, are used to obtain the radiation for exciting atoms of the samples. The X-rays emitted from atoms are directed to a detector by the help of analyser crystals (moved on a circle at a tangent to the sample and detector surface). The result is a spectrum where peaks allow the identification of chemical elements (but no crystal structure). Both instruments require sealed X-ray sources with moderate to high energy requirements.

18.2 Measured parameters

XRD: produces a set of peaks characteristic of individual crystalline materials, as a function of the X-ray source to detector angle (diffraction angle).

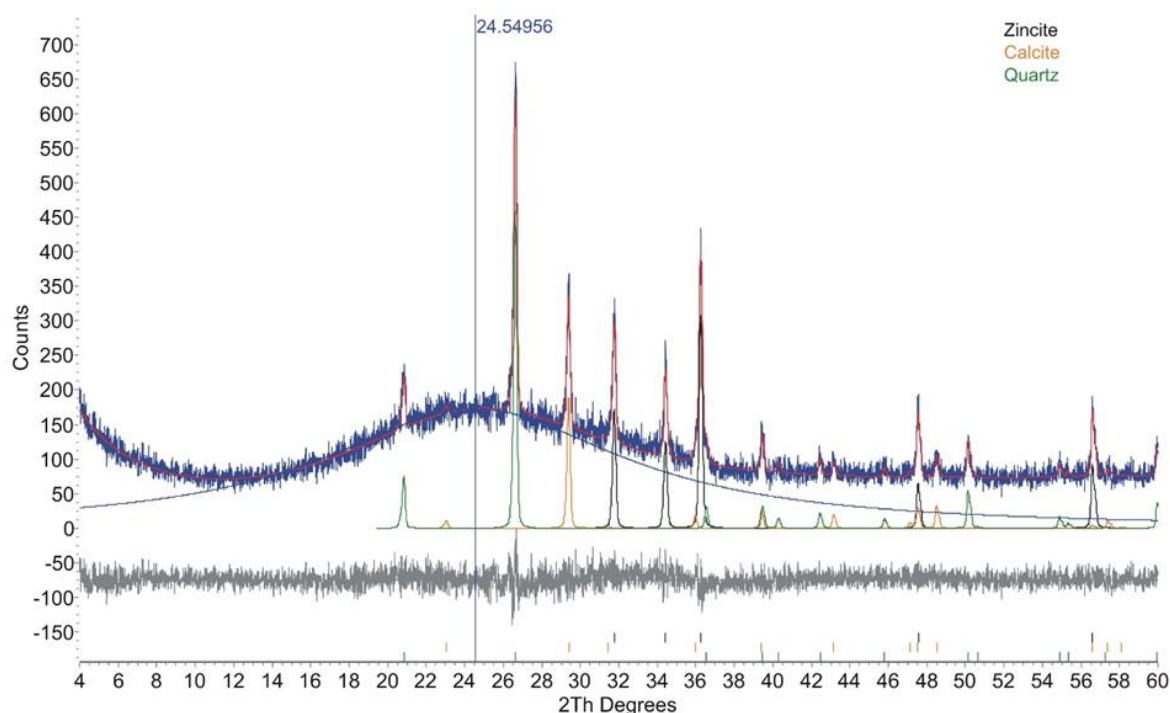


Figure 133. XRD pattern with characteristic peaks for specific minerals (coloured curves – calculated). Amorphous matter pattern is represented by hump on the blue measured – pattern.

XRF: produces a set of peaks characteristic for specific atoms, as a function of emitted photon energy or analyser crystal angle. Possible settings are wave-length dispersive mode (WDS) if using analyser crystals and detector or energy dispersive mode (EDS) if using SSD detectors to record emitted radiation.

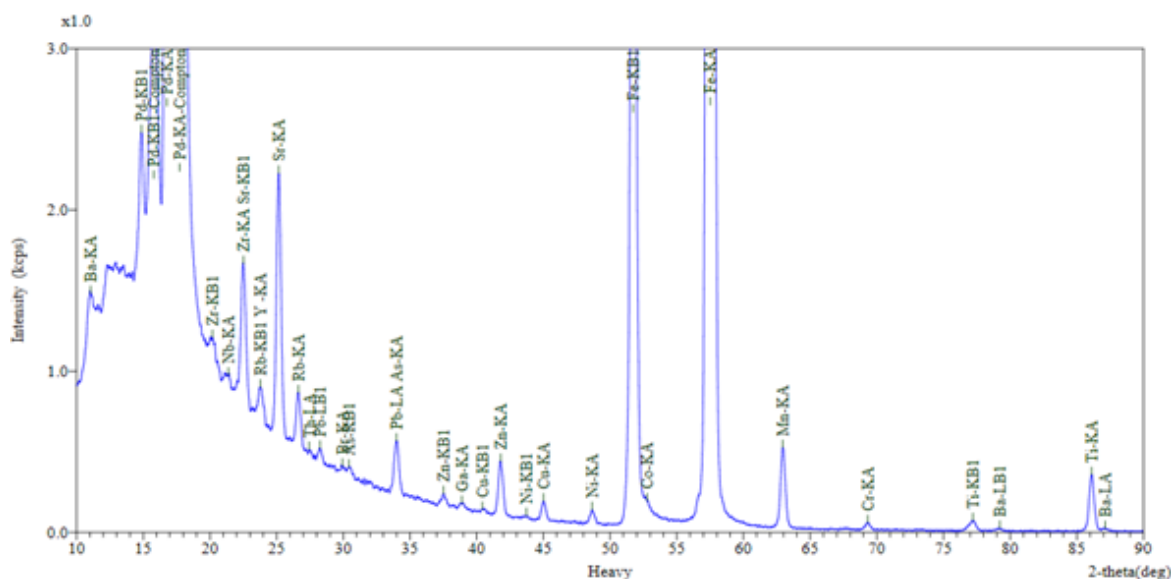


Figure 134. XRF spectrum, atomic elements and characteristic line types are plotted on the peaks

18.3 Measuring method

XRD: powder, solid or liquid samples with high to no sample preparation requirement; X-ray source set to 30 – 50 kV and 20 – 40 mA. Measurements require moving parts for the diffractometer setting or imaging plate, 2D detector for stationary beam and sample. Air scattering is a major part of the results, which have to be subtracted. Photons are quickly absorbed by matter, whether gases, liquids or solids.

XRF: powder, solid or liquid samples with high to no sample preparation requirement. Measurements require highly aligned analyser crystals (WDS) or high resolution SSD detector (Si-drift) (EDS). Measurement chamber is sealed and vacuumed to minimize absorption.

18.4 Target parameter

Mineralogical and chemical composition, both qualitative (compounds and chemical elements type) and quantitative (amount of each detected compound and chemical element)

18.5 Advantages of the methods

- Accurate and precise identification of minerals (XRD) and chemical compositions (XRF)

18.6 Disadvantages of the methods

- High efficiency X-ray photon absorption by water: the difference of density for air and water is high, water is almost 830 times denser at 20 °C than air (air: 1.2045kg/m³; water: 998.2 kg/m³), and, thus, the absorption is also much higher.

Table 17 shows that 100 µm of water column already causes almost 10% and 1 mm almost 2/3 drop in intensity. At about 4.5 mm 99% of the X-ray is absorbed, and no X-ray radiation is transmitted through 1.5

cm water column. Moreover the results are defined for clear water. But if the water contains dissolved ions, especially heavy metals, or colloids, the rate of absorption is be even higher.

0mm	0.0000%	1mm	63.8952%	5mm	99.3865%	10 mm	99.9962%
0.10 mm	9.6857%	1.5 mm	78.3056%	6 mm	99.7785%	11 mm	99.9986%
0.25 mm	22.484%	2 mm	86.9644%	7 mm	99.9200%	12 mm	99.9995%
0.50 mm	39.913%	3 mm	95.2935%	8 mm	99.9711%	13 mm	99.9998%
0.75 mm	53.423%	4 mm	98.3007%	9 mm	99.9896%	14 mm	99.9999%

Table 17. Absorption characteristics for Cu-K α in water

However, the Table 17 shows values only in one direction. However, it must be noted, that when using this technique under water, x-rays must travel from source located in submarine to the target, and then back. So actual absorption is much higher.

Based on this, it can be declared that the detected intensity will be at least exponentially lower than the emitted intensity (if the atomic absorption for initial X-ray radiation is not taken into consideration).

18.7 Conclusion

As a final conclusion, it is declared that neither technique (XRD / XRF) is applicable in water. The dimension and weight of the instruments are too large and also the X-ray sources need high amounts of energy. Moreover because of the high absorption ability of the water, the analysed surface would need to be extremely close to the X-ray source and detector, which cannot be solved mechanically in this project.

Suggested/Suggested with comment (suggested in 2.2)/Unsuggested methods

18.8 References

- [1] B.L. Henke, E.M. Gullikson, and J.C. Davis. **X-ray interactions: photoabsorption, scattering, transmission, and reflection at E=50-30000 eV, Z=1-92**
Atomic Data and Nuclear Data Tables Vol. 54 (no.2), 181-342 (July 1993).

From the three main areas (geophysical, optical and water analytical) we suggest to realise the methods listed below in Table 18 based on the prepared summarization.

		Developed in this project		Commercial main parts		Realized in other instrument		Placement		Output		Other requirements			
								On the surface of the robot hull	In the service hatch	Digital	Analog				
										Other calibration sensors	Direct water contact	Post Processing software	Interface electronics		
Geophysical methods	Magnetic field measurement	x	x	Speake & Co Llanfapley FGM-3 Series			x		x		6	x		x	x
	Natural (integral) gamma ray activity	x	x	Gammatech Kft. IH-99DNC dose rate meter				x	x		1				
	Sub-botom sonar	x	x	Garmin FishFinder 100				x	x		1			x	x
Water Testing Methods	Temperature					DVL					1				
	Pressure					DVL					1				
	pH	x	x	Corrinstruments High pressure glass based pH			x			x	1		x		x
		x	x	Corrinstruments Ph probe			x			x	1		x		x
	Electrical conductivity	x	x	Corrinstruments High pressure EC probe			x			x	1		x		x
	Water sampler unit	x						x			1		x		x
Optical methods	Hyper/Multispectral unit	x	x	HD cam											
	Fluorescent imaging	x					x		x		1		x	x	x

Table 18. Selected methods and their properties

19.1 Geophysical methods

Magnetic field measurement

Commercial sensor needed for the realisation with a unique designed mounting bracket. The suggested type of sensor for installation/use: Speake & Co Llanfapley, FGM-series Magnetic Field Sensors FGM-3 series.

During the implementation must be developed the mounting systems, the related sensors (e.g. tilt detector), and also the interface electronics and processing software.

The placement of the needed six sensors must be inside the pressure hull, as it is not necessary to have direct water contact with the sensor heads.

Installation is suggested for all of the planned three robots at the same time.

Natural (integral) gamma ray activity

Commercial sensor needed for the realisation with a unique designed mounting bracket. The suggested type of sensor for installation/use: Gammatech Ltd. IH-99DNC dose rate meter.

During the implementation must be developed the mounting systems and also the processing software.

The placement of the sensor could be inside the pressure hull, mounted at the modified service hatch. Not necessary to have direct water contact with the sensor heads.

Installation is suggested in only one robot occasionally.

Sub-bottom sonar

Extensive modification and adaptation of a commercial product is needed for the implementation. The suggested type of sensor for installation/use: Garmin FishFinder 100.

During the implementation must be developed the mounting systems, a complex electronics interface and also processing software.

The placement of the sensor could be inside the pressure hull, mounted at the modified service hatch. Not necessary to have direct water contact with the sensor heads.

Installation is suggested in only one robot occasionally.

19.2 Water Testing Methods

Temperature

The use of this sensor is suggested but the DVL instrument used for navigation also contains a probe like this, therefore the implementation (duplication) of this probe and the related equipment are not needed.

Installation is suggested for all of the planned three robots at the same time.

Pressure

The application of this sensor is suggested but the DVL instrument used for navigation also contains a probe like this, therefore the implementation (duplication) of this probe and the related equipment are not needed.

Installation is suggested for all of the planned three robots at the same time.

pH

Commercial sensor needed for the realisation with a unique designed mounting bracket. The suggested type of sensor for installation/use: Corrinstruments, High pressure glass based pH. For the proper operation needs the Reference probe using at same place and same time.

During the implementation must be developed the sealing and mounting systems, the interface electronics and also the processing software.

The placement of the needed 2 sensors (pH probe and reference probe) must be outside on the pressure hull, and it is necessary to have direct water contact with the sensor heads. Installation is suggested for at least one robot according the budget.

Electrical conductivity

Commercial sensor needed for the realisation with a unique designed mounting bracket. The suggested type of sensor for installation/use: Corr instruments, High pressure EC probe.

During the implementation must be developed the sealing and mounting systems, the interface electronics and also the processing software.

The placement of the needed 1 sensor must be outside the pressure hull and it is necessary to have direct water contact with the sensor heads.

Installation is suggested for all of the planned three robots at the same time.

Water sampler unit

The design and operation are relative complex, and it could be a brand new development during the project implementation. Commercial parts (valves, pumps, connectors, pipes, drives and motors) will be needed for the realisation.

During the implementation must be developed the whole system included the sealing and mounting systems, the related sensors (e.g. pressure probes), and the interface electronics and also the processing software.

The placement of the sensor could be inside the pressure hull, mounted at the modified service hatch. It is necessary to have direct water contact with numerous parts of the unit.

Installation is suggested in only one robot occasionally.

19.3 Optical methods

Hyper/Multispectral unit

The design and operation are relative complex, and it could be a brand new development during the project implementation. Commercial parts (pressure resist observing glass, camera, colour LEDs) will be needed for the realisation.

During the implementation must be developed the whole system included the sealing and mounting systems, and also the interface electronics and processing software.

The placement of the sensor could be inside the pressure hull, mounted at the modified service hatch. Not necessary to have direct water contact, but necessary to observe the ambient (outer) environment (mine wall and water as well) with optical parts through some pressure resistant windows.

Installation is suggested in only one robot occasionally.

Fluorescent imaging

Commercial UV LEDs could be used for the realisation and the synchronous operation with one or more HD camera used for navigation must be provided.

During the implementation must be developed the sealing and mounting systems, and also the interface electronics and processing software .

The placement of the needed one or more UV LEDs must be outside on the pressure hull in a sealed transparent cover.

The installation is suggested for all of the planned three robots at the same time.

The technical details of the summarised methods above will be worked out in the D2.2 deliverable of the UNEXMIN project.